Mineral Tanning Mechanisms – A Fundamental Study

Graham S Lampard

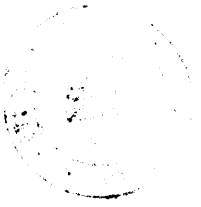

Thesis submitted for the degree of Doctor of Philosophy

Leicester University

University College Northampton

August 2000

ProQuest LLC
789 East Eisenhower Parkway
P.O. Box 1346
Ann Arbor, MI 48106-1346

Preface

'Even in a strictly theoretical evaluation of the potency of the tanning agent, it is advisable not to emphasise any particular property to the exclusion and detriment of any other criteria. Thus, characterisation of tannages from the point of view of the degree of hydrothermal stability attained in the final product by a certain tanning agent may lead to an erraneous conception.'

KH Gustavson

Dedication

To Emily and Jane whom I never knew, but dearly wish I had

Acknowledgements:

I wish to acknowledge, with thanks:

- Professor Paul O'Brien for his boundless enthusiasm, advice and support
- Professor Tony Covington for all the work which he has put into his role as supervisor
- The British School of Leather Technology for use of their facilities
- University College Northampton, formerly Nene College, for use of their facilities
- Leicester University for use of their library
- Pat Potter and Sue Maloney for their help and support during this work
- Drs Damien Murphy and Robert Farley at the EPSRC ENDOR facility, Universiy of Cardiff

Mineral tanning mechanisms - a fundamental study

Graham S Lampard

Abstract

A review across the periodic table of tanning effects of simple inorganic compounds reveals that many elements are capable of being used to make leather. But, if the practical criteria of effectiveness, availability, toxicity and cost are applied, the useful options reduce to chromium (III), the benchmark, or to titanium (IV), zirconium (IV), iron (II/III) and aluminium (III). For mainly environmental reasons, alternative tanning agents to chromium are needed. However, none so far investigated match the all round properties achieved with chromium (III) salts.

In tanning terms, the chemistry of titanium (IV) is dominated by the titanyl ion, TiO^{2+}, limiting its reactivity with collagen. An alternative approach to titanium tanning, using metastable titanium (III) salts as possible tanning agents, was investigated in this study. A method to determine the titanium content in leathers was developed.

Complexes of Ti (III) were investigated using various spectroscopic techniques, including uv/vis spectroscopy, electron spin resonance, electron nuclear double resonance and nuclear magnetic resonance dispersion spectroscopies. The complexes used in subsequent tanning studies were based on titanium (III) citrate, gluconate and tartrate. However, in comparative trials with chromium (III) salts, the study highlighted that titanium (III) salts were not suitable for tanning collagen. Titanium (III) salts were found to be useful in the production of semi-metal tannages.

The research was extended to investigate the hydrothermal shrinking of tanned collagen. Techniques such as extended x-ray absorption – fine structure and x-ray absorption near structure were used to investigate the interaction of chromium (III) tanning salts and titanium (III) complexes with collagen.

The research demonstrated that the shrinking reaction is independent of the tannage. It involves instead the breaking of hydrogen bonds, rather than the breakdown of the tannin-collagen molecule. From this work, and a reappraisal of older work on the shrinking reaction, a new theory of tanning has been formulated based on co-operating units and the role of crystallinity in stabilising the collagen structure. The influence of the solvent is also discussed.

Word Count: 36,600

1 Introduction

Leathermaking converts a byproduct from the meat industry - animal hides and skins - into a desirable, durable and useful material. The process stretches beyond prehistory and table 1.1 outlines the basic leathermaking processes, which have changed little over these years. The essence of leathermaking is to stabilise the skin's main protein, collagen, by tanning it.

1.1 Leather Processing

The basic leathermaking process is outlined below.

1.1.1 Preservation

Untreated hides have limited value once they have been removed from the carcass, since the protein, fat, sugar, blood and dung provide ideal nutrient conditions for bacterial growth. The conditions are such that putrefaction readily occurs because the saprophytic bacteria, which protect the pelt in the living animal, do not function. Natural enzymes cause autolysis, which leads to protein, triglyceride and carbohydrate breakdown. This activity, if left unchecked, will cause rapid deterioration of the hide, so the skin must be rendered non-putrescible by preserving it, either for the long or the short term.

For long term preservation there are only two practical options: drying is used in tropical countries, but in temperate conditions salting with sodium chloride is typical. Hides have salt spread on the flesh side and are then stacked, sandwiched with more salt. The salt draws water from the hides and the resulting brine solution penetrates the hide, preserving by an osmotic, bacteristatic action. Alternative long term preservation methods are limited, often based on reduced quantities of salt supplemented with bactericides, either inorganic or organic. One practical option is to use potassium chloride, which is a fertiliser rather than a soil pollutant.

Table 1.1: Leathermaking process

Process	Aim
Flaying	Removing the hide/skin from the carcass
Curing/preservation	Preserving the hide for transportation or storage
Soaking	Rehydrates and cleans the hide
Unhairing	Removal of hair, either intact by attacking the anchoring point at the base of follicle or by dissolving the keratin via attack at the sulfur-sulfur bond of cystine
Liming	Splits the collagen fibres by inducing swelling
Deliming	Neutralises the alkali used in unhairing and liming, typically using ammonium salts. pH falls from >12 to 7-9
Bating	A process using proteolytic enzymes to make the hide cleaner and softer by degrading the non collagenous proteins
Pickling	Brings the hide to the correct acidity for tanning
Tanning	Converts the putrescible pelt into non putrescible leather
Post tanning	A number of processes used to improve the organoleptic properties of the leather making it fit for use. This usually involves changing the colour, improving the softness and protecting the grain with a finish

Short-term preservation options are based on temperature reduction; this may take the form of simple chilling, but the most effective method uses biocide ice, that is ice made with the addition of a water soluble bactericide.

1.1.2 Soaking

When the cured hide is ready for processing, the preservative must be removed. This is achieved by soaking, which removes dirt, blood, dung, some soluble interfibrillary proteins, albumen, globulin and the glycosaminoglycan hyaluronic acid, while rehydrating the hide.

Many tanneries add surfactants, enzymes or other aids to rehydration called sharpening agents, eg sodium tetrasulfide, to speed up the soaking.

1.1.3 Liming

Once rehydrated, fat and flesh are removed mechanically and the hide is ready to be limed. This process removes hair and epidermis and swells the collagen. Under the alkaline, reducing conditions, removal of dermatan sulfate proteoglycan and swelling splits the collagen fibres at the fibril bundle level. The overall process is known as opening up and is crucial if the resultant leather is to be soft.

Unhairing involves nucleophilic attack at the sulfur-sulfur bond in cystine which is present in keratin, the hair protein. Sodium sulfide is the common reagent, although mercaptans and aliphatic amines are also effective. By adjusting the conditions, the hair may be dissolved or it may be removed intact; the latter is becoming the preferred option, for environmental impact reasons. The unhairing process occurs readily only at pH >12, conditions which are ensured by adding lime.

1.1.4 Deliming and bating

Having removed the hair and opened up the fibre structure, the pH is lowered for bating. Strong acids could be used for this, but it is difficult to exert sufficient control over the pH and too much acid will also cause excessive swelling. Ammonium chloride or sulfate is usually used to buffer at pH 8-9. The process is called deliming. Environmental concerns about ammoniacal nitrogen in effluent has meant that the industry is using carbon dioxide as an alternative, which reacts with calcium hydroxide to produce soluble calcium hydrogen carbonate reducing the pH to as low as pH 5.

$$Ca(OH)_2 + CO_2 \rightarrow CaCO_3 + H_2O$$

$$CaCO_3 + H_2O + CO_2 \rightarrow Ca(HCO_3)_2$$

At this point the pelts are treated with proteolytic enzymes in a process called bating. This solubilises the interfibrillary proteins, loosens epidermal tissue, hair roots and pigments, degrades fat cells and, depending on the activity of the proteolytic enzymes, may modify the fibre structure by degrading the elastin network in the grain layer.

1.1.5 Pickling and tanning

Following bating, the pelt is pickled with acid and salt. The addition of acid alone would lead to swelling, due to the imbalance of acid inside and outside the pelt, acting as a semi-permeable membrane, and to electrostatic repulsion in the cationically charged collagen. However, sodium chloride can curb this by controlling the electrolyte concentration gradient between the pelt and the bath. The minimum salt ionic strength needed is 0.5 mol dm^{-3}. In practice, 10% (w/v) brine solution is used and the pelts are soaked in this before the acid is added. Usually, organic and inorganic acids are used, eg methanoic and sulfuric acids. Pickling adjusts the pH of the stock ready for tannage, to acid pH values for tanning with metal salts or to neutral pH values for tanning with plant polyphenols.

1.1.6 Metal tanning

The tanning process is the focus of this thesis, particularly that involving mineral salts. Tanning converts skin into the non-putrescible material leather and the leather industry uses chromium salts for about 90% of leather production. The reasons being that chromium salts confer a high degree of hydrothermal stability and impart desirable mechanical properties to the resulting leather. There are many other metals capable of tanning and these will be discussed in more detail later.

1.1.7 Non-metal tannages

The alternative to simple inorganic tanning agents is organic tanning and there are currently several options that are open to the tanner.

1.1.8 Vegetable tannins

In the middle ages the tanner used to put hides into a vegetable tanning liquor for 'a year and a day' as a form of quality insurance. These days modern processing techniques can reduce that time to a few days. Many plant materials contain polyphenols which can be used for tanning; they react with protein primarily by hydrogen bonding at the peptide links along the chain. Vegetable tannins can be classified as either hydrolysable gallotannins or ellagitannins, based on pyrogallol, or condensed tannins based on the flavonoid skeleton, figure 1.1. In this work they have been used to investigate the interaction with metals and the synergistic effect of semi-metal tannages.

1.1.9 Semi-metal tannages

With semi metal tannages the collagen is first organically tanned, usually with hydrolysable vegetable tannin, then retanned with a metal salt. In industry, the preferred metal is aluminium (III). A synergistic reaction occurs at the pyrogallol group, to crosslink the bound polyphenol. This can raise the shrinkage temperature above 115°C. The process is probably as old as tawing, a stabilising process based on alum, but the alum would have been added as a mordant for dyeing rather than for its retanning effect.

1.1.10 Other organic tannages

The ideal tannage should match chromium (III) in its low degree of environmental impact and its ability to confer hydrothermal stability. The most difficult criterion to achieve is that of shrinkage temperature and the only established alternative method to produce leather with high hydrothermal stability is semi-metal tannages. However, recently it has been shown that equally stable leather can be made by the aldehydic crosslinking of condensed vegetable tannins using oxazolidine. This process has the advantage of not relying on any metal salt.

Also in that study, Covington[1] *et al* showed that oligomers of 2,4,6-tri amino-1,3,5-triazine/methanal (melamine/formaldehyde) resins can be crosslinked by aldehydic compounds

to achieve high shrinkage temperatures. The reaction is the first example of a totally synthetic organic tannage, which can compete with chromium (III).

1.2 Structure of collagen

About a third of the total skin weight is structural protein, the majority of which is collagen. The types of collagen found in skin are shown in table 1.2[2].

Table 1.2: Classification of collagen

Classification	Types (Examples)
Fibrous	I, II, III, V and X
Non-fibrous	IV, VIII, X
Fibril associated	IX, XII,XIV, XV
Filamentous	VI, VII

The basic structure of the collagen molecule is simple. The primary sequence is a tripeptide repeat of $(Gly\text{-}X\text{-}Y)_n$, n = 100-400 where X is often proline and Y is sometimes hydroxyproline. Glycine therefore occupies every third residue, while proline stabilises the α-helix by hindering rotation. The hydrogen side chain on the glycine allows these helices to pack in close contact and form a triple helix. This consists of 1,011 residues (3 x 337 Gly-X-Y units). In collagen I, there are two α I helices and one α II helix. The tropocollagen molecule is, thus, a long rigid rod, which in the fibrous collagen types is 1.5 nm by 300 nm. There is also a short telopeptide region, which differs from the main body of the molecule because it does not form a triple helical structure.

The tropocollagen molecule is stabilised by hydrogen bonds from the glycine residues to the peptide backbone of an adjacent chain. The larger polar and non-polar amino acids side chains face radially outwards from the cylindrical helix providing a charge profile along the molecule. It is this charge profile, which varies from regions of polarity to non polarity, that drives the

self assembly of the collagen molecules into the quarter stagger alignment of the collagen fibre and leads to the banded appearance of the fibre when stained.

The structural cohesion of tropocollagen can be traced to a number of factors. The peptide link provides a source of hydrogen bonding, dipole interaction and some double bond character, all of which stabilise the structure. The number of prolyl residues in the structure locks the protein chain and reduces the rotation. Gustavson[3] showed that as the hydroxyproline content of collagen in skin increases so does the shrinkage temperature.

Table 1.3: Shrinkage temperature and hydroxyproline content (*)

Fish	Hydroxyproline (g/100 g collagen)	Ts (°C)
Rock Cod	7.0	33-34
Alaska Pollak	8.2	36-39
Mackerel	9.7	52-54
Carp	11.0	56-58
Cattle hide	12.6	64-66

* selected results. Hydroxyproline determined by Neumann-Logan method

The role of the imino acids in general is now thought to be important; they increase the steric hindrance within the collagen structure, which leads to lower entropic values and so stabilises that structure.

Because there is a glycine molecule every third residue, a hydrogen is always at the centre of the tropocollagen molecule. This allows the close packing of the polypeptide chain. The role of water in stabilising the structure is thought to occur by allowing the formation of dipoles. Hydrogen bonded water varies from 1-3 moles per mole of collagen residue depending on that residue. There are also effects of hydrophobicity. Non polar amino acids, such as alanine or valine, hold the molecule together while the hydrophilic groups, which are mainly on the outside, make the protein soluble.

Bonding within the tropocollagen molecule is still the subject of much discussion. There are two models for the hydrogen bonding within the helix. According to the one hydrogen bond

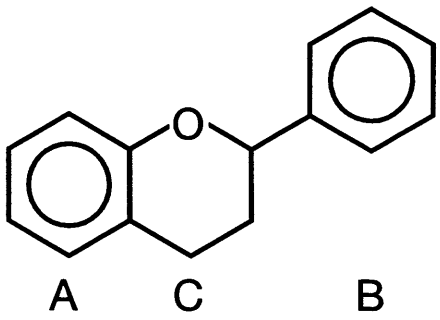

Figure 1.1: The flavonoid ring system

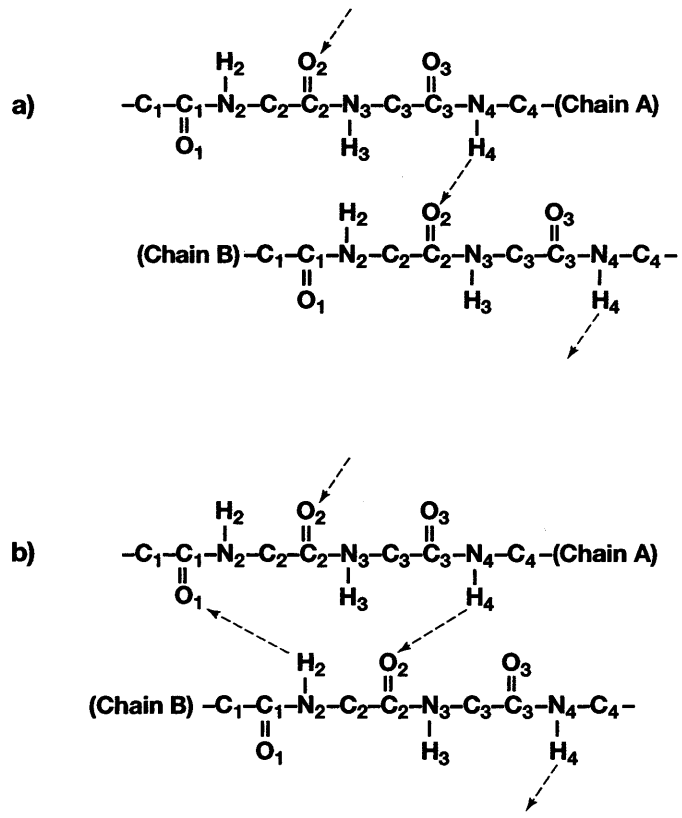

Figure 1.2: Different models of internal hydrogen bonding in collagen: (a) one hydrogen bonded model: (b) two bonded model[4]

model per Gly-X-Y triplet, postulated by Crick & Rich, the polypeptides are connected between the amide on the glycyl group, which is in the first position, polypeptide A, to the carbonyl of a residue in the second position of polypeptide B. Ramachandran *et al.* have suggested that there are two hydrogen bonds per Gly-X-Y residue, with the extra bond between the carbonyl of the glycyl and the amide of a residue in the second position of a triplet. This only occurs if an imino acid does not occupy this position, figure 1.2[4].

1.2.1 Assembly of collagen fibres

Once this primary structure has been formed, the tropocollagen molecule undergoes intramolecular crosslinking in the globular telopeptide regions of the two α I and one α II chains. This is an aldol reaction through the deaminated oxidised lysine/hydroxylysine amino acids to form the microfibril. Its formation is then thought to involve the minimisation of the surface exposed to the aqueous environment. There is disagreement as to how the microfibril is formed, with suggestions ranging from an hexagonal molecular lattice to other proposals that embody the idea that fibrils are composed of microfibrils, with models having two, four, five, seven, or eight arrays of tropocollagen molecules in each strand.

The microfibrils, approximately 7,000 of them, are then assembled by lateral association to form a fibril. Fibrils have a range of diameters linked through the glyco and mucoproteins. The fibrils, which show the characteristic striations associated with collagen 64-70 nm in size, assemble to form the fibres and fibre bundles.

1.3 Shrinkage and Mineral tannages

Native collagen is chemically and biologically relatively inert when dry, but it can absorb water readily, and when wet, is vulnerable to biochemical attack. Macroscopic fibre bundles of collagen can be induced to undergo an abrupt decrease in length at a characteristic shrinkage temperature, Ts, when subjected to slow heating in a solvent. Factors that govern this value

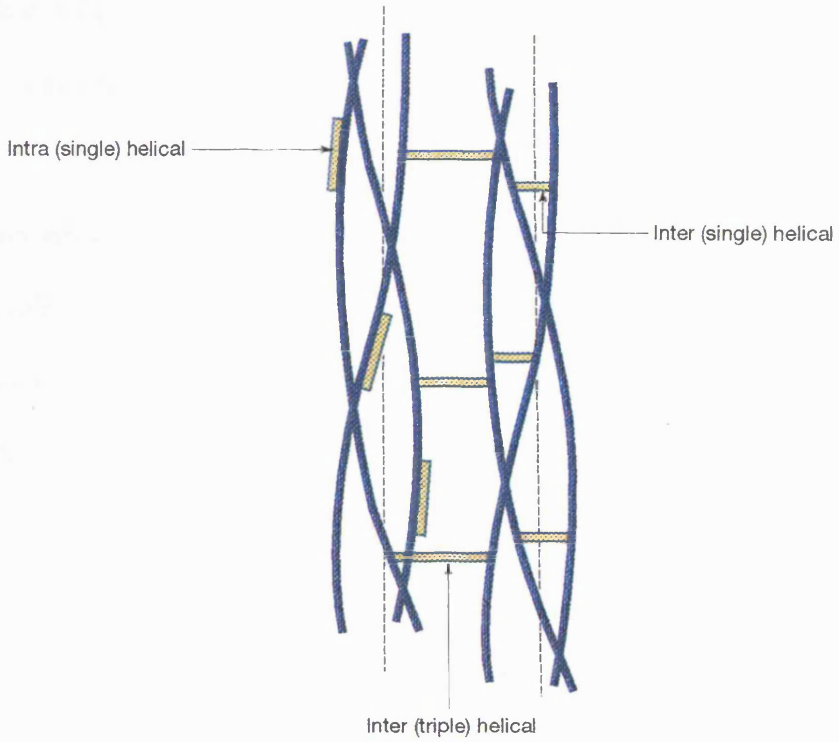

Figure 1.3: Intra and inter helical bonding sites on the tropocollagen molecule

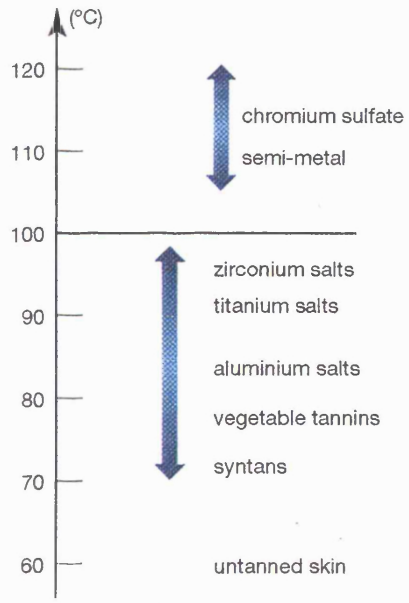

Figure 1.4: Schematic representation of the shrinkage temperature ranges for common tannages

include the chemical composition of the collagen, as shown by Gustavson; the nature of the solvent. In distilled water native collagen has a Ts of about 60°C, whereas in salt solutions the value can fall to below 40°C, depending on the concentration and type of salt used; the rate of heating.

The factors affecting shrinking include the intramolecular interactions and the superimposed intermolecular interactions. The latter is bought about by tanning and the sites available for tanning vary depending on the tanning agent. Figure 1.3[5] shows the intra and interhelical bonding sites on the tropocollagen molecule. The introduction of these crosslinks produces a more regular structure, decreases the entropy and so more energy is required to denature the collagen, hence, the shrinkage temperature rises. Also, metal tanning agents usually impart more hydrophobicity to the collagen making it more difficult to wet, thus, the shrinkage temperature is likely to rise.

Many elements of the periodic table are capable of tanning, but, if the practical criteria of effectiveness, availability, toxicity and cost are considered only aluminium (III), chromium (III), titanium (IV), zirconium (IV) and iron (II/III) are useful solo tanning agents. Current tanning technology is dominated by chromium (III): it was introduced about 130 years ago and by the turn of the century had begun to replace traditional vegetable tannages. The shrinkage temperatures produced from these tannages are shown in figure 1.4.

1.3.1 Chromium (III) salts

There is a fortuitous coincidence of reactivities in chromium (III) tanning. The reaction occurs at the ionised carboxyl groups of aspartic and glutamic acid. These side-chain carboxyls have pKa values 3.8 and 4.2 respectively, providing a reaction range at pH 2-6. Chromium (III) forms basic salts in the range pH 2-5.

Chromium (III) tanning is usually initiated at pH 2.5-3.0, using 33% basic chromium (III) sulfate in the form of spray dried powder, obtained from sulfur dioxide reduced chromium (VI)

acid; the empirical formula is $Cr(OH)SO_4$. During the course of the tanning process, the pH is raised to 3.5-4.0 causing the number of reaction sites on collagen to increase and the chromium species to increase in size. The formation of olated species was first suggested by Bjerrum to explain the hysteresis in delayed back titration of basified chromium (III) and the compound containing both hydroxy and sulfato bridges is well characterised. Further change, into the oxolated (oxo bridged) species, is postulated to happen during ageing after tanning.

The coordination of ligands, often methanoate, to chromium (III) prior to or during tanning is called masking. Masking agents may be applied at different ligand:metal ratios, depending upon the degree of masking desired; this produces a reduction of the cationic charge and the number of sites on the chromium (III) complex available for reaction. This makes the complex less reactive to collagen and, thus, increases the penetration rate. Masking may also increase the precipitation point of the complex. In these circumstances the final pH of the tannage may be elevated beyond that of the unmasked tannage, thereby enhancing the reactivity of the collagen. In this way the reaction rate can be accelerated, but without increasing the size of the chromium species.

Wet part processed chromium tanned leather is called wet-blue, the blue colour coming from the protein carboxy complexes of chromium (III); the colour also depends on the masking salts used and can range from pale green to purple. Wet-blue is highly versatile and can be used as the basis for producing a wide variety of leathers; the properties are modified by the addition of other tanning agents and lubricants.

The most remarkable property of wet-blue is its shrinkage temperature; values of 110°C or higher are easily achieved. Chromium (III) is unique among solo tanning agents in producing hydrothermally stable leather capable of resisting boiling water.

However, there has been research into alternatives, initially because the sources of chrome ore were in politically sensitive countries and then because of the worries about chromium being hazardous to health.

1.4 Other metal tannages

1.4.1 Aluminium

Aluminium has been known as a tanning agent for thousands of years. It is part of the tawing process. However, recent studies have shown that as a solo tanning agent it has low hydrothermal stability and the public perception of aluminium is not good. It has been used in combination with titanium (IV) to produce wet-white leather, with some success, but it cannot claim to be an alternative to chromium mainly because it does not impart high hydrothermal stability to the leather.

Aluminium (III) can be used in conjunction with vegetable tannins, *vide infra,* but it can also be used to accelerate chromium tanning. Following a pretreatment with aluminium (III), the incoming chromium displaces it. It is known that the exchange rate of solvate ligands is 10^7 times faster at Al(III) than at Cr(III). Covington[6] postulates that Al(III) can react quickly with other ligands, including collagen carboxyls, in a loose association that is entropy favoured. This allows orientation of the carboxylated side chains from the lowest energy of conformation to a conformation for reaction with metal salts, including crosslinking. When chromium (III) enters the system, the activation barrier is lower, so the reaction is accelerated. The use of aluminium (III) appears to be catalytic.

1.4.2 Zirconium

Zirconium is another transition metal that has been cited as a solo tanning agent. The development of zirconium tannage is relatively recent. However, although it imparts a higher shrinkage temperature than either aluminium or titanium, it gives the leather a fuller substance

and requires a high percentage addition to achieve the high stability. Again, this is not greater than 95-98°C, and to achieve that level of hydrothermal stability about 10% ZrO_2 is required compared with 2% Cr_2O_3.

Zirconium (IV) salts are characterised by 8-coordination and high affinity for oxygen, resulting in a tetrameric core structure. Zirconium (IV) is seldom used as a solo tannage, partly because of its ineffectiveness at raising the shrinkage temperature and partly because of the acidity of the salts which can induce osmotic swelling. Also, its tendency to polymerise as it becomes more basic causes a filling effect within the fibre structure, giving rise to comparisons with polyphenol tannage.

1.4.3 Iron

Iron salts were used in full scale manufacture during World War II but, although there have been a number of papers on the subject[7,8], the tanning mechanism, which is based on an electrostatic, weak complexing interaction, is still not fully understood. Moreover, this interaction confers a dark colour to the leather, due to the interaction with the polyphenols found in the vegetable tannins and syntans. This makes it unlikely that iron salts will be used as a main tannage.

1.4.4 Titanium

In tanning terms, titanium (IV) chemistry is intermediate to those of Al(III) and Cr(III). Its tanning chemistry is dominated by the titanyl ion, TiO^{2+}, but the species are chains of titanium ions bridged by hydroxy and sulfato ligands, like Cr(III). However, the coordinating power is weak with respect to carboxyl complexation, so the interaction is more electrostatic than covalent. As a solo tannage, Ti (IV) tanning is only moderately effective because large quantities are required to achieve high shrinkage temperatures, >95°C. This causes the leather to be overfilled and, therefore, less versatile.

1.5 Project introduction

It is apparent that a viable inorganic alternative to chromium still has to be found and those alternatives are limited. The titanium chemistry used so far in the leather industry has involved only the titanyl ion.

There is a possible alternative, titanium (III). This is an oxidation state with the potential for tanning, which has been investigated in this research through the use of novel techniques, including electron spin resonance (ESR), electron double nuclear resonance spectroscopy (ENDOR), nuclear magnetic resonance dispersion (NMRD) and extended x-ray absorption – fine structure (EXAFS). There has also been an investigation of its leather chemistry, which has involved developing a method for determining titanium in leather, investigating the masking interaction of ligands and the hydrolysis reaction of the titanium (III) ion.

1.6 The project

Initially, the aims of this work were three fold.

- To investigate titanium (III) complexes, their formation, stability to change in pH, temperature, time and oxidation
- To study the interaction of Ti (III) complexes with collagen and assess their tanning effectiveness
- To compare the mechanical and physical properties of Ti (III) tanned leather with those of the industry standard, chrome tanned leather

However, it soon became obvious that titanium (III) would not prove to be a tanning agent to rival chromium. It was decided to extend the project to investigate the factors involved in the tanning and shrinkage of leather, using tervalent titanium salts as an indicator where possible.

The unpaired electron made the salt ideal for the investigation of titanium complexes using ESR and ENDOR. Early on it was realised that the underlying principles of why leather

shrinks and what is involved in the shrinking mechanism were not clearly understood. Apart from investigating the titanium leather chemistry, the techniques mentioned above were also used to elucidate more about the shrinking of leather and the complexes involved in chromium tanning, which also tend to be paramagnetic.

Thus, the original aims of the project were extended to include other metals and to develop a theory of collagen shrinking. From this work, and by reinterpreting older work in the light of recent ideas, a new theory of tannage has been developed.

2 Titanium and titanium (III) chemistry

2.1 Introduction

This chapter is concerned with the aqueous chemistry of titanium (III). The aim of the research was to develop suitable complexes for use in tanning studies. These studies included masking with ligands and the interaction was investigated using uv/vis spectroscopy. The effect of ligation was measured by studying the changes in the absorption spectra and the changes in the titration curve of the titanium (III) salts.

The narrative is divided into a review of the work carried out by other authors who have investigated the hydrolysis of titanium (III) and relating this to the changes in the absorption spectra. This is followed by the research carried out in this study.

2.2 Background

Titanium is the ninth most abundant element by weight in the earth's crust. The main ores are ilmenite, $FeTiO_3$, and rutile, TiO_2. The electronic structure of titanium is given in table 2.1, along with that of other members of the titanium group. The known oxidation states are also given.

Table 2.1: Properties of group IVB metals

Element	Electronic structure	Oxidation states
Titanium	[Ar] $3d^2$ $4s^2$	(-I) 0 (II) III IV
Zirconium	[Kr] $4d^2$ $5s^2$	0 (II)(III) IV
Hafnium	[Xe] $4f^{14}$ $5d^2$ $6s^2$	0 (II)(III) IV

The states in brackets are transitory

Titanium is a commercially important element. Titanium (IV) oxide is used as a pigment and filler and the metal is important for its strength, low density and corrosion resistance properties. Titanium (III) chloride is important as a Ziegler Natta catalyst for making polythene and other polymers. The titanium (III) compounds have a d^1 configuration and are coloured and paramagnetic. Ti (III) is much more basic than Ti (IV) and the addition of alkali to Ti^{3+}

solutions precipitates $Ti_2O_3.x(H_2O)$, which is purple in colour. TiX_3 halide compounds are readily formed by reducing TiX_4. Thus, anhydrous titanium (III) chloride can be obtained as a violet powder by reducing titanium (IV) chloride with hydrogen at 600°C. This compound is unstable in air, being readily oxidised to the titanium (IV) state on contact with moisture. The solid was used in some of the experiments in this study.

The reduction with zinc of solutions containing titanium (IV) complexes gives the purple aqua ion, $Ti[H_2O_6]^{3+}$. Another way of producing the titanium (III) salt is direct combination of the metal with the acid of the salt required. This was the method most frequently employed in this work.

2.2.1 Solution chemistry of titanium (III) salts

Titanium (III) is unstable in air and under neutral or alkali conditions. In the acidity range 0.3 mol $dm^{-3} < [H^+] < 12$ mol dm^{-3} the potential is[9]:

$$Ti^{4+} + e^- \rightleftharpoons Ti^{3+} \qquad E_0 = -0.2 \text{ V}$$

The first work investigating the hydrolysis reaction of the hexa-aqua titanium (III) ion seems to be by Fletcher and Pecsok.[10] They stated that under acid conditions, below pH 2, the hydrolysis reaction is limited to

$$Ti(H_2O)^{3+} \rightleftharpoons Ti(OH)^{2+} + H_3O^+ \qquad (1)$$

with any polynuclear reactions only occurring above pH 2.7. They also suggest that the reaction

$$2\ Ti(OH)^{2+} \rightleftharpoons [Ti\text{-}O\text{-}Ti(OH)]^{3+} + H^+ \qquad (2)$$

occurs at pH 4.1. This is a higher pH value than any other reported results indicate, whether they are quoted in the literature or found in this work. It is also interesting to note that they assume the oxygen bridge between the titanium ions is a mono rather than a diol bridge as is usually suggested with chromium (III) salts. Pecsok stated that because their research indicated

the polynuclear reaction occurs at higher pH values, it did not affect significantly the first hydrolysis constant. However, work by Baes[11] indicates that there was a significant influence from the olation reactions. He suggests that the hydrolysis reaction

$$2Ti^{3+} + 2H_2O \rightleftharpoons [Ti_2(OH)_2]^{4+} + 2H^+ \qquad (3)$$

occurs at a pH lower than that suggested by Pecsok and so renders invalid the assumption that it does not interfere. Other researchers agree that reaction 1 gives rise to the first hydrolysis constant to be determined.[12]. In addition, the solutions studied contained small, but significant amounts of titanium (IV), the hydrolysis of which introduces additional uncertainty into the measurements.

Hugi et al[13] studied the water exchange mechanism at different temperatures and pressures on $[Ti(H_2O)_6]^{3+}$ using ^{17}O NMR. Samples, in up to 20% ^{17}O enriched water, containing titanium (III) and trifluoromethanesulfonate as the non co-ordinating ion were studied and the authors came to the conclusion that the interaction showed evidence for an associative interchange mechanism (I_a mechanism) in substitution reactions with $[Ti(H_2O)_6]^{3+}$. They found that the rate, k, was fast compared with other first row transition metals, see table 2.2. This was investigated using NMRD, see chapter 6.

Table 2.2: Rate constants for solvent exchange in 1st row transition metal hexa-aqua ions[14]

Electronic configuration	t_{2g}^1	t_{2g}^2	t_{2g}^3	$t_{2g}^3 e_g$
Cation	**Ti(III)**	**V(IV)**	**Cr (III)**	**Fe(III)**
k^{298} (s^{-1})	1.8×10^5	5.0×10^2	2.4×10^{-6}	1.6×10^2

Spectrophotometric and temperature jump techniques[15] have also been used to study the equilibria and kinetics of complex formation of titanium (III) with acetate, monochloroacetate and dichloroacetate in aqueous solution. Chaudhuri and Deibler[15] measured the stability constants of some Ti(III) complexes. These are shown in table 2.3.

Table 2.3: Stability complexes of titanium (III) salts

Ion	Stability constant (M^{-1})
$TiAc^{2+}$	390
$Ti(ClAc)^{2+}$	24
$Ti(Cl_2Ac)^{2+}$	5.2

15°C, ionic strength = 0.5 M

The kinetic data indicate that at least two reaction pathways contribute to the complex formation process. The second order rate constants generally increased with the basicity of the ligands. This behaviour also indicates appreciable associative character of the substitution process with $[Ti(H_2O)_6]^{3+}$ ions. The problems occur when assigning the reaction routes. The titanium hexa-aqua ion readily hydrolyses to give the mono hydroxyl ion. So, the reaction may proceed via

$$Ti^{3+} + L^- \rightleftharpoons TiL^{2+} \qquad (4)$$

Or it may be by

$$Ti(OH)^{2+} + HL^- \rightleftharpoons TiL^{2+} \qquad (5)$$

Interpretation of the results suggests that the reaction is via equation 4. Table 2.4 shows the interaction of titanium (III) with other ligands. It shows that the ion reactivity increases as the basicity increases and provides further strong evidence for an associative interchange mechanism. It may be that in the case of carboxylic acid anions the outer sphere association is somewhat stronger than with non-basic ligands, eg Cl^-, due to H-bond formation between the co-ordinated water and the acceptor ligand. The evidence for an associative interaction is also seen with chromium (III). The mechanism is viable because of the high positive charge of the central atom and the co-ordinative unsaturation of Cr(III), which facilitates the formation of a transition state of increased co-ordination number. This mechanism is confirmed by other work[16].

Table 2.4: Rate constants for the reaction of Ti^{3+} with various ligands[16]

Ligand	Rate constant	Experimental conditions
$ClCH_2COOH$	0.7×10^3	15°C, 0.5 M
CH_3COOH	1.0×10^3	15°C, 0.5 M
H_2O	1.0×10^5	25°C, 0.1 M
Cl_2CHCOO^-	1.1×10^5	15°C, 0.5 M
$ClCH_2COO^-$	2.1×10^5	15°C, 0.5 M
$HC_2O_4^-$	3.9×10^5	15°C, 0.5 M
CH_3COO^-	1.8×10^6	15°C, 0.5 M

Chaudhuri and Diebler[17] followed the complexation with oxalate as a function of the hydrogen ion concentration to show that the mechanism was most likely an associative mechanism. Hartmann and Schläfer[18] observed strong variations in the absorption spectrum of titanium (III), which was ascribed to hydrolysis at low concentrations and formation of chloro complexes in hydrochloric acid. In 2 mol dm^{-3} hydrochloric acid, the hexaaquo ion is the dominating species in the reddish purple solution. However, if the molarity of the acid is increased, the titanium (III) turns sky-blue with a shift to a double band about 660 nm and 525 nm. This is probably due to the chloro anion entering the inner sphere and displacing water ligands.

It has been suggested that in acid concentrations of that molarity the species present are $TiCl^{2+}$ and $TiCl_6^{2-}$ and so the composition of the mixed complex (III, IV) may be near to the neutral form, Ti_2Cl_7. This type of structure is suggested by Wessel and Ijdo[19] who state that each metal atom is octahedrally bonded to three terminal and three bridging chlorine atoms. For the titanium derivative of cesium titanium heptachloride, the bond lengths were determined as 25.2 nm (bridging) and 23.4 nm for a terminal bond.

2.2.2 Reaction pathways

The main use of titanium (III) is as a reducing agent. There have been papers investigating the reaction pathways involving titanium (III). Some of these suggest mechanisms that involve mixed complexes. The reduction of vanadium (V) by titanium (III)[20] is one. The first step of

the mechanism, equation 6, is thought to involve the olation of the titanium, followed by interaction with the VO^{2+} ion. At this point there is a mixed complex, which then involves an electron transfer, for oxidation of the titanium and reduction of the vanadium.

$$Ti^{3+} + H_2O \rightleftharpoons Ti(OH)^{2+} + H^+ \quad (6)$$

$$Ti(OH)^{2+} + VO^{2+} \rightleftharpoons Ti(OH)VO_2^{3+} \quad (7)$$

$$Ti(OH)VO_2^{3+} \rightleftharpoons TiOVO_2^{2+} + H^+ \quad (8)$$

$$TiOVO_2^{2+} \rightarrow Ti(IV) + V(IV) \quad (9)$$

The point here is that there is evidence for olation reactions that show such a mechanism can exist and secondly that they are stable enough to be analysed. If they can exist in redox reactions, it may be possible to use these reactions in tanning collagen.

2.2.3 Uv/vis spectra

The shape of a transition metal complex is determined by a number of factors including the tendency of the electron pairs to occupy positions as far away from each other as possible. The loss of degeneracy into the t_{2g} and e_g orbitals is due to the interelectronic repulsion of metal and ligand centred electrons.

According to the crystal field theory, in octahedral complexes the t_{2g} orbitals (d_{xy}, d_{xz} and d_{yz}) lie at a lower energy level than the e_g orbitals (d_x^2-d_y^2, d_z^2) when splitting is induced. According to Hund's rule, the d^1 electron will occupy one of the t_{2g} orbitals and so the molecular orbitals are non degenerate. This means that the repulsion of some ligands directly interacting with the occupied orbital will be greater than the repulsion felt by those interacting with unoccupied orbitals. The result is that the complex will become distorted from the regular octahedron expected from sp^3d^2 hybridisation. The Jahn Teller Theorem says that any non-linear complex in a degenerate state is unstable and will undergo distortion to remove that degeneracy. If the distortion occurs with the e_g orbitals, then in the case of an octahedral d^1

system, the tetragonal elongation, along the z axis should be observed in the uv/vis spectra. The electronic spectrum of the Ti (III) ion produces a d-d transition with a single peak at about 500 nm and the distortion is visible as a broad shoulder in the spectrum, figure 2.1.

Goroshchenko and Godneva[21] showed that on dissolving titanium (III) sulfate in sulfuric acid a violet solution was obtained. They also showed that this was due to the presence of Ti^{3+}, being independent of the anion, since the same violet colour is obtained when titanium (III) chloride is dissolved in hydrochloric acid. Around 608 nm, in concentrated solutions of sulfuric acid, ~80%(w/v), a blue colouration developed. This they assigned to either a complex involving the sulfate ion entering the titanium sphere, rather than acting simply as a counterion, or to a change in the hydration of the titanium (III) ion.

They determined that the addition of titanium (IV) sulfate shifted the λ_{max} towards the higher energy region (527 nm $\rightarrow$ 472 nm) and increased the absorbance. Up to 50% addition of Ti^{4+} shifted the spectrum, Figure 2.2. However, above that, no further change was noted. They suggest this violet/brown complex is a 1:1 ratio of Ti^{3+}/Ti^{4+}.

Work by Cservenyak et al[22] also showed that there is an enhanced absorption of titanium (III)/(IV) solutions in sulfuric acid. They believed this to result from intramolecular charge transfer in a mixed oxidation state intermediate incorporating sulfate.

The species formed were thought to be:

$$TiOSO_4 + Ti^{3+} + (p-2)H^+ + (q-1)SO_4^{2-} \rightleftharpoons [Ti^{IV}\ Ti^{III}(SO_4)_q(H^+)_p]^{(2q-3-p)-} \qquad (10)$$

The time dependence of the absorption maxima and the corresponding change in wavelength are shown in figure 2.3. The relatively rapid shift in the λ_{max} and the corresponding increase in the absorbance in the first hour reflects the formation of mixed Ti (III) – Ti (IV) sulfate complexes.

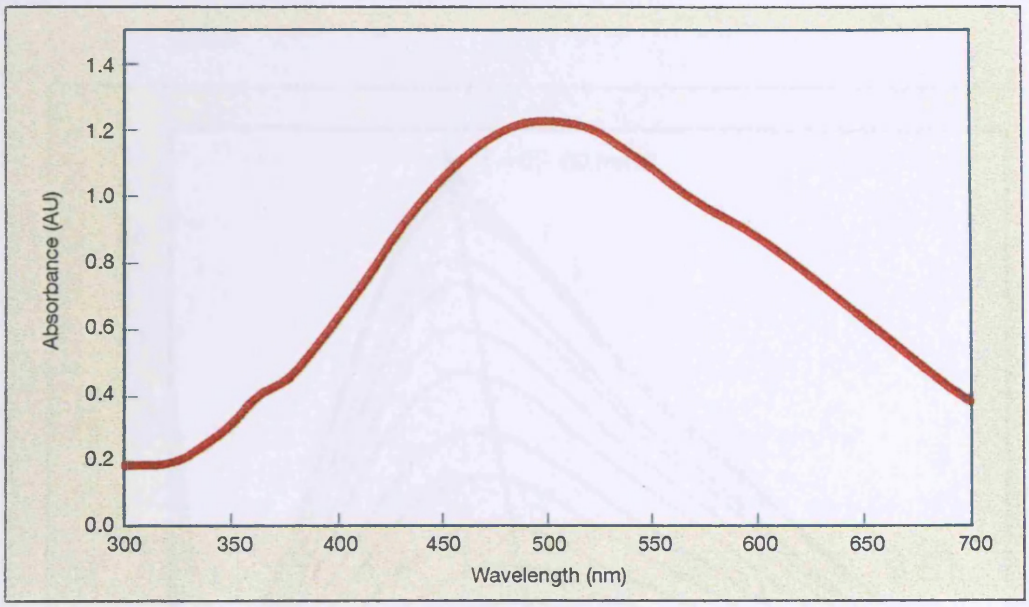

Figure 2.1: Absorption spectrum of titanium (III) sulfate

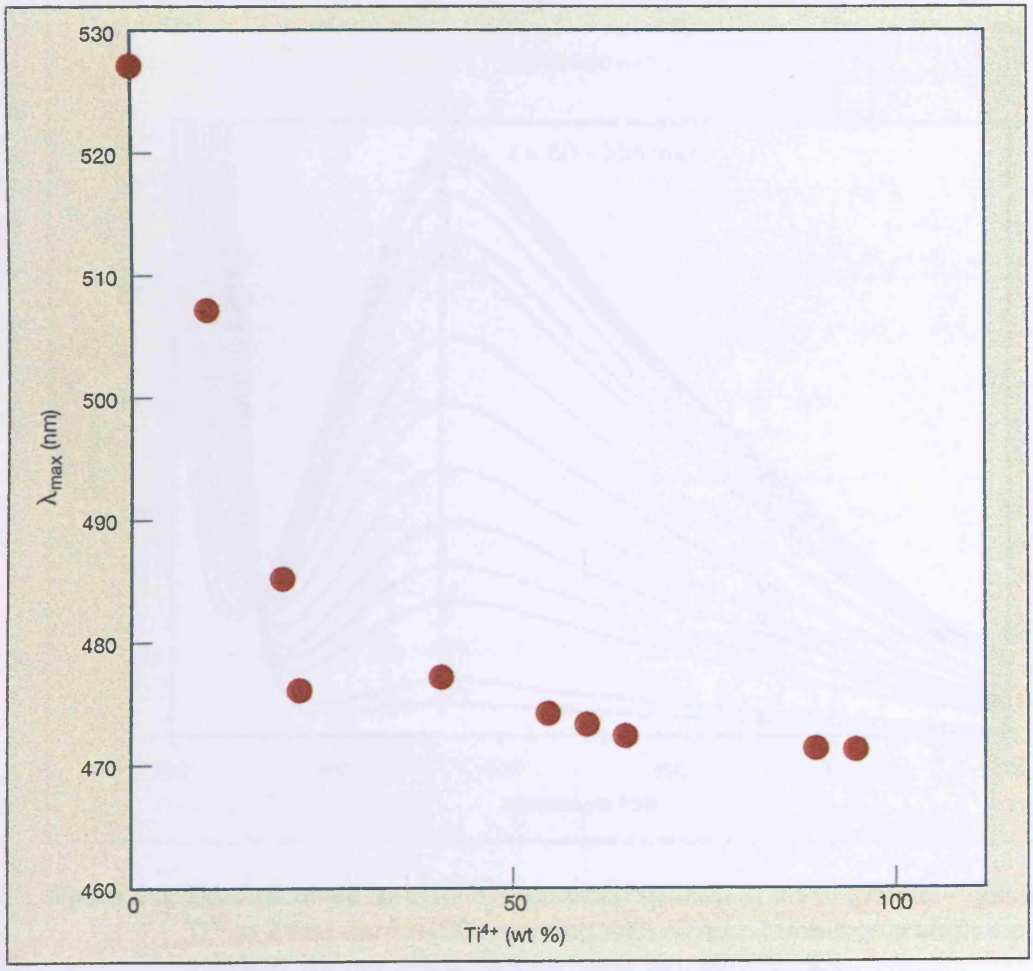

Figure 2.2: Change in λ_{max} on the addition of titanium (IV) ions to a solution of titanium (III)

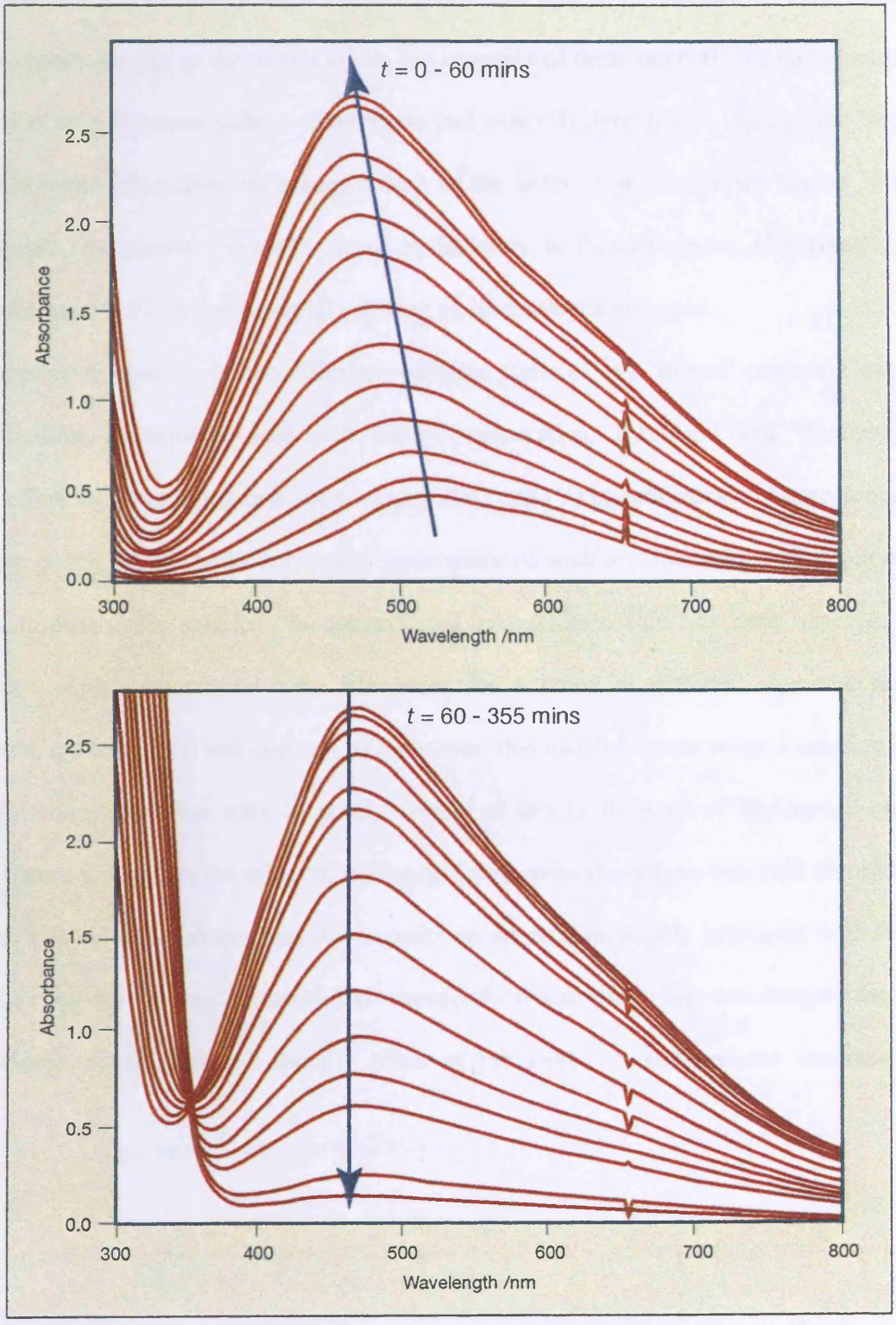

Figure 2.3: Time resolved uv-visible absorption spectra of 0.114 mol dm^{-3} dissolved Ti^{III} in 2 mol dm^{-3} H_2SO_4 reacting with oxygen bubbling through the solution. (Upper set: 0-60 min; lower set: 60-355 min)

2.2.4 Intervalence compounds

In analytical chemistry, the interaction of two elements can lead to an increase in absorption due to a phenomenon known as the matrix effect. An example of these intervalence compounds is the interaction seen between sodium dichromate and iron (II) perchlorate. Adding the iron salt to the dichromate intensifies the orange colour of the latter, even though the former is a colourless liquid. The reason for the increase in intensity is thought to be an interaction between the chromium (VI) and the iron (II) to form an intervalence complex.

Systems containing an element in two different oxidation states or in a 'mixed' oxidation state sometimes manifest abnormally deep and intense colouration. Davidson and Whitney[23] observed the effect by mixing solutions of antimony (III) and (V) in concentrated hydrochloric acid. They also noted the 'hitherto unreported occurrence of such an "interaction absorption" for mixed stannous-stannic solutions in concentrated hydrochloric acid has been observed.' Other instances of this interaction have been seen for a range of different elements and oxidation states, eg, copper (I) and copper (II). However, this usually occurs when a solution is doped with the other oxidation state. A good example of this is the work of McConnell and Davidson[24], Figure 2.4, where the effect of adding different chloride salts to iron (III) chloride, including iron (II) chloride, shows that the intensity in absorption is only increased with the addition of the iron. All the divalent halides are essentially colourless in this wavelength range. The data indicate the marked and specific effect of the oxidation state on the absorption spectra.

2.3 Experimental work

2.3.1 Production of titanium (III) salt

One of the problems with using titanium (III) salts is their poor stability in air. Solid titanium (III) chloride fumes in air and is easily oxidised to Ti (IV). However, under acid conditions the rate of oxidation can be reduced significantly.

Titanium metal (7 g) was added to a warm solution (40°C) of sulfuric acid (600 cm^3, 3 mol dm^{-3}) and left overnight to react. The following morning, the solution was diluted to 1 dm^3 and the purple solution of titanium (III) sulfate was analysed to determine the Ti content. This was typically about 0.15 mol dm^{-3} Ti. A uv/vis spectrum was collected to ensure that no Ti (IV) was present (λ_{max} 280 nm). The solution was then stored under nitrogen until used. In some experiments the acid was changed and hydrochloric and phosphoric acids were used, however, unless stated, the salt used is titanium (III) sulfate.

2.4 Effects of changes in uv/visible spectra

The solution chemistry of titanium (III) sulfate was investigated as a function of the pH, ageing and the rate of oxidation. This was monitored using uv/vis spectroscopy.

2.4.1 Apparatus assembly

To determine the uv/vis spectrum, a flow cell was used. The apparatus was set up as shown in figure 2.5. A peristaltic pump was used to transport the reaction mixture through a flow cell in the Perkin Elmer Lambda 2 uv/vis spectrometer. The reaction vessel was held at constant temperature by setting it up in a temperature controlled water bath. The flow cell had a path length of 10 mm and all the tubing had an internal diameter of 15 mm. The average flow rate was 0.5 $cm^3\ s^{-1}$.

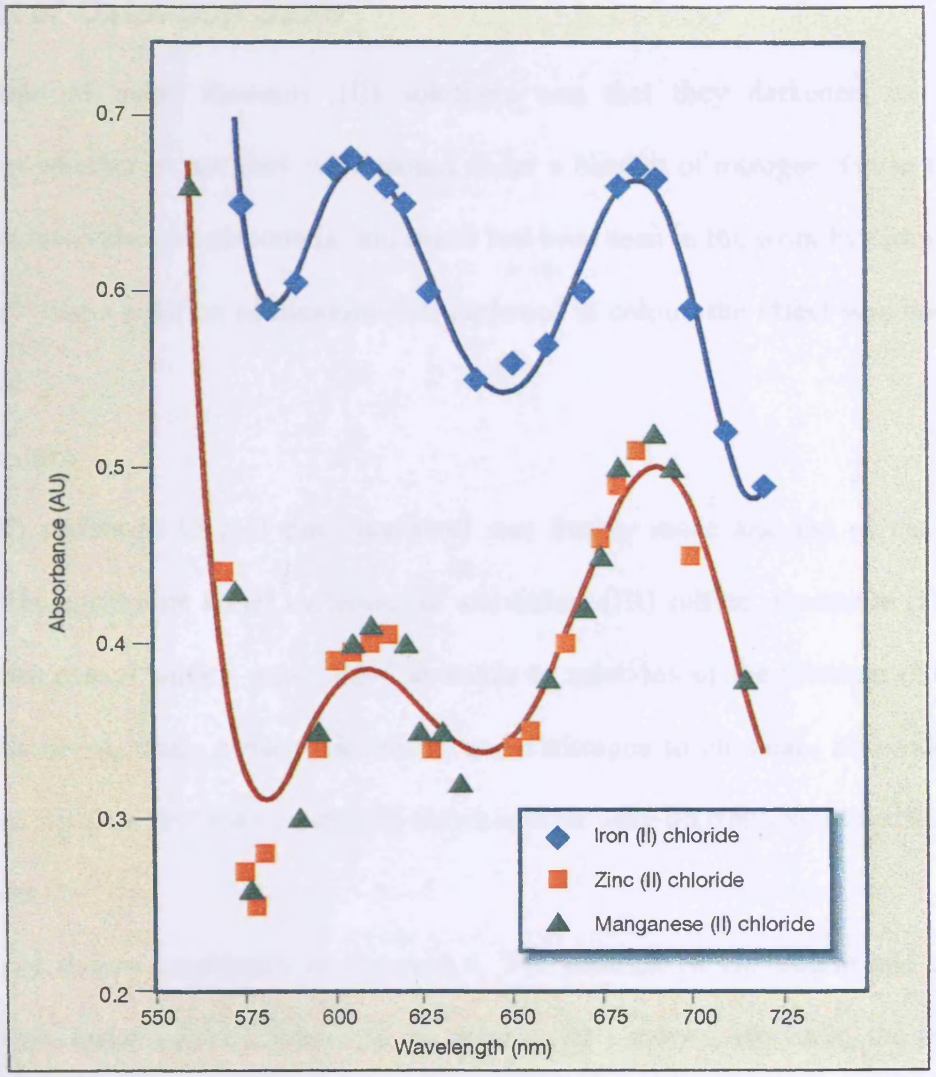

Figure 2.4: Effects of several salts on the absorption spectrum of iron (III) in 12 mol dm^{-3} HCl

Red line = absorbance of iron (III) chloride without salt addition

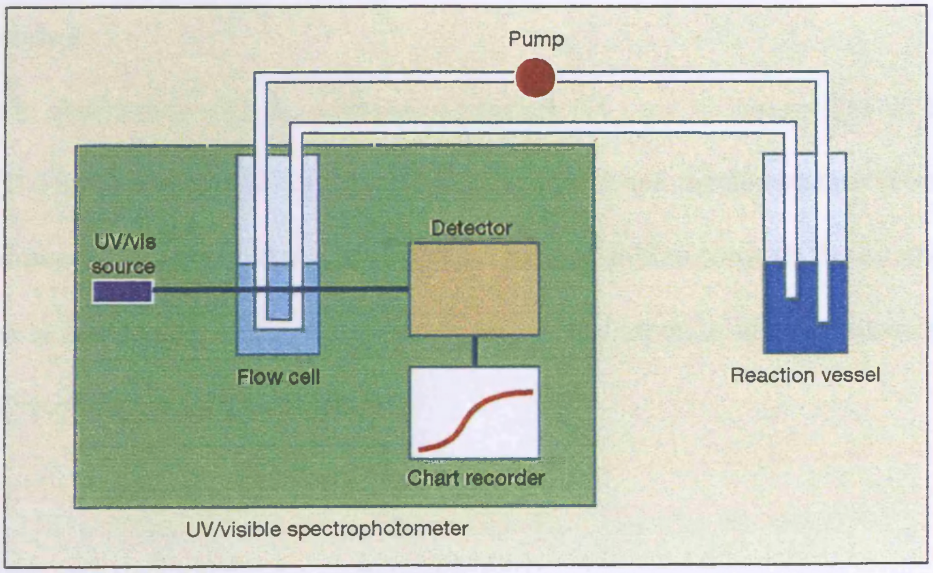

Figure 2.5: Schematic diagram of the equipment used to determine the uv/vis spectra

2.5 *Effect of Oxidation State*

An observation of using titanium (III) solutions was that they darkened on standing, irrespective of whether or not they were stored under a blanket of nitrogen. Given that other metals exhibit intervalence compounds, and that it had been seen in the work by Goroshchenko and Godneva[25] that a solution of titanium (III) darkened in colour, the effect was investigated for this metal.

2.5.1 Procedure

Titanium (III) sulfate (0.15 mol dm^{-3} titanium) was freshly made and the uv/vis spectrum determined. The equivalent metal molarities of aluminium (III) sulfate, zirconium (IV) sulfate and ammonium titanyl sulfate were added as solids to solutions of the titanium (III) sulfate. They were dissolved, using a magnetic stirrer, under nitrogen to eliminate air oxidation. All salts dissolved within a few minutes and the uv/vis spectra were determined immediately.

2.5.2 Results

The results are shown graphically in Figure 2.6. The addition of aluminium and zirconium sulfates does not make much difference to the titanium (III) spectra. However, the data in this figure clearly indicate that the effect of adding titanium (IV) ions is a marked increase in the absorbance.

2.5.3 Discussion

The increase in absorbance with the addition of titanium (IV) can be assigned to an interaction of titanium (III) and titanium (IV) to form a mixed complex and the absorbance from titanium (IV) alone. However, given that the λ_{max} at 505 nm has not shifted towards the uv, the increase in absorbance in this region is due to the matrix effect. The increase in absorbance below 350 nm is indicative of titanium (IV) complexes.

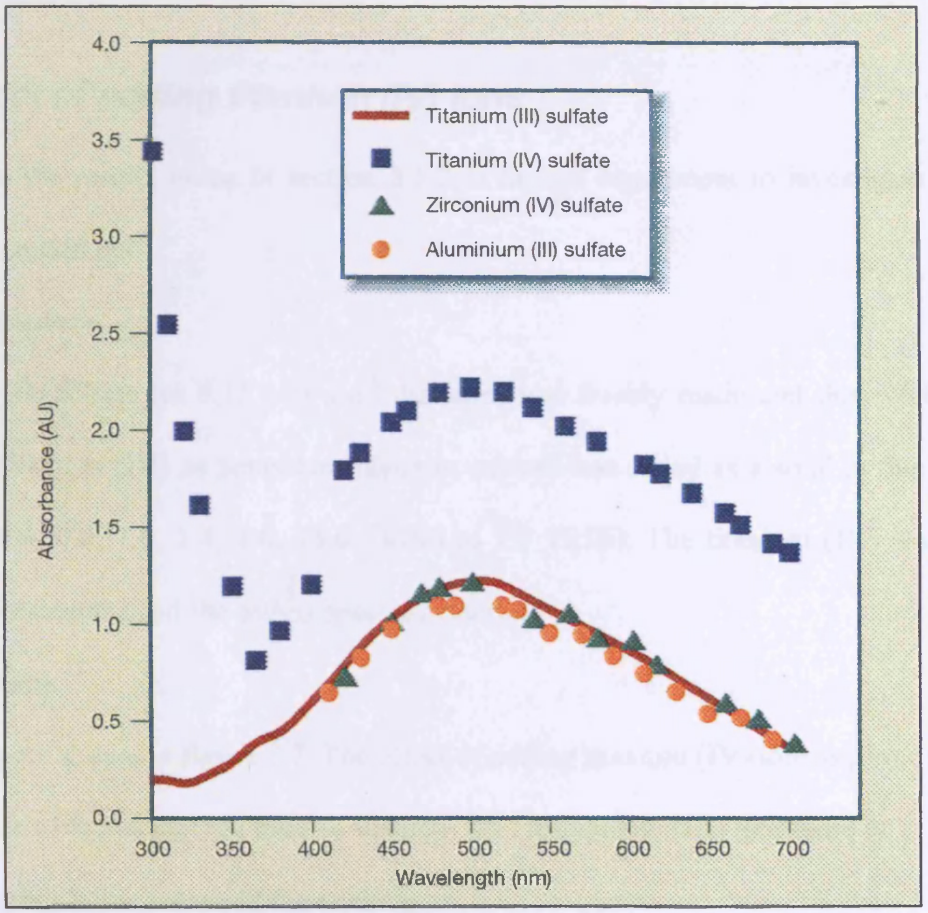

Figure 2.6: Effects of salts on the absorption spectrum of titanium (III) in 6 mol dm^{-3} sulfuric acid

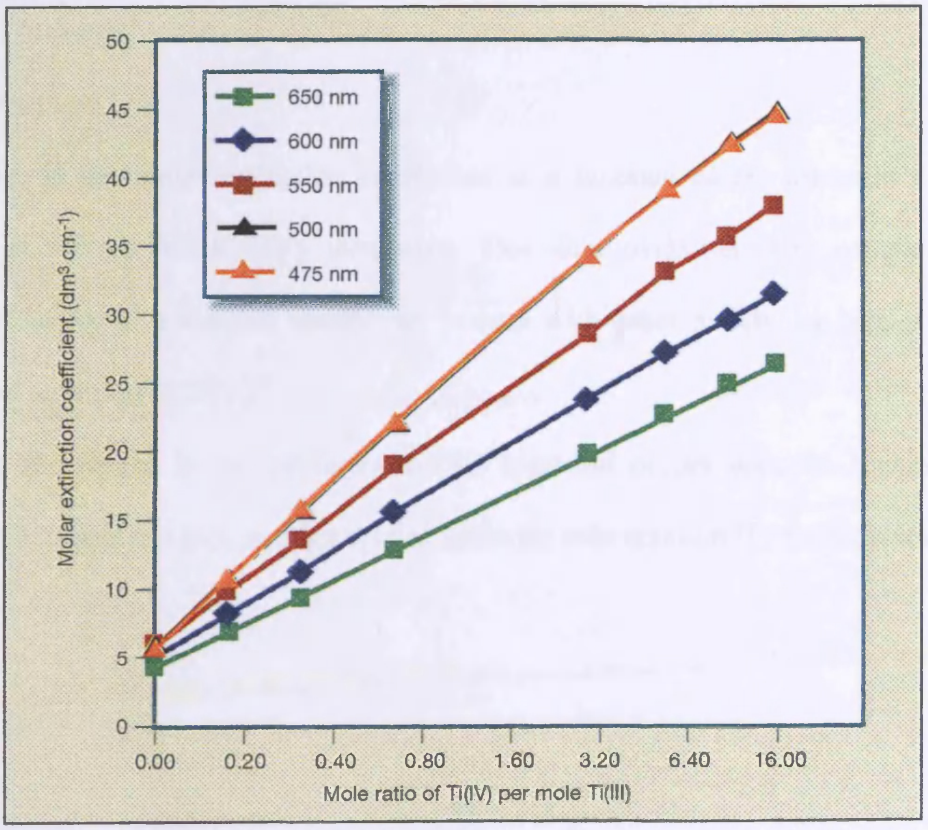

Figure 2.7: Effect of titanium (IV) concentration on the molar extinction coefficient

2.6 *Effect of adding titanium (IV) ions*

To confirm the results given in section 2.5.2, a further experiment to investigate the matrix effect was carried out.

2.6.1 Procedure

Titanium (III) sulfate (as 0.15 mol dm^{-3} titanium) was freshly made and the uv/vis spectrum acquired. Titanium (IV) as potassium titanium oxalate was added as a solid in the mole ratios of 0, 0.2, 0.4, 0.8, 1.6, 2.4, 4.0, 16.0 Ti(IV) to 1.0 Ti(III). The titanium (IV) was dissolved within a few minutes and the uv/vis spectra acquired.

2.6.2 Results

The results are shown in figure 2.7. The effect of adding titanium (IV) ions is pronounced. As a consequence of increasing the ratio of titanium (IV) to titanium (III) ions there is:

- a darkening in the colour of the solution.
- a strong absorbance in the uv region, which is absent when the spectrum of titanium (III) alone is measured.

2.6.3 Discussion

The increase in the molar extinction coefficient as a function of the ion ratio signifies the formation of mixed Ti (III)/(IV) complexes. This dual oxidation state complex, with an increase in the molar extinction coefficient, is seen with other metals, eg copper (I/II)[26], tin (II/IV)[27] and antimony (III/IV)[28]

The strong absorbance in the uv region of the spectrum occurs with the highest ratios of titanium (IV) to titanium (III) and is a typical value for solo titanium (IV) complexes.

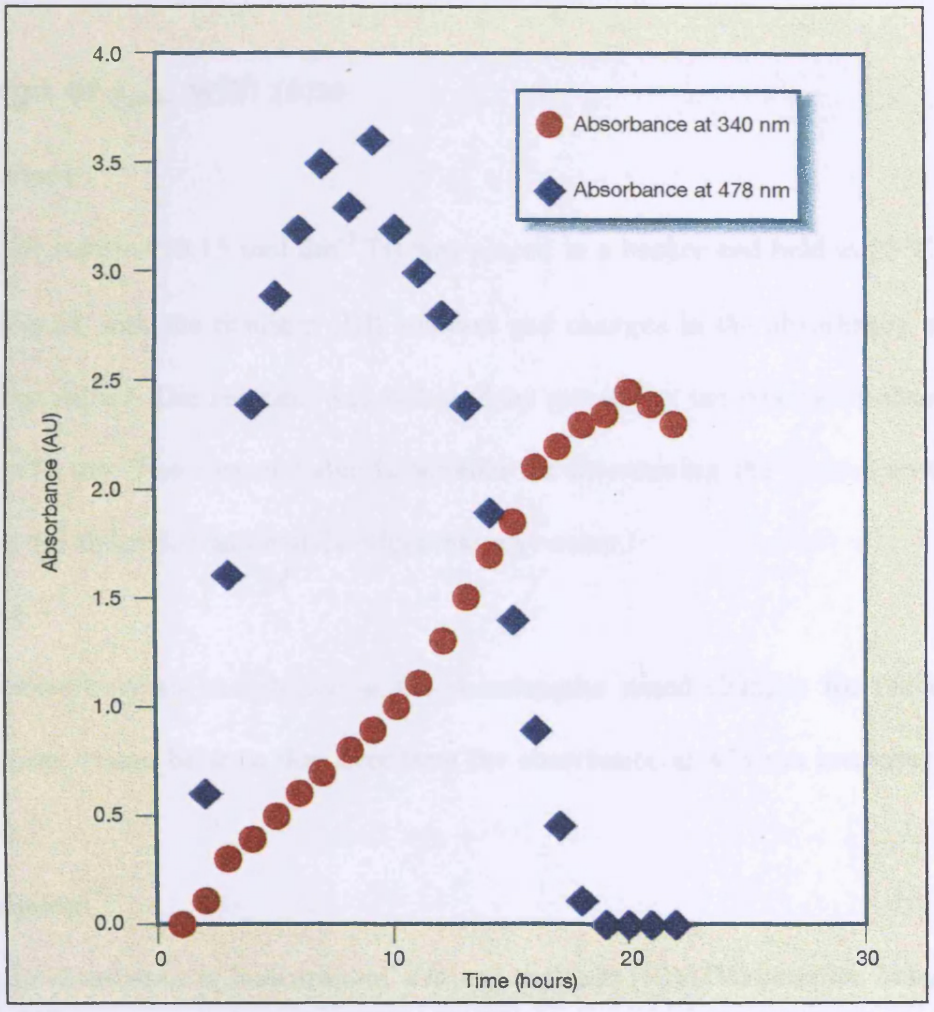

Figure 2.8: Change in λ_{max} of titanium (III) sulfate solution

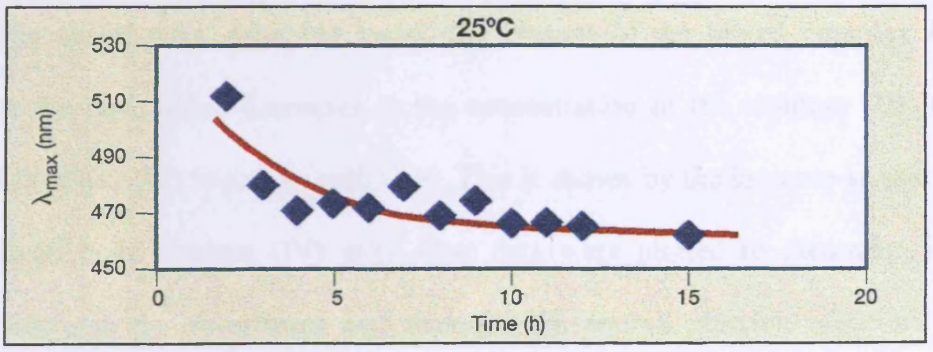

Figure 2.9a: Change in λ_{max} with time

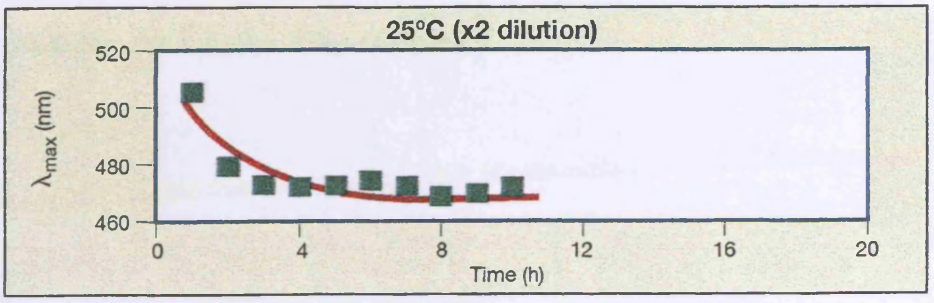

Figure 2.9b: Change in λ_{max} with time

2.7 Change of λ_{max} with time

2.7.1 Procedure

A titanium (III) solution (0.15 mol dm^{-3} Ti) was placed in a beaker and held at 25°C. Air was allowed to interact with the titanium (III) solution and changes in the absorbance at specific wavelengths measured. The reaction was followed by measuring the change in absorbance at 340 nm and 478 nm. The former value is suitable for determining the presence of titanium (IV), the latter for following any matrix effect that may occur.

2.7.2 Result

Figure 2.8 shows how an absorbance at the wavelengths stated changes for the unmasked titanium solution. It can be seen that over time the absorbance at 478 nm increases and then decreases.

2.7.3 Discussion

This change in absorbance is indicative of a mixed titanium (III)/(IV) complex being formed. In the early stages, the oxidation of titanium (III) induces an intervalence effect. This causes the increase in absorbance. After ten hours, the amount of the mixed complex formed is dependent on the rate, which decreases as the concentration of the titanium (III) falls. The formation of titanium (IV) increases with time. This is shown by the increase in absorbance at 340 nm, indicative of titanium (IV) salts. Rate data were plotted to determine whether a relationship between the absorbance and time for the overall reaction could be resolved, however, no meaningful results were found. Since it may well involve a series of parallel and consecutive reactions, the kinetics seem complex.

2.8 Change of λ_{max} with temperature, boiling, and ligation

To investigate the solution chemistry of titanium (III) further, experiments were developed that investigated the changes in the uv/vis spectra as a function of various physical and chemical parameters.

2.8.1 Procedure

Titanium (III) sulfate (0.15 mol dm^{-3} Ti) was placed in a beaker and held at the required temperature, 25, 45 or 60°C, under nitrogen. The nitrogen supply was then stopped and air allowed to interact with the titanium (III) solution. Scanning from 700 to 340 nm followed the reaction.

The λ_{max} was noted and plotted against time as a function of temperature. The experiment was repeated, but with a two-fold dilution.

In separate experiments, sodium gluconate and sodium citrate were added, in a ratio of 1 mole of masking agent to 1 mole of titanium, to fresh titanium (III) solutions. They were dissolved at room temperature, under nitrogen, and then subjected to the procedure described above.

2.8.2 Results

The changes in λ_{max} are plotted in Figures 2.9a to f.

- No dilution: Figures 2.9 (a),(c) and (e) show qualitatively that there are changes in the complex as the temperature increases. First, an intervalence complex is formed with the λ_{max} shifting to about 480 nm. The loss of solution colour which follows is indicative of oxidation of titanium (III) and the intervalence complex. The data collection end when there is no further absorbance in the range likely to indicate titanium (III).
- 2x dilution: Figures 2.9 (b),(d) and (f) show that diluting the solution has the same effect, but shortens the time of complexation.

- Citrate ligation: The change in λ_{max} showed that some degree of ligation had occurred, figure 2.9(g), (h) and (i). Compared with the unmasked solution, the data may indicate that the citrate is stabilising the trivalent state. The complex structure was determined using esr and endor and the results are discussed in chapter 4.
- Gluconate ligation: Again the change in λ_{max} suggests masking, figure 2.9 (j), (k), (l). The effects are similar to that of the sodium citrate, with the ligand seemingly stabilising the titanium (III). In both cases the stability is reduced as the temperature increases.

The kinetic of the reactions were analysed by using Guggenheim plots, but no reaction rates could be determined because there is no simple correlation between the reaction time and the change in absorbance. Again, this suggests that the kinetics is complex.

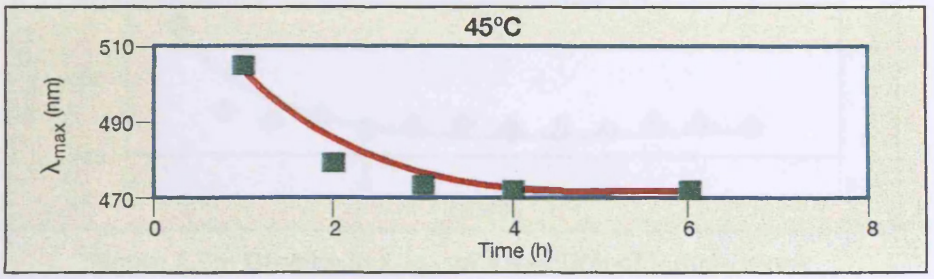

Figure 2.9c: Change in λ_{max} with time

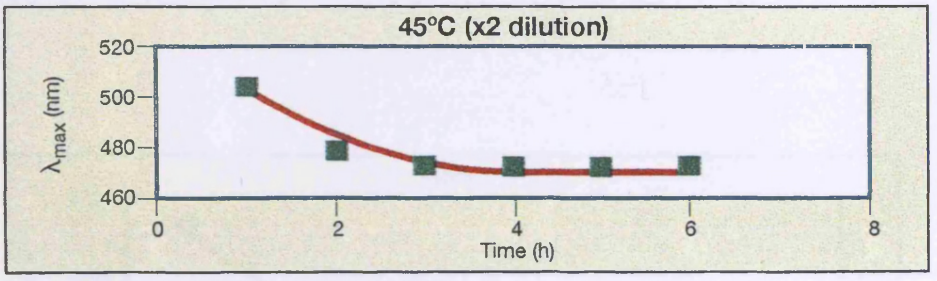

Figure 2.9d: Change in λ_{max} with time

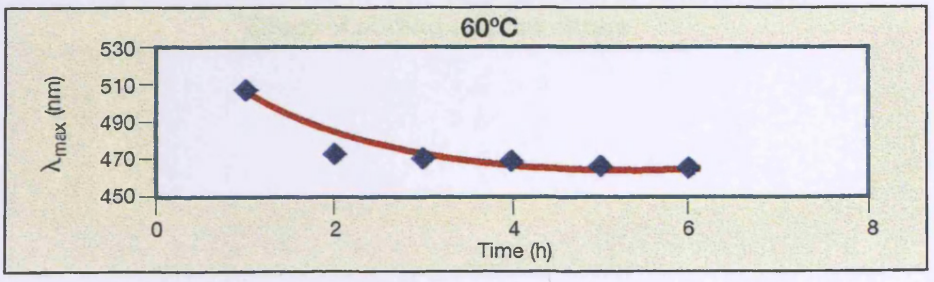

Figure 2.9e: Change in λ_{max} with time

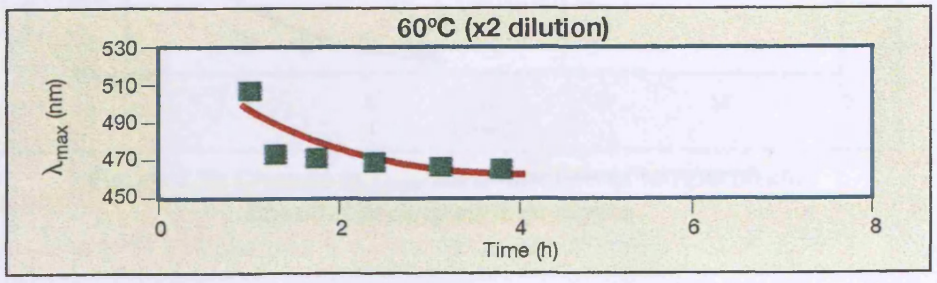

Figure 2.9f: Change in λ_{max} with time

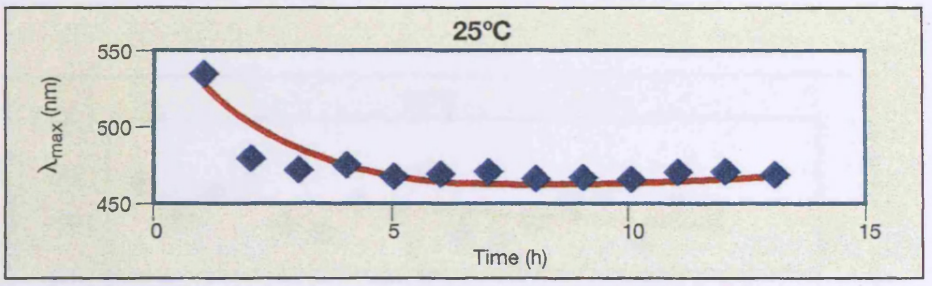

Figure 2.9g: Change in λ_{max} as a function of temperature: Effect of adding sodium citrate

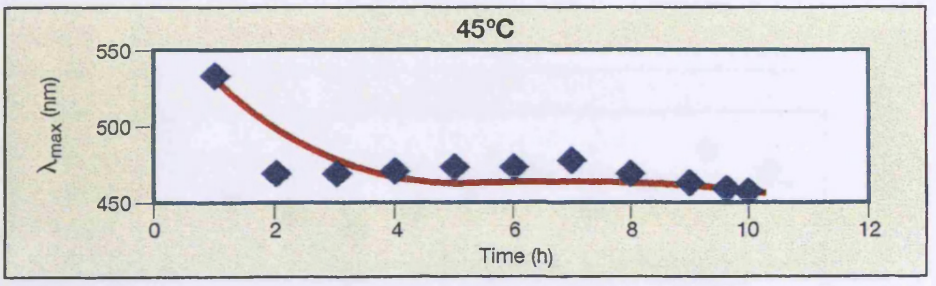

Figure 2.9h: Change in λ_{max} as a function of temperature: Effect of adding sodium citrate

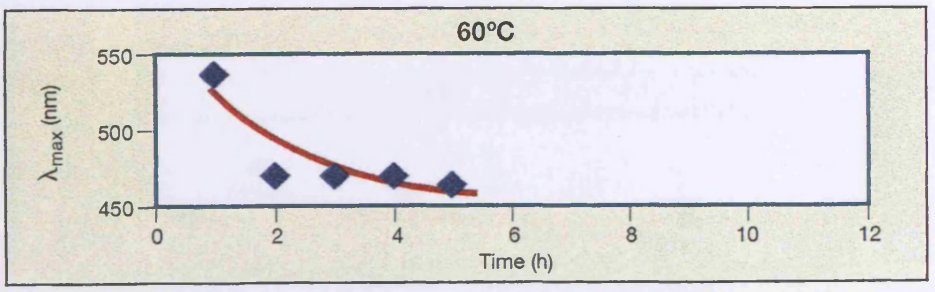

Figure 2.9i: Change in λ_{max} as a function of temperature: Effect of adding sodium citrate

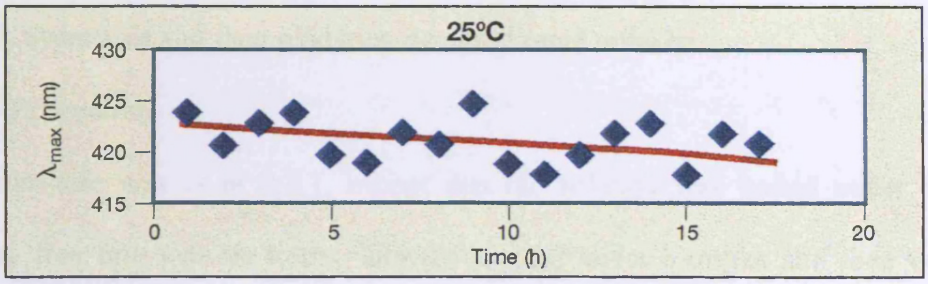

Figure 2.9k: Change in λ_{max} as a function of temperature: Effect of adding sodium gluconate

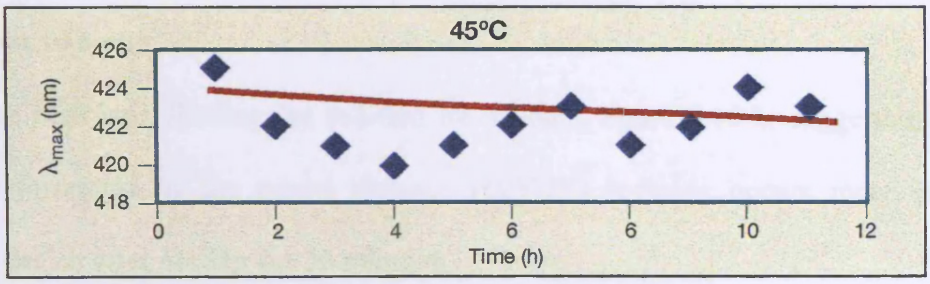

Figure 2.9j: Change in λ_{max} as a function of temperature: Effect of adding sodium gluconate

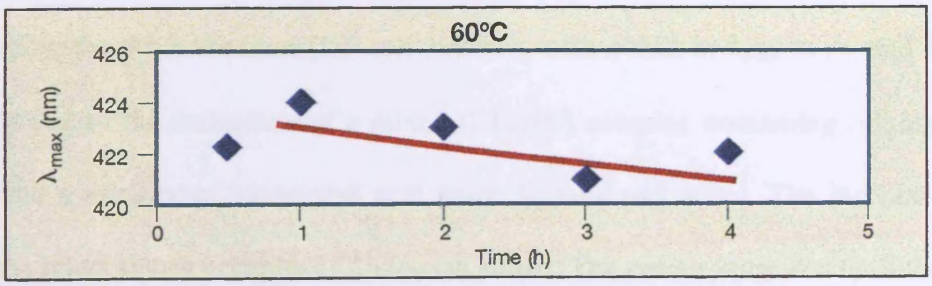

Figure 2.9l: Change in λ_{max} as a function of temperature: Effect of adding sodium gluconate

2.9 *Effect of boiling on the spectra*

The effect of boiling on the solution was investigated to determine whether interaction with the solvent, hydrolysis and then oxidation occurred more quickly.

2.9.1 Procedure

The procedure was as in 2.8.1, except that the solution was boiled under nitrogen for 30 minutes, four hours or six hours, allowed to cool under nitrogen and then the spectra were obtained in air until the absorbance was zero.

2.9.2 Results

The changes in λ_{max} are plotted in figures 2.10 a-c.

- 30 minute boil. Figure 2.10 a shows a shift in the λ_{max} from 511 nm, the expected wavelength for a hexa-aqua titanium (III) complex, towards the uv region. This occurs over about 10 hours.
- Four hour boil. Boiling the solution for 4 hours, figure 2.10 b, suggests qualitatively that the formation of the mixed titanium (III)/(IV) complex occurs more quickly than its formation after boiling for 30 minutes.
- Six hour boil. The effect on the λ_{max} of the titanium (III) solution of boiling for this length of time causes the hydrolysis reaction to occur much more quickly. The shift to higher energy radiation had happened before the testing in the spectrophotometer.

2.9.3 Discussion

The shape of the graphs from the previous experiments can be explained in the following way. On standing the fresh titanium (III) salt oxidises, with a shift in λ_{max} to around 480 nm. This is probably due to the formation of a mixed (III)/(IV) complex containing oligomers of Ti (III), Ti(IV) and a number of associated acid anion ligands and water. The increase in intensity is due to the intervalence complexes discussed above. The colour increases until the titanium (IV) formed is determined by the machine more readily than the Ti (III)/IV) complex. At this point

the colour gradually disappears. The degree of shift in λ_{max} is probably a result of the formation of sulfato/aquo complexes, analogous with titanium metal dissolved in hydrochloric acid as discussed by Gardner[17].

The effect of boiling is simply to speed up the hydrolysis process. Boiling for shorter periods of time, 30 minutes and four hours, seems to leave the $[Ti(H_2O)_6]^{3+}$ intact initially. Thus, the formation of the mixed complex can be assigned, qualitatively, as a function of the boiling time. Unfortunately, there seems to be no simple, direct relationship between the rate of complex formation and the change in absorption as a function of the time of boiling. The only observation is that there is an increase in the hydrolysis, noted by the change in absorption towards the ultra-violet, the longer the solution is boiled. Boiling the solution for six hours is a manifestation of this hydrolysis process. Once hydrolysis has started, oxidation is inevitable and, seemingly, irreversible.

Most likely, the associated colour changes are a result of complex consecutive and parallel reactions, but no quantitative data was obtained to confirm this.

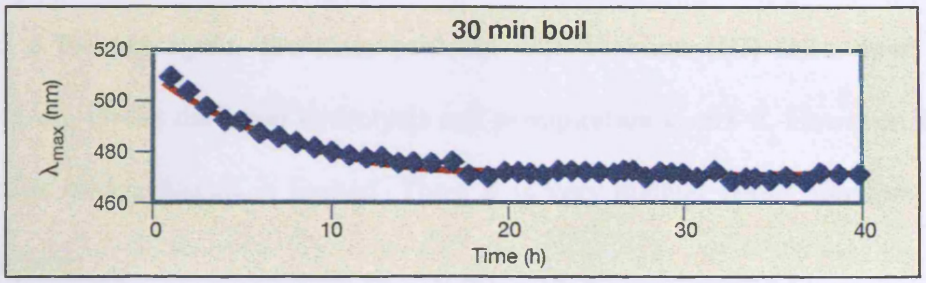

Figure 2.10a: Effect of varying the boiling time on the change in λ_{max}

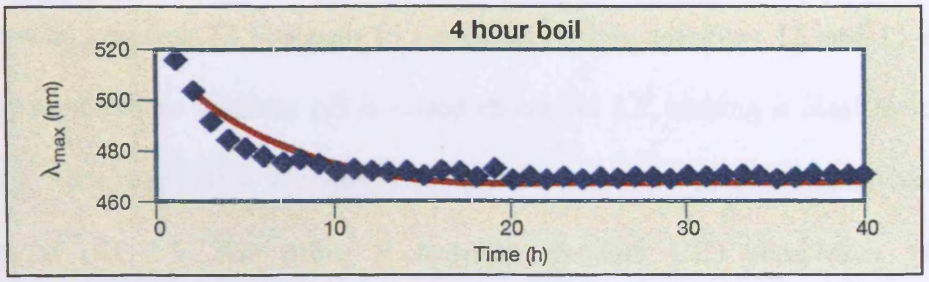

Figure 2.10b: Effect of varying the boiling time on the change in λ_{max}

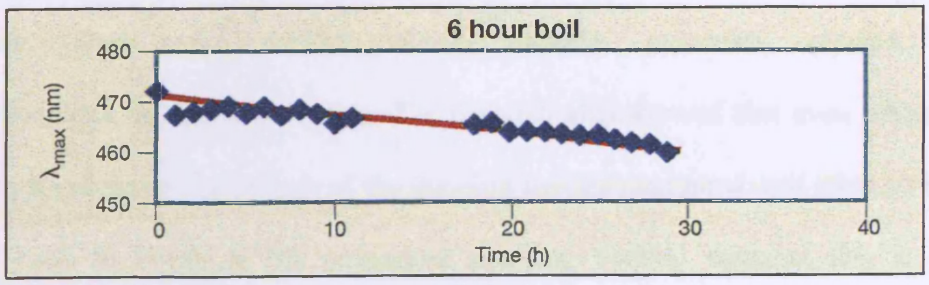

Figure 2.10c: Effect of varying the boiling time on the change in λ_{max}

2.10 Hydrolysis and olation

For use as a tanning agent, the main problem with titanium (III) salts, apart from their instability in air, lies in the rapid hydrolysis and precipitation at pH>2. However, below pH 2 the interaction with collagen is limited. Thus, it is very unclear which titanium species are involved tanning.

The primary hydrolysis reactions for titanium (III) salts, as for chromium (III) salts, are:

$$M_2(SO_4)_3 + 2H_2O \rightarrow 2M(OH)SO_4 + H_2SO_4 \quad (11)$$

$$2M(OH)SO_4 + 2H_2O \rightarrow [M(OH)_2]_2SO_4 + H_2SO_4 \quad (12)$$

$$[M(OH)_2]_2SO_4 + 2H_2O \rightarrow M(OH)_3 + H_2SO_4 \quad (13)$$

Where M = Cr (III) or Ti (III)

With chromium, reaction 11 proceeds to completion while reactions 12 and 13 do not take place to any great extent until the pH is raised above pH 3.5, making it ideal for crosslinking and tanning. However, with titanium (III) the reactions proceed simultaneously, and to completion, at pH 2.5. The result is hydrated titanium (III) complexes, of unknown composition.

2.11 Masking titanium (III) ions

2.11.1 Introduction

In a wide-ranging and thorough thesis, Swamy *et al.*[29] studied twenty-three ions that could possibly be used to mask titanium (IV) salts. They found that nine were suitable for further investigation. They were acetate, citrate, formate, gluconate, glycine, glycollate, hexametaphosphate, lactate and tartrate. The research also showed that even where there was masking, on standing the hydrolysis of the titanium species continued, and after 30 days the pH had fallen back to levels of the unmasked solution. Swamy suggests this is due to the hydrolysis reaction described in equations 11-13 and an oxolation reaction similar to that of

chromium (III) salts. The result was precipitation. Assuming that masking is a rate process, it seems that although complexation of titanium (IV) ions slows the hydrolysis, it is less effective than with chromium (III) salts.

Their work also showed that, generally, using ligands which contained hydroxy groups improved the stability of the titanium (IV) against precipitation longer than if the masking agents were simple organic acids. This was also noted by Celedes, who modified the collagen structure with compounds that contained hydroxy groups in an effort to improve the uptake of titanium (IV) salts.

The following titration experiments were carried out to determine the precipitation point of masked titanium (III) complexes. The aim was to raise the pH of precipitation to values that would allow titanium (III) complexes to successfully tan collagen.

2.11.2 Procedure

An aliquot of titanium (III) sulfate (0.15 mol dm^{-3}, 20 cm^3) was titrated with sodium hydroxide (0.956 mol dm^{-3}) every 30 seconds. Any changes in colour and precipitate were noted and the pH recorded. Complete precipitation was considered to have occurred when a black cross, drawn on piece of paper and placed underneath the conical flask, was obscured. Whether there was a precipitate or not the titration was continued until 20 cm^3 of alkali had been added. The solution was then either back titrated immediately with hydrochloric acid (1.004 mol dm^{-3}) or left for 24 hours before titrating with the acid.

The procedure was repeated with masked solutions (1 mole of masking agent to 1 mole of titanium).

2.11.3 Results

The results are shown in tables 2.7 and 2.8.

Table 2.7: Effect of titrating with alkali and then acid

Masking agent	Titration with alkali	Back titration immediately	Back titration after 24 hours
No masking	Precipitate at pH 2.8	Ti (IV) formed	-
Sodium gluconate	Opaque at pH 2-5. Precipitate then cleared at pH 12 to give orange/brown solution	Titrated back to Ti (III) solution, λ_{max} 505 nm	Formed a fine orange/brown precipitate overnight. On titrating this disappeared to leave a clear, colourless solution. Ti (IV)*
Sodium glycollate	Colour darkened and a fine precipitate was seen at pH 8.8	Precipitate redissolved to give Ti (III), λ_{max} 505 nm	Colour changed at pH 2.5 to grey and became cloudy at pH 1.1. On standing this redissolved to give a clear, colourless solution†
Sodium citrate	Colour changed to a deep blue on titrating	Titanium (III) solution restored, λ_{max} 505 nm.	Thick white curdy precipitate produced on standing. Redissolved to give clear, colourless solution at pH <2*
Sodium tartrate	Colour changed to green/brown	Titrated back to Ti (III), λ_{max} 505 nm	Colour changed from green/blue to a mustard yellow

Notes: * precipitate was a different colour
† redissolved precipitate left a faint pink solution, which turned colourless on standing
gluconate is $HO\text{-}CH_2\text{-}(CH_2OH)_4\text{-}COO\text{-}$
glycollate is hydroxyethanoate
citrate is trihydroxypropane-1,2,3-tricarboxylate
tartrate is dihydroxybutandioate

2.11.4 Discussion

The effect of titrating without a masking agent is to produce a black precipitate at pH 2.8. This turns white on standing overnight. The white colour probably indicates titanium (IV) salts. Immediate back titration with acid left a clear, colourless, solution, which may indicate Ti (IV) salts

The results also show that there is some ligand interaction with the titanium (III). Sodium tartrate seems to stabilise the titanium salt against oxidation to Ti (IV), even after standing for 24 hours. However, given that the other ligands do not stabilise the Ti (III) after 24 hours, indicated by the loss of λ_{max} at 505 nm, the colour change could be due to a complex of titanium (IV). ESR and ENDOR were used to elucidate the structures further and the results are discussed in chapter 4.

Table 2.8: pH values of titanium (III) salts titrated with alkali and acid

Masking agent	Alkali titration	immediate acid back titration	24 hour acid back titration
No masking	12.4	1.0	12.3 to 0.8
Sodium gluconate	12.3	1.3	12.3 to 1.2
Sodium glycollate	8.8	1.4	6.4 to 1.0
Sodium citrate	11.7	1.4	10.9 to 1.0
Sodium tartrate	9.3	1.0	7.3 to 1.0

All the initial pH values were less than pH 1.0

There seems to be some olation taking place with the ligated titanium (III) salts, at a rate faster than that seen for titanium (IV). Swamy, in his work, managed to stabilise the titanium (IV) solution for up to 15 days before precipitation.

The reactions, as explained earlier, are not discrete. The interesting result is with the addition of sodium glycollate, which produces a buffering effect, the pH only rising to 8.8, even though 20 cm^3 of alkali was added.

2.12 Additional masking agents

Given that Swamy found a limited number of simple ligands had a positive effect on stabilising titanium (IV) salts, it was decided to extend the range of masking agents used, to compare non-hydroxy acids with those used above.

2.12.1 Procedure

Aliquots of the titanium salt were diluted with acid to give a [Ti] = 0.06 mol dm^{-3} and different masking agents of 1, 2, 5 or 10 moles to 1 mole Ti were added. The solutions were refluxed

under nitrogen for 30 minutes to ensure dissolution and titration curves were determined by titrating aliquots with sodium hydroxide (0.9811 mol dm^{-3}, 15 cm^3) using Titralab 80, an automatic titrator from Radiometer Analytical SA, together with Tim Talk 8, a windows based software package. The ligands used are set out in table 2.9, which also shows the precipitation point of the complexes. The results are shown graphically in Figures 2.11a-f

Table 2.9: Effect of complexing salt on stability of titanium (III) salt

Complexing salt	Reaction with Ti (III)
None	Precipitation at pH2.2
Formate	Precipitate with all mole ratio at pH2-2.5
Acetate	Precipitate with all mole ratio at pH2-2.5
Propanoate	Precipitate with all mole ratio at pH2-2.5
Gluconate	No precipitate at mole ratio ≥ 2
Tartrate	No precipitate at mole ratio ≥ 5
Malonate	No precipitate at mole ratio ≥ 2
Citrate	No precipitate at mole ratio ≥ 2
Cinnamate	Salt precipitated on addition to Ti (III) solution
Maleate	No precipitate at mole ratio ≥ 2
Oxalate	Precipitate at 1 mol dm^{-3}, insoluble at other mole ratios

2.12.2 Results

Figures 2.11a to c show that the presence of formate, acetate and propanoate ligands had little effect on the precipitation point of the titanium. They all precipitated around pH 2.5, table 2.9.

2.12.3 Discussion

Even at high mole ratios of ligand to titanium the shape of the titration curve is little altered, and even where there is a change in shape, there is no effect on the precipitation point.

However, the addition of ligands containing hydroxyl groups (d-f) seems to have a positive effect on the stability of the Ti (III). The shapes of the titration curves alter, especially for the citrate and all the ligands increased the precipitation point of the salt, some to regions which may be useful for tanning. This was dependent on the mole ratio, with most of the hydroxy ligands not stabilising the titanium until at least 2 moles of ligand to 1 mole of titanium had

been used. Comparing them with the changes seen when chromium and aluminium are masked, suggests that the interaction is much more limited with titanium (III) salts. This work was presented at the IULTCS congress in Chennai.[30]

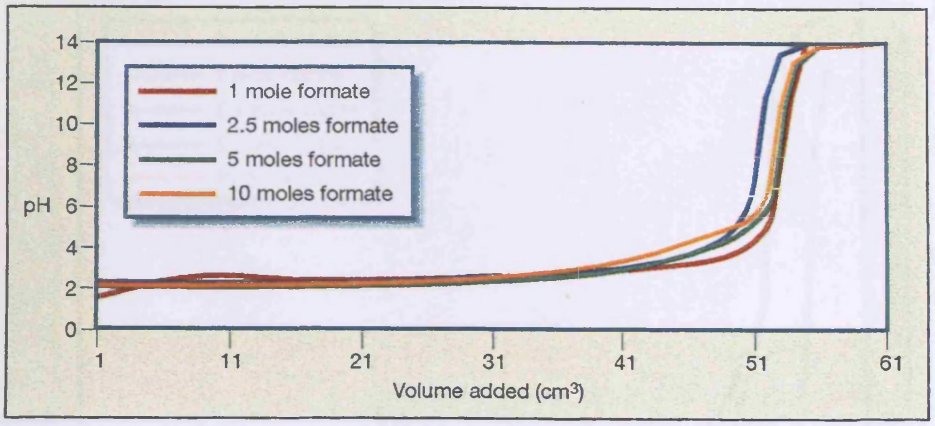

Figure 2.11a: Effect of masking titanium (III) with sodium formate

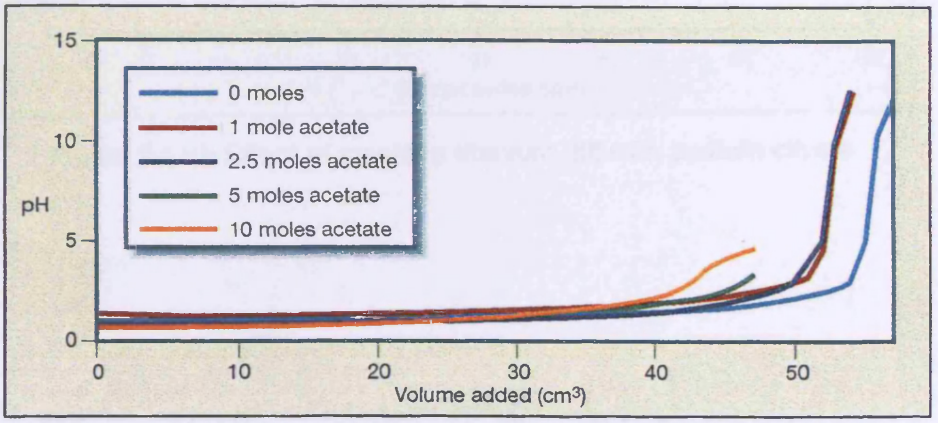

Figure 2.11b: Effect of masking titanium (III) with sodium acetate

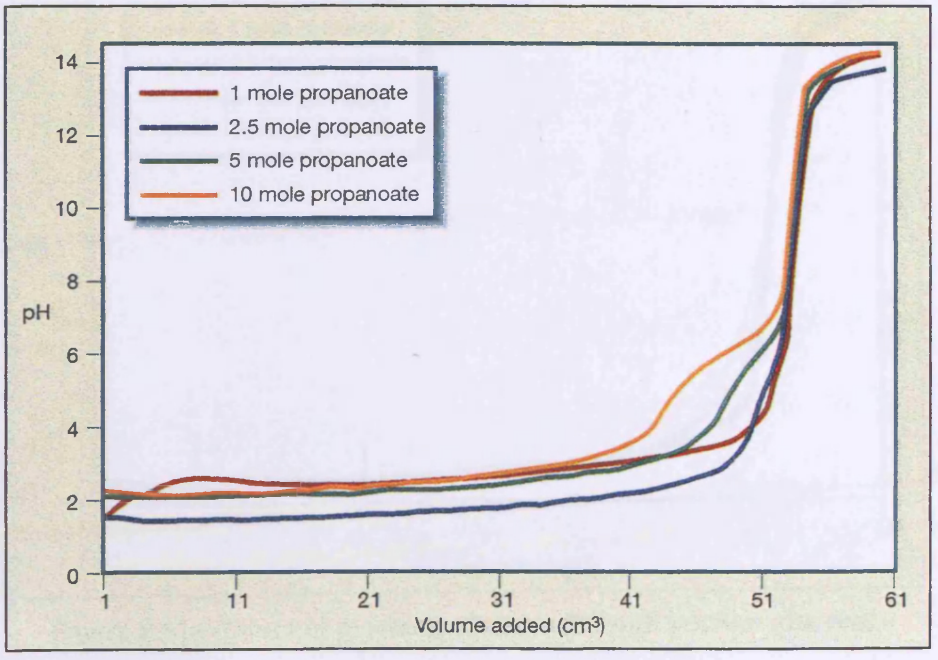

Figure 2.11c: Effect of masking titanium (III) with sodium propanoate

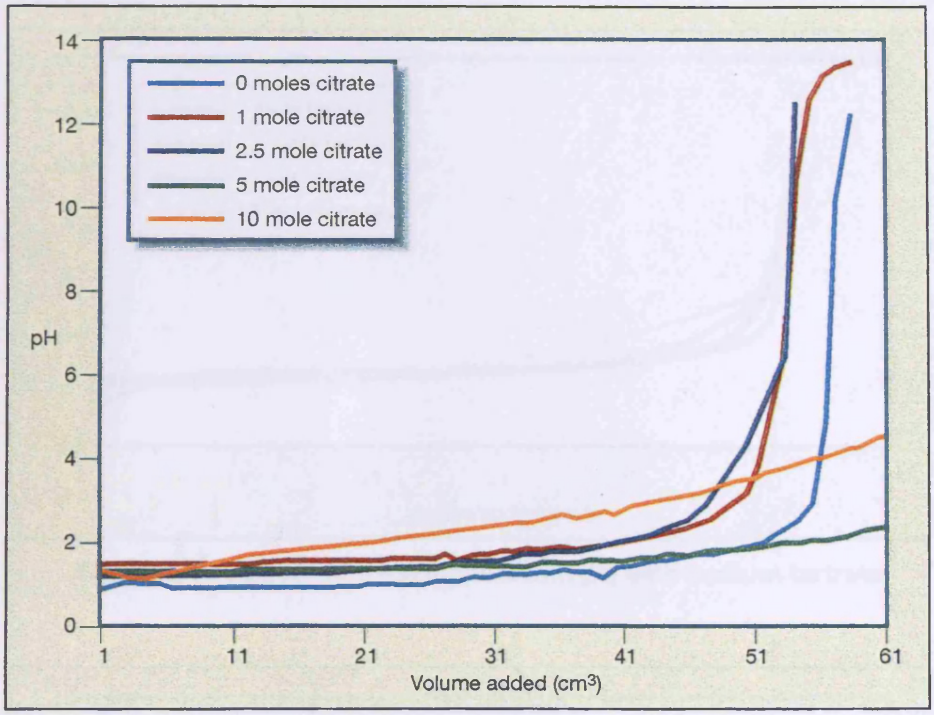

Figure 2.11d: Effect of masking titanium (III) with sodium citrate

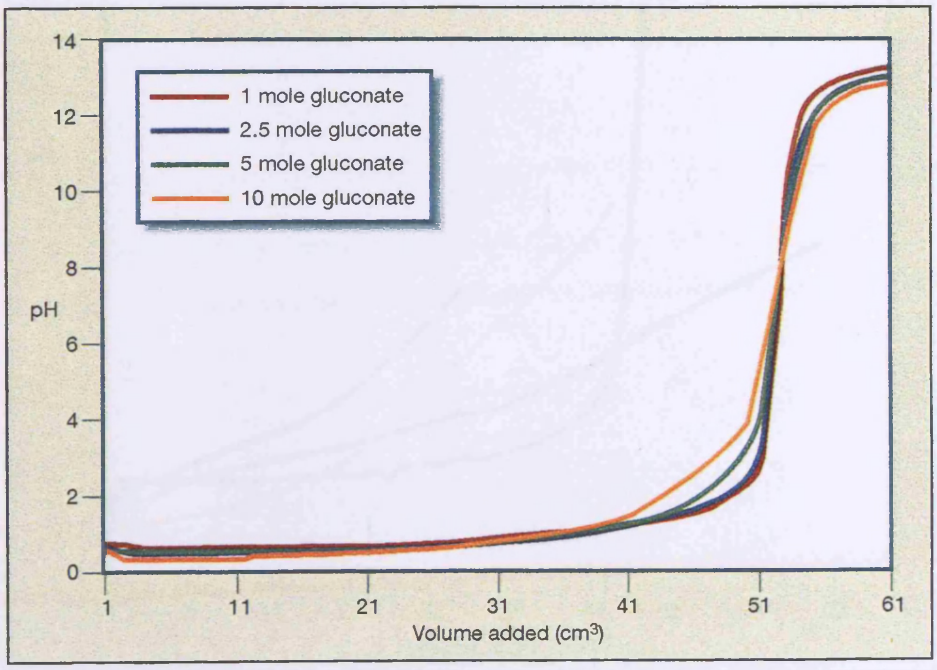

Figure 2.11e: Effect of masking titanium (III) with sodium gluconate

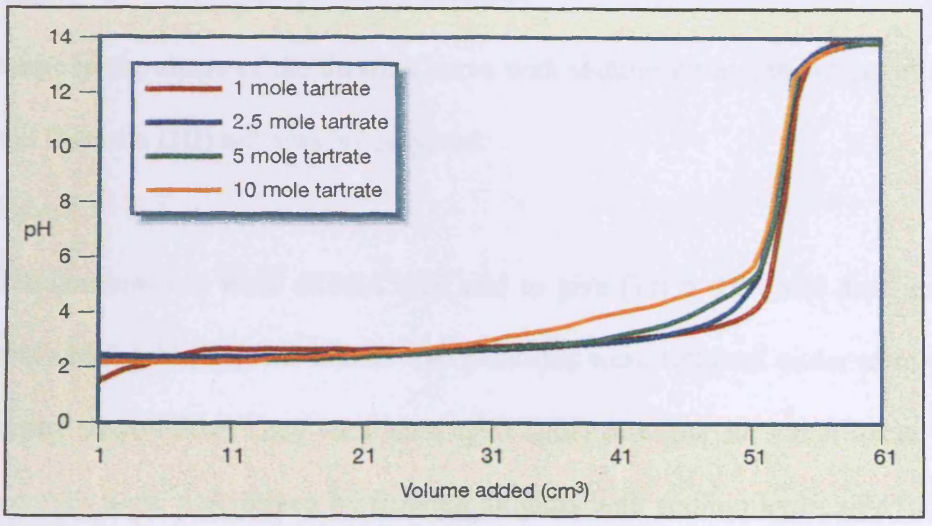

Figure 2.11f: Effect of masking titanium (III) with sodium tartrate

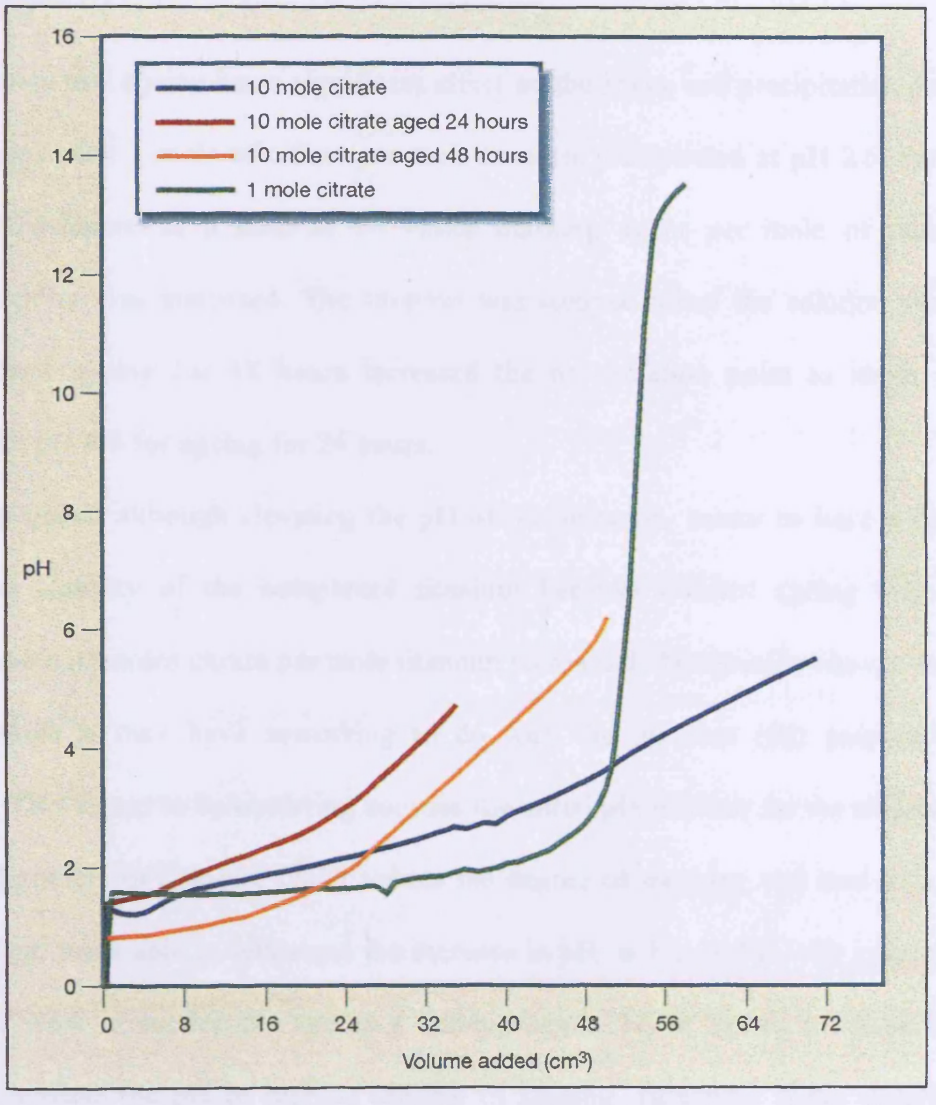

Figure 2.12: Effect of ageing on titration curve of titanium (III) sulfate masked with citrate

2.13 Ageing of titanium (III) masked salt

Given the change in the shape of the titration curve with sodium citrate, the effect of ageing on this complexed titanium (III) salt was investigated.

2.13.1 Procedure

Aliquots of the titanium salt were diluted with acid to give [Ti] = 0.06 Mol dm^{-3} and sodium citrate, 10 moles to 1 mole Ti, was added. The solutions were refluxed under nitrogen for 30 minutes to ensure dissolution. They were then aged under nitrogen for either 24 or 48 hours. The titration curves were determined by titrating aliquots with sodium hydroxide (0.9811 mol dm^{-3}, 15 cm^3) using the Radiometer Titralab 80 equipment described in section 2.12.1.

2.13.2 Results

Figure 12 shows that ageing has a significant effect on the shape and precipitation point of the ligated complex. The 1 mole of citrate per mole titanium precipitated at pH 2.6. But, as with the initial experiments at a ratio of 10 moles masking agent per mole of titanium, the precipitation point was increased. The titration was stopped when the solution was heavily precipitated and ageing for 48 hours increased the precipitation point to about 6.0. This compares with pH 4.8 for ageing for 24 hours.

The ageing process, although elevating the pH of precipitation, seems to have a detrimental effect on the stability of the complexed titanium because without ageing there was no precipitate when 10 moles citrate per mole titanium were used. The precise reasons for this are unclear although it may have something to do with the titanium (III) polymerising and hydrolysing. This seems to be occurring because the initial pH is lower for the aliquot aged for 48 hours. Oligomers of titanium could reduce the degree of masking and lead to a complex which, although more able to withstand the increase in pH, is less stable with respect to time. This may be what is needed for use as a tanning agent. There has to be some degree of stability, to increase the pH to regions capable of tanning. However, if the stability of the

complex is greater than the stability of the titanium/collagen complex, then there is no reason for the latter to form.

2.13.3 Discussion

Under nitrogen, as the titanium (III) complexes are formed there is a change in the wavelength and the precipitation point of the complex. However, when exposed to air the complexes are oxidised and oligomers of a mixed oxidation state are formed.

The addition of ligands to titanium (III) salts produces a stabilising effect. However, the rates at which olation and oxolation occur seem to be much faster than with titanium (IV) or chromium (III). Precipitation is seen after a few hours even with the citrate masked complex, which is faster than with either the equivalent titanium (IV) salts or chromium (III) salts. The reasons for this are related to the co-ordination of the complexes. Chromium (III) complexes are kinetically inert and covalent in nature. They are inner orbital complexes and so coordinate very well with the masking ligand and the collagen. Both titanium (III) and (IV) exhibit outer orbital coordination, are electrovalent in nature and, consequently, they are less stable with respect to the olation and oxolation reactions taking place.

On exposure to air the complexes formed are probably based on titanium (III)/(IV) mixed oxidation states and the limited stability they exhibit is a function of adding ligands in a mole ratio of greater than 2. It is likely that these mixed oxidation state complexes are formed in any tanning interaction. The addition of ligands containing hydroxy groups seems to have a positive effect on the stability of the titanium ion. Complexes of titanium (III) masked with sodium citrate, tartrate and gluconate were used in the subsequent tanning trials. These complexes were also examined in ESR studies.

2.13.4 Conclusion

The data collected in the experiments confirmed the initial observations that titanium (III) salts are unlikely to produce a tanning agent to rival chromium.

When titanium (III) and titanium (IV) ions interact they give rise to an intervalence complex. Because this effect can occur even when the solution is stored under nitrogen, the likehood of producing a complex for practical tanning purposes comprising of only titanium (III) moieties, is poor.

3 Tanning studies using transition metal salts

3.1 Introduction

The work set out in this chapter develops the use of titanium (III) as a tanning agent. In the first section, a method for determining the amount of titanium in the leather is discussed. The work then focuses on trying to stabilise the titanous ion at pH values that would allow a covalent, rather than electrostatic interaction, with collagen. In most cases the tannage was compared with titanium (IV) salts, usually potassium titanium oxalate. In some instances the tannage was compared with chromium, aluminium or another metal.

It was quickly realised that as a solo tannage titanium (III) offered no advantages over chromium or indeed titanium (IV). In fact, from the solution chemistry work, it is likely that the tanning species was titanium (IV) in all cases. Thus, the tanning work turned to comparing the metals in a semi-metal tannage. In these trials a range of metals was used, including lanthanides and other 'd' block transition metals. The results are used to further develop the theory of shrinking.

3.2 Determination of titanium in leather

Petroselli[31] commented that:

'Hydrogen peroxide reacts with titanium to produce a yellow/orange colour. The more intense the colour, the more titanium is present. Presumably, once the process has been established, this reaction could be used to determine the amount of titanium left in solution by using colorimetry.'

There is no official method for the determination of titanium in leather. Thus, one of the first aims of this research was to develop such a method.

Samples of leather were digested using the wet oxidation method for chromium analysis, SLC 8 [IUP/8][32]. A small amount of chromium (III) sulfate powder (ca 3 mg) was added to

determine when the oxidation process was complete. This addition converted the solution from a green colour to orange. It is necessary since the titanium solution is colourless and there is no visible colour change.

A method for determining the amount of titanium, using hydrogen peroxide, was then employed[33]. The solution was diluted to 250 cm^3. An aliquot was taken, to give a final solution containing 2-25 mg l^{-1} of titanium and 10 cm^3 of hydrogen peroxide (3%[v/v]) was added and diluted to 100 cm^3 with 1 mol dm^{-3} sulfuric acid. A blank of the reagents minus the hydrogen peroxide was used in the reference cell and the absorbance was measured at 410 nm[a].

3.2.1 Calibration curve

Potassium titanyl sulfate (3.68 g) was weighed into a Kjeldahl flask and to it was added ammonium sulfate (8 g) and sulfuric acid (100 cm^3, conc). The mixture was refluxed for 10 minutes. After cooling, the solution was poured into distilled water (750 cm^3) and diluted to 1 dm^3. The concentration of the titanium is 0.5 mg cm^{-1}. The graph is shown in figure 3.1.

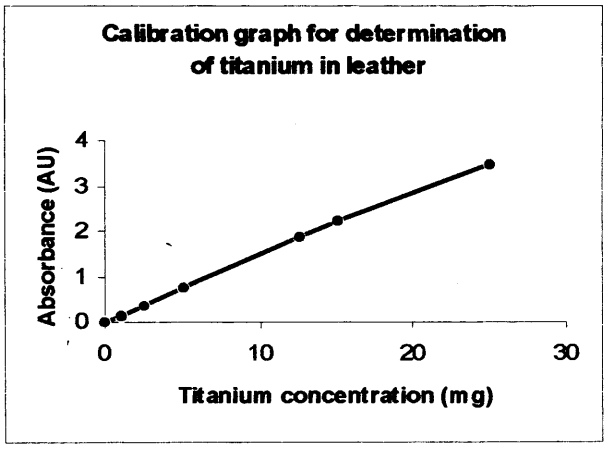

Figure 3.1: **Determination of titanium (III) in solution**

The molarity of the titanium (III) solutions was determined using the following method. 5 cm^3 of phosphoric acid was added to an aliquot of the titanium (III) solution, which was titrated

[a] Peng Biyu[37] *et al* developed a similar method, although they were developed separately.

with potassium dichromate (0.0167 mol dm^{-3}) and the end point was noted by observing the colour change with barium diphenylamine sulfonate indicator.

3.3 Tanning with titanium (III) sulfate

The titanium (III) salt used in these experiments was produced using the method set out in section 2.3.1. The following experiments were carried out to determine the parameters of titanium (III) tannage. All experiments were carried out in a water bath under a flow of nitrogen to reduce the amount of air getting to the solution.

3.3.1 Effect of titanium offer on the shrinkage temperature of pickled pelt

The offer of titanium salt, added to depickled pelt at pH 4, was varied to determine the optimum shrinkage temperature achievable. The process is set out in appendix 1.

3.3.1.1 Results

The leathers produced were white and the shrinkage temperature was measured using SLP18. The results are shown in table 3.1.

Table 3.1: Effect of Ti offer on shrinkage temperature

% offered	0.5	1.0	2.5	5.0
Ts/°C	66 ± 2	64 ± 1	74 ± 3	79 ± 2

errors are standard deviations

3.3.1.2 Discussion

While the actual values are unremarkable, they do show that as the amount of titanium offered increases the shrinkage temperature increases. This suggests there is some positive interaction with the collagen. However, a 4.5% increase in the amount of titanium offered results in only a 16°C increase in temperature. It would seem that the effect of adding titanium is to increase the stability of the collagen structure via non-specific crosslinking interactions, similar to vegetable tannin rather than chromium (III) tannage.

3.3.2 Effect of temperature

The experiment was repeated at two higher temperatures to see if there was an effect due to a change in temperature. The tannage is shown in appendix 1.

3.3.2.1 Results

The results are shown in table 3.2.

Table 3.2: Effect of bath temperature on shrinkage temperature of titanium leathers

% offered	0.5	1.0	2.5	5.0
Ts_{20}/°C	62 ± 2	67 ± 1	71 ± 2	80 ± 2
Ts_{25}/°C	66 ± 2	64 ± 1	74 ± 3	79 ± 2
Ts_{30}/°C	-	63 ± 1	74 ± 1	77 ± 3

errors are standard deviations

3.3.2.2 Discussion

There is no discernible pattern in the shrinkage temperatures as a function of the temperature of the processing bath. Shrinkage temperatures for the lowest percentage of titanium (III) sulfate added could not be measured, as the samples showed signs of gelatinisation. This may be a function of the low pH of processing and the temperature. The interaction with the collagen probably does not occur to any great extent until basification takes place. Hence the effect of heating the processing bath during tannage is negated.

3.3.3 Effect of heating the bath on the Ts of pickled pelt

In chromium (III) tannages the temperature of the bath during tanning is important. Covington[34] showed that to achieve the optimum shrinkage temperature the tanning bath should be heated at the end of processing. The process set out in appendix 1 was repeated. However, the titanium was added as titanium (III) sulfate on the pickled weight, and processed for 3 hours at 25°C. The temperature was then increased to 35°C for 2 hours and basified with sodium bicarbonate to pH 4 over 2 hours. The leathers produced were again white and the shrinkage temperature was measured as before. The results are shown in table 3.3.

Table 3.3: Effect of heating the bath at the end of tannage

% offered	0.5	1.0	2.5	5.0
Ts/°C	67	70	72	75

3.3.3.1 Discussion

There was little effect in increasing the temperature at which the tannage was carried out. If anything, the results are slightly lower than in the first trial, table 3.1. This may be due to the titanium complex hydrolysing when the heat is applied.

3.3.4 Role of the basifying agent

Rusakova[35] showed that the basifying agent was an important factor in attaining hydrothermally stable leather. The results of his work suggest that by using hexamethylenetetramine (HMT) the stability of the titanium tanned leather could be increased by up to 10°C compared with other basification systems, table 3.4

Table 3.4: Effect of basifying regime on stability of titanium (IV) tanned leathers

Basifying agent	Phthalate	Glutarate	Tartrate	Average Ts/°C
HMT	83 ± 3	82 ± 2	79 ± 4	**81 ± 3**
MgO	78 ± 2	72 ± 1	69 ± 1	**73 ± 4**
NH_4OH	74 ± 1	71 ± 3	71 ± 2	**72 ± 2**
Average Ts/°C	**78 ± 4**	**75 ± 5**	**73 ± 4**	**75 ± 3**

Errors are standard deviations

3.3.4.1 Discussion

The effect compared with magnesium oxide or ammonia shows an enhanced effect. It also highlights how well the HMT works as a basifying agent compared with the sodium bicarbonate basification carried out in section 3.3.2.

3.3.5 Effect of HMT concentration on the hydrothermal stability of the tannage

To determine whether the effects of HMT would be beneficial to titanium (III) tannages, the amount of HMT added in basifying was varied to determine the optimum conditions to achieve hydrothermally stable leather. The process is set out in appendix 1.

3.3.5.1 Results

The results are given in table 3.5.

Samples of the leathers were then split into three layers and a stratographic analysis of the titanium in each layer determined using the new procedure presented in section 3.2. Table 3.6 shows the percentage of titanium in the grain, middle and flesh layers of samples from each concentration of HMT used.

Table 3.5: Effect of HMT concentration on Ts of Ti(III) leathers

% HMT	0	1	2	5	10
Ts /°C	74 ± 2	76 ± 1	85 ± 1	88 ± 2	86 ± 1

Errors are standard deviation
HMT = hexamethylenetetramine

Table 3.6: Distribution of titanium in leather

% titanium in each layer					
	% HMT used to basify sample				
Layer	*0*	*1*	*2*	*5*	*10*
Grain	30	34	29	35	33
Middle	20	23	23	24	25
Flesh	50	43	48	41	42
Uptake	**65**	**67**	**73**	**78**	**68**

Uptake of titanium determined as a percentage of the total added.
The amount of titanium in each layer is a percentage of the total in the leather.

3.3.5.2 Discussion

The maximum effect of the HMT seems to be around 5% of the compound on the pickled weight. The majority of the titanium seems to be on the flesh and grain surfaces. This may be due to basifying the samples too quickly, or it may be a function of the polymerisation of the tannage, reducing the ability to penetrate the skin. The results show that, compared with the sample which was not basified with HMT (0 in the table), the HMT distributes the titanium through the cross-section more evenly. This is reflected in the increase in shrinkage temperature compared with the non HMT basified tannage.

3.4 Conclusion

As a single tanning agent it seems that titanium (III) has limited use, so the work moved to investigating ways that the tanning salt could be stabilised sufficiently to increase the pH into the range 3-4. This would allow a better interaction with the aspartic and glutamic acids on the collagen. One of the methods used to increase the precipitation point is to add ligands to mask the tanning salt.

3.5 Role of masking in stabilising the titanium ion

3.5.1 Introduction

Masking changes the reactivity of the tanning complex for the collagen. The masked complexes are less cationic and this acts to reduce the astringency of the tannage, increase the penetration through the substrate and give a more even distribution of the salt.

The effects of adding masking agents are seen to advantage with iron tannages. Using iron (II) sulfate, the solo tannage leaves the leather over tanned on the surface. If tartaric acid is added as a masking agent, the reactivity is reduced and the leathers are tight with a fine grain. With the addition of suitable syntans and fatliquors, the handle becomes rounded and soft and the leather is usable[36].

Secondly, ligating the tanning salt can be used to increase the precipitation point of that salt. With chromium, the addition of almost any organic acid will result in masking and an increase in the precipitation point of the tanning salt. This, however, proved not to be the case with titanium (III). As was seen in chapter 2, the use of ligands containing a large number of hydroxyl groups raised the precipitation point of the titanium salt. Some of these were used in the tanning studies.

3.5.2 Effect of masking agents on the shrinkage temperature of pickled sheepskin

3.5.2.1 Background

Celades[37] showed that by increasing the number of hydroxyl groups on a substrate the uptake of titanium (IV) could be significantly improved. In order to increase and modify the affinity of the titanium, he determined the most suitable active groups with respect to the substrate. The substrates used are shown in table 3.7:

Table 3.7: Substrate affinity for titanium salts

	Composition	Reactivity
Pickled pelt	Collagenic protein	reference
Wool	Collagen without hydroxyproline and with disulfide bridges	without hydroxy groups
Cotton	Polysaccharides	hydroxyl groups
Nylon	Polyamide	peptide groups
Acrylic fibre	Polyacrylonitrile	cyano groups

The absorption and fixation of the titanium salt is shown in table 3.8.

Table 3.8: Uptake and fixation of titanium as a function of the substrate

	Ti absorption(%)[‡]	Ti fixation(%)[‡]
Pickled Pelt	90	90
Wool	72	16
Cotton	77	45
Nylon	72	12
Acrylic fibre	75	30

[‡] at pH 2.5

The importance of the hydroxyl groups in fixation is indicated by the results obtained for cotton (45%) and for wool (16%). The low percentage for wool is attributed to the fact that wool lacks hydroxyl groups. It suggests that titanium has a propensity for OH^- groups.

Peng[38] has also shown the effectiveness of coordinating titanium ions with hydroxy groups. He developed tanning systems using titanium (IV) masked with citrate, sulfosalicylate, tartrate and 'HPZ', a multi-coordinating syntan, and produced leathers with shrinkage temperatures of 100-102°C. The leather produced was soft and supple and of an 'acceptable quality'.

Rusakova showed that the influence of phthalate and glutarate was important in increasing the hydrothermal stability of titanium (IV) leathers and Swamy[39] used citrate, tartrate and lactate to mask ammonium titanium (IV) sulfate successfully. He measured the stratigraphic distribution of the titanium in leathers tanned with these masked solutions and found that citrate produced the most even distribution.

3.5.2.2 Effect of masked titanium (III) salts on the hydrothermal stability of collagen

This experiment makes comparisons between the masking agents and the effects they have on the shrinkage temperature of the pickled skin. The work also compared titanium (IV) with titanium (III). The tannage is set out in appendix 1.3.

3.5.2.3 Results

The shrinkage temperature was measured using the method set out in SLP18 and the results are shown in table 3.9.

Table 3.9: Effect of masking agent on hydrothermal stability of titanium tanned leathers

	Ts /°C	
Masking agent	*Ti (III)*	*Ti (IV)*
None	72	75
Citrate	81	83
Gluconate	81	80
Tartrate	84	82

3.5.2.4 Discussion

Under the conditions used, the shrinkage temperatures are similar for the titanium salts. The crusted leathers are cream coloured and have a firm handle. Initially, however, the titanium (III) leathers were blue/grey in colour, with the change in colour to cream taking place overnight. This would be consistent with oxidation to titanium (IV). On the results of this trial there is no advantage to using titanium (III). The average shrinkage temperatures [Ti (III) = 79.5 ± 4.5°C compared with the Ti (IV) = 80 ± 3.5°C] are the same. However, there is an

advantage to masking the titanium (III) with the ligands used, the shrinkage temperature increases by about 10°C for the titanium (III) salt compared with 6°C for titanium (IV).

3.5.3 Effect of masking agents and HMT on the hydrothermal stability of Ti (III) leathers

Although the results did not show that masking significantly improved the stability of a titanium (III) tannage, it was decided to investigate titanium (III) tannage by using the best masking agent, sodium citrate and the optimum amount of hexamethylenetetramine. The conditions of tannage are set out in appendix 1.

3.5.3.1 Results

The results are set out in table 3.10.

Table 3.10: Effect of masking agents on the stability of Ti(III) leathers

Masking agent	None	Citrate	Maleate	Fumarate
Ts/°C	84	91	88	90

3.5.3.2 Discussion

The results proved inconclusive, other than to confirm that adding sodium citrate, together with HMT, improved the hydrothermal stability of the leathers. The addition of HMT alone increases the shrinkage temperature from around the middle 70s to the middle 80s. This reflects some 'masking' by the HMT ligand.

3.6 Effect of geometric isomers on the shrinkage temperature

The effect of sodium fumarate and sodium maleate was investigated because Francke[40] has shown that maleate, the trans and hence crosslinking isomer, positively influences the stability of chromium tanned leathers. He also showed that fumarate, the cis isomer, did not increase the hydrothermal stability presumably because it chelates and is unable to crosslink. There does seem to be an effect, table 3.10, caused by the addition of a crosslinking ligand compared with

a chelating ligand, but given that method states results are ± 2°C, this is not statistically significant.

3.7 Effect of pretanning on the hydrothermal stability of titanium (III) tanned skins

Celades[36] produced leathers with a higher shrinkage temperature after he had treated sheepskin with oxidised starch. Using this idea, the uptake of titanium (III) and titanium (IV) was investigated as a function of the effect of pretannage. The syntans used are given in table 3.11a and the process is set out in appendix 1.

Table 3.11a: Syntans used in the experiment

Syntan	Type
None	-
Paramel SMC	Styrene/maleic acid
Relugan GTW	Glutaraldehyde
-	5-sulfosalcylic acid
Paramel PA	Sodium polyacrylate
Retingan R5	Aryl sulfonic/dicyanamide
-	Starch
Neosyn BS3	Naphthalene based syntan

The samples were wetted back in water overnight and the shrinkage temperature was measured following SLP 18.

The samples were analysed for titanium content and the leathers were subjected to various physical tests. Analysis of variance, ANOVA, was carried out on results from each test, including the construction of 95% confidence intervals. Full statistical results are shown in appendix 2.

3.8 Analysis of the results

The results are set out in tables 3.11b to 3.11g.

3.8.1 Shrinkage temperature

Table 3.11b shows the results for titanium (III) tanned leathers, while table 3.11c shows the results for titanium (IV). Table 3.11d compares the change in shrinkage temperature between the pretanned stock and the tanned leathers. In this case it was found that there were no significant differences in shrinkage temperature as a function of the titanium oxidation state ($p = 0.018$). However, there were found to be significant differences between the samples as a function of pretannage. Column 7 of table 3.11d shows that adding titanium (III) salts generally increases the shrinkage temperature of the pretanned skins more than adding Ti(IV). The exception is with the glutaraldehyde sample where shrinkage values fell by 14°C for Ti(III) and 7°C for Ti(IV). This was probably due to the low pH of the initial tannage using titanium salts, breaking down the dialdehyde. Then, on basifying, the glutaraldehyde was unable to recombine to the same extent. The increase in the shrinkage temperature of the sample tanned with 5-sulfosalicylic acid and then retanned with titanium (III) is marked, especially when compared with titanium (IV). The actual value is not high, indeed it seems to be the titanium (IV) value that is low. However, there is no indication in the energy of shrinkage that the samples tested were damaged. The values are lower than with the other pretannages, but this is probably a function of the acidic nature of the pretannage and tannage disrupting the structure rather than previously damaged samples. The results can be recast, table 3.11e, to show whether there is a synergistic effect of the pretannage and titanium tannage. Again, the effect of the glutaraldehyde stands out. There is also an interesting result with the starch. It seems that although the starch increased the amount of titanium in the leather, table 3.11d, it had no synergistic effect on the shrinkage temperature. However, there is an interaction between the titanium and the starch because the energies of shrinkage for the starch pretanned samples are higher than the average value. But, this interaction does not seem to play a significant role in the hydrothermal stability of the leather.

There seems to be a positive influence on the shrinkage temperature from pretanning and then adding titanium (IV) compared with titanium (III). However, this is not statistically significant at the 95% confidence interval. The synergistic effects from adding the titanium (IV), 3.11f, seem greater than with titanium (III). In the case of a positive effect, that effect is greater, eg styrene + titanium (III) is +2 while with titanium (IV), the effect is +10. Conversely, the negative effects are less with titanium (IV) when compared with titanium (III), eg glutaraldehyde and starch. This may be a function of the acidity of the titanium (III) tannage. Perhaps, initially, the pretannage was reversed and any subsequent effect is due as much to the interaction of a pretannage/titanium (III) 'complex' as it is to the titanium (III) attaching itself to a modified collagen structure. Unfortunately, this 'complex' interaction is not as powerful as an interaction to modified collagen.

The milder conditions of the titanium (IV) tannage meant that the pretannage, which had reacted with the collagen, remained intact, allowing the titanium (IV) to bind with it there. This argument could explain the effect of the glutaraldehyde, where with titanium (III) there is a significant loss in hydrothermal stability. The titanous ions then combine with the glutaraldehyde in solution before being deposited on the collagen during basification or, the glutaraldehyde is simply lost in the effluent and the lower result is due to there being less aldehyde in the leather. With titanium (IV) these effects are reduced because the pH is higher.

Table 3.11b: Physical test results for leather with different pretanning agents, Ti(III)

Titanium (III) Pretanning agent	Average Thickness (mm)	Tear Strength (N/mm)	Grain Crack (mm)	Burst kgf/mm	Ts (°C)	Energy of Shrinking (J/g)
None	1.22	63.7	9.6	2.6	74	37.6
Styrene/maleic acid	1.54	43.5	7.3	2.7	81	32.3
Glutaraldehyde	1.54	47.0	7.3	3.5	75	27.4
5-sulfosalicylic acid	1.28	56.3	8.1	3.3	74	12.7
Sodium polyacrylate	1.71	45.3	7.6	2.8	79	13.3
Aryl sulfonic/dicyanamide	1.40	44.5	6.8	3.2	74	13.1
Starch	1.48	48.2	8.2	2.8	71	39.4
Naphthalene based syntan	1.50	60.5	8.3	3.5	75	26.4
Average value	**1.46**	**51.1**	**7.9**	**3.1**	**75**	**25.3**

Table 3.11c:Physical test results for leather with different pretanning agents, Ti(IV)

Titanium (IV) Pretanning agent	Average Thickness (mm)	Tear Strength (N/mm)	Grain Crack (mm)	Burst Kgf/mm	Ts (°C)	Energy of shrinking (J/g)
None	1.03	105.3	8.9	2.9	66	21.1
Styrene/maleic acid	1.27	55.7	8.5	2.6	81	20.4
Glutaraldehyde	0.98	80.8	7.7	2.8	82	25.3
5-sulfosalicylic acid	1.18	72.3	7.4	3.8	61	15.9
Sodium polyacrylate	1.39	55.0	6.4	3.0	76	27.3
Aryl sulfonic/dicyanamide	1.06	59.0	6.7	2.8	73	28.9
Starch	0.78	83.1	9.2	2.9	66	37.5
Naphthalene based syntan	0.80	64.0	7.4	2.9	71	20.4
Average value	**1.06**	**71.8**	**7.8**	**3.0**	**72**	**24.6**

Table 3.11d: Functional group affinity for Ti salts, Ts (°C)

Pretanning agent	Pretan	Ti(III)	$diff_1$	Ti(IV)	$diff_2$	δ diff	%Ti(III)	%Ti(IV)
None	58	74	16	66	8	8	4.22	2.20
Styrene/maleic acid	63	81	18	81	18	0	3.15	3.08
Glutaraldehyde	89	75	-14	82	-7	-7	4.00	3.08
5-sulfosalicylic acid	52	74	23	61	11	12	2.81	2.24
Sodium polyacrylate	60	79	19	76	16	3	4.25	4.14
Aryl sulfonic acid/dicyanamide	63	74	11	73	10	1	3.05	3.76
Starch	65	71	6	66	1	5	4.36	3.14
Naphthalene based syntan	67	75	9	71	4	5	3.36	4.16
Average	**64**	**75**	**11**	**72**	**8**	**3**	**3.65**	**3.23**

δ diff = $diff_1 - diff_2$

Table 3.11e: Effect of pretannage and Ti^{III} interaction on shrinkage temperature of pelt

Pretannage	Pretan ΔTs /°C	Metal +Pretan $\Delta Ts/°C_{(theory)}$	Metal +Pretan $\Delta Ts/°C_{(actual)}$	Difference /°C
Styrene/maleic acid	+ 5	+21	+23	+2
Gluraraldehyde	+31	+47	+17	-30
5-sulfosalicylic acid	-6	+10	+16	+6
Sodium polyacrylate	+2	+18	+21	+3
Aryl sulfonic acid/dicyanamide	+5	+21	+16	-5
Starch	+7	+23	+13	-10
Naphthalene based syntan	+9	+25	+17	-8

Shrinkage temperature of pickled pelt = 58°C
Metal alone increased Ts by 16°C

Table 3.11f: Effect of pretannage and Ti^{IV} interaction on shrinkage temperature of pelt

Pretannage	Pretan ΔTs /°C	Metal +Pretan $\Delta Ts/°C_{(theory)}$	Metal +Pretan $\Delta Ts/°C_{(actual)}$	Difference /°C
Styrene/maleic acid	+ 5	+13	+23	+10
Gluraraldehyde	+31	+39	+24	-15
5-sulfosalicylic acid	-6	+2	+3	+1
Sodium polyacrylate	+2	+10	+18	+8
Aryl sulfonic acid/dicyanamide	+5	+13	+15	+2
Starch	+7	+15	+8	-7
Naphthalene based syntan	+9	+17	+13	-4

Shrinkage temperature of pickled pelt = 58°C
Metal alone increased Ts by 8°C

Table 3.11g: Effect of pretannage on tear strength

Pretanning agent	Titanium (III) Tear Strength (N/mm)	Titanium (IV) Tear Strength (N/mm)	Average Tear Strength (N/mm)
None	63.6	105.2	**84.4**
Styrene/maleic acid	43.5	55.7	**49.3**
Glutaraldehyde	46.9	80.8	**63.9**
5-sulfosalicylic acid	56.3	72.3	**64.3**
Sodium polyacrylate	45.2	55.0	**50.1**
Aryl sulfonic acid/dicyanamide	44.5	59.0	**51.7**
Starch	48.1	83.1	**65.6**
Naphthalene based syntan	60.5	64.0	**62.3**
Average (J/g)	**51.1**	**71.8**	**61.5**

Table 3.11h: Effect of pretannage on thickness

Pretanning agent	Titanium (III) Thickness (mm)	Titanium (IV) Thickness (mm)	Average Thickness (mm)
None	1.22	1.03	**1.13**
Styrene/maleic acid	1.54	1.27	**1.41**
Glutaraldehyde	1.54	0.98	**1.26**
5-sulfosalicylic acid	1.28	1.18	**1.23**
Sodium polyacrylate	1.71	1.39	**1.55**
Aryl sulfonic acid/dicyanamide	1.40	1.06	**1.23**
Starch	1.48	0.78	**1.13**
Naphthalene based syntan	1.50	0.80	**1.15**
Average (mm)	**1.46**	**1.06**	**1.26**

3.8.2 Uptake of titanium

The naphthalene based syntan and the sodium polyacrylate produce the highest uptake of titanium, for both the (III) and the (IV), 3.11d. Overall, there is more titanium in the leathers tanned with titanium (III) than those tanned with titanium (IV). One reason for this could be that on initial contact with the titanium (III) salt, the pelt swelled, making the structure more open, and hence physically allowing more titanium to get into the pelt. This was then fixed in the subsequent basification. This hypothesis is borne out by the thickness values.

3.8.3 Tear strength

The tear strength, table 3.11g, is seen to be a function of the titanium tannage. The leathers tanned with titanium (III) are significantly weaker than those tanned with titanium (IV) ($p = 0.04$). This is probably also due to the acidic nature of the titanium (III) tannage. The initial pH of the reaction may well disrupt the fibre structure and weaken the leather subsequently produced. Also the filling nature of tannage will have an adverse effect of the tear strength.

Overall, the effects of the pretanning is to reduce the tear strength of the leathers, with those pretanned with styrene/maleic anhydride, sodium polyacrylate and the mixed aryl sulfonic acid/dicyanamide polymer being significantly weaker. This is in line with the general

understanding that tanning reduces the strength of collagen. This effect is also seen with the lastometer values.

3.8.4 Thickness

The titanium (III) leathers were significantly thicker than their titanium (IV) counterparts ($p = 0.001$), table 3.11h. As the tannage probably polymerises as well, the thickness would increase in a manner similar to that of vegetable tanning.

3.8.5 Discussion

Titanium(III) salts produce a white leather which, at maximum, has a Ts of about 90°C. This is comparable with other metal tannages such as titanium (IV) and zirconium (IV). However, it is not comparable with chromium (III). At pH values <3.0 the capacity of collagen to covalently bind metal salts through the acid groups is limited, thus reducing the likelihood of producing hydrothermally stable leather. This was borne out by the initial trials and the low shrinkage temperature values indicated no significant covalent interaction. From the chemistry discussed before it seems that a balance needs to be achieved between increasing the pH to allow for interaction with the collagen and the ionisation of the carboxy groups and the need to limit oligomerisation of the metal tanning ion. With titanium (III), excessive polymerisation above pH 2 is one of the factors that reduce the ability of the ion to produce high hydrothermally stable leather. The second factor is the precipitation point of the unmasked titanium (III) salt as discussed in chapter 2. Thus, in terms of tanning, with titanium (III) alone this compromise is probably unachievable simply because, unlike with chromium, there is no coincidence of pH, needed to stabilise suitable Ti(III) complexes, and chemical reactivity, which is required for the complexes to interact strongly with collagen.

3.9 *Effect of metal type on the physical and hydrothermal properties of semi-metal leathers*

3.9.1 Background

Vegetable tanning agents can be divided into two groups, hydrolysable and condensed tannins. There are structural differences between the two types and by reacting hydrolysable vegetable tannins (gallotannins or ellagitannins) with metal salts, leathers exhibiting high shrinkage temperatures, to match those obtained with chrome tannage, can be achieved. This can be viewed as extending the multiple interactions between the polyphenol molecules and collagen by creating a crosslinked but, more importantly, by reducing rotations within the protein matrix[41]. In this way, there is a positive effect on both the crystallinity and the effective cooperating unit, which leads to an increased hydrothermal stability.

The question of how the metal interacts with the vegetable tannin has led to a number of investigations. Slabbert[42] has studied the combination of mimosa tannage and aluminium sulfate retannage. He suggested that the aluminium ions are fixed to the already bound flavanoid units of the, in this case, mimosa via complexation. This was based on the work of Sykes, Hancock and Orszulik[43], who showed that aluminium complexes with mixed σ-phenolate and carboxylate groups. Slabbert suggested the binding occurs as in figure 3.2:

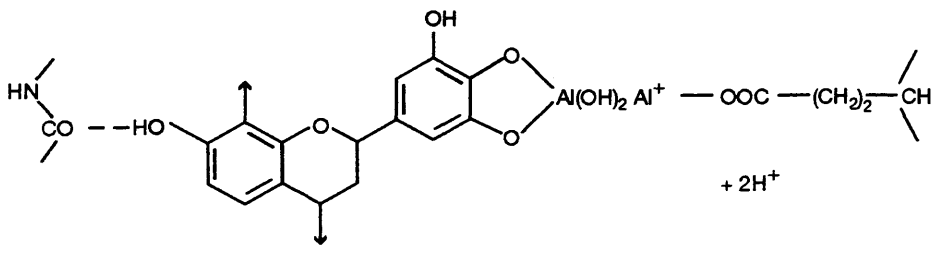

Mimosa-Al crosslink

Figure 3.2: Binding of metal and vegetable tannin

Kallenberger[44] set out to contradict the notion that any covalent or co-ordinate covalent ties to the collagen are formed by the tannin/aluminium treatment. To demonstrate the lack of importance of the protein/metal interaction in producing a very heat stable leather, he used metals that have little or no conventional tanning power.

The metals were chosen for their multivalent nature in the belief that there was a need to link the tannin into polymers to achieve stability. The commercial stock from which the samples were taken was a wet vegetable tanned hide from an American tannery. At that time tanners were using a blend of chestnut, wattle and quebracho. Most varied the mix depending upon price, so if quebracho was cheap, that was increased while higher priced components were cut. Generally, wattle and quebracho were the principal tannins with a little chestnut added for colour[45]. Thus, the effects were not optimised. Some of the results are set out in table 3.12.

Table 3.12: Shrinkage temperature of vegetable tanned grain split strips and pickled hide splits treated with metal salts

	Veg tanned strips	Pickled strips
Metal salt solution	**Ts/ °C**	**Ts /°C**
Sodium chloride + acid	86	62
Cobalt chloride	112	61
Manganese Acetate	91	58
Manganese (II) sulfate	90	56
Iron (III) chloride	101	57
Nickel sulfate	107	63
Nickel phosphate	105	68

Although the vegetable tannins are not identified, the valence states of the metals ions chosen not unequivocal and the offers used not stated, there are a number of general conclusions that can be drawn. Covington recast the results in terms of three interactions: metal collagen, metal veg tanned and metal veg tannin. These are shown in table 3.13.

Table 3.13: The collagen/vegetable tannin/metal ion system: 1st row transition metals[46]

Parameter	Changes in shrinkage temperature (°C)							
	$Mn^{(II)}$ Sulfate	$Mn^{(II)}$ Acetate	Δ	$Fe^{(III)}$ Chloride	$Co^{(II)}$ Chloride	$Ni^{(II)}$ Sulfate	$Ni^{(II)}$ phosphate	Δ
Metal – collagen interaction								
	-6	-4	+2	-5	-1	+1	+6	+5
Metal – vegetable tanned collagen interaction								
	+4	+5	+1	+15	+26	+21	+19	-2
Metal – vegetable tannin interaction								
	+10	+9	-1	+20	+27	+20	+13	-7

Δ = the effect of counterion with respect to sulfate

The data show that in most cases there is a powerful interaction due to the addition of the vegetable tanning agent into the system. Even with the manganese (II), which is not a known tanning agent as can be seen from effect of metal alone on the collagen stability, the effect of adding the vegetable tanning agent is to increase the shrinkage temperature by 10°C. With other metals the effect is more dramatic. The most interesting results are those for metal-vegetable tannin interaction. When the metal salts were used, the effect is the same for Fe(III), Ni(II) and Co(II), but smaller, although still marked, for manganese (II). The results do not necessarily show that Slabbert's model can be discounted because although the metal-vegetable tannin interaction is large it is not, in general, greater than the metal-veg tanned collagen interaction. Hence, the results are not inconsistent with Slabbert's postulate of a mixed crosslinking system as shown in figure 3.2.

In a review paper Covington[47] suggests that the synergistic interaction between the polyphenol and the aluminium may arise from one of the following options:

Collagen-Al-Veg-Al-Collagen

Collagen-Veg-Al-Veg-Collagen

Collagen-Veg-Al-Collagen

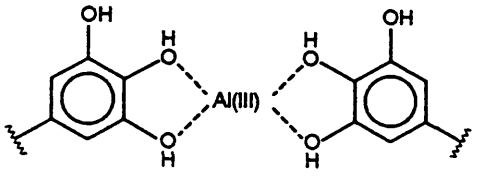

Figure 3.3: Crosslinking of polyphenol with aluminium (III)

He contends that since it is known that applying the metal salt before the vegetable tannin produces only moderate shrinkage temperature, the first and third options are unlikely. The metal is likely to crosslink the vegetable tannin, figure 3.3, and, in effect, the crosslinked polyphenol is itself crosslinked, to form a matrix within the collagen matrix. In other words the reaction appears to be dominated by polyphenol complexation. The collagen is then stabilised by a multiplicity of connected hydrogen bonds.

Table 3.14 lists some of the semi-metal tannages used by various researchers in an effort to achieve high hydrothermal stability.

Table 3.14: Effect of retanning on the initial shrinkage temperature of tannages

Tannage	Retannage	Ts_t °C	Ts_r °C	Difference °C
Vegetable	Methanal[48]	87	108	21
Vegetable	Cobalt	86	112	26
Vegetable	Manganese	86	94	8
Vegetable	Nickel	86	107	21
Vegetable	Iron	86	111	25
Vegetable	Aluminium[49]	76	117	41
PMA	Aluminium[50]	42	105	63
Titanium	Vegetable[51]	84	106	22

Ts_t = shrinkage temperature of first tannage
Ts_r = shrinkage temperature after retannage
Unless referenced, values are from Kallenberger & Hernandez[41]

Extending this further, there is an analogous reaction for condensed tannins, in which the flavanoid ring systems are crosslinked with oxazolidine to produce similar imposed structures, resulting in high shrinkage temperatures, > 110°C[52,53].

With the semi-metal tannages it is likely that the addition of a metal will make the leather more hydrophobic and as will be discussed in chapter 6 this is likely to have a positive effect on the shrinkage temperature.

3.9.2 Experimental work

A number of metals were used to determine their interaction with four types of vegetable tannins. The four vegetable tannins were myrabalams, sumach, quebracho and mimosa. The effect of vegetable tannin type is also investigated.

Thirty-two sheepskin flesh splits were cut down the backbone and divided into four groups of sixteen for vegetable tannage and eight groups of eight for metal tannage. The four groups were tanned with the vegetable tannages mentioned above according to the recipe set out in appendix 1.

As a comparison the isoelectronic vanadium (IV) was also used on a sample of mimosa tanned leather, using the same process as in appendix 1.

A series of physical tests was carried out on the leathers. The hydrothermal stability and the energy of shrinkage of the leathers, as well as the values for the vegetable tanned leathers were determined using differential scanning calorimetry [DSC]. The heating rate was 2°C/min and the average sample size 20 mg. The results are set out in tables 3.15 and 3.16.

Table 3.15: Physical parameters of semi-metal leathers

Metal	Shrinkage temperature (°C)	Energy of shrinkage (J/g)
Chromium (III)	101 ± 1	31± 3
Titanium (IV)	104 ± 1	22 ± 3
Titanium (III)	103 ± 1	27 ± 3
Aluminium (III)	95 ± 1	25 ± 2
Vanadium (IV)*	100	-

*with mimosa only

Table 3.16: Physical parameters of semi-metal leathers

Vegetable tannin	Type	Shrinkage temperature (°C)	Energy of shrinkage (J/g)
Mimosa	Hydrolysable	102 ± 0	27 ± 3
Quebracho	Hydrolysable	99 ± 1	24 ± 3
Myrabalams	Condensed	100 ± 1	25± 3
Sumach	Condensed	101 ± 1	29 ± 3

The results reveal that the Ti(III) tanned semi-metal leathers performed extremely well. The physical properties, table 3.17, show that the titanium (III) tanned leather is at least as good as the industry standard, semi-alum leather. The leather tanned with the different oxidation states of titanium developed the same colour. The orange colour of the leather is characteristic of titanium-oxy complexes, the best known being the reaction between acidic titanium (IV) salts and hydrogen peroxide. The colour suggests that a redox reaction, Ti(III) oxidation to Ti(IV), occurs. However, the physical properties of the Ti(III) leathers were usually better than that of Ti (IV), which suggests a different route to the same final complex[54].

Table 3.17: Physical properties of semi-metal leathers as a function of metal salt

Metal	Tear Strength (N/mm)	Tensile Strength (N/m^2) x 10^3	Softness (mm)	Thickness (mm)
Chromium (III)	65 ± 4	24 ± 1	7.7 ± 0.7	1.07 ± 0.13
Titanium (IV)	51 ± 5	21 ± 2	7.5 ± 0.5	1.07 ± 0.99
Titanium (III)	72 ± 4	23 ± 2	7.7 ± 1.1	1.06 ± 0.07
Aluminium (III)	76 ± 4	22 ± 1	7.9 ± 0.4	1.01 ± 0.19

Table 3.18: Physical properties of semi-metal leathers as a function of veg tannin

Vegetable tannin	Tear Strength (N/mm)	Tensile Strength (N/m^2) x 10^3	Softness (mm)	Thickness (mm)
Myrabalams	61 ± 4	22 ± 2	8.1 ± 0.7	1.08 ± 0.19
Mimosa	64 ± 4	22 ± 3	7.0 ± 0.7	1.08 ± 0.13
Quebracho	71 ± 5	24 ± 0	7.6 ± 0.4	1.03 ± 0.07
Sumach	69 ± 4	23 ± 2	8.1 ± 0.4	1.02 ± 0.07

3.9.3 Other semi-metal tannage processes

To further investigate the effects of metal on the hydrothermal stability of vegetable leathers, various metals were used to retan the leathers tanned with myrabalams or sumach. Initially, small samples of the vegetable tannages were retanned in petri dishes with different metals using 1% metal on the weight of the sample of vegetable tanned leather. The metals used, together with the pH and shrinkage temperatures recorded at different time intervals, are set out in table 3.19.

Table 3.19: Effect of metal on the shrinkage temperature of veg tanned leathers

Metal	$pH_{initial}^{(\pi)}$	pH_{24}	$Ts_{24(*)}$	pH_{96}	Ts_{96}	Ts_{720}	Solo $Ts^{(\psi)}$
None	-	-	-	-	-	-	61
Copper (II) sulfate	2.73	$3.45^{(\dagger)}$	81	3.32	78	-	67
Nickel (II) sulfate	3.79	$4.75^{(\dagger)}$	90	3.87	90	-	63
Zinc (II) sulfate	3.68	4.32	88	4.19	88	90	58
Iron (II) sulfate	2.25	3.10	100	2.75	100	-	59
Dysprosium (III) sulfate	3.08	4.59	91	4.85	92	-	50
Yttrium (III) sulfate	3.16	3.57	89	3.57	89	-	51
Ytterbium (III) sulfate	3.00	3.87	94	3.89	94	-	51
Lanthanum (III) sulfate	3.22	3.82	88	3.78	88	-	53
Titanium (III) sulfate	0.89	3.14	98	-	-	>100	74
Titanium (IV) sulfate	3.79	3.38	>100	-	-	94	79
Zirconium (IV) sulfate	1.54	2.11	91	-	-	-	77
Terbium (III/IV) peroxide	3.97	4.15	91	-	-	96	56
Cerium (IV) sulfate	2.26	3.24	89			-	-
Uranium (IV) sulfate	3.32	2.95	92	2.89	99	93	-
Vanadium (IV) sulfate	2.27	2.00	95	1.94	90	60	-
Aluminium (III) sulfate	2.46	3.45	89			94	-

(*) all samples basified to pH ~4 after one hour in solution
(†) pH of precipitation was about pH 7, thus basified to pH 7
(ψ) shrinkage temperature of solo tannage after 24 hours – basified to pH 4
(π) figures in subscript indicate the time in hours at which the measurement was made

3.1.4 Kinetic studies of the mechanism of shrinkage

It has been shown[55] that, except at low temperatures, and after a short period of induction, shrinking follows approximately an exponential function of time, expressed by the following equation.

$l_t = l_0 - l_\infty \exp(-kt) + l_\infty$

where l_t = length of sample at time, t

l_∞ = the initial length

l_∞ = length of sample at infinity, in this case when shrinkage had stopped

k = rate constant and t = time in seconds

A graph of ln (l_t -l_∞) verses t should yield a straight line of slope –k.

The readings were taken by noting the time the leather shrank past a graduation until no further measurable shrinkage. This was carried out at a constant temperature.

Some of the semi-metal tannage samples were subjected to measurement of the rate of reaction. This procedure followed that developed by Weir, and used the standard shrinkage apparatus, as set out in SLP 18, with a 0.5 cm graduated scale added to the arm holding the sample. The leather was held at the previously determined shrinkage temperature in the apparatus in a water bath and allowed to shrink. The first result was noted after 10 seconds, to allow for relaxation of the sample, when the dial was reset to vertical. The readings were taken by noting the time the leather shrank past a graduation until no further measurable shrinkage was noted. All the initial tannages were with mimosa unless stated. A graph of ln l_t verses t was plotted which should yield data about the rate constant, k. Guggenheim plots for various metals are shown in figures 3.5a to 3.5h and the rate constant data is given in table 3.20.

Table 3.20: Rate constant data

Metal	Rate constant (s^{-1}) x 10^{-2}	Ts (°C)
Aluminium	4.06	94
Cerium	5.44	89
Lanthanum	7.26	88
Uranium	2.02	93
Terbium	3.20	96
Zirconium	3.65	91
Titanium (III)$^{\omega}$	0.51	98
Vanadium (IV)$^{\omega}$	0.57	95

$^{\omega}$ = tannage was myrabalams

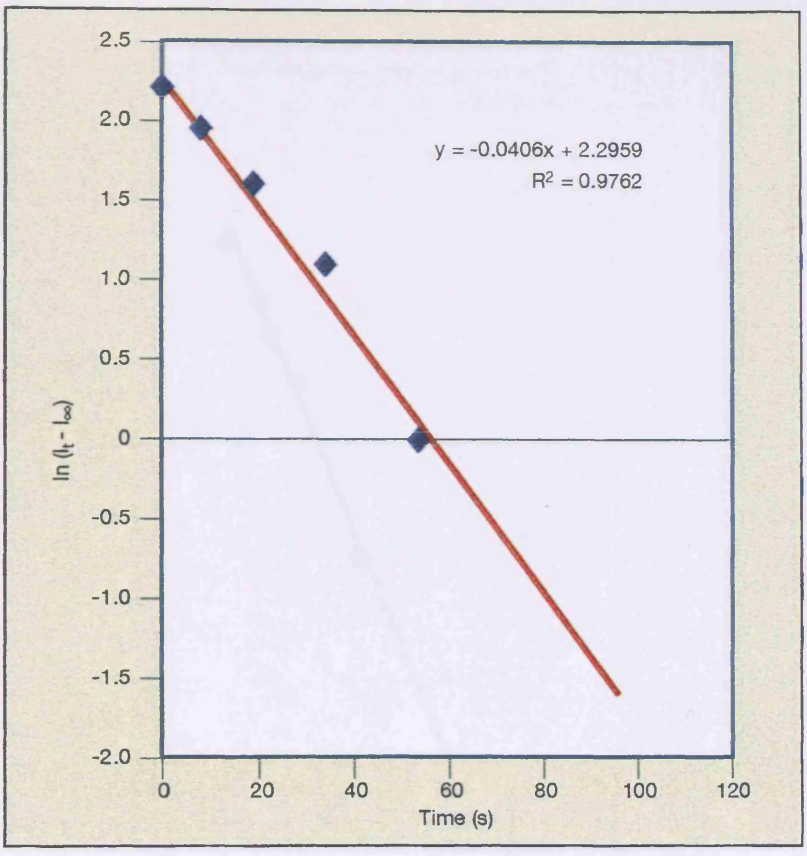

Figure 3.5a: Graph showing shrinkage of semi-aluminium

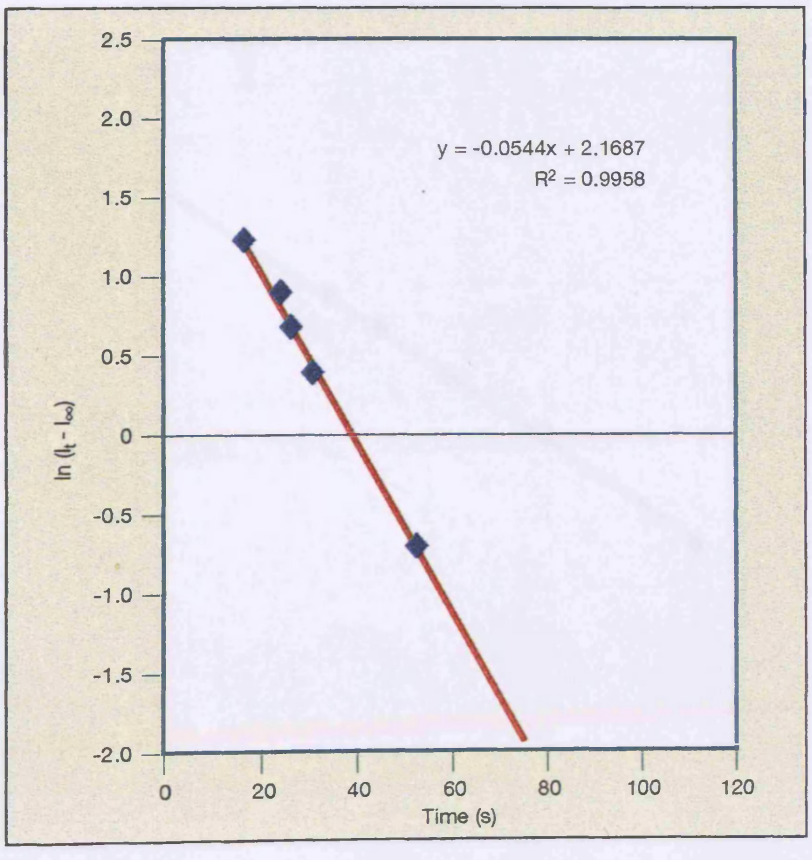

Figure 3.5b: Graph showing shrinkage of semi-cerium tannage

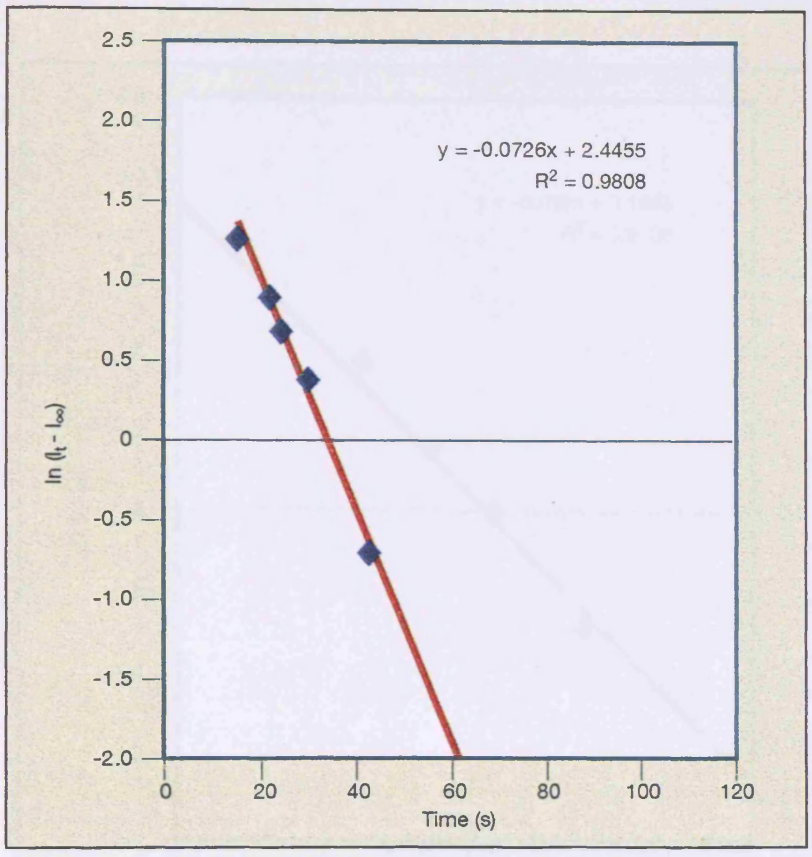

Figure 3.5c: Graph showing shrinkage of semi-lanthanum tannage

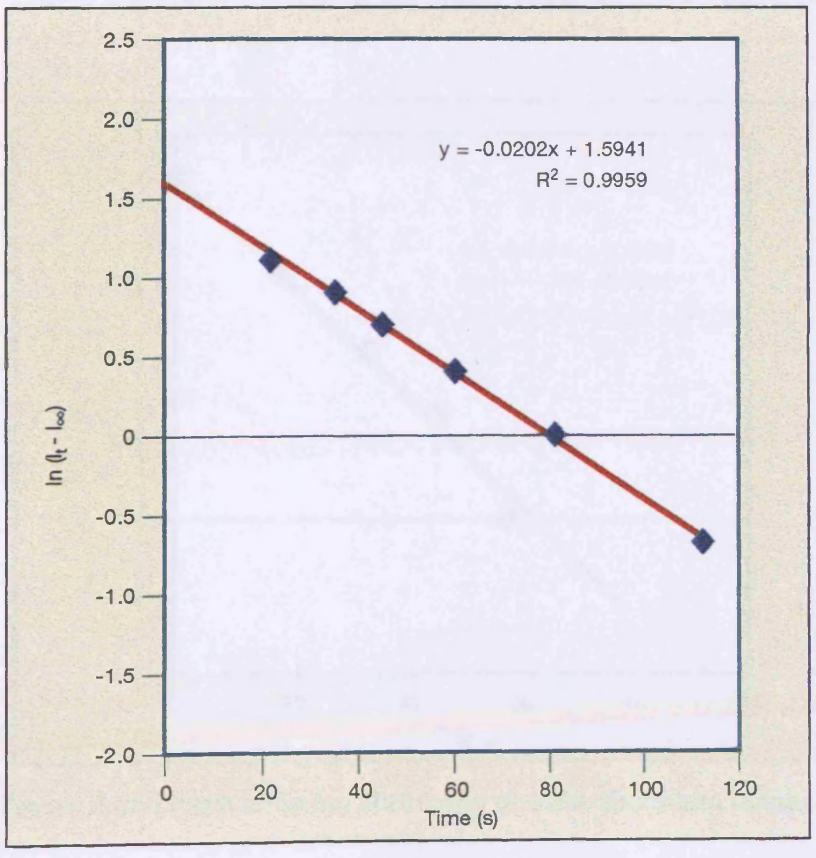

Figure 3.5d: Graph showing shrinkage of semi-uranium tannage

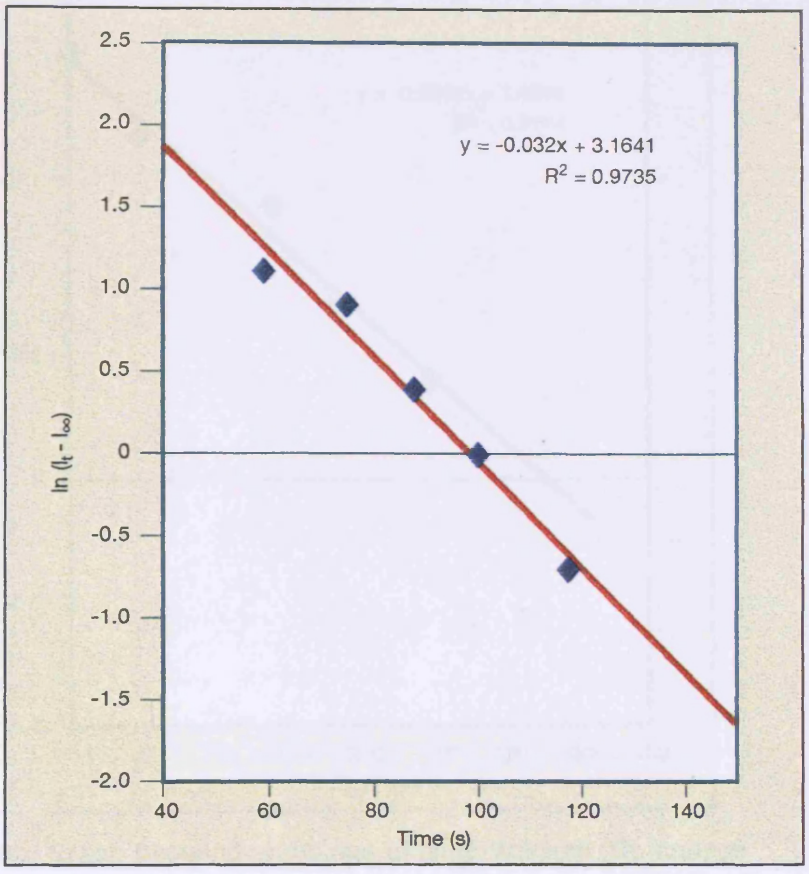

Figure 3.5e: Graph showing shrinkage of semi-terbium tannage

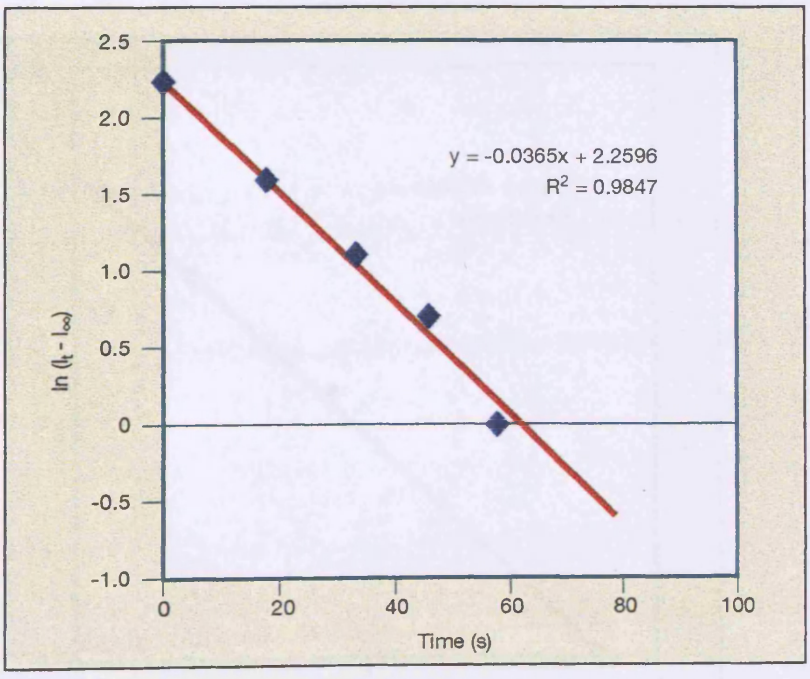

Figure 3.5f: Graph showing shrinkage of semi-zirconium tannage

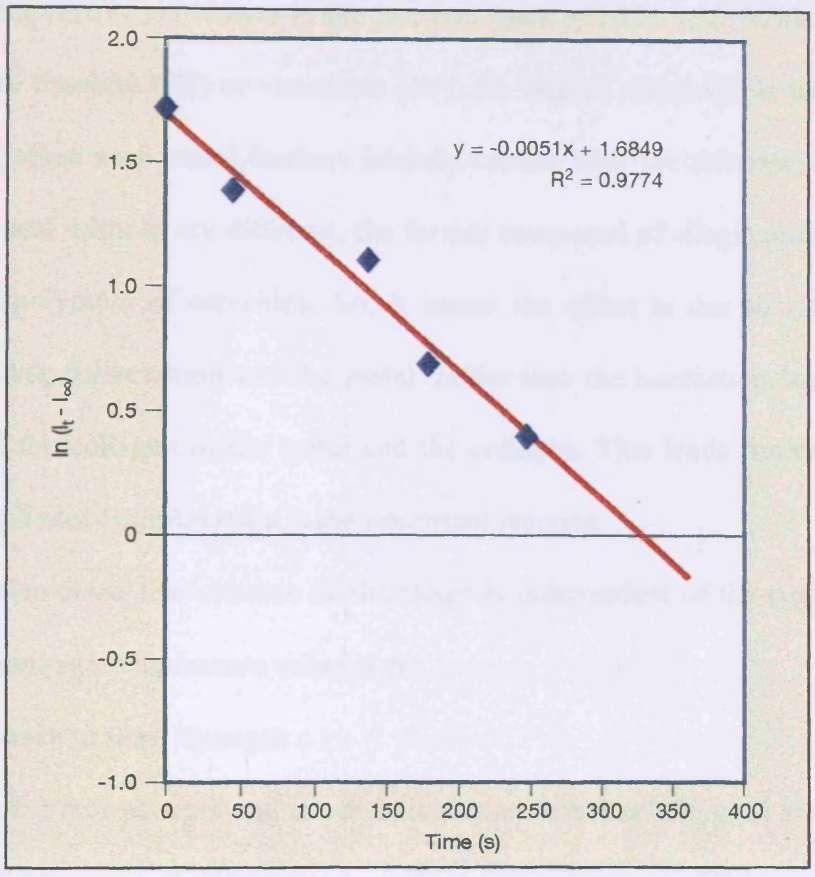

Figure 3.5g: Graph showing shrinkage of semi-titanium (III) tannage

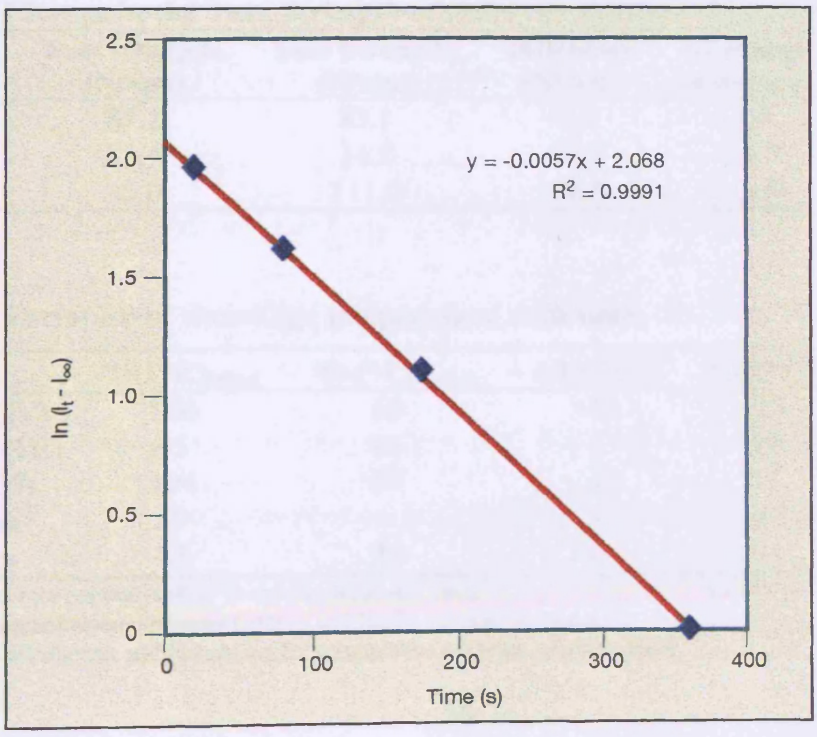

Figure 3.5h: Graph showing shrinkage of semi-vanadium tannage

The interesting results are shown in the last two rows of table 3.20. With myrabalams leather retanned with titanium (III) or vanadium (IV), the rate of shrinkage is ten times slower than some of the other semi metal leathers initially tanned with the mimosa. The composition of myrabalams and mimosa are different, the former composed of ellagitannins, while the latter is made up of polymers of catechins. So, it seems the effect is due to a different interaction between the vegetable tannin and the metal, rather than the interaction between the metal/veg complex and the collagen or the metal and the collagen. This lends further weight to the idea that the polyphenol complexation is the important reaction.

The results also show that the rate of shrinkage is independent of the type of metal, although the actual shrinkage temperature value is not.

3.1.5 Anomaly in tear strength

Periodically, the tear strength and the shrinkage temperature of the semi metal leathers were re-examined to determine if there was any effect due to storage. All leathers were stored in a conditioned room at 20°C, 68% relative humidiy. The change in tear strength and shrinkage are shown in tables 3.21 and 3.22 after storage for two years.

Table 3.21: Change in the Tear Strength of different semi-metal leathers

Metal	Tear strength$_1$ (N/mm)	Tear Strength$_2$ (N/mm)	Difference (N/mm)	% change in strength
Aluminium	87.2	83.1	-4.0	-4.5
Vanadium	81.4	34.2	-47.2	-58.0
Titanium	95.0	111.0	+16.0	+16.8

Table 3.22: Variation of shrinkage temperature with time

Metal	Ts (°C)$_{initial}$	Ts (°C)$_{2\ years}$	ΔTs(°C)$^{\psi}$	ΔTs(°C)$^{\tau}$
Vanadium (IV)	100	60	-40	-15
Aluminium (III)	95	96	1	14
Titanium (III)	104	98	-6	13
Molybdenum$^{\Upsilon}$	69	-	-	-16
Mimosa only	85	85	-	-

ψ = value is difference between initial Ts and the value at 2 years

τ = value is difference between mimosa tannage and the Ts value at two years

Υ = value from Kallenberger and Hernandez for comparative purposes, see discussion

There appears to be a severe detrimental effect of tanning with vanadium (IV) salts.

The reduction in shrinkage temperature of the semi-metal leather with vanadium (IV) is pronounced. The leather has been completely detanned. The tear strength has also fallen by two thirds.

3.1.6 Discussion

A marked fall in the shrinkage temperature was also seen by Kallenberger when he retanned vegetable tanned stock was with a molybdenum salt, table 3.22[44]. Unfortunately, the salt nor oxidation state of the metal is given. However, the effect is to reduce the shrinkage temperature of the leather by about 15°C compared with the control.

The loss of physical properties seems to be a function of the metal because the shrinkage temperature of the vegetable tanned stock shows no decrease in hydrothermal stability on storage. However, the loss of properties is likely to be caused by a reversal of the metal-veg complexation, eg through hydrolysis or, more probably, catalytic degradation of the veg tan-collagen interaction by oxidative reactions with the polyphenol resulting in disruption of the framework. It is thought to be a function of the metal's ability to act as a catalyst.

The effect of pH may also be important, because similar decreases in hydrothermal stability are seen with iron tannages and if leathers, eg bookbinding leathers, are exposed to acidic atmospheres.

There is a decrease in the shrinkage temperature of the semi metal leather retanned with titanium (III) salts, which are added under very acidic conditions. However, the effect is significantly smaller and there seems to be no detrimental effect on the tear strength of these leathers. The cause may simply be the titanium (III) oxidising to titanium (IV). Results obtained in other experiments, see section 3.9.3, indicate that vegetable tanned leather retanned with titanium (IV) also shows a reduction in the shrinkage temperature with time, table 3.19.

The effect of the solo metal tannages is also worth noting. Column 8 of table 3.19 highlights the shrinkage temperatures produced when the pelt was tanned with the metal alone. Table 3.23 shows the difference in shrinkage temperature compared with the shrinkage temperature of the starting material.

Table 3.23: Effect of metal tannage on shrinkage temperature

Metal(*)	Change in Ts/°C
None	0
Copper (II) sulfate	6
Nickel (II) sulfate	6
Zinc (II) sulfate	-3
Iron (II) sulfate	-2
Dysprosium (III) sulfate	-11
Yttrium (III) sulfate	-10
Ytterbium (III) sulfate	-10
Lanthanum (III) sulfate	-8
Titanium (III) sulfate	13
Titanium (IV) sulfate	18
Zirconium (IV) sulfate	16
Terbium peroxide	-5

(*) all samples basified to pH 4 after one hour in solution
values measured after 24 hours

The values show that some metals reduce the shrinkage temperature of the collagen compared with raw skin. These we define as a 'negative' tannage[56]. The influence tends to be seen with the lanthanide metals and is probably attributable to a powerful entropic effect. The metal disrupts the solvation of the collagen molecule leading to increased disorder. In tannages such as titanium, zirconium and aluminium, this disruption is overcome by strong enthalpic effects. However, with the lanthanides the enthalpic interaction is weak, hence the measured shrinkage temperature falls.

3.10 Comparative trials

3.10.1 Introduction

In this section, leathers tanned with a titanium (III) tannage were compared with the industry standard, chromium. As this project has demonstrated, the solo tanning abilities of titanium (III) are limited, however, it was decided to compare the tannage with the industry standard, chromium (III). The process carried out was a standard tannage for sheepskins from Hodgson Chemicals Ltd. Six of the skins were offered 2% chromium oxide and six with 2% titanium (III) oxide.

The process is outlined in appendix 3. The leathers were finished at H Goodman and Sons Ltd, Kettering, England.

3.10.2 Results

Samples were subjected to a series of physical tests. The results are shown in table 3.24.

Subjective analysis of the leathers suggested that the titanium (III) leathers were much firmer than the chrome controls. It was also noticed that the titanium (III) tanned leather were weak and easily torn.

Table 3.24: Physical test results of leathers in the comparative trial

	Average thickness (mm)	Tear strength N/mm	Grain Crack mm	kg	Burst mm	kg
Chromium tanned	0.84	43.3	8.9	14	10.5	21
Titanium tanned	0.85	29.3	9.5	15	10.3	18

The fullness of the leathers was determined using the Pierce Flex test. This was a method developed by Pierce and Conabere[57], and the test assesses three parameters:

- The bending length, which is a measure of the draping quality of the leather defined as that length of leather which will bend under its own weight, to a defined length. The lower the value the more drape the leather has.
- the flexural rigidity, which is the force required to bend unit length through unit angle. In simple terms, the lower the value the softer the leather
- the bending modulus. This is a measure of the intrinsic stiffness of the leather and is the inverse of fullness, ie the smaller the bending modulus the more full the leather

The average results of the six leathers in for the two tannages are set out in table 3.25.

Table 3.25: Assessment of fullness for the tannages

Tannage	Bending length (cm)	Flexural rigidity ($g\ cm^3$)	Bending modulus ($kg\ cm^{-3}$)
Titanium	3.05	2.40	41.78
Chromium	3.58	1.25	20.73

3.10.3 Discussion

The Pierce Flex test shows that the chromium tanned leathers have better physical properties. This was noted simply from handling the leathers: it was obvious the titanium tanned leathers were of poorer performance, in terms of handle, than the controls.

The leathers with the properties of a titanium (III) tannage compared with that of chromium are less likely to replace chromium.

Where Ti(III) seems to be effective is in semi-metal tannages. The addition of it to certain vegetable tannins produces boil-proof leathers with excellent physical properties when compared with the semi-chromium controls.

4 ESR and ENDOR spectroscopy of titanium (III) complexes

This chapter is concerned with work carried out to investigate the titanium (III) complexes developed in chapter 3 . Before analysing the ESR and ENDOR spectra of the metal complexes presented in the next section, it is necessary to review some of the fundamental principles of the technique, as these basic principles will aid in the interpretation of the data .

4.1 Basic electron magnetic resonance (EMR) theory[58]

In electron spin resonance (ESR) spectroscopy, the absorption of microwave radiation is measured as a function of a changing magnetic field (analogous to NMR, in which absorption of energy in the radio frequency region occurs). The basic mechanism by which the system absorbs energy is due to two properties of the electron, the spin and the associated magnetic moment.

An electron is a negatively charged particle, which moves in orbitals around the nucleus. As a result of this movement it has orbital angular momentum. Because it also spins about its own axis, it has spin angular momentum within the orbit (or simply spin, S) which, in a given direction (eg, the z direction), can only assume values of $M_S = +½$ and $M_S = -½$ in units of $h/2\pi$ where h= Planck's constant:

$$\textit{Spin Angular Momentum}\ (S_Z) = M_S\, h/2\pi \qquad (1)$$

Any spinning charge carries an associated magnetic field or magnetic moment. Therefore, the electron also carries a magnetic moment (μ_S) which is co-linear and anti-parallel to the spin angular momentum itself or in classical terms, with the axis of rotation. The two properties of magnetic moment (μ_S) and spin angular momentum (S) are related in equation 2:

$$\mu_S = - g_e\, \mu_B\, S \qquad (2)$$

where g_e is the spectroscopic splitting factor, the g value or the Landé splitting factor (g_e = 2.0023) and μ_B is a fundamental constant, the Bohr Magneton.

Just as when two magnets interact with each other, the magnetic moment of the electron can interact with the magnetic moment of an applied magnetic field. Classically, the energy (E) of this interaction is given by the relation:

$$E = -\mu_S \mathbf{B} \qquad (3)$$

where **B** is the magnetic flux density, which is usually measured in Tesla (T) or in Gauss (G). However, in quantum mechanics the μ vector is replaced by the corresponding operator leading to the following Hamiltonian, ie, the energy operator:

$$H = g_e \mu_B \mathbf{S} \mathbf{B} \qquad (4)$$

Assuming B lies in the z direction, the interaction energy (H) corresponds to:

$$H = g_e \mu_B \mathbf{B} S_z \qquad (5)$$

This is the simplest form of a spin Hamiltonian, the equation that describes the interaction of an electron with an applied magnetic field. Remembering that S_z can have values of $\pm \frac{1}{2}$, the energies corresponding to the two allowed orientations of the spin are given by:

$$E = (\pm \tfrac{1}{2})\, g_e \mu_B \mathbf{B} \qquad (6)$$

The lowest spin state has $M_S = -\frac{1}{2}$, so that the spin is anti-parallel to the field, while the magnetic moment is parallel to the field in accordance with physical expectations. These two energy levels are often referred to as the Zeeman levels. The difference between the two is known as the Zeeman splitting:

$$\Delta E = E_1 - E_2 \quad \text{or} \quad \Delta E = g_e \mu_B \mathbf{B} \qquad (7)$$

Since $\Delta E \propto B$, then the difference between the two energy levels is directly proportional to the external applied magnetic field. Transitions between the two Zeeman levels can be induced by irradiating the paramagnetic system with suitable electromagnetic radiation providing the frequency, ν, fulfils the resonance condition

$$\Delta \mathbf{E} = g\, \mu_B \mathbf{B} = h\nu \qquad (8)$$

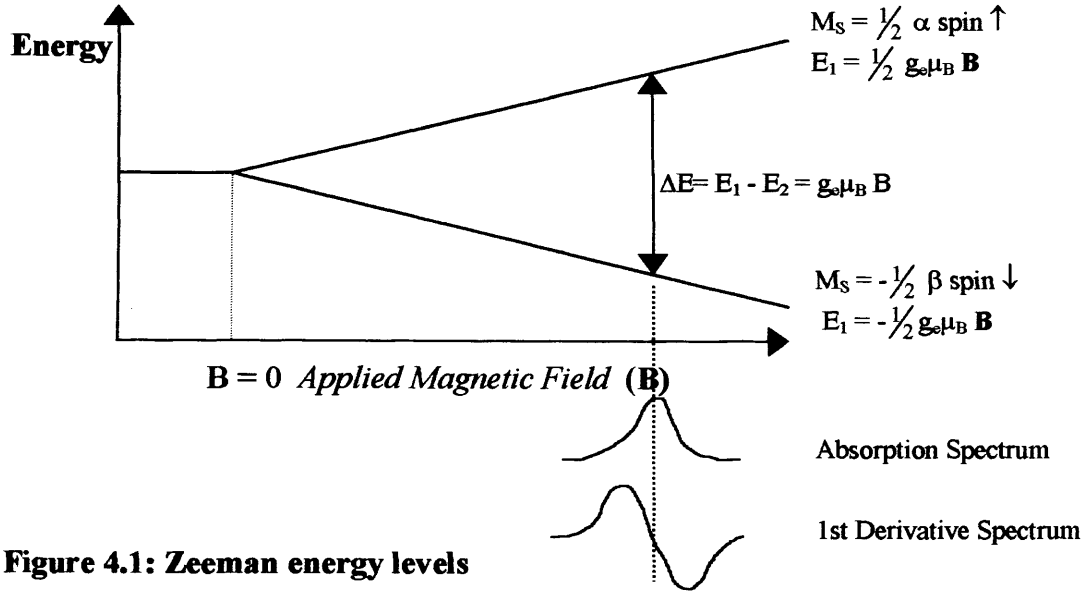

Figure 4.1: Zeeman energy levels

The existence of two Zeeman levels and the possibility of inducing transitions from the lower energy level to the higher energy level are the basis of ESR spectroscopy. The experiment can be conducted in two ways; either the magnetic field is kept constant and the applied frequency varied, or, the applied frequency is held constant and the magnetic field is varied. In ESR spectroscopy the latter case is usually used, since it is far easier to vary the magnetic field over a wide range than to change the microwave frequency.

4.2 Basic interaction of the electron with its environment

The above equations describe the energies of the electron spin states whose only interaction is with an applied magnetic field, (ie, a free electron), and they illustrate how transitions between these states can be induced and detected. This is an idealised model because in reality the electron, localised in a particular orbital of a metal cation for example, will undergo a variety of electrostatic and magnetic interactions, which complicate the resonance. It is, therefore,

necessary to examine how the electron interacts with its environment, resulting in the real ESR spectrum.

Magnetic Resonance spectroscopists seek to characterise and interpret ESR spectra quantitatively using the spin Hamiltonian. The ESR spectrum is essentially interpreted as the allowed transitions between the eigenvalues of this spin Hamiltonian. The spin Hamiltonian contains terms that reflect the interactions between the electron and nuclei spins with the applied magnetic field and with each other. Analysis of a spectrum amounts to identifying which interactions are involved. The two most important terms in the equation are the g tensor and the A tensor.

4.2.1 The g tensor: significance and origin

Equation 8 described the g value simply as the numerical factor or proportionality constant relating the frequency to the value of the applied magnetic field at which the resonance is observed. In practice, g often deviates from free spin so that $g \neq g_e$. It is then more appropriate to modify equation 4 to:

$$H = g\,\mu_B\,\mathbf{B}\,\mathbf{S} \qquad (9)$$

where g is characteristic of the sample and something to be determined by experiment. The 'real' g value will vary from g_e depending on the paramagnetic species in question. For organic radicals the deviations are small, usually less than 1%, but for systems containing heavier atoms such as transition metals ions, and particularly rare earth metals, the variations can be much larger. The main reason for the deviation in g comes from the fact that there is a spin-orbit coupling resulting in an orbital contribution to the magnetic moment (μ_L instead of μ_S). This arises due to the effect of the orbital angular momentum, L, that is non-zero in the case of orbitals exhibiting p or d character. (Spin orbit coupling is a magnetic interaction: the orbital motion of an electron can be viewed as generating a magnetic field with which the spin moment interacts). In this case the spin is no longer exactly quantised along the direction of

the external field so the g value can no longer be expressed by a scalar quantity but becomes a tensor. Put simply, the magnetic moment associated with the electron spinning on its axis ($\mu_S = \mu_B$ **S**) and the magnetic moment associated with the electron moving in the orbital ($\mu_L = \mu_B$ **L**) must be added vectorially.

The g_e scalar value reported in equation 8 is now replaced by **g**. This is a second rank tensor that represents the anisotropy of the interaction between the unpaired electron and the external magnetic field. The orbital contribution to the electronic magnetic momentum may be different along different molecular axes.

$$H = \mu_B \mathbf{B}\,\mathbf{g}\,\mathbf{S} \qquad (10)$$

In other words, the magnetic moment of the odd electron in a real paramagnetic system is not exactly anti-parallel to the spin and its magnitude is not that of a free electron, but depends on the orientation of the system in the applied magnetic field.

The g tensor is often depicted as an ellipsoid whose principal values, g_{xx}, g_{yy}, g_{zz}, depend upon the orientation of the symmetry axes of the paramagnetic moiety with respect to the applied magnetic field, figure 4.2. The most general consequence of the anisotropy of g, from an experimental point of view, is that the resonance field of a paramagnetic species for a given frequency depends on the orientation of the paramagnetic centre in the field itself.

Figure 4.2

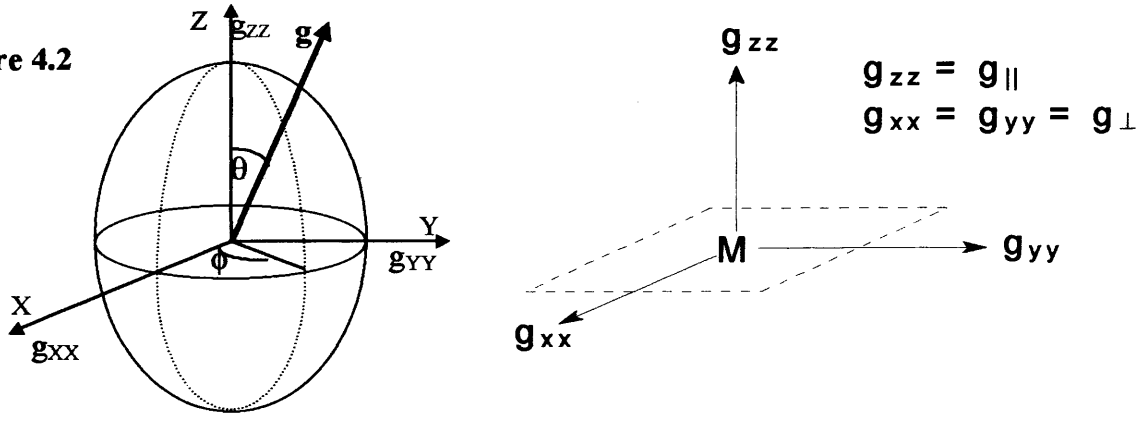

For example, if the x, y and z directions are all equivalent then a spectrum with *isotropic* character results (ie, $g_{xx} = g_{yy} = g_{zz} = g_{iso}$). This is very rare in inorganic systems, except for complexes with very high symmetry such as O_h. It is more common for inorganic systems to display axial or orthorhombic ESR symmetry. In the case of axial symmetry of the system, if z is the principal symmetry axis of the species and θ the angle between z and the magnetic field, the x and y directions are equivalent and the angle ϕ thus becomes meaningless, figure 4.2. In

Figure 4.3

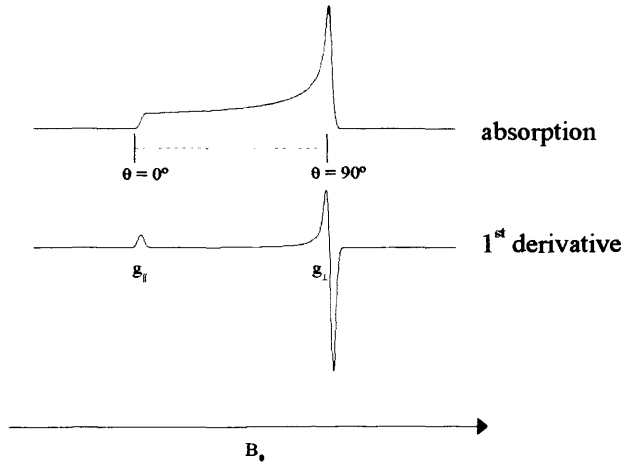

this case one observes an axial ESR spectrum as shown above in figure 4.3. This situation occurs for the vanadium and titanium complexes studied in this thesis.

The $g_{||}$ and $g_{\perp}$ values are the g values measured when the axis of the paramagnetic species is respectively parallel and perpendicular to the applied magnetic field as shown in figure 4.4.

Figure 4.4: Measured $g_{||}$ and $g_{\perp}$ values

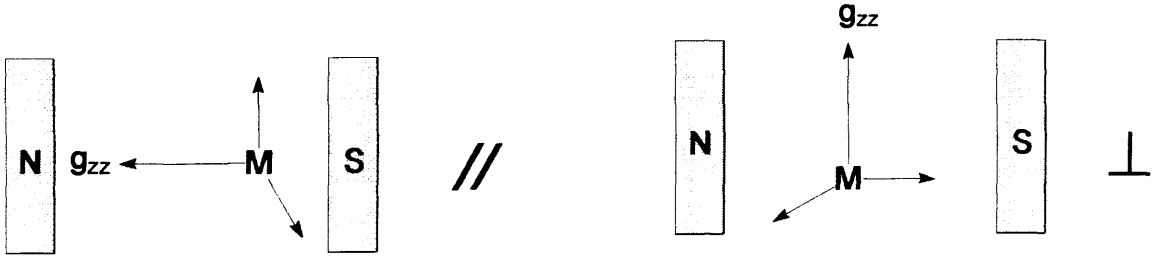

The spectrum is obtained by freezing the solution. In this work the sample was taken down to 10 K using liquid helium. The complex spectrum is an envelope of the individual lines corresponding to all possible orientations in the whole range of θ. Assuming the microcrystals are randomly distributed, it can be shown that the absorption intensity, which is proportional to the number of microcrystals at resonance for a given θ value, is maximum when $\theta = \pi/2$ ($B_\perp$). It is minimum for $\theta = 0$ ($B_\parallel$). This allows the extraction of the $g_\parallel$ and $g_\perp$ values which correspond to the turning points in the spectrum.

To further complicate the spectra, the above profile analysis of the ESR spectrum does not take into consideration the presence of hyperfine interactions. These arise from the central nucleus, where that nucleus has a value of $I \neq 1$ or 0, such as $I = 7/2$ for ^{51}V. Finally, there are super-hyperfine interactions, which arise from the nuclei on the surrounding ligands such as ^{31}P where $I = ½$)

4.2.2 The A tensor: significance and origin

Most ESR spectra are split into a number of lines that generally have simple intensity ratios and, provided the spectrum is not spread over large fields, probably forms a centrosymmetric pattern. The source of this splitting is the magnetic interaction between the electron spin and neighbouring nuclear spins; this hyperfine interaction gives rise to hyperfine structure in the spectra.

So, how does the hyperfine structure arise? A nearby magnetic nucleus gives rise to a local field, B_{local}, which is compounded with the applied magnetic field B in order to satisfy the basic ESR condition $h\nu = g_e \mu_B B$. Equation 8 is rewritten as:

$$h\nu = g_e \mu_B (B + B_{local}) \qquad (11)$$

The value of B required to achieve resonance will depend on B_{local} so the effects of nuclei with magnetic moments on the electron spin and, hence, the ESR spectrum becomes significant.

When the paramagnetic centre contains one or more nuclei with non zero nuclear spin ($I \neq 0$), the interaction between the unpaired electron and the nucleus gives rise to further splitting of the Zeeman energies and, consequently, to new transitions responsible for the so called hyperfine structure of the ESR spectrum.

Two types of electron spin-nuclear spin interactions must be considered: isotropic and anisotropic in nature. The former is a quantum interaction related to the finite probability of finding the unpaired electron at the nucleus and is termed the Fermi contact interaction. The corresponding constant is called the isotropic hyperfine coupling constant, A. The isotropic interaction concerns s-type orbitals or orbitals with partial s character (like hybrid orbitals constructed from s-type orbitals) because only these orbitals have finite probability density at the nucleus. Since s orbitals have high electron density at the nucleus, the hyperfine coupling constant will be large and since s orbitals are symmetrical, it is independent of direction.

The anisotropic interaction occurs for an electron in a p or d orbital, where there is no electron density at the nucleus (ie, the electron is some distance away from the nucleus). The interaction between it and the nucleus will be like two magnetic dipoles and, consequently, the interaction will be small and dependent on the direction of the orbital with respect to the applied magnetic field as well as to their separation. Anisotropic electron-nuclear (hyperfine) couplings are due to the dipolar interaction between the nuclear and the electron magnetic moments. The coupling arises from the dipolar interaction between magnetic moments whose energy is given by

$$E = \mu_s \mu_n / r^3 - 3(\mu_s r)(\mu_n r)/r^5 \qquad (27)$$

where r is the vector relating the distance between the electron and the nucleus. Knowledge of the anisotropic coupling constant obtained from the experimental spectrum is useful for estimating distances in paramagnetic systems.

4.2.3 ENDOR and EIE

These techniques are related to ESR[59]. ENDOR is a resolution enhancement technique. A spectrum is observed at one frequency while simultaneously irradiating at another. The first frequency is the standard ESR, while the second frequency, in ENDOR, observes the effect of an NMR transition. Determining this transition produces greater sensitivity of the ESR and, hence, allows better evaluation of the spectra.

An EIE (ENDOR induced ESR) spectrum is achieved by sweeping the ENDOR signal with the ESR frequency. This separates out the ENDOR peaks, allowing greater clarification of these peaks. The basic theory of EMR holds for both techniques.

4.3 Use of ESR to study transition metal complexes

ESR spectroscopy is widely used to study the structure and geometry of *d*-transition metal ions (TMI) in inorganic complexes, in biological systems and in catalysts. Information obtained through analysis of the spectrum varies from simple identification of the metal centre to a thorough description of the electronic structure of the complex. At a simple level, the main interactions experienced by the TMI which consequently influence the ESR spectra are:

- the electronic Zeeman effect
- the interaction between the electron and the nuclear spin.

In the first case, the interaction is expressed using the g tensor, which carries information on electronic structure and, in the second case, the metal hyperfine interaction is expressed by the A tensor (*cf* 4.2.1 and 4.2.2 above).

The ground state of paramagnetic transition metal ions may be inferred from the dependence of the g tensor values on the crystal field parameters. In other words the g values of d TMI elements depends on the values of the spin-orbit coupling constant (λ) and crystal field (CF) symmetry and strength, as shown in figure 4.5

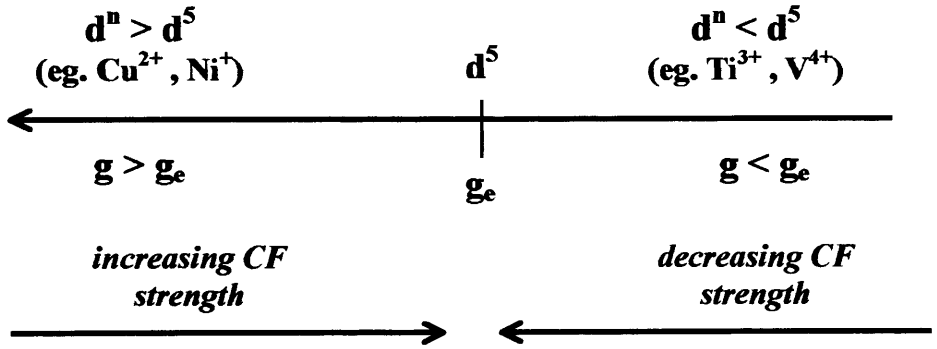

figure 4.5: Effect of crystal field strength on the g tensor

High spin highly symmetric d^5 ions (eg, Mn^{2+}) as well as organic radicals and some non-metal inorganic radicals show g values close to g_e. With increasing crystal field strength the deviations from the g_e value decrease for d-block elements. For f-block elements, due to the

effective screening of the f shell by the external s, p and d orbitals, the spin-orbit coupling is undisturbed by the crystal field, so g values are unaffected. When the separation between the ground state and excited levels is small, the relaxation time is very short which makes it difficult to observe ESR spectra unless very low temperatures are used.

Two representative examples may be discussed for d^1 and d^9 systems. The simplest case arises for d^1 TMIs. For a tetragonally distorted octahedral field, experiencing compression along the 4-fold axis (D_{4h}), the nondegenerate d_{xy} state lies lowest in energy and for a slight distortion the low lying 2-fold degenerate excited states (d_{xz}, d_{yz}) are close to the ground state, figure 4.6a. The small energy separation, Δ_1, results in a short relaxation time and the ESR signal can only be observed at low temperatures. Greater distortions lead to longer relaxation times, so that the ESR signals become observable at increasingly higher temperatures, with g values of $g_{\|} = g_e - 8\lambda/\Delta_2$ and $g_{\perp} = g_e - 2\lambda/\Delta_1$ (ie, $g_{\perp} > g_{\|}$). In the case of elongation along the 4-fold axis, the unpaired electron now occupies a doubly degenerate ground state (d_{xz}, d_{yz}) and no ESR signal is observed. However if the ion now experiences a trigonal distortion with a resulting point symmetry of D_{3d}, then the electron occupies the d_z^2 orbital so the order of the g values changes or becomes 'inverted' (ie, $g_{\|} > g_{\perp}$), since $g_{\|} = g_e$ and $g_{\perp} = g_e - 2\lambda/\Delta_1 - 4\lambda/\Delta_2$, figure 4.6b.

This may be explained another way. The single electron of the d^1 ion in a tetragonally distorted octahedral environment occupies a d_{xy} orbital. When an external magnetic field is applied along the z axis (ie, the parallel direction) the electron can commute weakly from the d_{xy} to the d_{x2-y2} orbital. Therefore, the effect of the applied field, B, is to make the electron 'rotate' about the z axis. This gives rise to a small current flowing in a circle and as a result a small magnetic field $B^{\dagger}$ occurs, which opposes B. In order to achieve the original field at the electron for resonance to occur the original field must be increased by $B^{\dagger}$. ie,

$$h\nu = g_{\|}\,\mu_B\,B \qquad \text{now becomes} \qquad h\nu = g_{\|}\,\mu_B\,(B + B^{\dagger})$$

Since the frequency ν is a constant, g, along the x axis, must now be less than 2.0023 to maintain the right hand side of the equation equal to $h\nu$. If the applied field was perpendicular to z, ie, along x or y, the d_{xy} may commute with d_{xz} and d_{yz} with the effect that $g_\perp < 2.0023$. Some examples include Ti^{3+} for which $g_\perp = 1.995$ and $g_\parallel = 1.992$, Cr^{5+} with $g_{XX} = g_{YY} = (g_\perp) = 1.9498$, $g_{ZZ} = (g_\parallel) = 1.9936$, and V^{4+} with $g_\perp = 1.9807$ and $g_\parallel = 1.9343$.

The Cu^{2+} ion is another example of an $S = ½$ transition metal which gives readily observed ESR spectra, and which forms a range of complexes of interest in both inorganic and biological sciences. The d^9 configuration corresponds to a one electron hole in the d shell, which in octahedral type complexes leads to the so called Jahn-Teller effect; ie, spontaneous distortion into a tetragonally distorted octahedron with a d_{x2-y2} or d_{z2} ground state for elongated or compressed octahedron, respectively. In the former case, the g values are given by the following equations

$$g_\parallel = g_e - 8\lambda/\Delta_1 \qquad \text{and} \qquad g_\perp = g_e - 2\lambda/\Delta_2$$

where $\Delta_1 = (E_{x2-y2} - E_{xy})$ and $\Delta_2 = (E_{x2-y2} - E_{xy,yz})$. The spin orbit coupling constant is negative for d^9 ions, and since $\Delta_1 < \Delta_2$, the above equation leads to the following sequence of g values; $g_\parallel > g_\perp > g_e$. The d^9 ion may be treated in a similar manner to the d^1 situation, by considering the missing electron as a positive hole. In this case the resonance occurs at $h\nu = g_\parallel \mu_B (B - B^\dagger)$ giving rise to g values larger than 2.0023.

For a compressed octahedron, the g components are given by the relations

$$g_\parallel = g_e \qquad \text{and} \qquad g_\perp = g_e - 6\lambda/\Delta_3$$

where $\Delta_3 = (E_{z2} - E_{xz,yz})$ which gives the relative order $g_\perp > g_\parallel \approx g_e$.

As shown above, the point symmetry at the metal can be reflected in the g values, but the A values can also be influenced in a similar manner. Furthermore, depending on the point symmetry, the principal axes of g and A may or may not be coincident. The relationship

between these tensors, the ESR symmetry and the point symmetry of the metal are shown in table 4.1. The importance of these relationships is that each type of ESR behaviour is associated with a restricted number of point symmetries which places constraints upon the geometrical structures of the paramagnetic ion. For example, if the paramagnet is known to have rhombic symmetry, then the associated geometry must belong to one of the point groups D_{2h}, C_{2v} or D_2, table 4.1. It would be incorrect to assign a structure that belongs to a more symmetric arrangement, eg, D_{4h} which is strictly axial. Therefore, for a system with unknown structure, if the ESR symmetry can be determined, table 4.1, invaluable structural information can be determined since the ion under detection can only belong to a restricted range of point symmetries.

Table 4.1: Relationship between g and A tensor, ESR symmetry and the point symmetry of the paramagnetic ion

ESR Symmetry	g and A tensor	Coincidence of tensor axis	Molecular Point Symmetry
Isotropic	$g_{xx} = g_{yy} = g_{zz}$ $A_{xx} = A_{yy} = A_{zz}$	All coincident	O_h T_d O T_h T
Axial	$g_{xx} = g_{yy} \neq g_{zz}$ $A_{xx} = A_{yy} \neq A_{zz}$	All coincident	D_{4h} C_{4v} D_4 D_{2d} D_{6h} C_{6v} D_6 D_{3h} D_{3d} C_{3v} D_3
Rhombic	$g_{xx} \neq g_{yy} \neq g_{zz}$ $A_{xx} \neq A_{yy} \neq A_{zz}$	All coincident	D_{2h} C_{2v} D_2
Monoclinic	$g_{xx} \neq g_{yy} \neq g_{zz}$ $A_{xx} \neq A_{yy} \neq A_{zz}$	One axis of g and A coincident	C_{2h} C_s C_2
Triclinic	$g_{xx} \neq g_{yy} \neq g_{zz}$ $A_{xx} \neq A_{yy} \neq A_{zz}$	Complete non-coincidence	C_1 C_I
Axial non-collinear	$g_{xx} = g_{yy} \neq g_{zz}$ $A_{xx} = A_{yy} \neq A_{zz}$	Only g_{zz} and A_{zz} coincident	C_3 S_6 C_4 S_4 C_{4h} C_6 C_{3h} C_{6h}

Analysis of the ESR spectra from titanium (III) and vanadium (IV) complexes used in this work will be discussed in the next section.

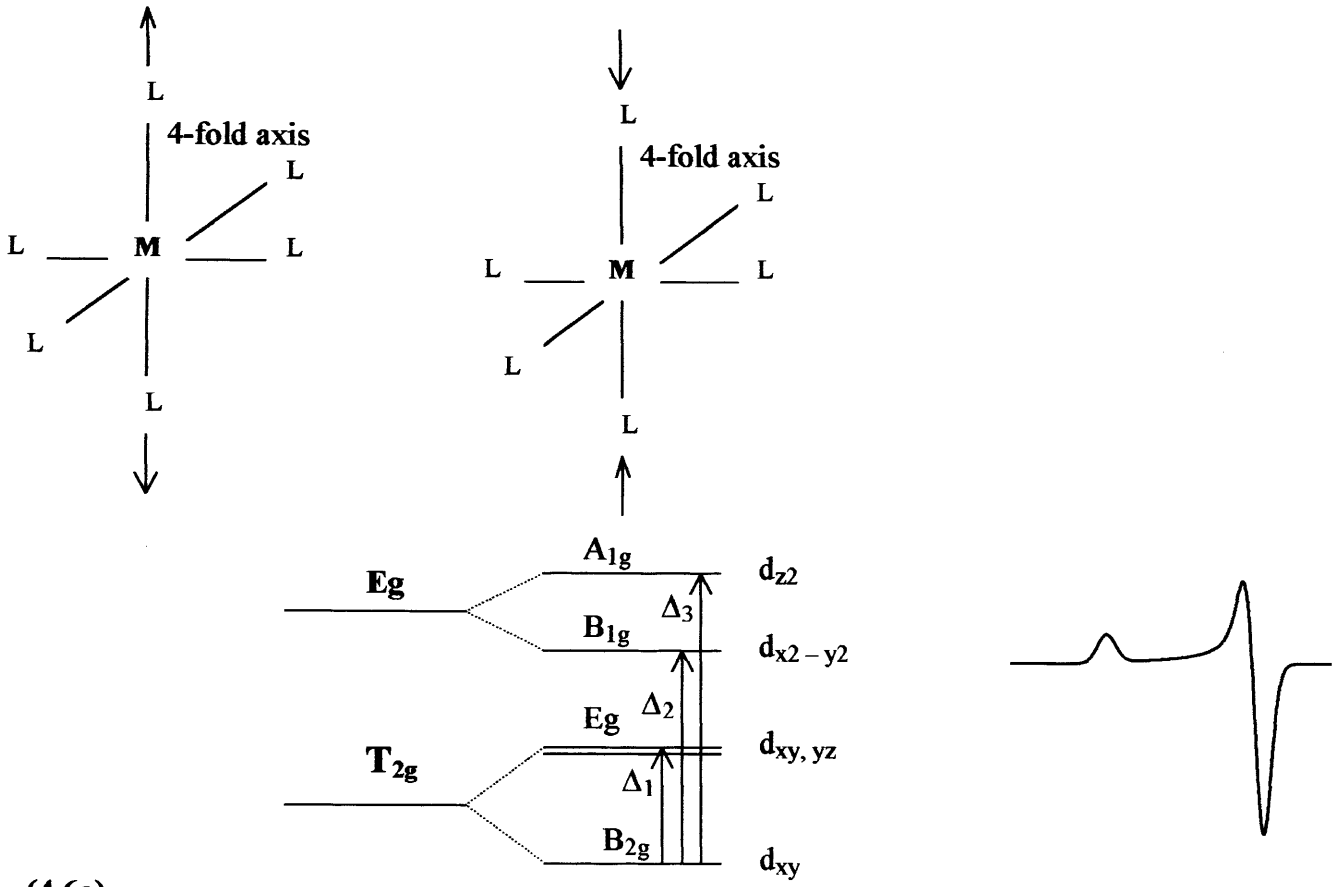

(4.6a)

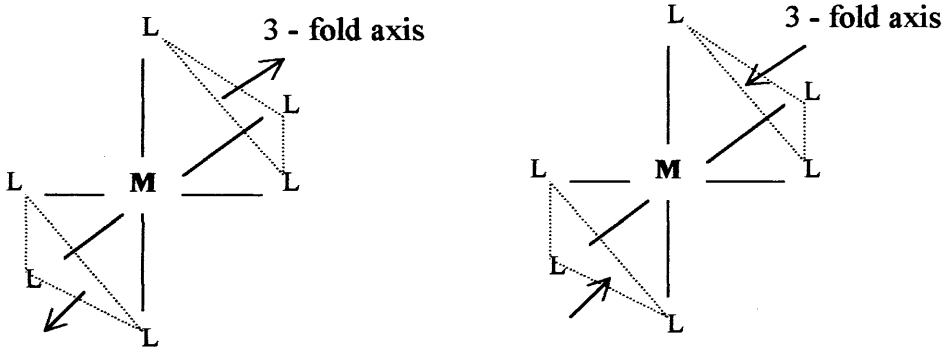

Elongation

Compression

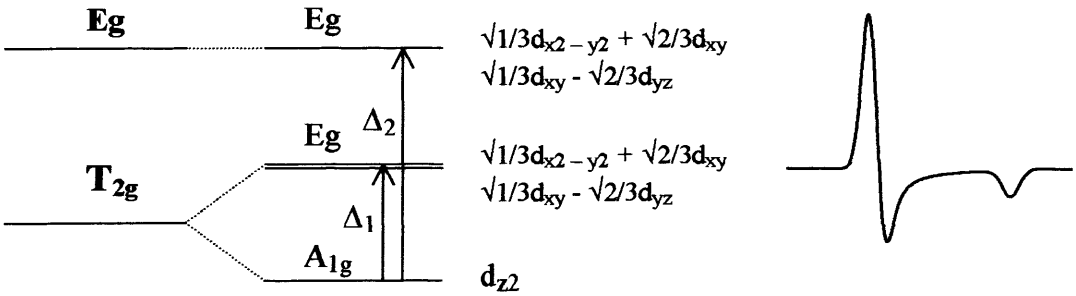

(4.6b)

4.4 Background

Titanium (III) has a single unpaired electron in a 3*d* orbital giving a ^2D state for the free ion. In an octahedral crystal field however, this fivefold degenerate state will be split into an orbital doublet, ^2E_g, and an orbital triplet, ^2T_g, the triplet having the lower energy. Under these circumstances, the observed g values for the ion will depend a great deal on the interplay of the orbital angular momentum, the spin-orbit interaction, and any deviations from distortions to the octahedral symmetry.

Wilson and Myers[60] studied the ESR features and spin relaxation processes for the $[Ti(H_2O)_6]^{3+}$ ion in aqueous solution. The spectra were characterised by g values of $g_{\|} = 1.988$ and $g_{\perp} = 1.892$. The fact that the g values have the form $g_{\|} > g_{\perp}$ and that $g_{\|}$ is close to the free electron value was explained on the basis of a trigonally distorted octahedron or D_{3d} symmetry. Premović and West[61] studied the effect of different anions on the ESR spectra of titanium (III). In strongly acidic titanium (III) chloride, bromide, iodide or sulfate, they showed that an identical spectrum is observed for each sample with $g_{\|} = 1.994$ and $g_{\perp} = 1.896$. Since the spectrum was independent of anion type, the counterion is unlikely to be in the first or second co-ordination shell of the titanous ion. They also pointed out that a maximum signal was observed at 6-8 mol dm^{-3} of added anion, indicating that not all the titanium (III) species were ESR active. Analysing the spectra indicated that the symmetry of the titanium (III) ion is approximately octahedral with a small axial trigonal distortion, D_{3d} symmetry. The work of Tachikawa et al[62] showed that this distortion is due to the Jahn Teller effect. They also showed that the unpaired electron is situated mainly in the d_z^2 orbital. The values they give for $g_{\|}$ (= 1.994) and $g_{\perp}$ (= 1.896) are in agreement with those of other authors.

4.5 Experimental

4.5.1 Sample preparation

4.5.1.1 titanium (III) sulfate

Titanium (III) sulfate was freshly prepared using the method shown in section 2.3.1. The molarity was determined using the method set out in section 3.3.

4.5.1.2 masked titanium (III) salts

Aliquots of the freshly prepared titanium (III) sulfate were masked with 1 mole of the sodium citrate or sodium gluconate per mole of titanium (III). The ESR and ENDOR spectra were collected immediately.

4.5.1.3 vanadium (IV) sulfate

Vanadium (IV) oxysulfate (1 g) (ex BDH, 99.99% pure) was dissolved in distilled water (100 g).

4.5.1.4 semi-metal leathers

Samples of previously processed semi-metal tanned leathers were analysed. The process details are given in appendix 1. The leathers were ground using a Wiley Mill to produce a fine powder.

4.6 ESR/ENDOR experimental methods

4.6.1 Solutions

The samples were first dissolved in water/methanol, as these solvents produce the best glass when frozen at low temperature, and gently degassed by repeated freeze-pump-thaw cycles on a vacuum line to remove all traces of dioxygen from the sample.

4.6.2 leathers

The powders were gently degassed by repeated freeze-pump-thaw cycles on a vacuum line to remove all traces of dioxygen from the sample.

4.6.3 Spectra

The ESR/ENDOR spectra were recorded on a CW X-band *Bruker ESP 300E* series spectrometer equipped with an ESP360 DICE ENDOR unit, operating at 12.5 kHz field modulation in a Bruker ER 200 ENB cavity. All spectra (ESR and ENDOR) were recorded at 10 K; the ENDOR spectra were obtained at 4 mW microwave power, 8 dB RF power from a ENI A-300 RF amplifier and 199 kHz RF modulation depth, again at 12.5 kHz modulation frequency. Computer simulations of the ESR spectra were performed on a commercial programme from Bruker (SIMFONIA). Accurate g values were obtained using a Bruker ER 035M NMR Gaussmeter. The position of the probe in the field relative to the sample was corrected for by using a sample of the perylene radical cation ($g = 2.002569 \pm 0.000006$) in H_2SO_4.[63]

4.7 Results

4.7.1 ESR and ENDOR of the model VO sulfate complex

The ESR spectrum of a frozen solution (10 K) of the vanadium sulfate in DCM/toluene solvent is shown in figure 4.7. The corresponding computer simulation of the spectrum is also shown in figure 4.7 (dotted trace), and the resulting spin Hamiltonian parameters are listed in table 4.2. Since the spectrum is well simulated, based on a pure $g_{\|}$ and $g_{\perp}$ tensor, it means that the magnetic symmetry is almost perfectly axial for this hydrated complex.

Table 4.2: Spin Hamiltonian parameters for the vanadyl complex

V(IV) Sample	$g_{\|}$	$g_{\perp}$	$A_{\|}$ / MHz	$A_{\perp}$ / MHz
VO – sulfate	1.932	1.9768	546.2	208.3
VO-tanned leather	1.938	1.9768	517	193

The strong anisotropy of the vanadyl hyperfine splitting tensor, together with its axial symmetry, offers the opportunity to obtain well-resolved 'single-crystal like' ENDOR spectra, with high orientational selectivity, by saturating selected turning points in the ESR spectrum.

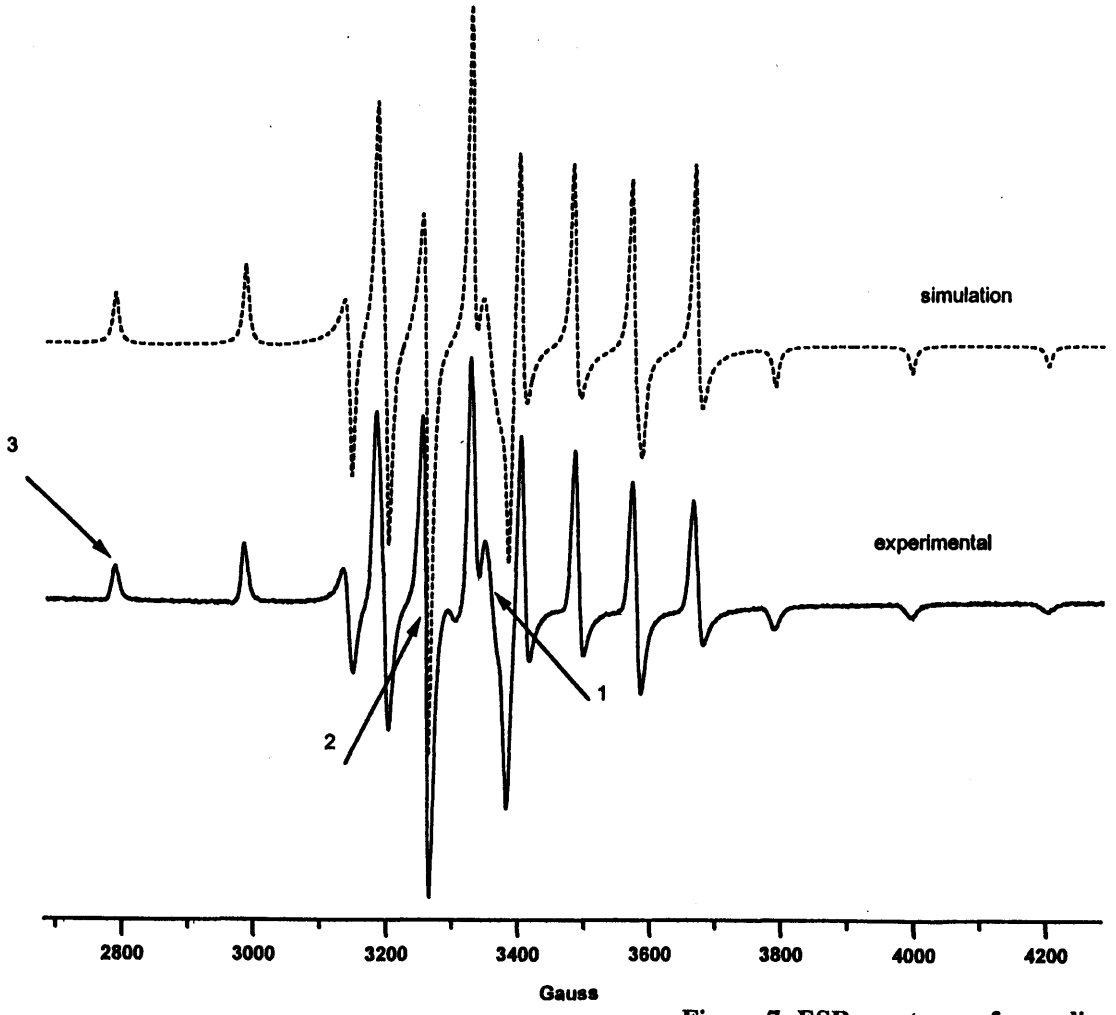

Figure 7: ESR spectrum of vanadium sulfate

Field settings marked 1, 2 and 3 in figure 4.7 indicate the ESR peaks which were saturated in order to obtain respectively the ENDOR spectrum from all orientations, a pure perpendicular ENDOR spectrum ($\perp$) and a pure parallel ENDOR spectrum ($\|$), shown in figure 4.8 (a-c respectively). Note that the $\|$ and $\perp$ symbols refer to the V=O bond direction. The measured proton couplings for the complex are listed below in table 4.3.

Table 4.3: ^{1}H couplings for the hydrated VO complex

Proton	$A_{\|}$ / MHz	$A_{\perp}$ / MHz
H_{Ax}	6.0	2.9
H_{Eq}	4.7	<2.5

The ENDOR Induced ESR spectrum (EIE) of the VO complex was subsequently recorded and is shown in figure 4.9. The EIE experiment is obtained by positioning the NMR frequency on one of the $\|$ and $\perp$ ENDOR lines (positions 1 and 2 respectively in figure 4.8), and the intensity changes of this line are recorded while the external magnetic field is swept over the range of ESR absorptions. Since the EIE experiment represents the amplitude change of the first derivative ENDOR line, it has the appearance of an absorption spectrum. The EIE method is generally used in EMR spectroscopy for deconvoluting complex ESR spectra, containing signals from more than one species. In the present case, the EIE approach was adopted in order to clarify whether the true parallel and perpendicular directions were chosen using the proton hyperfine tensor as a reference frame. In other words, the feature at position 1 in figure 4.8 corresponds to the axial proton of the hydrated complex, with its local magnetic field parallel to the V=O direction (ie, $\theta = 0°$). This produces the features in the EIE spectrum which arise purely from the parallel components, figure 4.9a. Again, the feature in figure 4.8b at position 2 corresponds to the axial proton with its local magnetic field perpendicular to the V=O direction (ie, $\theta = 90°$) and similarly gives the pure perpendicular EIE spectrum, figure 4.9c.

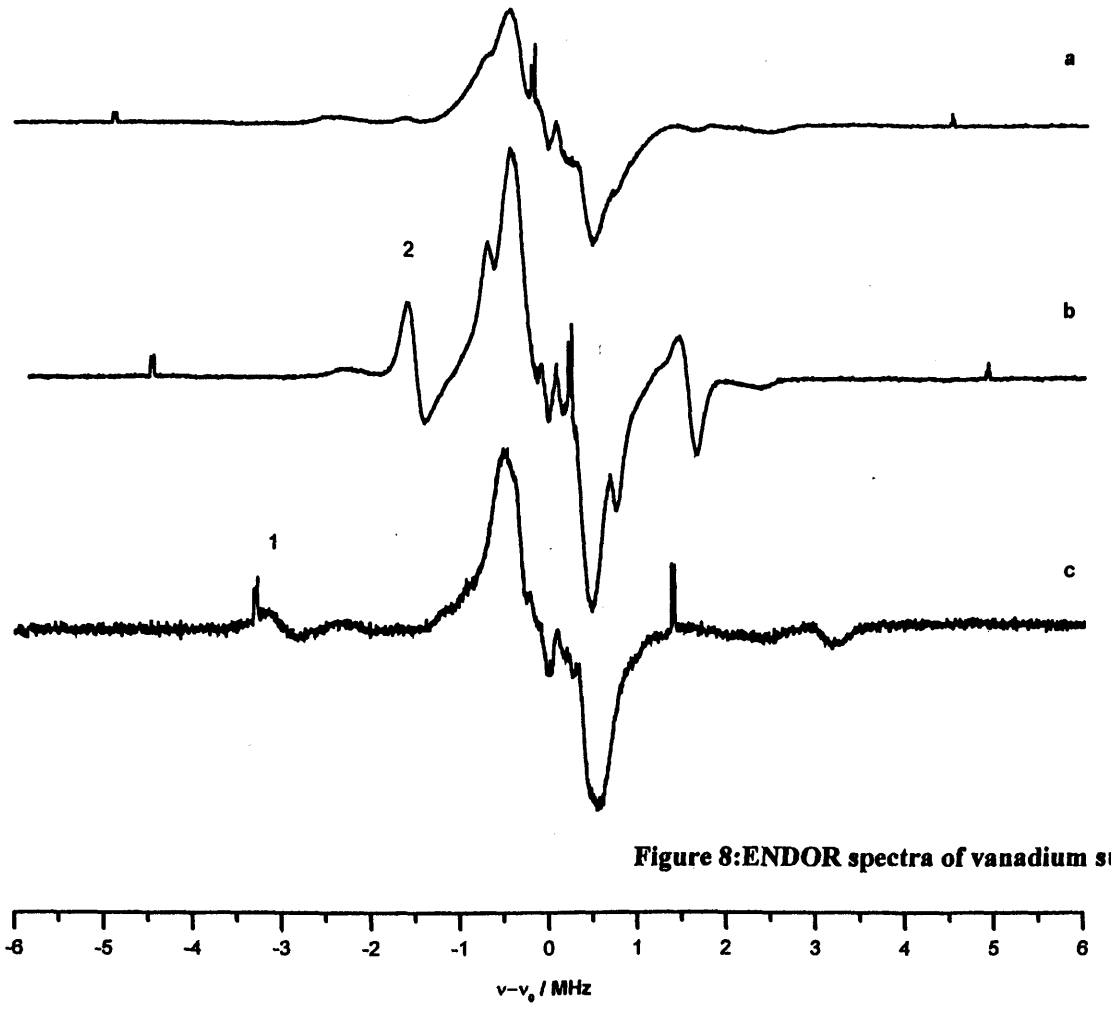

Figure 8:ENDOR spectra of vanadium sulfate

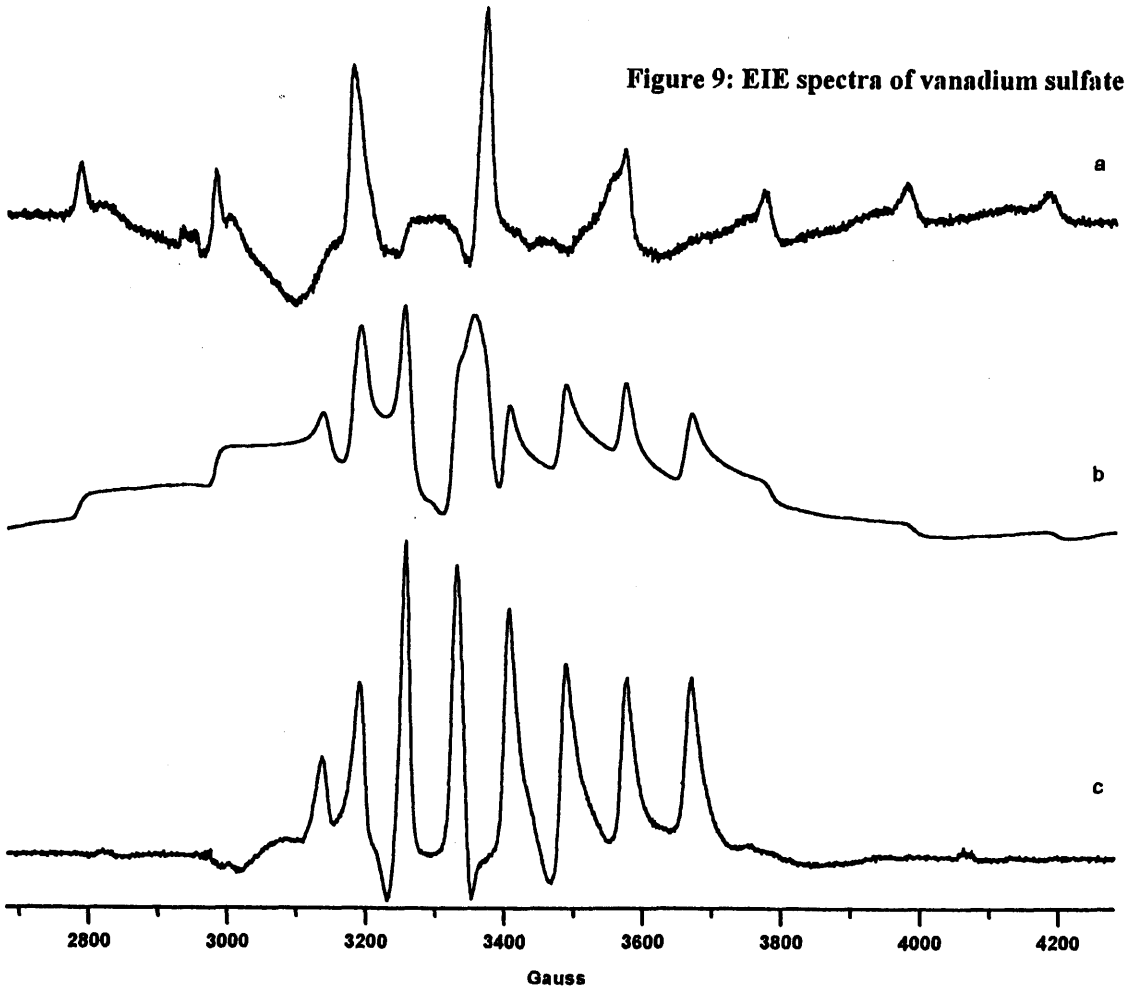

Figure 9: EIE spectra of vanadium sulfate

4.7.2 ESR and ENDOR of VO-SO_4 tanned leather

The above ESR and ENDOR spectra represent the situation observed for the model complex, hydrated VO sulfate in solution, and offers an excellent comparison for the spectra obtained in the case of the tanned leather sample. The ESR and ENDOR spectra of the tanned leather are shown in figures 4.10 and 4.11 respectively. The 10K ESR spectrum of the vanadyl tanned leather is shown in figure 4.10. The corresponding computer simulations are again shown in the figure (dotted trace) and the resulting spin Hamiltonian parameters listed in table 4.2. It is clear that the two ESR spectra, figures 4.7 and 4.10, have significantly different line widths. Nevertheless, the measured spin Hamiltonian values are quite similar, except for the very small decrease in hyperfine couplings for the tanned leather sample. This slight decrease in the hyperfine coupling suggests a small lowering in the symmetry of the complex, very likely induced by the distortions of the water ligands. The slightly broadened line widths of the tanned leather are expected considering the heterogeneity and non-uniformity of the leather sample. Essentially, there will be a small contribution to the ESR line width from the small anisotropic distortions from the surrounding medium.

The corresponding ENDOR spectra were measured at the same field positions as those described above for the pure hydrated VO case; the resulting spectra are shown in figure 4.11. For comparison, the analogous ENDOR spectra for the pure VO complex are superimposed (shown in grey) on the ENDOR spectra for the tanned leather sample. Although the signal to noise ratio is not good for the leather sample, nevertheless there is some similarity between the two spectra. Only in the case of the mixed and pure perpendicular spectra, figure 4.11a and b, are there significant differences (ie, the unknown lines marked with the * symbol).

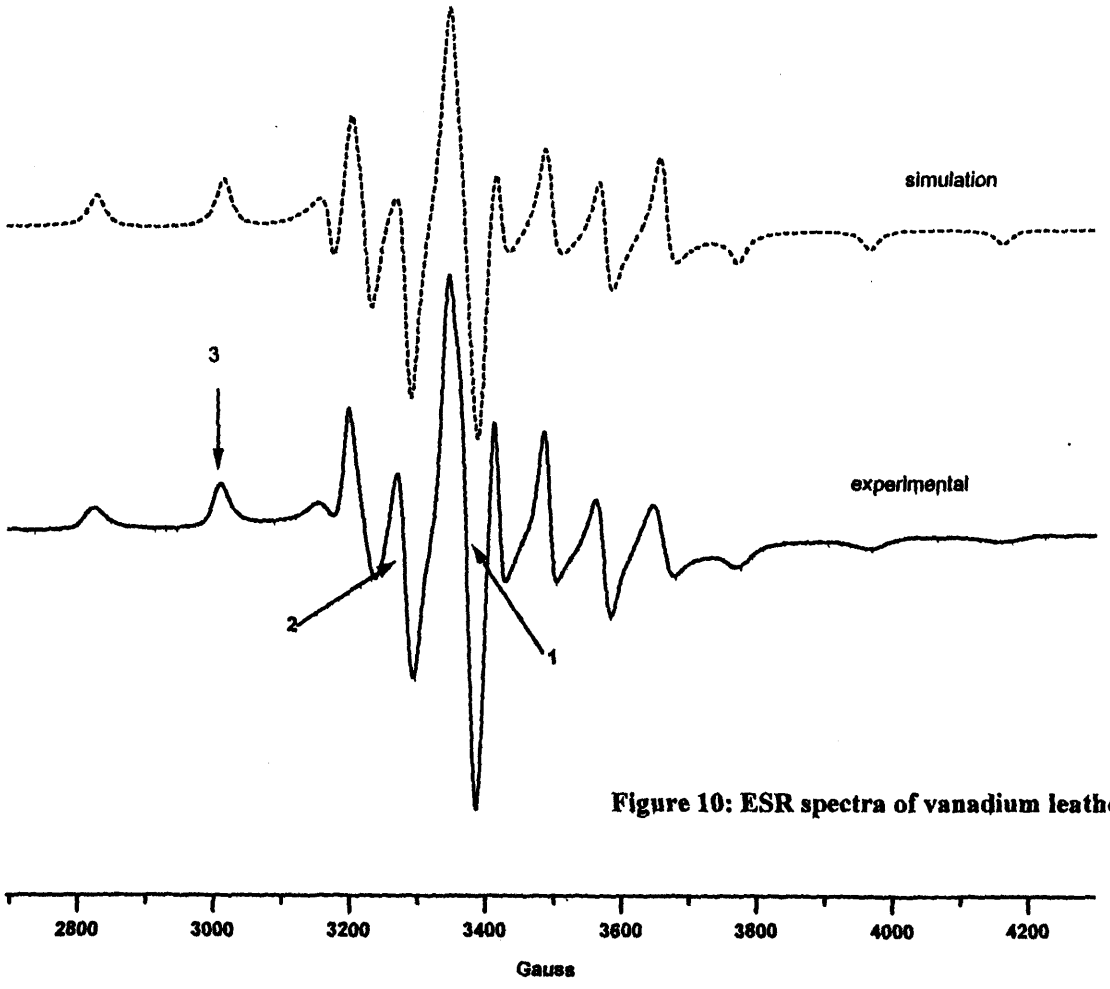

Figure 10: ESR spectra of vanadium leather

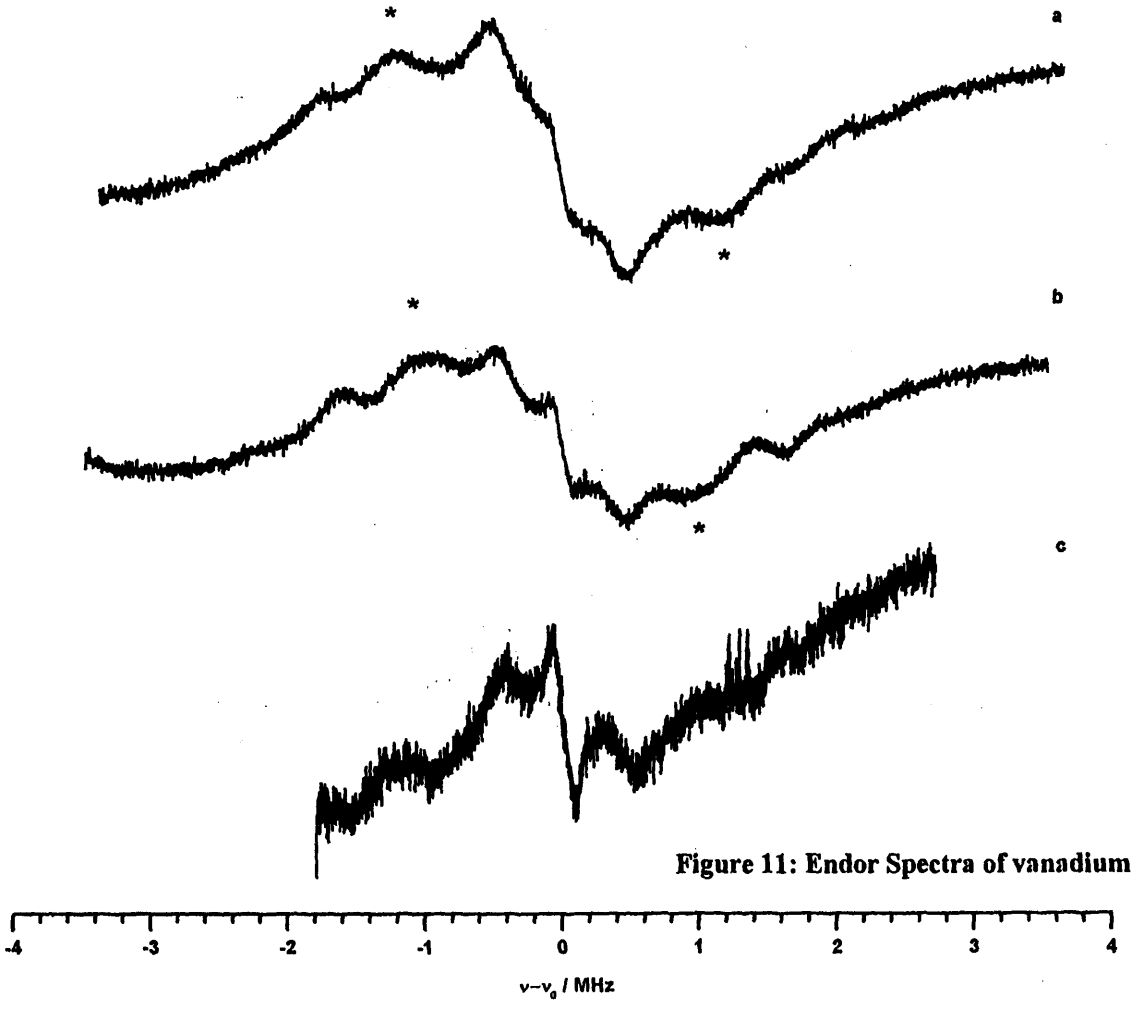

Figure 11: Endor Spectra of vanadium leather

4.7.3 ESR and ENDOR spectra of the titanium (III) sulfate, gluconate and citrate complexes

The ESR spectrum of the titanium sulfate complex at 10K is shown in figure 4.12. As before, the computer simulation of the ESR spectrum is also shown in figure 4.12, and the corresponding spin Hamiltonian parameters are given in table 4.4. Owing to the small g anisotropy of the Ti ion, the ESR spectrum is not as well resolved compared with the vanadium case described above, and the line widths appear quite broad. The corresponding ENDOR spectra are shown in figure 4.13. These spectra were measured at the magnetic field positions marked 1 and 2 in figure 4.12, corresponding to the perpendicular and parallel orientations respectively. For comparison, the corresponding ENDOR spectra of the pure $\perp$ and $\|$ VO-sulfate are shown in figure 4.14b and d. The analogous $\perp$ and $\|$ Ti-sulfate are shown in 4.14a and c. There are some clear and distinctive differences between the two and these differences have implications for the structural co-ordination of the transition metal ions in solution as discussed in the next section.

Table 4.4: Spin Hamiltonian parameters for the titanium complexes of sulfate, gluconate and citrate

Ti(III) Sample	$g_{\|}$	$g_{\perp}$
Ti – sulfate	1.993	1.903
Ti – gluconate	1.978	1.942
Ti – citrate	1.977	1.937

The ESR spectra for the Ti gluconate and citrate complexes are shown in figure 4.15. The ENDOR spectra for the gluconate and citrate samples were also measured at 10K and the resulting spectra are shown in figures 4.16 and 4.17. As described above the ENDOR spectra were measured at the appropriate turning points in the ESR spectrum corresponding to the $\|$ and $\perp$ directions. In the case of the Ti(III) sulfate sample, the measured proton couplings are listed in table 4.5.

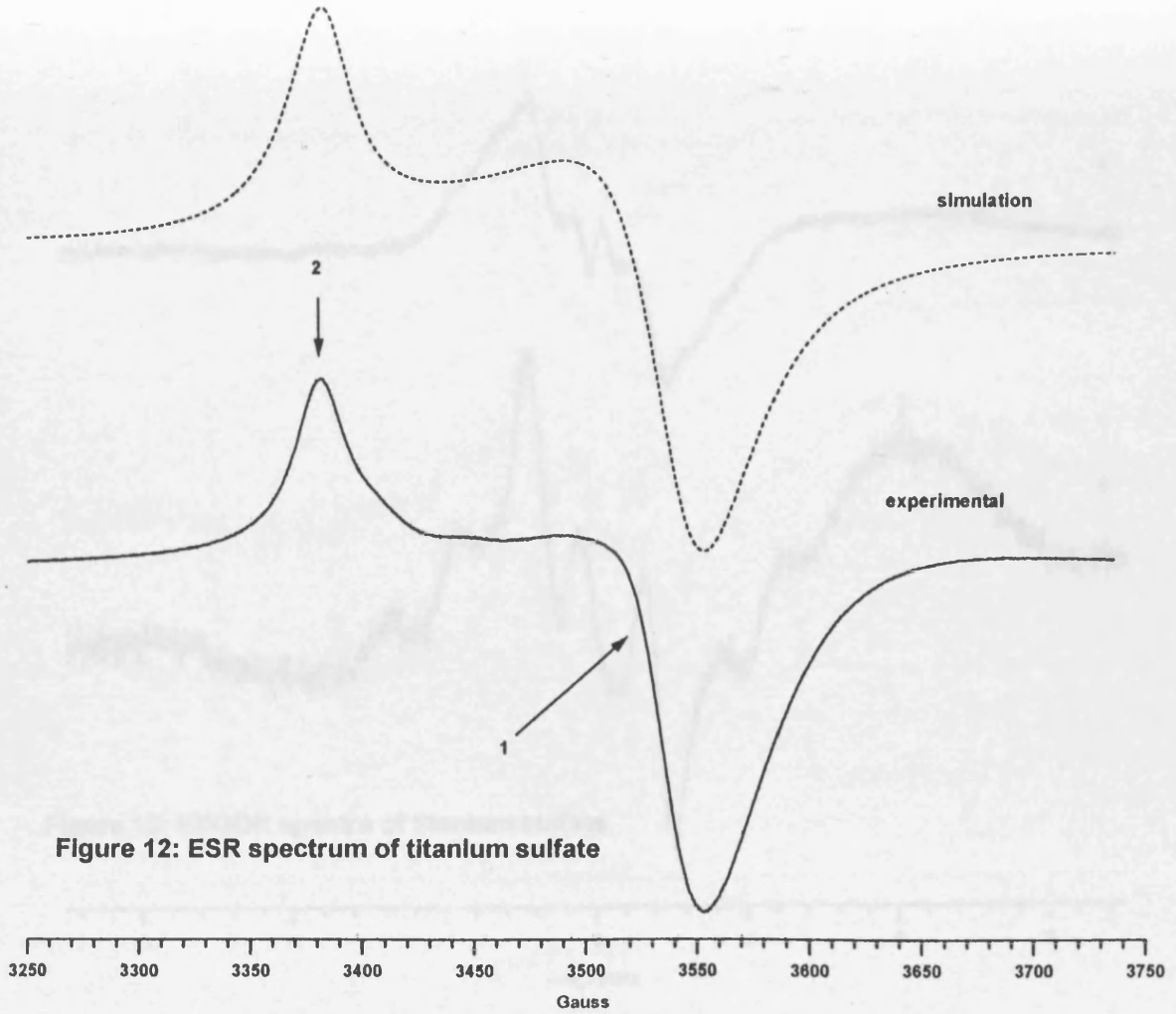

Figure 12: ESR spectrum of titanium sulfate

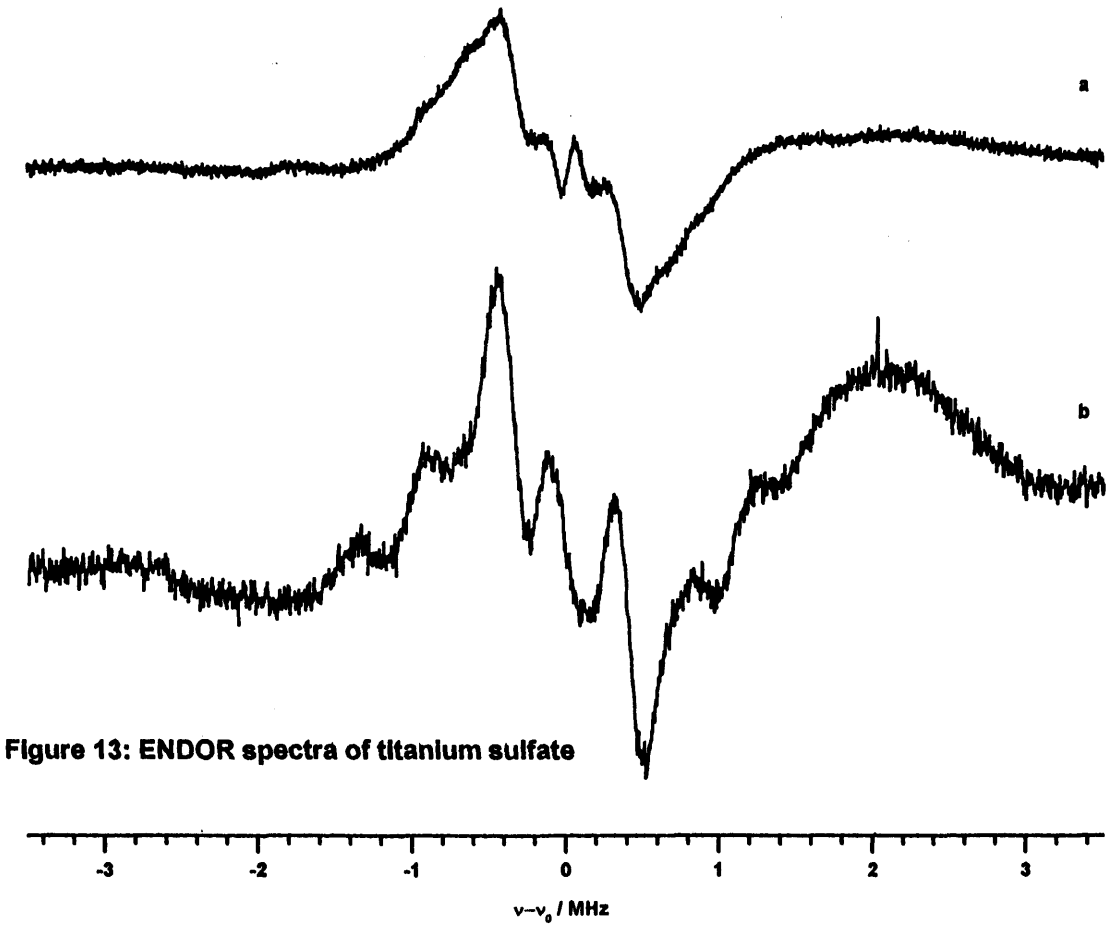

Figure 13: ENDOR spectra of titanium sulfate

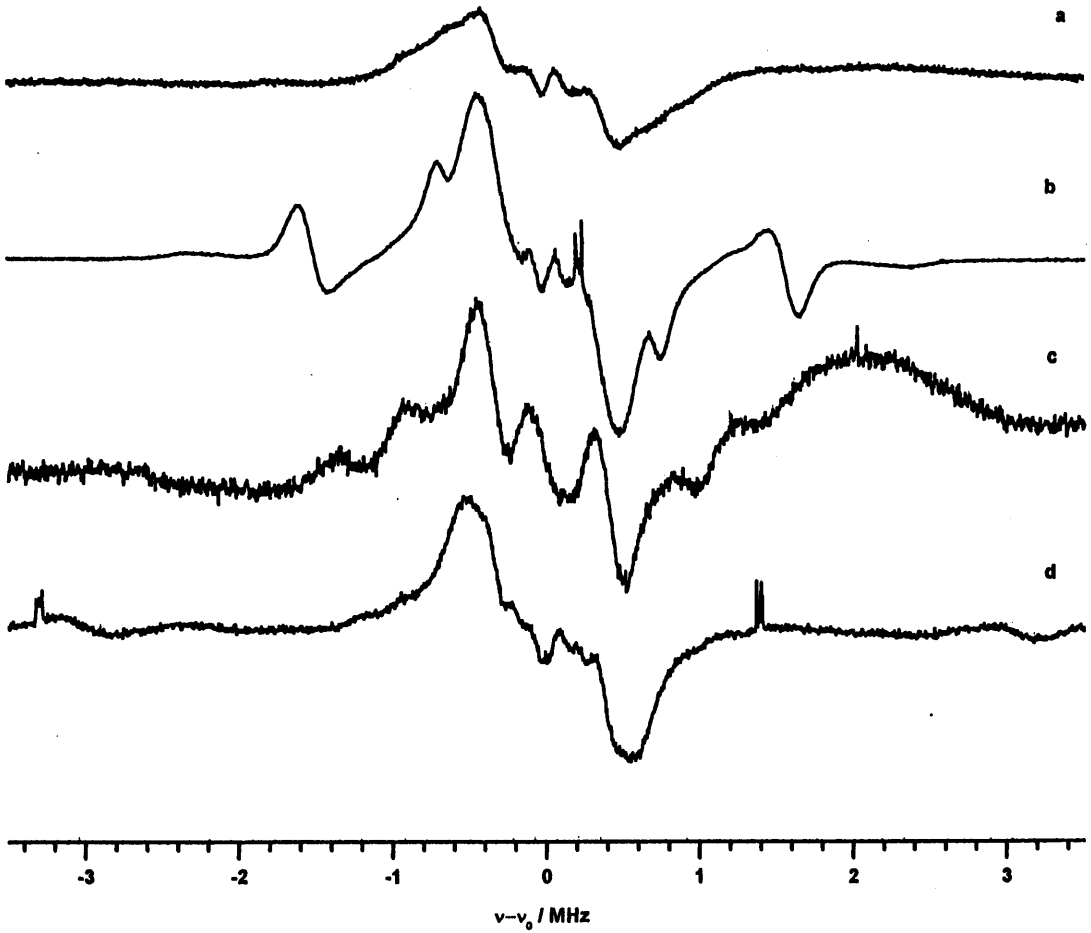

Figure 14: ENDOR spectra for vanadium and titanium sulfate

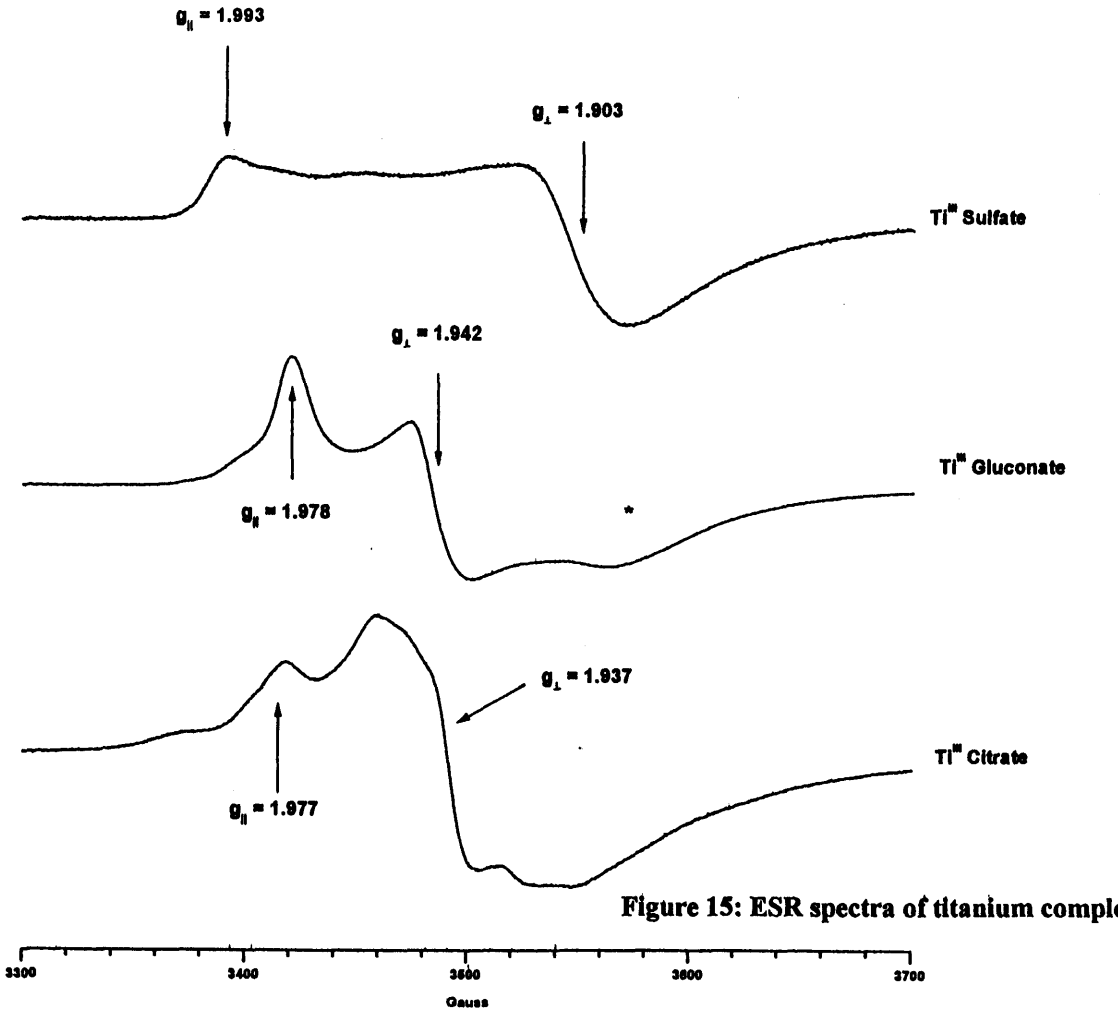

Figure 15: ESR spectra of titanium complexes

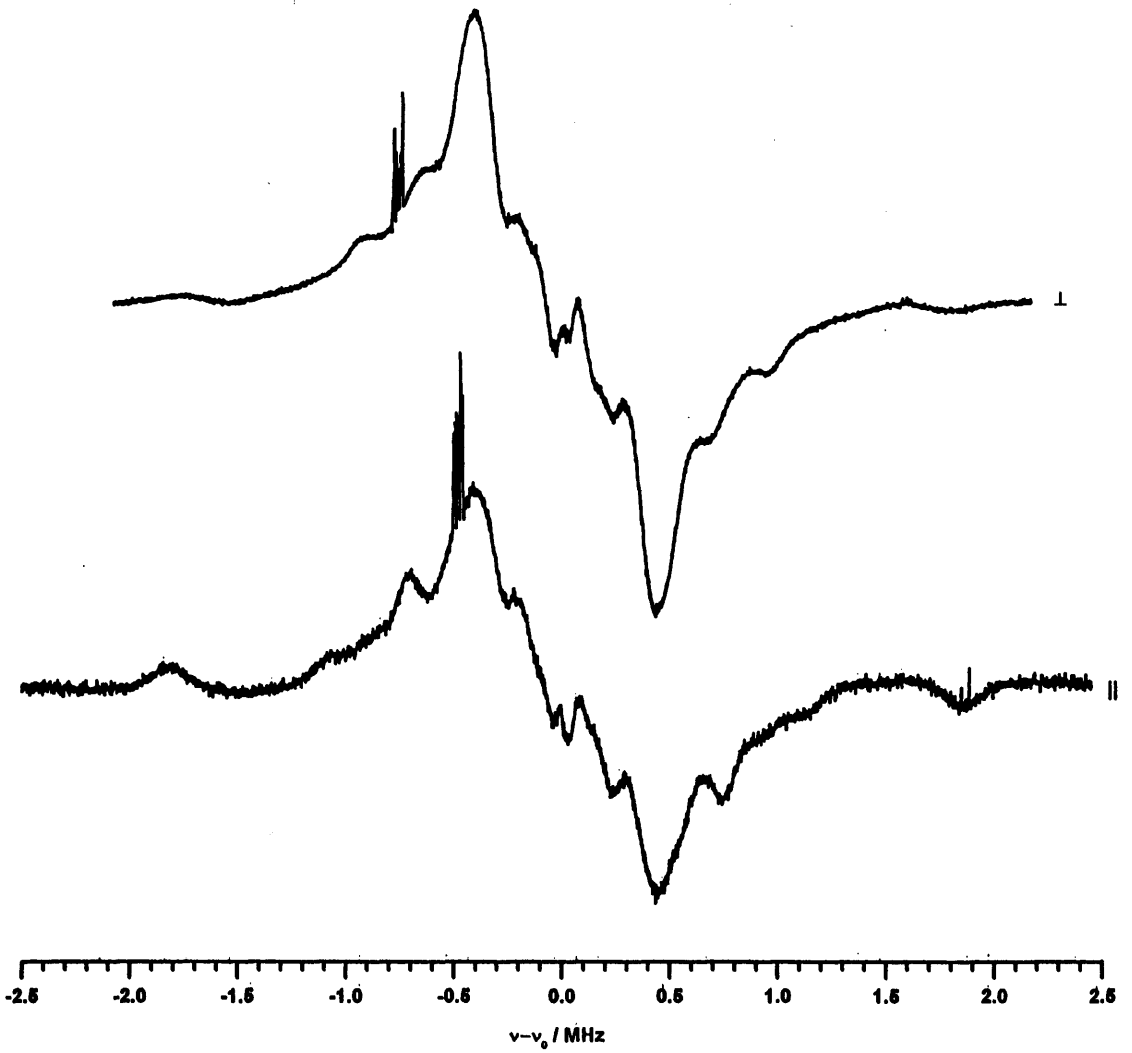

Figure 16: ENDOR spectra for titanium gluconate

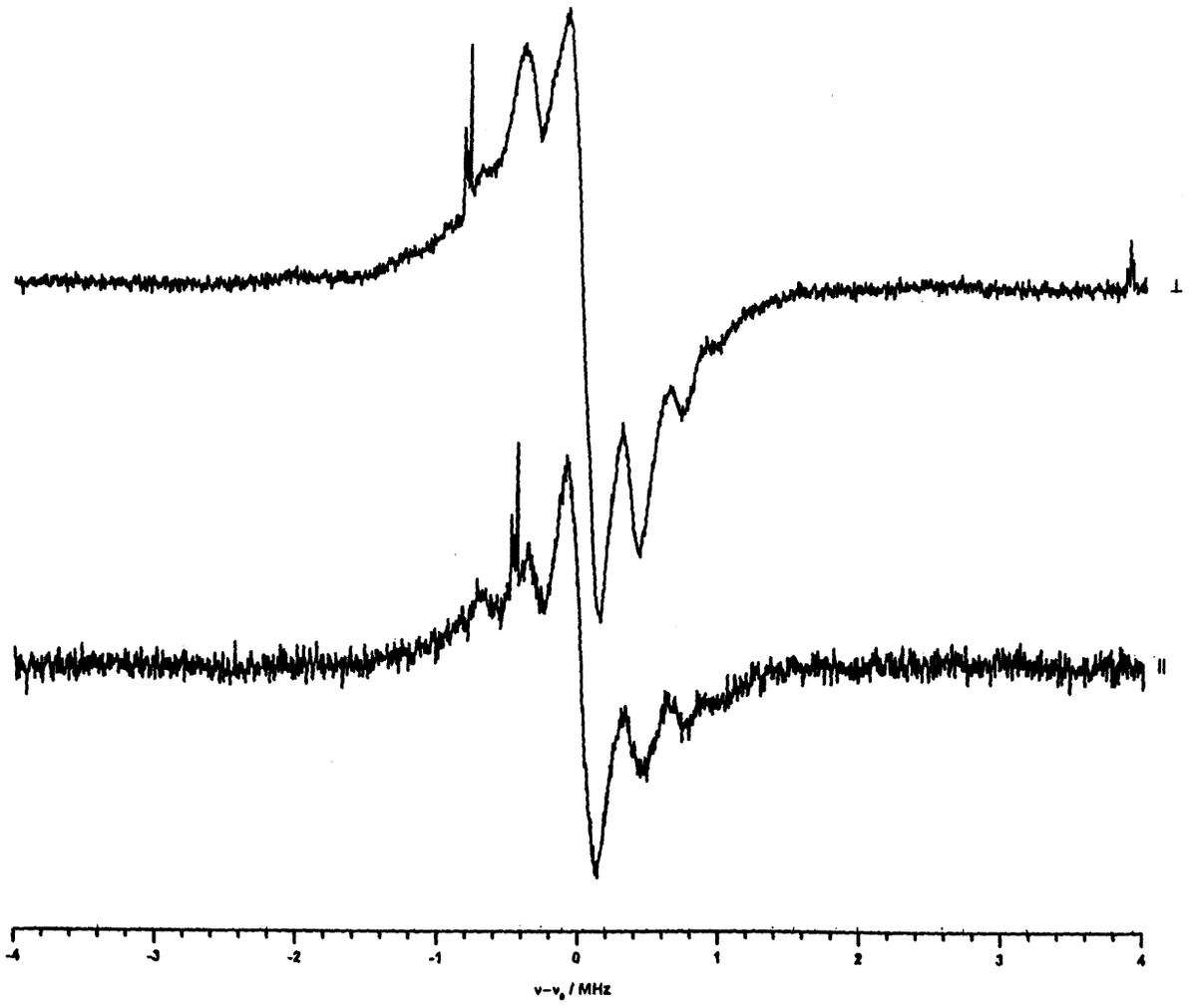

Figure 17: Endor of titanium citrate

Table 4.5: Measured ^1H couplings for the hydrated Ti(III) sulfate complex

Proton	A_1 / MHz	A_2 / MHz	A_3 /MHz
H_{Ax}	1.9	1.8	3.4
H_{Eq}	1.0	1.0	1.4

4.7.4 ESR of titanium (III) tanned leather

The ESR spectrum of a sample of titanium (III) tanned leather is shown in figure 4.18. Unlike the spectrum recorded for the vanadyl tanned leather sample, the spectrum is weak, poorly resolved and arises from the presence of more than one paramagnetic species. There are certainly traces of titanium (III) species, with characteristic g values typical of those observed for the hydrated $TiSO_4$ case. However, the well defined geometry and characteristic profile of the Ti(III) species is not observed, indicating significant distortions to the surrounding Ti(III) environment. The sharp signal at 2.0036 is unidentified, but most certainly arises from a carbon centred radical impurity. Such radicals generally produce a symmetric resonance around the free spin g value, and their precise assignment to a specific carbon centred fragment cannot be easily made, based only on the ESR measurements. The low field resonances at $g > 2$ are not fully understood. Because the electron g value is greater than 2.0023, these signals cannot arise from any Ti(III) state, for which the g value is always less than 2.0023, or any carbon based radical state, for which the g values are always close to free spin g=2.0023. The only remaining alternative assignments are:

- the presence of oxygen centred radicals, such as oxy- or peroxy- type radical (eg, $RO_x^{\bullet}$), quite common when there are carbon centred radicals in the presence of an oxygen environment, or
- another impurity transition metal ion with an electron configuration of greater than d^5. In that case the g values are expected to be greater than 2.0023.

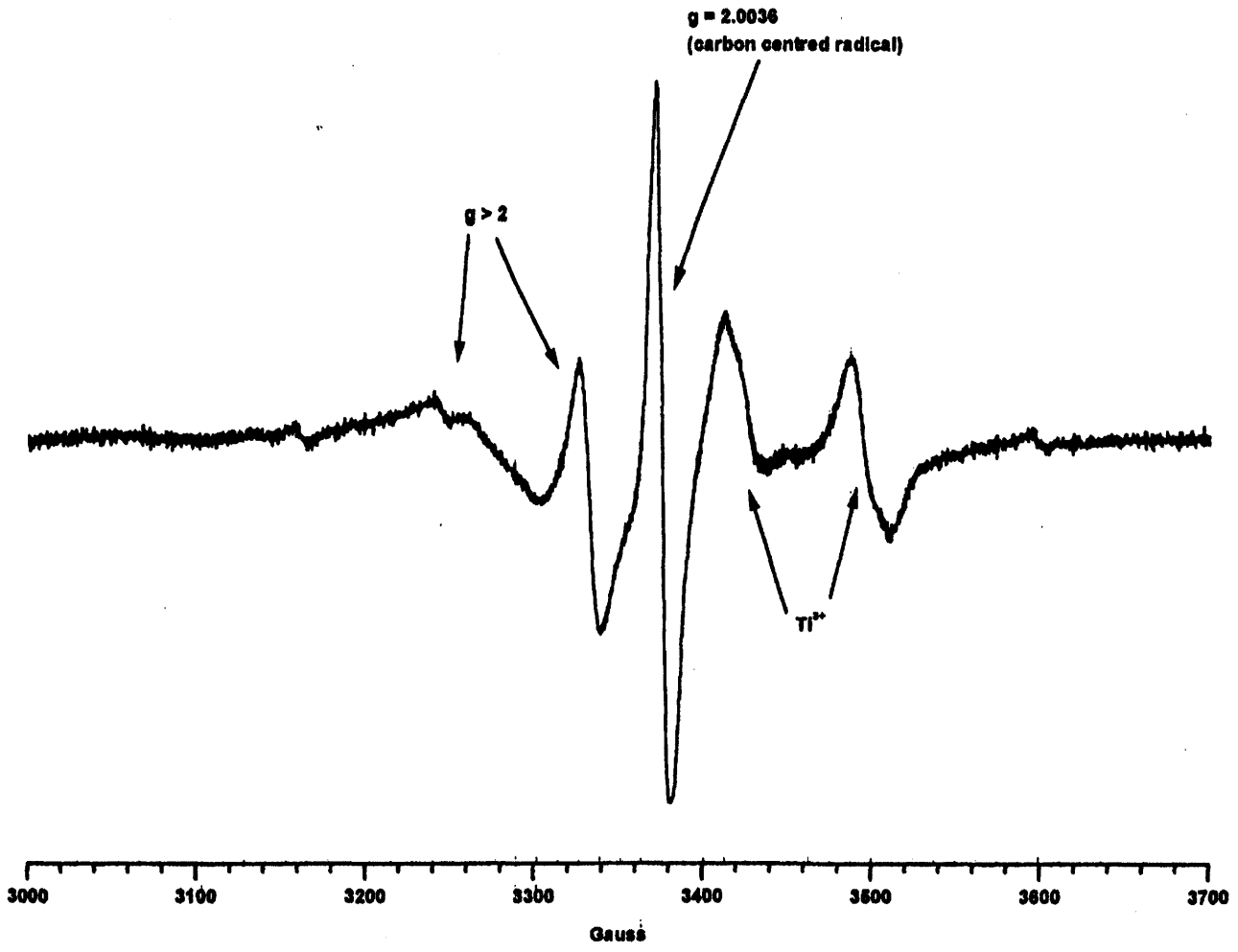

Figure 18: ESR of titanium leather

4.8 Discussion

4.8.1 ESR spectra of the hydrated titanium and vanadium ions

It was mentioned in the theory section that ESR has played a paramount role in the study of transition metal ions in inorganic complexes, biologically important molecules, such as metalloenzymes, and solid materials. The interpretation of the spectra for paramagnets with S>½ can, however, be complex. Fortunately, for d^1 transition metal ions such as Ti^{3+} and V^{4+}, the ESR spectra are more straight forward to analyse.

Ti^{3+} and V^{4+} usually exhibit octahedral or tetrahedral symmetry in co-ordination compounds, which splits the five-fold degenerate state of the free ion into two states, t_{2g} and e_g, which are, respectively, triply and doubly degenerate. The degeneracy of these two states is further lifted by other effects, which lead to structural distortions. The two most common cases experienced in ESR are tetragonal or trigonal distortion. These occur by compression or elongation of the tetrahedral or octahedral structures. The g values in the two cases are then evaluated on the basis of perturbation theory. In certain cases, such as tetragonally distorted tetrahedral crystal fields or a trigonally distorted octahedral field (D_{3d} symmetry), the 'theoretically' predicted g values have the form $g_{||} = g_e$ and $g_{\perp} = g_e - 6\lambda/\Delta$ (ie, $g_{||} > g_{\perp}$). In the common instance of tetragonally distorted octahedral fields, the g values take the form $g_{\perp} = g_e - 2\lambda/\Delta$ and $g_{||} = g_e - 8\lambda/\Delta$ (ie, $g_{\perp} > g_{||}$). In the former case, due to a small amount of spin orbit coupling, the $g_{||}$ value is never exactly 2.0023.

The ESR spectrum of the vanadium (IV) hydrated complex has the form $g_{\perp} > g_{||}$, while the titanium (III) complexes have the form $g_{||} > g_{\perp}$, table 4.2 and 4.3. This means that from the ESR viewpoint the paramagnetic vanadium species experiences a tetragonal distortion to the octahedral field, while the paramagnetic titanium species experiences either a tetragonally distorted tetrahedral environment or a trigonally distorted octahedral environment (D_{3d}

symmetry). Considering that the titanium ions should be completely hydrated in the aqueous solution, as $[Ti(H_2O)_6]^{3+}$ species, the trigonally distorted octahedral field is the most favourable symmetry case and is in agreement with the suggested symmetry quoted in the papers cited in the introduction.

Because of the low abundance of ^{47}Ti and ^{49}Ti, which have a nuclear spin of 5/2 and 7/2 respectively, no hyperfine interaction is observed. $^{48}Ti^{3+}$, which has I = 0, cannot exhibit hyperfine structure.

The ESR spectra of the gluconate and citrate samples are more complex, figure 4.15. Although they have a predominant g tensor of $g_{\|} > g_{\perp}$, indicating trigonal distortion, the magnitude of the g values indicates that the extent of this distortion or splitting is different compared with the Ti(III) sulfate case. These complex spectra, observed for the gluconate and citrate samples, can be interpreted based either on a non-axial g tensor (such as an orthorhombic) or a heterogeneity of complexed titanium (III) ions in solution. Given the nature of the tanning bath, which contains a number of different metal complex species, the latter explanation would be more appropriate. The consequences of these interpretations for the structure of the hydrated complexes based on the ^1H ENDOR data will be discussed later.

The V^{4+} ion has a similar d^1 electronic structure to Ti^{3+}, and based on the g values given in table 4.2, it is most likely that the ion possesses a tetragonally distorted octahedral environment. In this case, the high abundance of ^{51}V dominates the V^{4+} spectrum, with two overlapping 8-line hyperfine patterns (I=7/2, number of lines is therefore 2I+1 = 8). The presence of this large A anisotropy is very important because it allows well resolved ^1H ENDOR spectra to be obtained.

4.8.2 ^1H ENDOR spectra of the hydrated $[Ti(H_2O)_6]^{3+}$ and $[VO(H_2O)_5]^{4+}$ ions

The ESR data has provided evidence on the nature of the point symmetry for the hydrated metal ions in aqueous solution. The presence of different sets of water molecules can be

detected in the ENDOR spectrum, as described in detail by Li *et al*[64]. The ^{1}H ENDOR measurements, however, provide far more information on the spatial orientation of the surrounding protons in the hydrated complex. By combining the information from both techniques, a detailed structural view of the hydrated complexes can be constructed. The aim of this work is to examine the perturbation and changes to the structure of the hydrated complexes in solution after interaction with the carboxylic acid groups of the collagen or the interaction seen with the vegetable tannin.

4.8.2.1 Structure of the hydrated $[VO(H_2O)_5]^{4+}$ complex and the VO tanned leather

The measured ^{1}H couplings from the ENDOR spectrum, figure 4.8 and table 4.3, show there are two sets of equivalent protons in the hydrated vanadyl complex. Based on the ESR spectrum shown in figure 4.7, a g tensor which is characteristic of a tetragonally distorted octahedral species can be observed. This suggests that the hydrated complex has a structure analogous to that shown in figure 4.19. The ligated water molecule in the *z* direction (V=O bond direction) is regarded as the source of the 'axial' protons, while the water molecules in the *xy* plane produce the ^{1}H couplings for the 'equatorial' protons.

The proposed structure must possess a high degree of symmetry, because the superhyperfine couplings with the water protons have their principal axis pointing exactly along the direction of the g axis framework. In other words, the parallel direction of the axial protons lies directly along the V=O bond, while the parallel direction of the equatorial protons lies in the *xy* plane. If the four equivalent water molecules in the *xy* plane experienced some form of distortion, effectively lifting them out of the xy plane, then the fourfold equivalency of protons would be removed and the resulting ENDOR spectra would contain characteristic peaks indicative of three or more sets of protons. This is not the case, providing strong evidence that all four equatorial water molecules lie in the plane.

The couplings reported in table 4.3 are also quite large compared with those observed for the titanium species, and this indicates that the water molecules are tightly co-ordinated to the VO centre. In particular the axial water molecule, bonded along the z direction, is more strongly coordinated, having the largest coupling, compared with the equatorial waters.

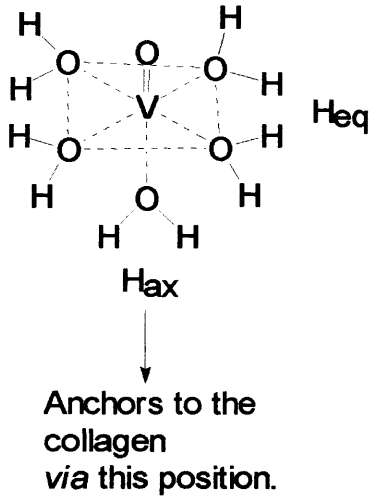

Figure 4.19 (a): Hydrated vanadyl complex

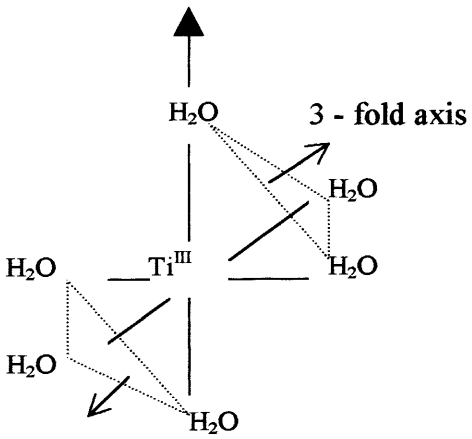

Scheme 4.19 (b): Hydrated titanyl complex

The ENDOR spectrum of the VO tanned leather sample was not as intense or well resolved compared with the pure hydrated VO solution, figure 4.11. Nevertheless some unmistakable

characteristics may be observed. The ^1H couplings associated with the axial water molecules are absent; although the couplings characteristic of the equatorial waters appear to remain, an additional coupling of approximately the same magnitude can be seen (marked with the * symbol). One interpretation for this spectrum is that the partially hydrated VO complex has bonded to the vegetable tannin or collagen surface perpendicular to the V=O (ie, the axial water molecule is removed, and the empty coordination replaced by a surface group). The spatial distribution of the equatorial waters (protons) is clearly more complicated in this case, and at least two sets of equatorial water groups could exist. Again such a distribution of proton ligands in the equatorial plane is not surprising if the VO species is bonded along the OV→ direction, perturbing the orientation of the ligands out of the *xy* plane.

4.8.2.2 (b) Structure of the hydrated $[Ti(H_2O)_6]^{3+}$ complexes and Ti tanned leather

The ESR spectra of the aqueous Ti(III) ions in the presence of various ligating ions including sulfate, gluconate and citrate are shown in figure 4.15 (a-c) respectively, while the corresponding ENDOR spectra are shown in figure 4.14, 4.16 and 4.17. Despite the changes and complexity of the individual ESR spectra, the g values all have the form $g_{\|} > g_{\perp}$. As discussed above this indicates a trigonally distorted octahedral environment for the ion. In addition, since the magnitude of the $g_{\|}$ values vary depending on the nature of the ligating ion, it is clear that the extent of the trigonal distortion is affected by the complexing ions in the solution, ie there is some ligation. The biggest effect can be seen by comparing the ESR spectra of the titanium (III) sulfate, figure 4.15a, and titanium (III) gluconate, figure 4.15b, where both $g_{\|}$ and $g_{\perp}$ values varied significantly.

The ESR spectrum of the titanium (III) sulfate species possesses almost pure axial symmetry, with little interference from additional features and, therefore, the ENDOR spectra of this complex were examined in detail. Depending on the extent of the distortions, the Ti - H_2O distance will vary so there should be more than one set of equivalent protons (or water

molecules). Assuming maximum distortion along the *z*-axis, then the six water molecules will at the simplest level split into two groups; the first group lying along the *z*-axis while the second group of four should lie in the *xy*-plane. However, with further distortions in the *xy*-plane, then three or more groups of water molecules would be expected.

It is clear from the analysis of the ^1H hyperfine tensors, table 4.5, that only two sets of equivalent protons are present in this hydrated complex. Based on the symmetry information derived from analysis of the g tensor components, the structure shown in figure 4.19 (b) can be proposed for this complex.

Analysis of the ENDOR spectrum for Ti(III) sulfate reveals the presence of two sets of proton couplings, see figure 4.14. Unlike the case observed for $[VO(H_2O)_5]^{4+}$, the A tensor of the protons is not positioned exactly along the principal g axis framework of the complex, so an orthorhombic A tensor is observed. In addition, the magnitude of the ^1H couplings for the hydrated titanium (III) complex are slightly less than those for the VO case, indicating that the water ligands are bound less tightly by the trivalent titanium cation. By comparison, the ^1H ENDOR spectrum of the Ti(III) gluconate system, figure 4.16, is far more complicated and reveals the presence of at least three distinctive couplings. One explanation for this is extra distortion to the water ligands in the *xy* plane (in a sense generating three sets of equivalent proton groups, for example from D_{3d} to a lower point symmetry such as D_{2d}). Such an assignment is supported by the orthorhombic g tensor observed in the ESR spectrum, figure 4.15b, indicative of a lowering of the point symmetry around the cation. However, it is impossible to rule out the possibility of a mixed ESR spectrum; in other words, the high field peak in figure 4.15b (labelled *) arises from the $g_\perp$ value of the hydrated Ti(III) sulfate species at $g_\perp = 1.903$. In this case, some of the hydrated Ti(III) cations in the presence of gluconate, produce a trigonally distorted octahedral symmetry as shown in figure 4.19b, while others have a slightly different spatial orientation of the surrounding water ligands. This effect would

ultimately produce a mixed ENDOR spectrum with contributions coming from both hydrated complexes. Accurate assignment becomes very difficult in such cases. An analogous situation exists for the Ti(III) citrate sample. The ESR spectrum, figure 4.15, is too complicated to be explained exclusively on the basis of a single Ti(III) complex, and more likely arises from a mixture of slightly different hydrated complexes.

However, it is interesting to note that the overall magnitude of the proton couplings, measured from the ENDOR spectra, decreases from Ti(III) gluconate, to sulfate to citrate. In other words, the water ligands are less tightly bound to the cation from gluconate to citrate. This may have consequences for anchoring the Ti(III) complex to the collagen. The more weakly complexed water molecules of the Ti(III) citrate may be more favourable for interaction with the ionised carboxylic groups on the collagen or allow a more powerful electrostatic interaction between the charged centres.

Unlike the case for the ESR spectra of the VO tanned leather sample, the ESR spectra for the Ti(III) tanned leather is extremely weak. It was not possible to measure the ENDOR spectra in order to study the structure of the anchored titanium complex. The ESR spectrum itself, figure 4.18, is quite weak, and suggests that only a small fraction of the Ti is in the paramagnetic state. Furthermore, at least two distinctive Ti(III) peaks can be observed, indicating two slightly different co-ordination environments (locations) for the anchored titanium species.

4.9 Conclusion

EMR studies have shown that even though titanium as the trivalent salt was used to tan the collagen, the majority of the species involved in tanning are tetravalent titanium. Thus, in terms of tanning, it would be simpler to start with a solid titanium (IV) salt, such as ammonium titanyl sulfate.

The fact that emr analysis of vanadium (IV) species has highlighted specific metal binding sites indicates that ESR and related techniques may be a useful tool in investigating the interaction of metals with collagen.

5 Spectroscopic investigations

A number of spectroscopic techniques have been used in this study to understand, at the molecular level, the mechanisms involved in mineral tannages. The first three, nuclear magnetic resonance dispersion (NMRD), extended x-ray absorption – fine structure (EXAFS) and x-ray absorption – near structure (XANES) are discussed in detail.

Other techniques, such, higher band electron spin resonance and solid state nuclear magnetic resonance (SS-NMR) were also investigated. The results from these investigations are discussed at the end of the chapter.

5.1 Nuclear Magnetic Resonance Dispersion

5.1.1 Introduction

In this section, the work involved an investigation into the role of water in stabilising the collagen structure in the presence of tanning agents. NMRD, a technique that measures the relaxation rate of water molecules in proteins, was used. First, the background to this technique is reviewed and then the results, comparing the interaction of titanium (III) and chromium (III) with soluble collagen, are discussed.

5.2 Background [65,66]

5.2.1 Spin

Spin is a fundamental property of nature, like electrical charge or mass. It comes in multiples of ½ and can be + or -. Protons, electrons, and neutrons possess spin and individual unpaired electrons, protons, and neutrons each possesses a spin of ½.

In the hydrogen atom (^{1}H), with one unpaired electron and one unpaired proton, the total electronic spin = ½ and the total nuclear spin = ½.

Two or more particles with spins having opposite signs can pair up to eliminate the observable manifestations of spin. An example is helium. In nuclear magnetic resonance, it is unpaired nuclear spins that are of importance.

5.2.2 Properties of Spin

When placed in a magnetic field of strength B, a particle with a net spin of ν can absorb a photon, of frequency λ. The frequency depends on the gyromagnetic ratio, γ, of the particle.

$\nu = \gamma B$

For hydrogen this is 42.58 MHz.

5.2.3 Nuclei with Spin

Almost every element in the periodic table has an isotope with a non zero nuclear spin. NMR can only be performed on isotopes whose natural abundance is high enough to be detected. Some of the nuclei that are of interest in NMRD are listed below.

Table 5.1: Properties of nuclei used in NMRD

Nuclei	Unpaired Protons	Unpaired Neutrons	Net Spin	Frequency (MHz)
^{1}H	1	0	½	42.58
^{2}H	1	1	1	6.54
^{31}P	0	1	½	17.25
^{23}Na	0	1	$\frac{3}{2}$	11.27
^{14}N	1	1	1	3.08
^{13}C	0	1	½	10.71
^{19}F	0	1	½	40.08

5.2.4 Energy Levels

To understand how particles with spin behave in a magnetic field, consider a proton. The spin of this proton has a magnetic moment vector, causing the proton to behave like a tiny magnet with a north and south pole. When the proton is placed in an external magnetic field, the spin vector of the particle aligns itself with the external field, just like a magnet would. There is a low energy state where the poles are aligned N-S-N-S and a high energy state N-N-S-S.

5.2.5 Transitions

This particle can undergo a transition between the two energy states by the absorption of a photon. A particle in the lower energy state absorbs a photon and is promoted to the upper energy state. The energy of this photon must exactly match the energy difference between the two states. The energy, E, of a photon is related to its frequency, ν, by Plank's constant (h = 6.626x10-34 J/s).

$E = h\nu$

In NMR and NMRD, the quantity, ν, is called the resonance, or Larmor frequency.

Given that $\nu = \gamma B$ and $E = h\nu$, the energy of the photon needed to cause a transition between the two spin states is

$E = h\gamma B$

When the energy of the photon matches the energy difference between the two spin states absorption of energy occurs. In NMR, the frequency of the photon is in the radio frequency (RF) range. With conventional NMR the frequency used is between 60 and 1000 MHz for hydrogen nuclei. In NMRD it is lower; between 15 and 100 MHz for hydrogen imaging, specifically used to detect water molecules.

5.2.6 Boltzmann Statistics

When a group of spins is placed in a magnetic field, each spin aligns in one of the two possible orientations. At room temperature, the number of spins in the lower energy level, N^+, slightly outnumbers the number in the upper level, N^-. Boltzmann statistics tells us that

$N^-/N^+ = e^{-E/kT}$

E is the energy difference between the spin states; k is Boltzmann's constant, 1.3805×10^{-23} J/K; and T is the temperature in Kelvin. As the temperature decreases, so does the ratio N^-/N^+. As the temperature increases, the ratio approaches one.

The signal in NMR spectroscopy results from the difference between the energy absorbed by the spins. This make a transition from the lower energy state to the higher energy state, and the energy emitted by the spins, which simultaneously make a transition from the higher energy state to the lower energy state. The signal is thus proportional to the population difference between the states. NMR is a sensitive spectroscopy since it is capable of detecting these very small population differences. It is the resonance, or exchange of energy at a specific frequency between the spins and the spectrometer, which gives NMR its sensitivity.

5.2.7 Relaxation times

Taking the analogy that the magnetic moments are like bar magnets, the question of why they do not all line up immediately with the external magnetic field, so that they all occupy the lowest energy state, must be addressed. As shown above the Boltzmann distribution is important but there are also mechanisms by which the excess spin energy can be dissipated. This involves sharing the energy with the surroundings or with other nuclei, and is referred to as a relaxation process: the time taken for a fraction of the excess energy to be dissipated is called the relaxation time. Thus, relaxation is the return of a system to equilibrium after perturbation.

Two different relaxation processes can occur for nuclei. In the first the excess spin energy equilibrates with the surroundings by spin/lattice relaxation, called the longitudinal relaxation time, T_1. NMRD concentrates on measuring this parameter.

The second way of sharing excess spin energy is directly between nuclei, via spin/spin relaxation, called the transverse relaxation time, T_2.

Electron and/or nuclear spin relaxation phenomena are crucial to all magnetic resonance spectroscopies and NMRD is based on the differences in nuclear relaxation between and within different proteins and tissues. In the case of Magnetic Resonance Imaging, the technique is used extensively to determine cancerous areas and other diseases within body organs.

Both electron and nuclear spins relax by coupling, ie exchanging energy, with the lattice. The types of energy exchange between spin systems are shown in figure 5.1 [67].

The observed water proton longitudinal relaxation time, T_1, in a solution containing a paramagnetic metal complex is given by the sum of three contributions:

$$T_1^{obs} = T_{1p}^{is} + T_{1p}^{os} + T_1^{w}$$

T_{1p}^{w} is the water relaxation rate in the absence of the paramagnetic ion

T_{1p}^{is} represents the contribution due to exchange of water molecules from the inner coordination sphere of the metal ion to the bulk water

T_{1p}^{os} is the contribution of solvent molecules diffusing in the outer coordination sphere of the paramagnetic centre.

The overall paramagnetic relaxation enhancement:

$$T_{1p}^{is} + T_{1p}^{os}$$

defined as a 1mM concentration of a given paramagnetic ion, is called the relaxivity[68].

Data for the dependence of T_1^{-1} against the magnitude of the external field Bo, the Larmour frequency, is termed a nuclear magnetic resonance dispersion profile [69].

5.3 Experimental

Samples of soluble collagen type I (ex Aldrich), titanium (III) chloride (solid, ex BDH) and chromium (III) acetate (ex BDH) were taken to the Consorzio Interuniversitario Risonanze Magnetiche Metalloproteine Paramagnetiche (CIRMMP) large scale nmr facility, which is

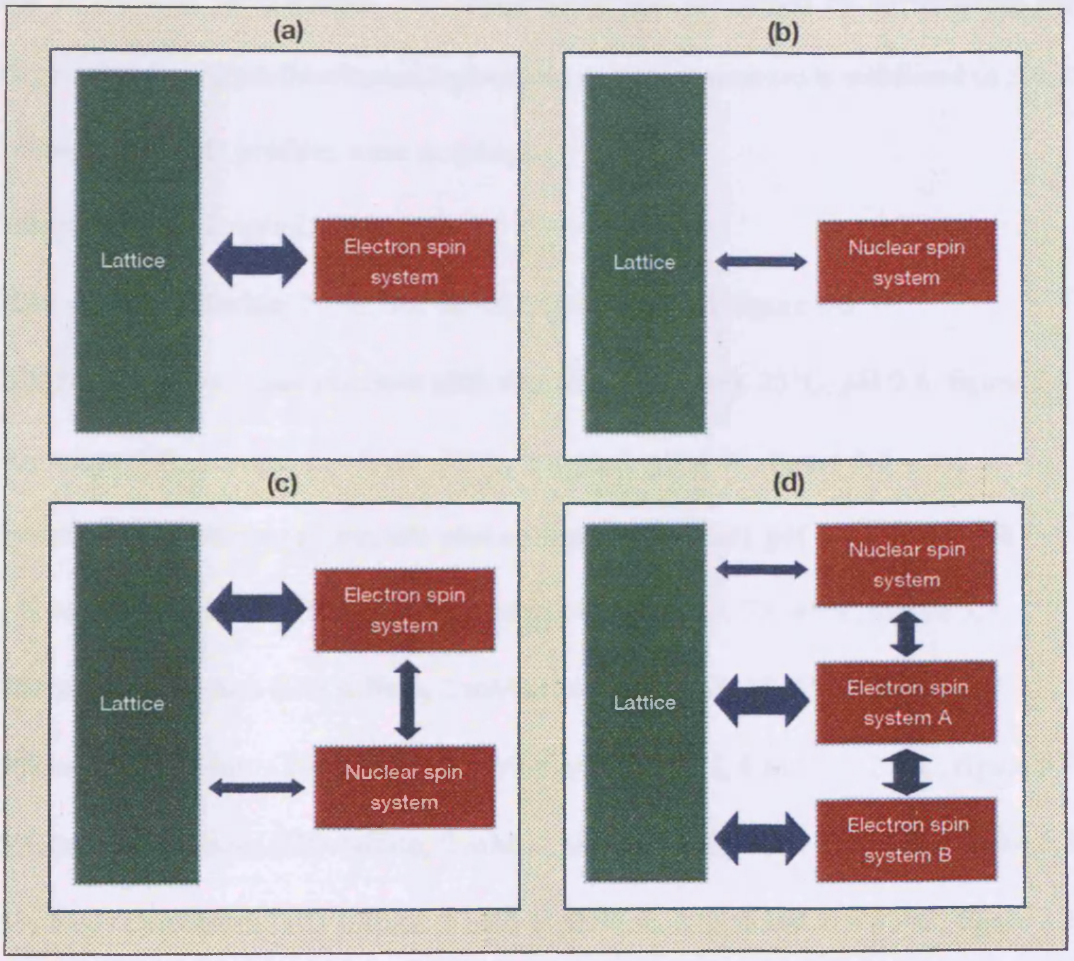

Figure 5.1: Energy exchange between spin systems and the lattice and between different spin systems. The size of the arrows indicates the efficiency of the exchange (bigger = better)

based at the University of Florence, Italy. A Stelar fast field cycling NMR relaxometer was used to acquire dispersion profiles of the longitudinal relaxation times as a function of the field intensity at constant temperature. The temperature was controlled by surrounding the sample with circulating liquid perfluorinated hydrocarbon. Its temperature is stabilised to ± 0.2°C.

The following NMRD profiles were acquired:

1. Collagen, 25°C, 2mg/ml, figure 5.2
2. Titanium (III) chloride, 25°C, 35, 40°C 2mg/ml, pH 0.6, figure 5.3
3. Collagen (1 mg/ml) plus titanium (III) chloride (1 mg/ml), 25°C, pH 0.6, figure 5.4
4. Chromium (III) acetate, 5, 15, 25, 35°C, 2 mg/ml, pH 4.03, figure 5.5
5. Chromium (III) acetate (1 mg/ml) plus collagen (1 mg/ml), pH 4.03, figure 5.6
6. 33% basic chromium (III) sulfate, 2 mM at pH 2, T = 25, 35, 45°C, figure 5.7
7. 42% basic chromium (III) sulfate, 2 mM at pH 3, T = 25, 35, 45°C, figure 5.8
8. 33% basic chromium (III) sulfate, 2 mM at pH 0, 1, 2, 3, 4 and T = 25°C, figure 5.9
9. 33% basic chromium (III) sulfate, 2 mM at pH 0, 1, 2, 3, 4 and T = 35°C, figure 5.10
10. 33% basic chromium (III) sulfate, 2 mM at pH 0, 1, 2, 3, 4 and T = 45°C, figure 5.11

5.4 Results

The relaxation rates increased with repeating the measurements subsequently. It was noticed that after 24 hours the increase in the relaxation rate was about 30%. This is comparable with the change due to the increase of temperature from 25 to 45°C. Thus the profiles were acquired just after the preparation of the solutions, without waiting for any stabilisation of the species present in solution.

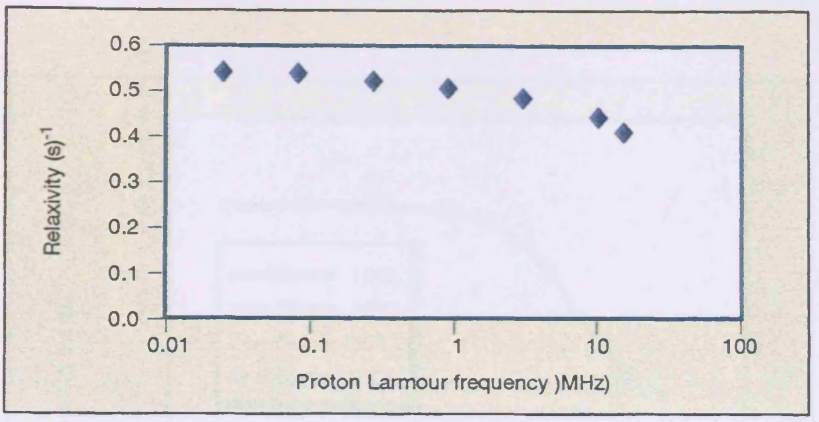

Figure 5.2: Relaxivity of collagen at 25°C, pH 4.4

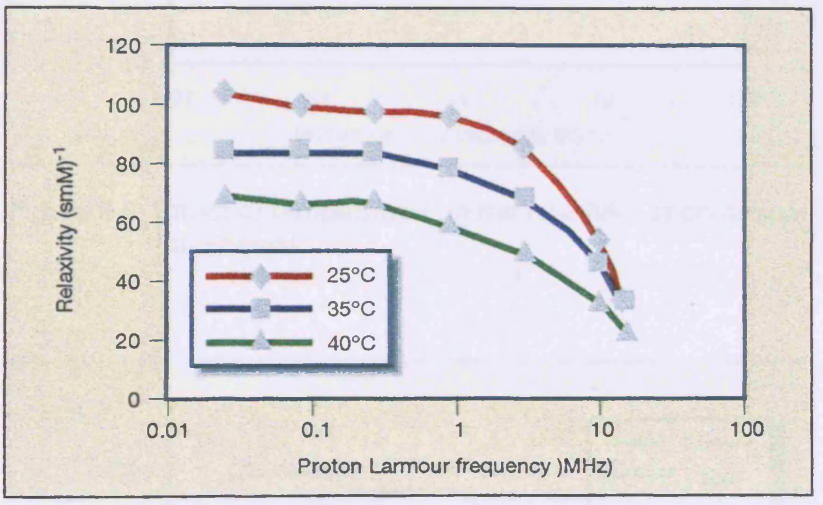

Figure 5.3: Relaxivity of titanium (III) chloride

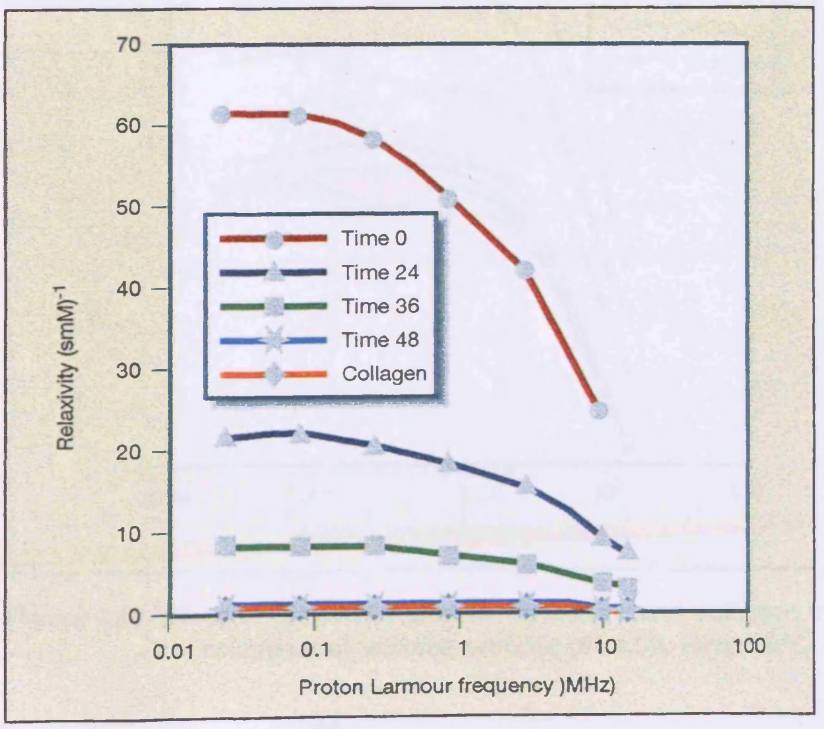

Figure 5.4: Interaction of collagen with titanium (III) chloride, 25°C

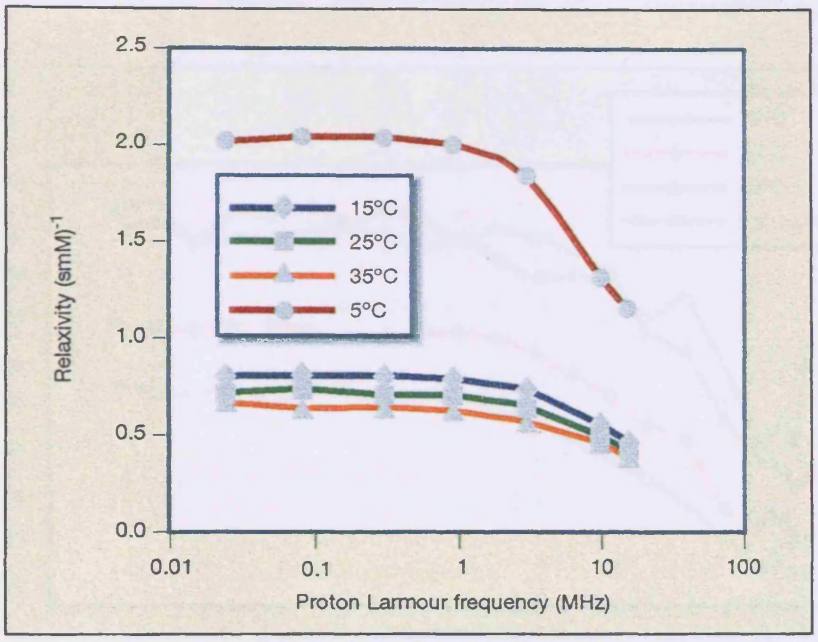

Figure 5.5: Effect of temperature on the relaxivity of chromium (III) acetate

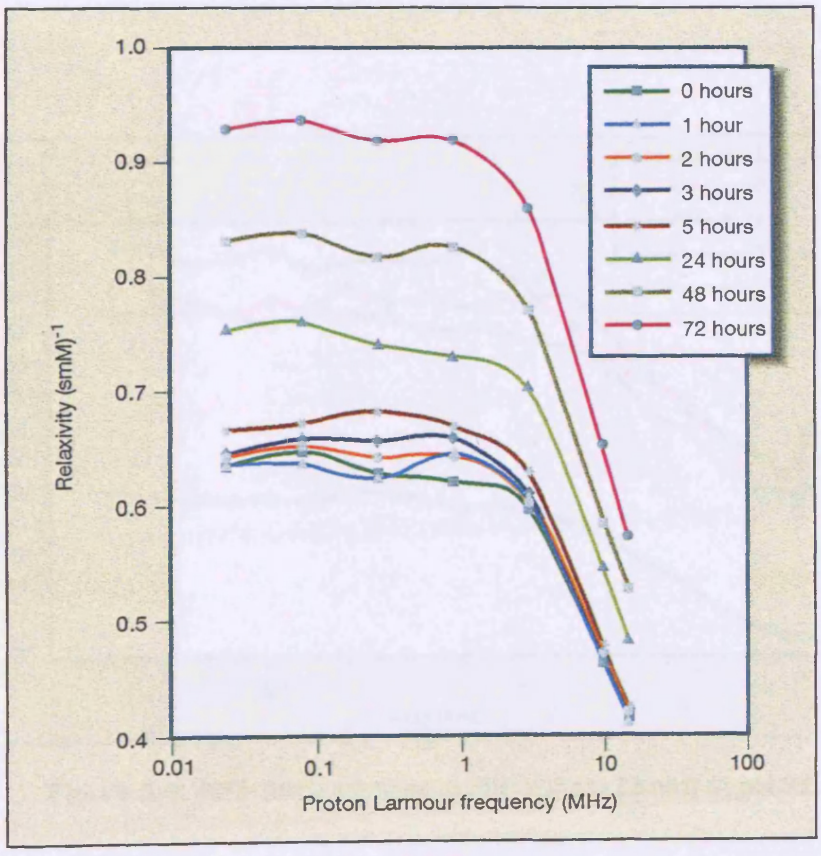

Figure 5.6: Effect of the interaction of chromium and collagen on the relaxivity of solvent protons pH 4.03, temp 35°C

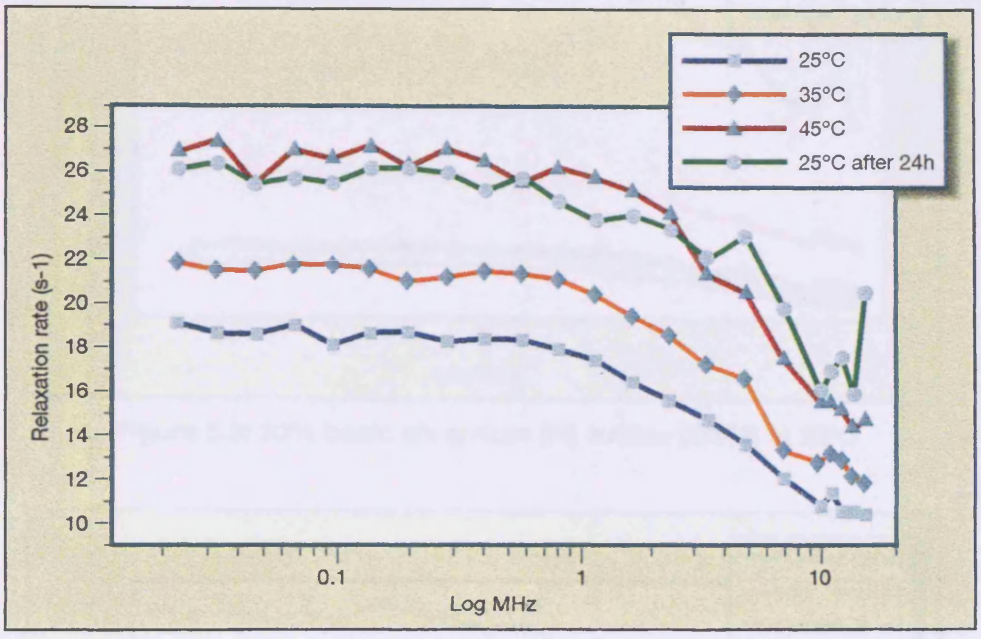

Figure 5.7: 33% basic chromium (III) sulfate [2mM] at pH 2.0

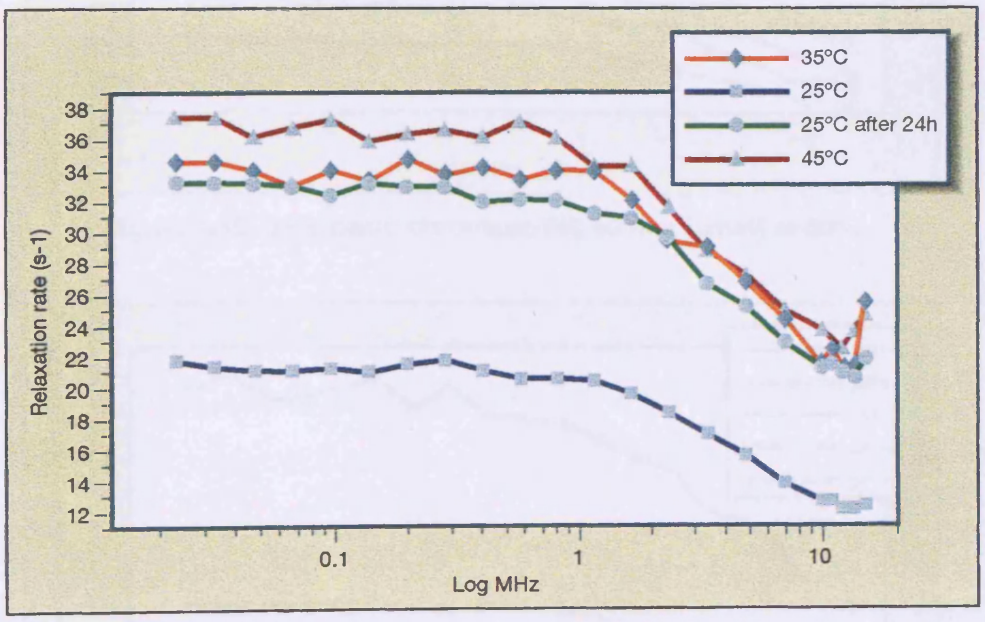

Figure 5.8: 42% basic chromium (III) sulfate [2mM] at pH 3.0

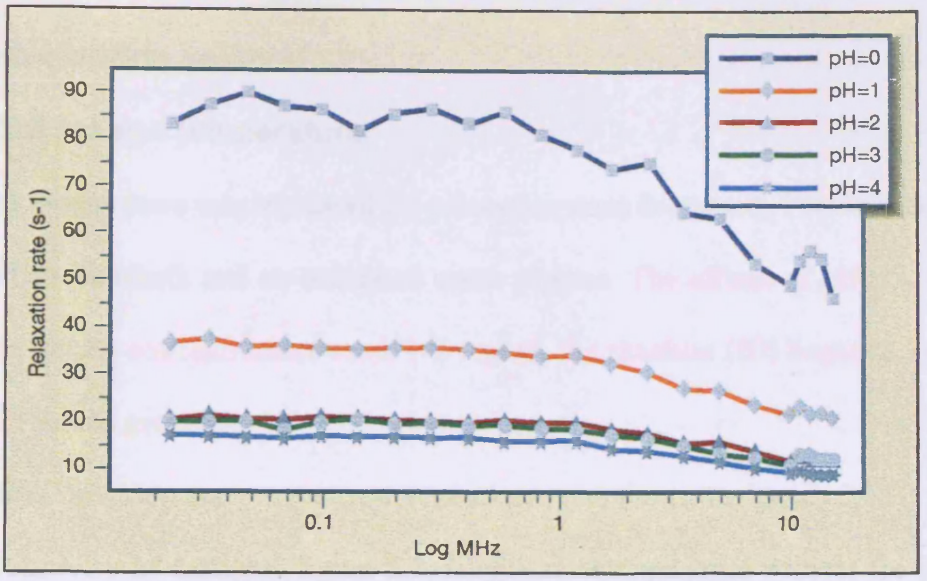

Figure 5.9: 33% basic chromium (III) sulfate [2mM] at 25°C

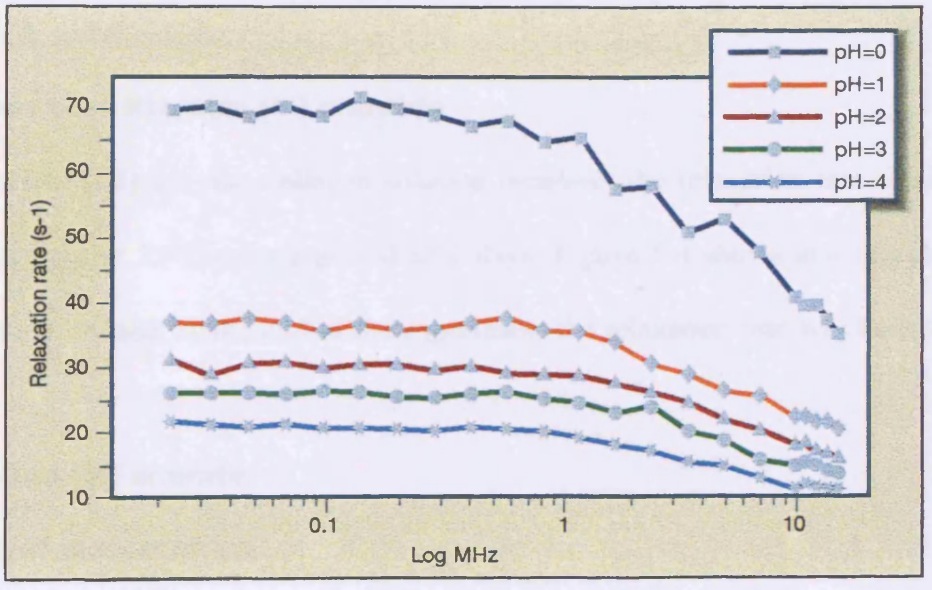

Figure 5.10: 33% basic chromium (III) sulfate [2mM] at 35°C

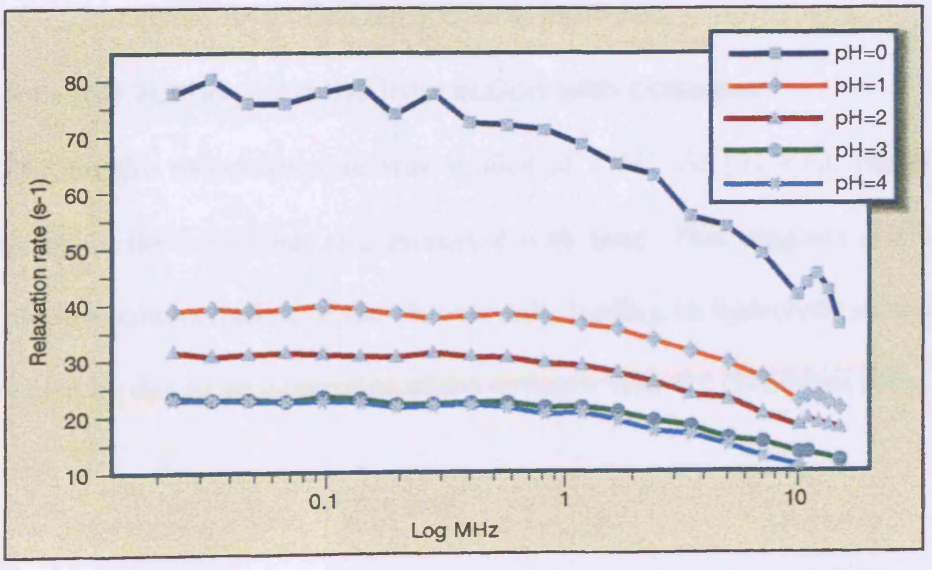

Figure 5.11: 33% basic chromium (III) sulfate [2mM] at 45°C

5.4.1 Titanium chloride solution

5.4.1.1 Effect of pH and temperature

In general, as the temperature was increased the relaxation rates decreased. This is indicative of a fast exchange between bulk and co-ordinated water protons. The effects of pH could not be measured because at the concentrations used, 1-2 mg/ml, the titanium (III) began to hydrolyse above pH 1.5 and would precipitate.

5.4.2 Collagen

The measured relaxivity of collagen, figure 5.2, is typical of a spectrum without the influence of a paramagnetic species. The rate is slow and indicates that the exchange between bound water and the bulk water is slow.

5.4.3 Collagen plus titanium (III) chloride

Introducing titanium (III) into the collagen solution increases the relaxation rate significantly. The sample was held at 25°C over a period of 2 days. Figure 5.4 shows that rate decreased notably in that time, indeed by the end of the experiment the relaxation rate was back to that of collagen alone.

5.4.4 Chromium (III) acetate

5.4.4.1 Effect of temperature

As the temperature increases the relaxivity decreases. This is particularly marked for the measurement at 5°C, compared with other temperatures measured.

5.4.5 Chromium (III) acetate and the interaction with collagen

The effect of time on the relaxation rate was studied at 35°C. At pH 4.03, the pH of the chromium (III) acetate, the relaxation rate increased with time. This suggests that the effect may be due to the low concentration of the chrome salt, leading to hydrolysis of the species. However, it may also be due to an interaction of the collagen with the chromium (III).

Also, the relaxivity is larger than that for the aqua-ion solution at the same temperature. Such increases could also be caused by processes that lead to stabilisation of the chromium salts with time, an effect that is probably also present with increasing temperature.

5.4.6 Chromium tanning powders

5.4.6.1 Effect of pH

The profiles exhibit a large decrease in relaxation rate, about 50%, on increasing the pH from 0 to 1, figures 5.7 to 5.9. The relaxation rates continue to decrease with increasing pH. This is true for all the temperatures.

5.4.6.2 Effect of temperature

From figures 5.10 and 5.11, the relaxation rates increase with increasing temperature. This indicates a slow exchange between bulk and co-ordinated water protons.

5.4.6.3 Effect of time

The effect of time on the relaxation rate was studied at 25°C. The results are shown as part of figures 5.10 and 5.11. At pH 2.4, the pH of the 33% basic chromium (III) sulfate, the relaxation rate has increased with time. This suggests that olation is taking place at this pH. However, the effect may simply have something to do with the low concentration of the chrome salt, leading to hydrolysis of the species. Furthermore, the values of relaxation rate are larger than those in the aqua-ion solution. Such increases could also be caused by processes that lead to stabilisation of the chromium salts with time, an effect that is probably also present with increasing temperature.

5.5 Discussion

5.5.1 Titanium

Bertini *et al*,[70] when they investigated the effect of temperature on titanium (III) (and vanadium (IV)), also found that as the temperature increased the relaxation rate fell. This is an opposite effect to the one seen with chromium (III) salts. They commented that, at all three

temperatures, there was only one dispersion. This is ascribed to the dipolar ω_s dispersion, an electronic relaxation, which suggests that the relaxation is via spin lattice interaction rather than spin/spin relaxation. The result, according to Bertini, shows that the electron relaxes via a specific mechanistic route, known as an Orbach mechanism.

In terms of tanning, the result shows that titanium (III) is unsuitable as a tanning agent because as the temperature is increased there is a transformation towards longer polymeric molecules. This is in agreement with the theory of shrinking, which states that polymerisation in metal tannages reduces the chances of a hydrothermally stable tannage, see chapter 6.

5.5.2 Collagen and titanium (III) interaction

There are a number of possible explanations for a change in the relaxation rate.These include:

- dilution. A sample at concentration of 2 mg/ml will have a relaxation rate about twice that of the same compound at 1 mg/ml.
- interaction. Generally, if there is a reaction, eg crosslinking, there is a reduction in the relaxation rate because the number of water molecules surrounding the central atom is reduced.
- viscosity. As the viscosity increases the relaxation rate increases. This is due to the number of relaxation pathways being increased.
- loss of paramagnetism leads to a reduction in the relaxation rate.

Thus, the reduction in the titanium (III)-collagen relaxation rate could be due to an interaction between the collagen and the titanium (III). It could also be due to the titanium (III) oxidising to titanium (IV) and, hence, losing its paramagnetism. The latter seems more likely, given that the rate of fall in the relaxation was fast. If there had been crosslinking there may have been signs of a reduced rate of fall, because, assuming that tanning would increase the viscosity of the collagen, this effect should increase the relaxation rate. The overall effect would probably have been to reduce the relaxation rate, but at a slower rate.

The second point favouring loss of paramagnetism is that the final spectra for the collagen-titanium (III) and the collagen alone are indistinguishable. This would be unlikely to occur if the collagen had been successfully crosslinked.

5.5.3 Chromium acetate

The values obtained show that the chromium (III) is interacting with the collagen. Again, there is only one dispersion visible, a dipolar interaction. The rise in relaxivity can be ascribed to an increase in the viscosity of the solution, which was noticeable when the sample was shaken. This increase can be explained by the crosslinking. An alternative explanation is that the collagen began to swell on standing. It was noticeable that the stock solution of collagen, at a concentration of 2 mg/ml, was a gel after a week of standing. It had initially been a solution. Although the time period was less, the effects of the commencement of gelation may have been picked up by the sensitive technique.

5.5.4 Chromium

The measurements indicate that as the pH and temperature increase there is a transformation

- towards species with an increased number of water protons which stabilise with time.
- towards species with a smaller number of co-ordinated water protons. These species increase with the rise in pH.

However, at the higher pH values, the relaxivity always remains much smaller than that measured at the lowest values of pH. This is consistent with the idea that the dominant species at pH 0 is probably monomer chromium (III) and as the pH increases the proportion of the polymeric species increases. This is, of course, in line with what the leather chemist expects in theory and the tanner knows in practice.

All the NMRD profiles acquired with chromium (III) sulphate solutions at different pH values (0, 1, 2, 3, 4) and temperatures (25, 35, 45°C) exhibit only one stretched dispersion centered at about 3 MHz of proton Larmor frequency. The profiles show one dispersion over the range of

temperatures investigated. This is ascribed to the dipolar ω_s dispersion. Since relaxation increases with increasing temperature, the system is in a slow exchange regime, as expected from the pH0 Cr(III) aqua-ion water solution. There is no evidence of the contact, spin/spin, dispersion. The profiles acquired at different pH values for the same 33% basic Cr(III) sulfate solution, 2 mM, show a decrease in relaxation rate with increasing the pH. Such a decrease can be related to the lower number of waters coordinated to the chromium ion. In leather science terms, the experiment shows that olation occurs as the pH increases.

It has been shown that a technique such as NMRD can pick up changes in the speciation studies of chromium and, to a lesser extent, titanium. These changes can then be related to what is already understood by the tanner. These results suggest that the technique could be used to investigate many aspects of tanning chemistry such as the rate of masking and the effects of soluble collagen interactions with chromium.

5.6 x-ray absorption techniques for structural analysis

5.6.1 Introduction

The work carried out using x-ray absorption techniques is discussed in this section. The aim was to elucidate structural changes in chromium and titanium tanned leathers. Extended x-ray absorption - fine structure, EXAFS, was used to investigate the detailed structure of titanium (III) tanned leathers and compare the resulting structural details with those of titanium (IV) and chromium (III) tanned leathers. For titanium tanned leathers another related technique, x-ray absorption - near edge structure, XANES was used to determine the oxidation state of semi-titanium leathers.

5.6.2 Background

When an x-ray photon, produced in this case from a synchrotron source, is tuned to the binding energy of some core level of an atom, there is an abrupt increase in the absorption coefficient, due to a core electron from the target metal being emitted. The outgoing photoelectron can be

thought of as a spherical wave with the epicentre at the nucleus of the target metal. When the wave reaches a neighbouring atom it is back scattered and this scattering interferes with the original wave. If it is in phase with the original wave, constructive interference occurs and the absorption of the x-ray is enhanced, while if it is out of phase, there is destructive interference and the x-ray absorption is reduced. The result is that the detector detects a variation in the x-ray absorption close to a transition, the so-called absorption edge. The absorption edge corresponds to an x-ray photon having enough energy to just free a bound electron in the atom. When the electrons are in the most tightly bound n = 1 shell the edge is called the K edge. For the next most tightly bound shell of electrons, the n = 2 shell, the corresponding edges are called the L edges. EXAFS refers to the oscillatory variation of the x-ray absorption as a function of the photon energy beyond this edge [71]. EXAFS spectra generally refer to the region 40-1000 eV above the absorption edge. A typical absorption for chromium (III), is shown in figure 5.12.

The signal oscillation depends on the number, nature and distance of the surrounding atoms from which the wave is back scattered. An advantage of this technique is that the relative sizes and energies of the oscillations are important rather than the total absorption. The background can, therefore, be allowed for and removed by computer. The phase of the electron wave depends on the distance of the scattering atom from the original atom, while the number of atoms at each different distance affects the amplitude. The Debye-Waller factor, a term added to take account of the thermal disorder encountered in the analysis, also plays an important role in EXAFS spectroscopy. It contains important structural and chemical information relating to the static disorder and thermal vibrations of the sample being analysed.

XANES, x-ray absorption near edge structure, refers to the region from 30-60 eV. There is overlap in the definition and there are different interpretations of where the XANES ends and the EXAFS begins[72].

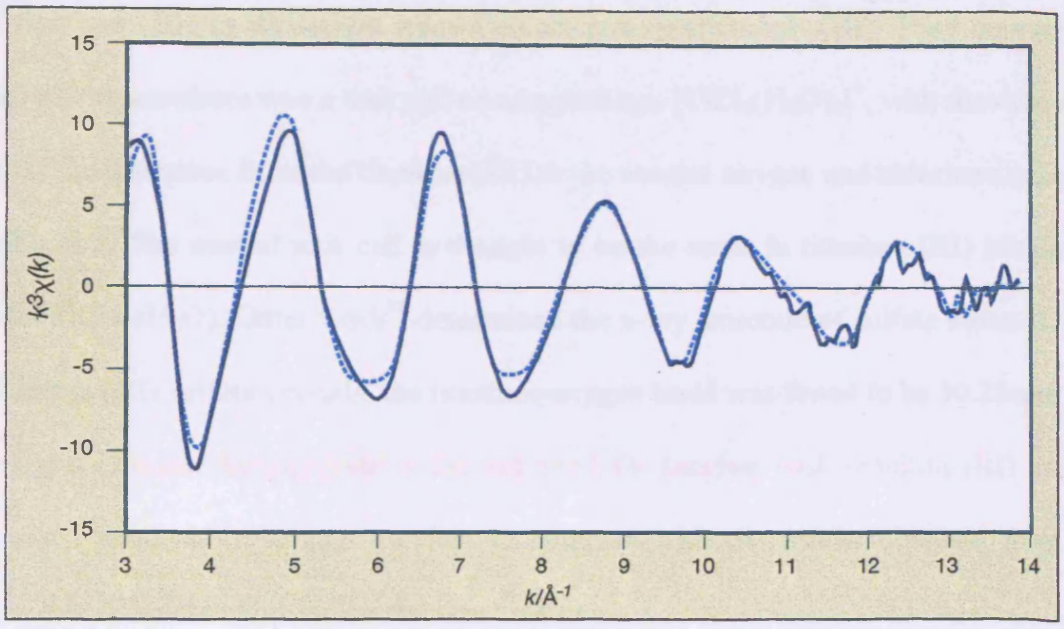

Figure 5.12: Cr K-edge EXAFS spectrum (k^3 weighted) for a sample of leather

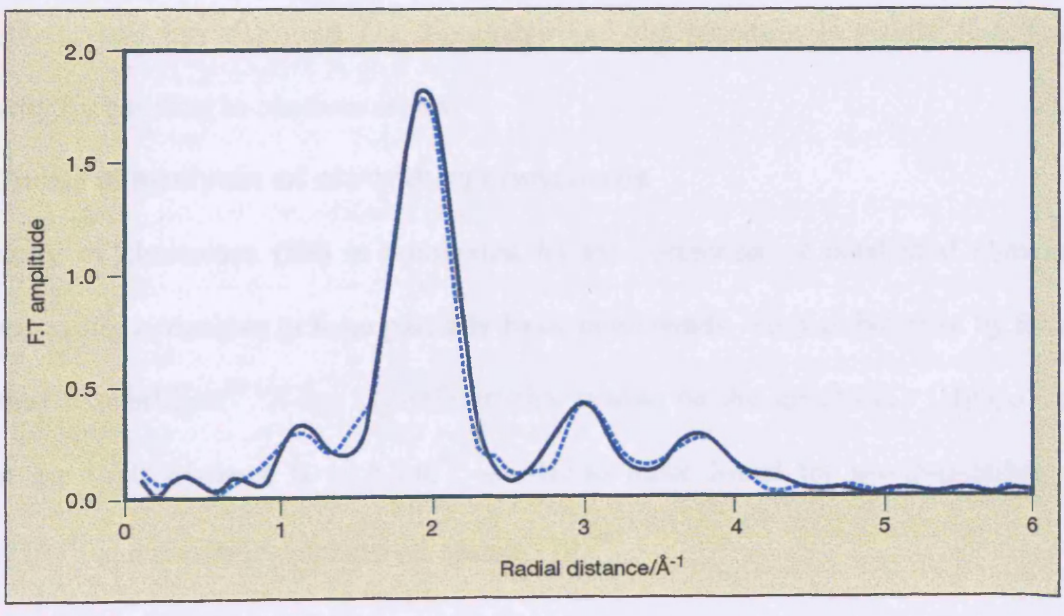

Figure 5.13: Fourier transform of the Cr K edge EXAFS spectrum

5.6.3 Structural analysis of titanium complexes

McCarthy and Richardson[73] determined the crystal structure and low temperature crystal spectra of titanium (III) in dicaesium trans-dichlorotetraaquotitanium (III). They determined that the central chromophore was a unit cell of composition, $[TiCl_2(H_2O)_4]^+$, with titanium (III) at the centre. The distances from the titanium (III) to the nearest oxygen and chlorine atoms are given in table 5.2. The central unit cell is thought to be the same in titanium (III) trichloride hexahydrate ($TiCl_3.6H_2O$). Other work[74] determined the x-ray structure of sulfate alums. Using caesium titanium (III) sulfate crystals, the titanium-oxygen bond was found to be 20.28nm. Titanium (III) trichloride hexahydrate is the salt used for tanning with titanium (III) and it, therefore, seems reasonable to use this data to compare with the results obtained from the EXAFS and XANES data recorded on the synchrotron.

Table 5.2: Some distances in the $[TiCl_2(H_2O)_4]^+$ unit cell[69]

Atom	Distance (nm)
Ti-O	20.33
Ti-O	20.46
Ti-Cl	24.00

The $TiCl_2O_4$ crystal has distorted D_{4h} symmetry and the structure is rigidly linked three dimensionally by bonding to caesium atoms.

5.6.4 Structural analysis of chromium complexes

The chemistry of chromium (III) is dominated by the formation of octahedral complexes, which often readily hydrolyse to form partially basic compounds. They polymerise by forming hydroxyl then oxo bridges[75]. X-ray crystallographic studies on the species $[Cr(H_2O)_6]^{3+}$ have shown that the Cr-O distance is 19.6 nm[76], similar to those found for μ-oxo-μ-carboxylato chromium (III)[77] and μ-oxo-μ-sulphato chromium (III)[78].

5.6.5 Methods

5.6.5.1 Sample preparation

The titanium and chromium tannages used in the experiments are described in appendix 1. Samples of the leather were ground on a Wiley mill. Basic chromium (III) sulfate salts were supplied by Elementis Chromium, Eaglescliffe, UK, as typical tanning salts, containing 25% Cr_2O_3 and about 25% sodium sulfate hydrate.

5.6.5.2 EXAFS sample preparation

For EXAFS study, the salts were diluted with boron nitride before being compressed into a thin 13 mm diameter pellet in a press. The amount of salt in the pellet was adjusted to give a change of ~1 in x-ray absorption coefficient (μ= incident intensity / transmitted intensity) at the metal K-edge. For the titanium salt, potassium titanium oxalate was used. Satisfactory measurements were made on leathers by preparing pellets from leather powder alone: they were not diluted with boron nitride.

EXAFS spectra were collected on Station 8.1 at the CLRC Daresbury Synchrotron Radiation Source. The synchrotron has electron energy of 2 GeV and the average current during the measurements was 150 mA. Station 8.1 is designed specifically for EXAFS measurements of dilute samples of 3d transition elements. It is equipped with an order sorting double silicon (III) monochromator that can be offset from the Bragg angle, to reject harmonic contaminants from the monochromator beam. The harmonic rejection was set at 50%. EXAFS spectra in the experiments were collected mostly in transmission mode, using gas filled ion chamber detectors, although fluorescence detection was used to collect some of the titanium spectra, to improve the signal to noise ratio.

Scans were taken beyond the absorption edge, to a k value of 140 nm and several scans were collected for each sample and averaged to improve the signal to noise ratio. The data were

processed in the conventional manner, using Daresbury's suite of EXAFS programs: EXCALIB, EXBACK and EXCURV92. Phase shifts were derived from *ab-initio* calculations within EXCURV92; this program contains a least squares fitting routine. Using this program, the EXAFS spectrum can be fitted to a structural model. The data in the k range 20-140 nm were analysed to yield a best fit, by iterating the radial distances, the Debye-Waller factors, A = $2\sigma^2$ and the co-ordination number, CN. The quality of the fit is measured by an R factor, given as a percentage (B) and the errors in the radial distance, RD, are expected to be ± 0.2 nm and ± 20% in A and CN respectively.

5.7 Results

5.7.1 Chromium (III)

The Cr K-edge EXAFS spectrum for a sample of leather tanned with chromium(III) tanning salt at 33% basicity is shown in figure 5.12. Figure 5.13 is the corresponding Fourier transform. These plots are typical of all the samples investigated, both the tanning salts and the tanned leather. The Fourier transform in figure 5.13 shows one main peak at ~20 nm, and two smaller peaks at ~30 nm and ~38 nm. These peaks were assigned to the co-ordination shells of oxygen, chromium and oxygen respectively and the data were analysed on this model. The best-fit parameters yield the broken lines in figure 5.13. Tables 5.3 and 5.4 list the best-fit parameters for all the samples examined.

Table 5.3: EXAFS results for basic chromium (III) tanning salts

Basicity (%)	Shell	CN	Error	RD (nm)	Error (nm)	$2\sigma^2$ (nm^2)	Error (nm^2)	R (%)
	Oxygen	6.034	0.212	19.64	0.03	0.10	0.01	
33	*Chromium*	2.0*	-	30.39	0.06	0.15	0.01	26.738
	Oxygen	5.215	1.794	38.36	0.19	0.21	0.10	
	Oxygen	5.804	0.147	19.62	0.02	0.09	0.01	
42	*Chromium*	2.113	0.409	30.40	0.06	0.19	0.03	21.167
	Oxygen	4.253	1.183	38.35	0.15	0.16	0.07	
	Oxygen	6.063	0.165	19.65	0.02	0.09	0.01	
50	*Chromium*	1.908	0.355	30.23	0.06	0.16	0.03	22.324
	Oxygen	3.802	1.061	38.31	0.14	0.12	0.05	
	Oxygen	5.410	0.120	19.76	0.02	0.08	0.01	
100	*Chromium*	2 236	0.223	30.06	0.03	0.14	0.02	18.144
	Oxygen	2 486	0.827	38.61	0.16	0.14	0.07	

*chromium co-ordination number (CN) held at 2.0 in the fitting

Table 5.4: EXAFS results for leather tanned with basic chromium (III) tanning salts

Basicity (%)	Shell	CN	Error	RD (nm)	Error (nm)	$2\sigma^2$ (nm^2)	Error (nm^2)	R (%)
	Oxygen	6.294	0.137	19.65	0.01	0.09	0.01	
33	*Chromium*	1.454	0.296	29.80	0.06	0.15	0.03	18.442
	Oxygen	7.436	1.372	38.24	0.10	0.21	0.05	
	Oxygen	6.456	0.178	19.65	0.02	0.10	0.01	
42	*Chromium*	1.424	0.344	29.73	0.08	0.16	0.04	20.936
	Oxygen	5.545	1.460	38.42	0.14	0.19	0.07	
	Oxygen	6.540	0.165	19.66	0.02	0.10	0.01	
50	*Chromium*	1.448	0.318	29.84	0.06	0.14	0.03	20.455
	Oxygen	5.851	1.458	38.41	0.14	0.20	0.07	

The overall R factor and the errors of the individual parameters are also listed. The errors are largest for the third shell, which are approaching the limits of the analysis.

5.8 Discussion

It can be seen in Table 5.3 that the chromium ions in the tanning salts are hexacoordinated by oxygen, at a distance of 19.6 nm. This is in agreement with the work of Nakahanada and Finholt[74] mentioned above. Each chromium atom has two other chromium atoms as next nearest neighbours, at a distance of 30 nm.

The analysis of the EXAFS data for the different basicity salts is consistent, indicating that the crystallinity of the salts has the effect of making all the chromium atoms equivalent. An

interesting variation is the number of the nearest oxygen atoms in the third co-ordination shell, which varies inversely with the basicity of the salts. Why this should be so is not understood.

The analysis of the leathers demonstrates some differences in the chromium (III) peaks when compared with the salts. This is because the chromium ions are effectively isolated on the collagen molecule. In the first co-ordination shell there are still six oxygen atoms at 19.7 nm away, but the number of nearest chromium atoms, also still at 30 nm distance, is consistently lower than in the salts. This result is consistent with, since the carboxylate groups would compete effectively with hydroxide for chromium in these acidic solutions and the effect would be to reduce the oligomerisation of any chromium complexes formed.

Unlike the salts, the next nearest oxygen atoms are consistent in number, also in agreement with the expected number by calculation. It is possible that this measurement is influenced by the presence of co-ordinated carboxyl groups, which although bound by a single valency, contain two equivalent oxygen atoms.

Conventional reactions, with a range of basicities of chromium (III) salts, show that the average size of the salts fixed to collagen depends on the final pH condition, rather than on the basicity of the starting compounds. This will typically result in linear chromium species, whether the species is bound to a single collagen carboxyl or is involved in crosslinking more than one carboxyl. It may be a feature of the unique tanning ability of chromium (III) that it is able to form such linear complexes under tanning conditions, of the right size to form enough crosslinks to confer the high hydrothermal stability observed in routine leather production.

5.8.1 Titanium - EXAFS

Examples of the Ti K-edge EXAFS spectrum for leather tanned with titanium are shown in appendix 4. The plots show the EXAFS $\chi(k)$, weighted by k^3 versus k. Unfortunately, the spectra are too noisy to analyse; the highest peak at around 18 nm is indicative of this. The use of the fluorescence detector proved no better.

5.8.2 Titanium

The results for the titanium tanned leathers were inconclusive. The EXAFS spectra proved elusive and yielded little useful information. Analysis of the spectra suggest that there is a high degree of polymerisation, but this is circumstantial evidence, based on studies of many titanium EXAFS spectra and extrapolating the information from the data seen in appendix 4[79].

5.9 Titanium - XANES

5.9.1 Sample Preparation

XANES spectra of the titanium tanned leathers used in the EXAFS determination were collected. The XANES spectra were also collected on Station 8.1 at the CLRC Daresbury Synchrotron Radiation Source. The synchrotron has electron energy of 2 GeV and the average current during the measurements was 165 mA. As with the EXAFS determination the harmonic rejection was set at 50%. XANES spectra in the experiments were collected in transmission mode, using gas filled ion chamber detectors.

5.9.2 Results

The XANES spectra proved difficult to analyse. The differences between the vegetable tanned leathers, seen in the physical properties of the leathers, see chapter 3, are also seen in the XANES spectra, however, how these differences can be related to molecular structure is not understood. Spectral differences between samples D and B (titanium (IV) tanned) and A and C (titanium (III) tanned, are visible, figure 5.14. However, what these differences mean is not understood because of the complexity of system[80].

Analysing leather with such techniques has never before been attempted. The main problem encountered was trying to decipher what the spectra meant, especially with the amorphous areas within the structure. Analysis of these areas proved impossible: indeed analysis of the titanium spectra was not possible either, probably because of the polymeric nature of the

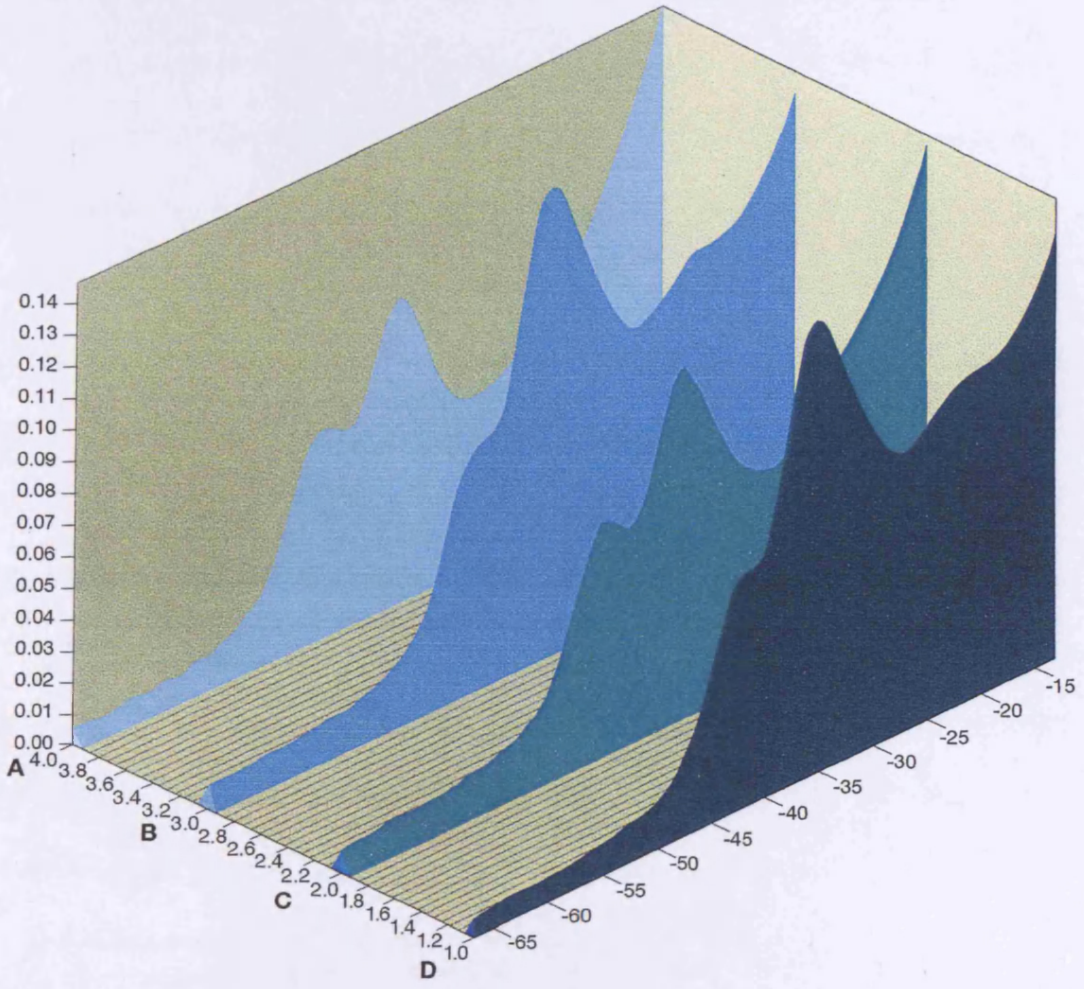

Figure 5.14: XANES spectra of titanium (III) and titanium (IV) leather
A and C are titanium (III) tanned leather samples
B and D are titanium (IV) tanned leather samples

tannage. However, the discrete nature of the oligomers formed by chromium during tanning allows structural changes due to differences in processing to be determined.

5.10 Other spectroscopic techniques

5.10.1 Higher band ESR

Although ESR active, one of the reasons for the poor spectra produced with the titanium (III) was the low concentration of paramagnetic ions. This meant that any signal obtained was either accompanied with excessive noise or the signal was masked by signals from other sources.

In an effort to overcome these deficiencies, a sample of the ground semi-titanium (III) leather was sent to the University of Manchester's ESR facility. There they have more powerful machines including a Q band ESR, which was used to try and expand the spectrum obtained from the semi-titanium leather to elucidate further structural information.

5.10.2 Results

Three of the spectra obtained are presented in appendix 5.

Even using the higher band machine, assigning a signal due to the titanium (III) proved impossible. This was mainly because there was a high degree of inhomogeneity in the sample. There is a sharp signal at about 3400 G, which is almost certainly a free radical. This is enhanced when the temperature is reduced (Appendix 5, figure 5.3). There are weak signals below 2500 Gauss and these could be assigned to high spin iron (III) atoms, probably an impurity from the processing, or possibly there was some iron in the titanium metal used to make the titanium (III) solution. The broad features between 4500 G and 2500 G are impossible to interpret because there is no resolved hyperfine structure. In addition, the features are not reproducible and there is a free radical signal sitting on top of some of the other signals. The broadness of the spectrum suggests that it is coming from more than one type of centre. So, even using a higher frequency machine did not bring out any hyperfine structure that could be assigned definitively.

5.11 Solid state nuclear magnetic resonance

Samples of semi-metal leathers were sent to a solid state NMR facility at Durham University. These metals have at least one NMR active isotope, table 5.5.

Table 5.5: metals used for NMR studies

Metal	Isotope
Copper(II) sulfate	^{63}Cu
Nickel (II) sulfate	^{61}Ni
Iron (II) sulfate	^{53}Fe
Dysprosium (III) sulfate	^{161}Dy
Yttrium (III) sulfate	^{89}Y
Ytterbium (III) sulfate	^{171}Yb

The leathers were processed according to the procedure set out in appendix 1. Shrunk and control samples of these leathers were sent for comparison, to determine whether there were differences in the inner or outer coordination spheres of the metal atom after shrinking.

Previous work, using ^{27}Al NMR[81], showed that the inner coordination sphere around the aluminum in shrunk aluminium tanned hide powder does not differ from the control samples. This suggests that there is no hydrolysis of the aluminium during the shrinking transition.

5.11.1 Results

Although NMR spectra of the metal isotope were requested, their concentration in the leather was too low to obtain a signal from. Thus, ^{13}C spectra were collected. A typical result is shown in the figure 5.15a (control), and 5.15(b) (shrunk).

The resolution of the tanned samples is not as good as for the soluble collagen, figure 5.15c (taken from the work of Brown *et al*[82]) because these samples were solid. However, certain peaks can be assigned. Between 170-190 ppm are peaks due to carboxyl and amide carbons. Further down the spectra, the carbons associated with proline and hydroxyproline can be assigned to the peaks at 60-80 ppm. Unfortunately, the resolution is not high enough to pick up changes between the raw collagen and the tanned samples. Nor does there seem to be any difference between the ^{13}C NMR before and after the samples were shrunk.

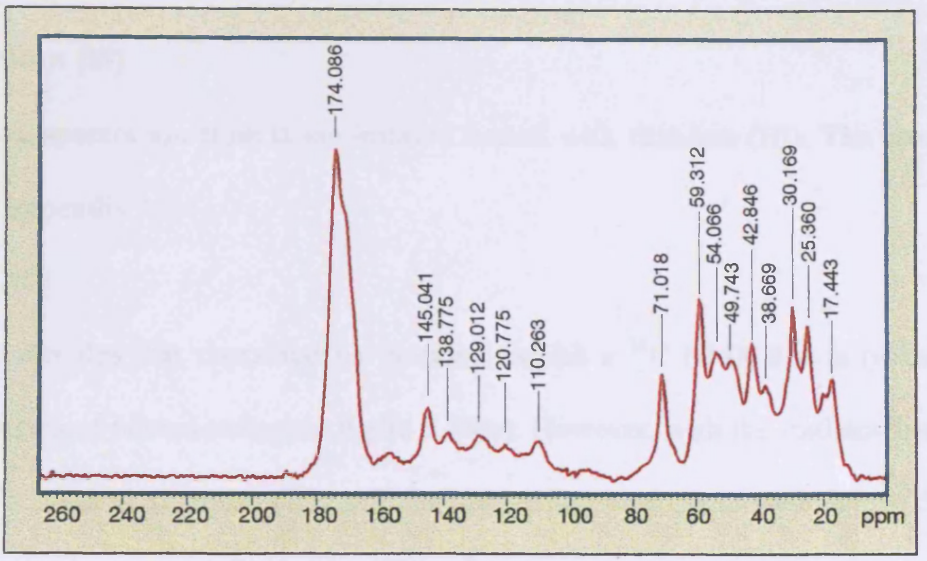

Figure 5.15a: ^{13}C NMR spectrum of mimosa tanned leather, retanned with ytterbium sulfate. Unshrunk

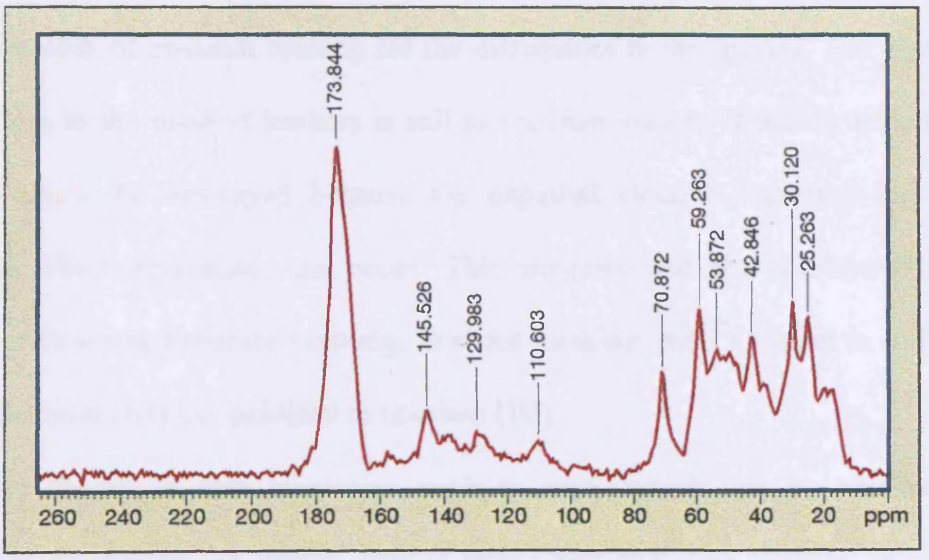

Figure 5.15b: ^{13}C NMR spectrum of mimosa tanned leather, retanned with ytterbium sulfate. Shrunk

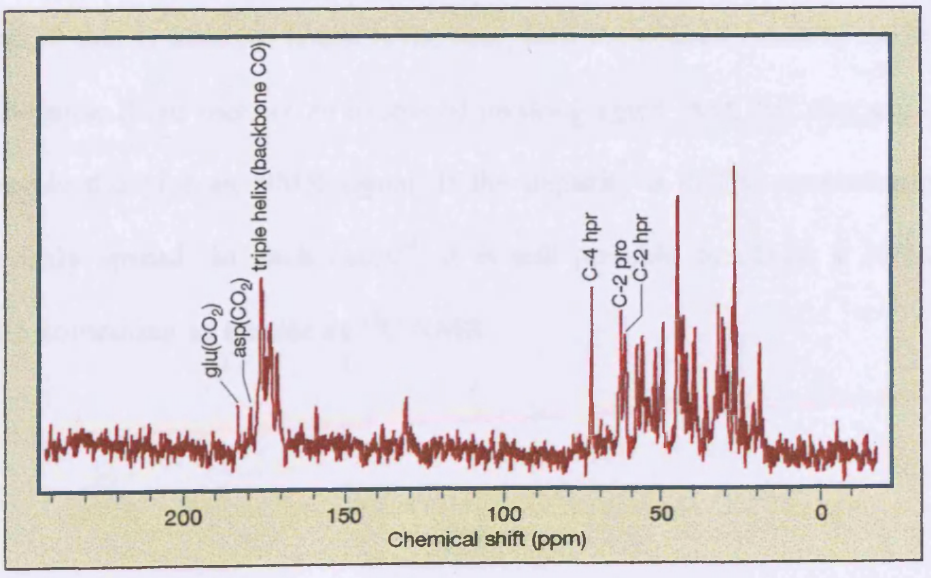

Figure 5.15c: ^{13}C NMR spectrum of soluble collagen

5.11.2 Titanium (III)

The interesting spectra are from those leathers tanned with titanium (III). The process details are set out in appendix 1.

5.11.3 Results

The titanium samples that contained no masking exhibit a ^{13}C NMR that is typical of a low resolution spectra of tanned collagen, figure 5.16(a). However, with the leathers that have been tanned with a masked titanium (III) salt the signal has been destroyed, figure 5.16(b) and 5.16(c).

5.11.4 Discussion

There are a number of possible reasons for the differences in the spectra. The obvious one is that the titanium in the masked leathers is still as the titanous ion. If that is the case, then the NMR signal could be destroyed because the unpaired electron increases the number of pathways via which relaxation can occur. This suggests that the titanium (III) ions are stabilised by maleate or fumarate masking. Without masking, the ^{13}C signal is still detectable, because the titanium (III) has oxidised to titanium (IV).

An alternative theory is that impurities such as iron, which can be paramagnetic, are responsible for destroying the signal. This is seen when analysing samples of clays[83]. But, there is no reason why the iron in the masked sample should not destroy the signal in those samples unless it, too, is masked. If that is the case, then the concentration of the iron impurity must be low because there was not an excess of masking agent. And that may explain why the unmasked sample did give an NMR signal. If the impurity is in low concentration, it is not necessarily evenly spread. In such cases[84], it is still possible to obtain a NMR spectrum, especially with something as routine as ^{13}C NMR

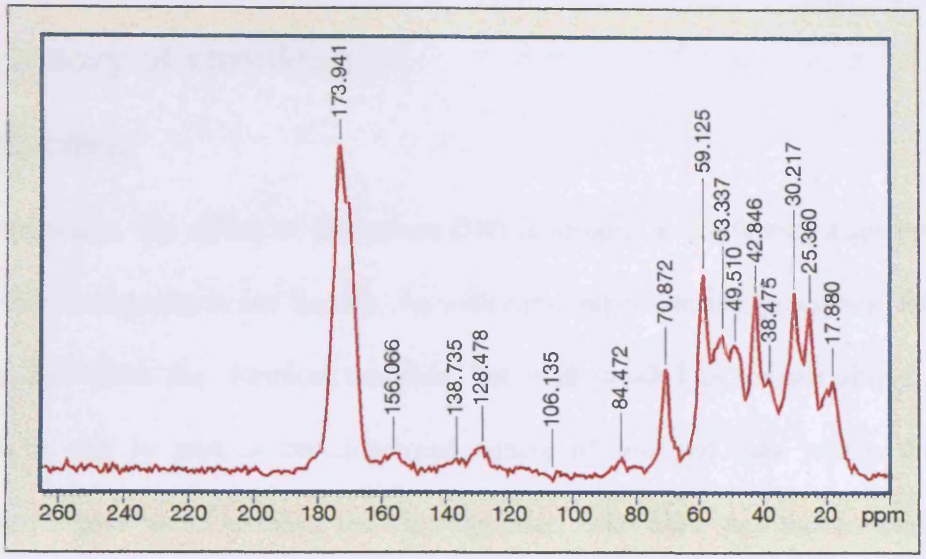

Figure 5.16a: ^{13}C NMR of titanium (III) tanned leather: Unmasked

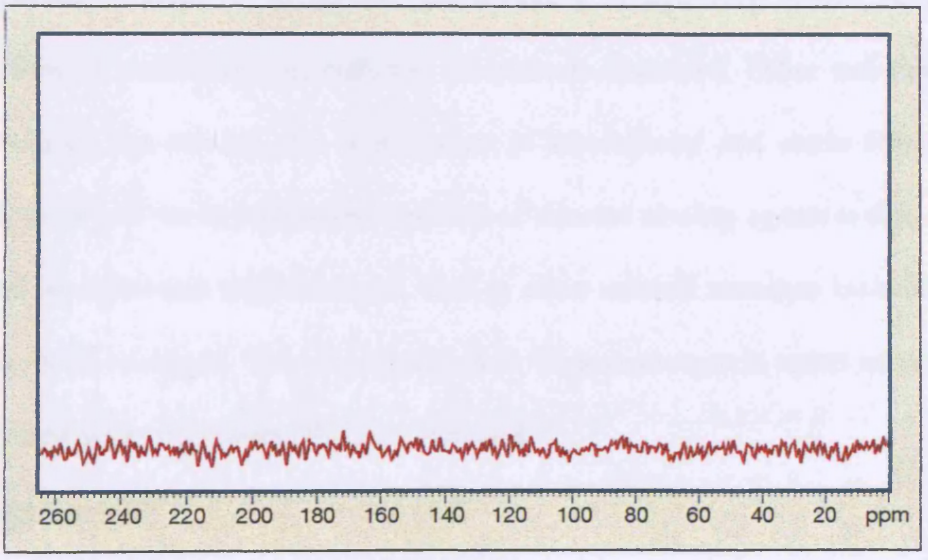

Figure 5.16b: ^{13}C NMR of titanium (III) tanned leather: maleate masked

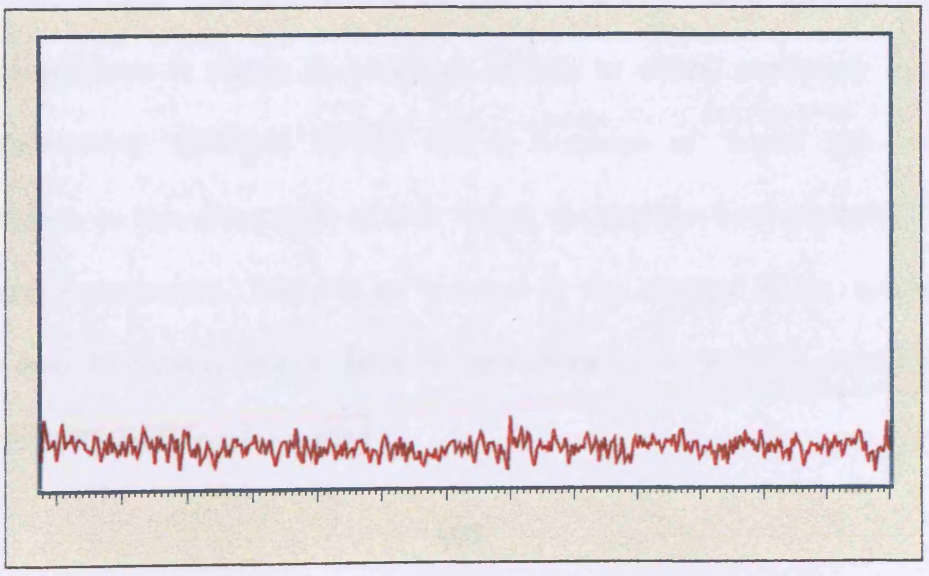

Figure 5.16c: ^{13}C NMR of titanium (III) tanned leather: Fumarate masked

6 A new theory of shrinking

6.1 Introduction

Among solo tannages, the effect of chromium (III) is unique in conferring high hydrothermal stability, but the reason why is not known. As with most other tanning processes, this is typical of our knowledge about the chemical reaction, but with much less known about the tanning reaction. This is due in part to the dispersed nature of relevant data within the technical literature. This chapter seeks to bring the data together, from older and more recent literature, together with the new research into titanium tanned and semi-metal leathers.

Collagen shrinking is believed to involve the breaking of hydrogen bonds, so the role of hydrogen bonding in stabilising the collagen structure is discussed. Other stabilising factors, such as the role of the solvent, the significance of crystallinity and steric effects are also considered. A theory of the hydrothermal stability of mineral tanning agents is then developed. This is applied to chromium (III) tannages, then to other mineral tannages including titanium (III) and semi metal tannages. The reasons for their limited success in terms of hydrothermal stability compared with chromium (III) are discussed.

6.2 Background

6.2.1 Definition of tannage

Dr Dorothy Jordan Lloyd[85] stated that there are four criteria by which tannage can be defined. One is the temperature at which the collagen shrinks in water, commonly known as the shrinkage temperature. 'Collagen shrinks due to breakage of 'lateral links between the polypeptide chains, so that along parts of their length, the peptides have changed from ordered to a disordered arrangement. There is an increase in the entropy of the system. Tanning increases the lateral cohesive forces either by strengthening the existing crosslinks or, more probably, by forming additional crosslinks.'

The other three criteria are resistance, when moist, to attack by enzymes and micro-organisms, chemical stability and the physical properties of the resulting leather.

Gustavson entered a plea for consideration when defining tanning: 'The criteria given for the properties of tanned collagen and the definition of leather must be applied with due consideration of its intended use. Even in a strictly theoretical evaluation of the potency of a tanning agent, it is advisable not to emphasize any particular property or constant to the exclusion or detriment of any other criteria. Thus, characterisation of tannages mainly from the point of view of the degree of hydrothermal stability attained in the final product by a certain tanning agent may lead to an erroneous conception, or even invalidate the conclusion drawn from accentuating one property at the sacrifice of the other criteria. Hence, it is advisable to include all the criteria given in a consensus of the degree of efficiency of a tanning agent.[86]

The chemical nature of collagen allows it to react with a variety of agents, often resulting in its conversion to leather. Of the changes in appearance and properties that are a consequence of tanning, one of the more important is the increase in hydrothermal stability. This can be measured by observing the point at which a specimen shrinks when it is held in water and heated at a rate of 2°C per minute. This is the conventionally measured shrinkage temperature, Ts.

The most common way of defining tanning is to state the shrinkage temperature of the leather concerned. However, this led to a situation where many in the industry assume something is not 'tanned' unless it has a shrinkage temperature above 100°C. As Gustavson implies in the quote above, the important factor is not necessarily a fixed temperature, but whether the article is fit for purpose.

6.2.2 Raw collagen stability and the effects of heat

The structure of collagen was discussed in chapter 1. In this section, the role of hydrogen bonding, its importance in stabilising the structure and the influence of the pyrrolidine residues is further developed.

It was Pauling[87] who first suggested that long chain protein molecules are held together by hydrogen bond linkages and Wilson[88] pointed out that although the hydrogen bond is extremely stable with respect to temperature and humidity under normal conditions, when swollen in acid or alkali the structure is lost. Braybrooks[89] showed that the peptide chain in collagen would coil upon the removal of the restraining hydrogen bonds and, since a rise in temperature increases the vibrational energy of the molecule, it was seen as natural for the collagen fibres to contract on heating.

Astbury[90], in the first Procter Memorial Lecture to the Society of Leather Technologists and Chemists, said that 'when the thermal agitation is sufficient to overcome the interchain attractions, the chain bundles may be said to melt and the chains collapse upon themselves. It follows that anything that interferes with this process must inevitably influence the thermal transformation temperature.' He further pointed out that coiling and uncoiling of peptide chains is very common in proteins.

It was Weir and Carter who were the first to suggest that hydrothermal shrinking of collagen was due to hydrogen bonds breaking[91]. They suggested this theory from work carried out into the role of different solvents on the shrinkage of collagen. Their argument was that if ionic linkages were stabilising the collagen structure, and involved in the shrinkage process: 'it would be expected that the enthalpy should increase by virtue of the lowering of the dielectric constant of the solutions and the increased cohesive energy of the collagen.' In fact, the opposite was observed. They also rejected the idea that salt bonds were involved in shrinkage for a number of other reasons:

- the number of such linkages is probably small because of the spatial requirements involved
- hydrogen bonds out number the salt linkages 7to1
- salt bonds existing in an aqueous medium of the type used in shrinkage measurements are expected to be labile.

The mechanism they favoured, involving hydrogen bonding, was as follows: 'Inasmuch as variations in chain spacing, spatial orientation and chemical structure probably exist in pure collagen, it is not likely that all crosslinks possess equal energies, or even that extremely small, arbitrary regions contain equal numbers of such linkages. Thus, a small region containing few linkages of low energy is considered to represent a site favourable for initiation of shrinkage.' Weir called this area the shrinking nucleus. Due to kinetic and thermal bombardment, any particular non-imposed crosslink, eg hydrogen bonds, may rupture and a degree of freedom imparted to the chains broken, even at low temperature. On breaking, the sites of the former bond can be saturated with solvent molecules, held by secondary forces. At low temperature, the collagen chain is not likely to contract, simply because the rigidity of neighbouring crosslinks will stabilise the structure and the probability that the broken crosslink will reform. However, as the temperature of the bath is raised, more energy is available for bond rupture and the number of bonds broken per unit time becomes larger. It can be assumed that at some point the number of bonds breaking will so weaken the structure that the nucleus will proceed to a more stable configuration, ie the shrunken or chain folded state. For this process to occur there has to be cooperation between many chains; that is many chains have to shrink simultaneously. These shrinking nuclei occur randomly through the collagen structure. The process is dependent on temperature and time and, so, could occur at room temperature, although the probability of such an occurrence is prohibitively small.

The idea that collagen has thermally labile regions is also thought likely by Miles and Bailey. In a paper given to the Indian Academy of Science[92], they show that shrinking is an irreversible

rate process, in which the uncoupling of the α-chains initially occurs in an area devoid of hydroxyproline residues. These areas are near the C-terminal and, when the helices have been formed into the quarter stagger, the shrinking nucleus, to use Weir's nomenclature, is in the gap region. Once the chains in the region are uncoupled, the structure 'unzips' and folds.

6.2.3 Role of hydroxyproline and hydrogen bonding

The assumption that the stability of the triple helix is founded on hydrogen bonding is still something of a debate. That hydroxyproline plays an important role in the stability is in no doubt. But, its role in that stabilising effect is still something of a mystery. There seem to be two models, one involving hydroxyproline and water, the other hydroxyproline and inductive effects.

It was Gustavson[93] who first observed that the shrinkage temperature of raw skin increased with increasing pyrrolidine (proline + hydroxyproline) content. The effect on shrinkage temperature is shown in table 6.1.

Table 6.1: Shrinkage temperature and imino acid content[94]

Source	Total number of imino acid residues†	T_s (°C)
Calf	232	65
Carp	197	54
Cod	155	40

† per 1000 residues

Berg and Prockop[95] extracted protocollagen, a non-hydroxylated form of collagen, with cold acetic acid and showed that it consisted of polypeptides of the same dimensions as the α I and α II chains of collagen. Having established that the optical rotatory properties were similar to that of collagen, they measured the thermal transition and found it was 15°C lower than for hydroxylated collagen. This is evidence of the important role of hydroxyproline in stabilising the collagen structure.

However, there is still some contention about the role of the solvent, usually water, in stabilising the collagen triple helix. There are different models of what is believed to be happening.

6.2.3.1 Solvent stabilisation of collagen

Privalov thought that the hydroxy group on the proline bound water molecules, via hydrogen bonding, which aided the structural stability of the collagen[96]. He believed that water bridges were playing a large role in stabilising the structure and investigated these effects on the energy required to denature collagen.

He thought that the additional hydrogen bond per amino acid triplet, formed through a water molecule, ie the Ramachandran[97] model of water bridged collagen, could not be solely responsible for the high collagen denaturation energy. He said the stabilisation energy probably included wider layers of water, adjacent to the regular collagen structure. In another paper[98] he states that: 'Having in mind the tendency of water molecules to co-operate with their neighbours, it does not seem improbable that hydroxyprolyl can serve as an initiator to an extensive co-operative network of hydrogen bonds. This envelops the collagen molecule and might be responsible for the exceptional thermodynamic properties of collagen.' Bella[99] *et al* confirm this idea. They synthesised a triple helical peptide with a collagen like structure containing (Pro-Hyp-Gly)$_4$-Pro-Hyp-Ala-(Pro-Hyp-Gly)$_5$, which provided the first precise experimental proof for the existence of water bridges in a collagen like structure. They showed the triple helices in the crystal structure were surrounded extensively by a cylinder of hydration, and the Hyp residues seemed to act as 'keystones' connecting the water network to the peptide molecules. Figure 6.1 illustrates the hydration of the synthesised peptide. The grooves on the triple helix are filled with solvent molecules directly bonded to the anchoring groups on the peptide, or connected to those waters in the first hydrogen bonded shell. The third shell of waters complete the cylinder of hydration.

While it was realised that without the Hyp residue there were only localised regions of water structure, the role of the Hyp was not understood until Kramer showed that it was important in the development of an extended hydration network[100]. She suggests that the presence of hydroxyproline acts as a nucleus for water bridges. Their presence extends the hydration network far beyond what would be expected and that it is critical for the lateral assembly and supermolecular structure of collagen.

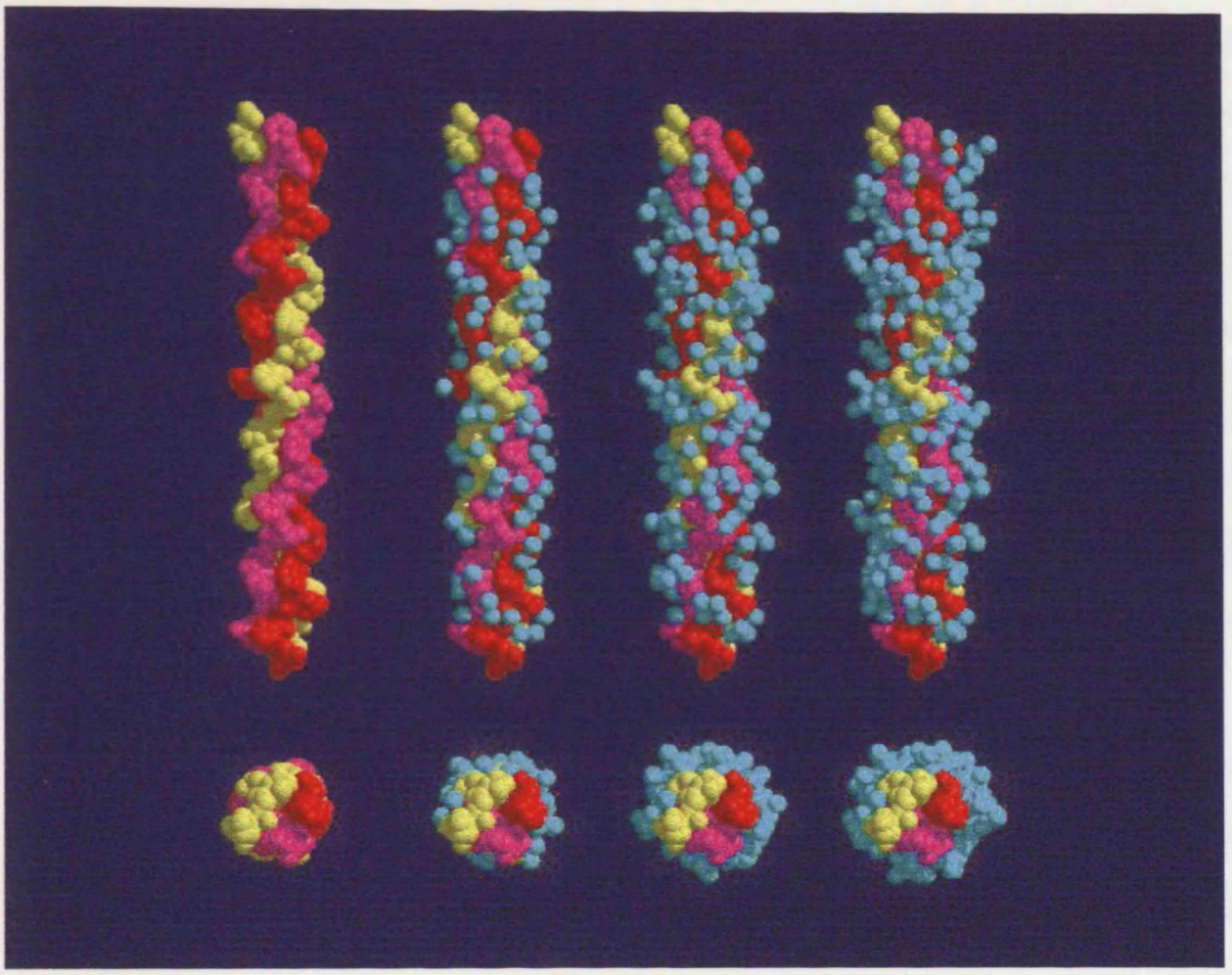

Figure 6.1: Space filling representation for the progressive hydration of the Gly→Ala peptide.

The views in the top row are perpendicular to the molecular axis, whereas those in the bottom row are parallel to the molecular axis. From left to right, a view of the naked triple helix, the three peptide chains are shown in different colours; incorporation of the first shell of water molecules, directly hydrogen bonded to carboxyl, hydroxyl, or even amide groups on the peptide surface; incorporation of the second hydration shell, hydrogen bonded to the ones in the first shell; the third shell of water molecules. *(Graphic courtesy of Berman laboratories, Rutgers University, Piscataway, USA)*

While that is one view of the role of solvent in stabilising collagen, an alternative theory comes from those who believe that inductive effects are paramount. They suggest that water does not play a major role in stabilising the structure. It was thought by Cooper that structural stabilisation may originate in solvent organisation around the triple helix[101]. However, he also suggests that the severe rotational restrictions placed on a polypeptide chain by the presence of pyrrolidine residues act to stabilise the triple helical structure by reducing the total conformational entropy change in the helix → non-helix transition. He goes on to say: 'This is not to deny the importance of hydrogen bonding in structural considerations of the protein, but it would seem, in the case of collagen, that the peptide/peptide hydrogen bonds differ little in stability from the peptide/water interactions.' So, it is the conformational restrictions that play the important role in stability.

In an interesting piece of unpublished work, Williams[102] measured the shrinkage temperature of raw calfskin in lithium bromide solution, a known hydrogen bond breaker. He found that soaking the sample in 1% (w/v) lithium bromide solution overnight led to a 5°C drop in hydrothermal stability when the analysis was performed in toluene. He suggested this drop in value was due to hydrogen bonds breaking. This idea is given credence by the effect of giving another sample the same treatment but then following it with a prolonged wash. The shrinkage temperature was restored to the original value. This, he suggests, is due to the hydrogen bonds reforming.

However, the question remains as to whether aqueous scaffolding could stabilise a macromolecular structure. While Berman and Kramer believe it can, Engel *et al* came to the conclusion that it could not. They demonstrated[103] that in a comparison of peptides of the same length, those with hydroxyproline residues induced an increased thermal stability compared with those without the Hyp. However, they showed that the presence of water was not essential by proving the same increase in thermal stability using non-aqueous solvents. Thus, it seemed

the role of Hyp residues, while stabilising the structure, does not rely totally on water to support a macrostructure. Raines[104] came to the conclusion that in fact it was not possible energetically to build and stabilise an 'aqueous scaffolding' on the scale required, which he said would involve 500 water molecules per triple helix. He said the energies would be enormous, but seems to have ignored the fact that collagen does indeed have a very high enthalpy of denaturation compared with other proteins[88].

Raines takes the argument further. While agreeing that the hydroxy group on proline helps to stabilise the collagen structure, rather than using hydrogen bonding to impart the stability, he suggests the important effect is due to the inductive effects. His group synthesised $(ProFlpGly)_{10}$, where Flp is a 4(R)-fluoroproline residue, fluorine being used because it is the most electronegative element. The other advantage of using fluorine is that organic fluorine is a poor hydrogen bond acceptor, thus any stabilising effects must come from another source. By comparing the circular dichroism spectra, they showed that the structure of the polymer did not differ from $(ProHypGly)_{10}$, but that it did increase the temperature of folding, table 6.2. Indeed temperatures of up to 91°C were achieved. The positive effect of adding hydroxyproline can also be seen clearly.

Table 6.2: Effect of structure on the shrinkage of the polymer

Polymer	Tm (°C)
$(ProProGly)_{10}$	41 ± 1
$(ProHypGly)_{10}$	69 ± 1
$(ProFlpGly)_{10}$	91 ± 1

The conclusion was that, because the fluorine atom exerts a greater inductive effect than the hydroxyl group and cannot hydrogen bond water molecules, the Flp residue contributes more to the collagen stability, via inductive effects, than do the hydroxyproline residues. This would

agree with Cooper's comments about reducing the number of conformation changes in going from a helical structure to a non-helical one.

6.3 Theory of shrinkage

6.3.1 Entropic effects

The shrinkage temperature of raw collagen as a function of swelling has been extensively studied and as a general rule the swelling is inversely proportional to the shrinkage temperature, as Theis and Steinhardt showed,[105] see figure 6.2. The addition of salts such as sodium sulfate introduces steric hindrance and Hofmeister[106] developed a classification, the Hofmeister series, that puts cations and anions into a rank, depending on how greatly a particular ion induces lyotropic swelling in gelatin. This series is usually discussed in relation to swelling in the beamhouse processes, but it has relevance here as well.

Using the change in optical rotation as a measure of the collagen folding, Von Hippel and Wang[107] showed the rate of mutarotation was equal to:

$$\log(\frac{d\alpha}{dt}) = \log(\frac{d\alpha}{dt})_0 + k_0 m$$

Where:

log ($d[\alpha]/dt$) = change in mutarotation at a given temperature and stated value of Hg line,

log $(d[\alpha]/dt)_0$ is the value at time zero,

k_0 = the slope of fitted line

m = molarity

Plotting log ($d[\alpha]/dt$) against the molarity gives a straight line, figure 6.3, and shows that collagen folding depends on the salt used. This explains why the addition of salts such as sodium sulfate, which follow the Hofmeister series, stabilises the collagen structure with

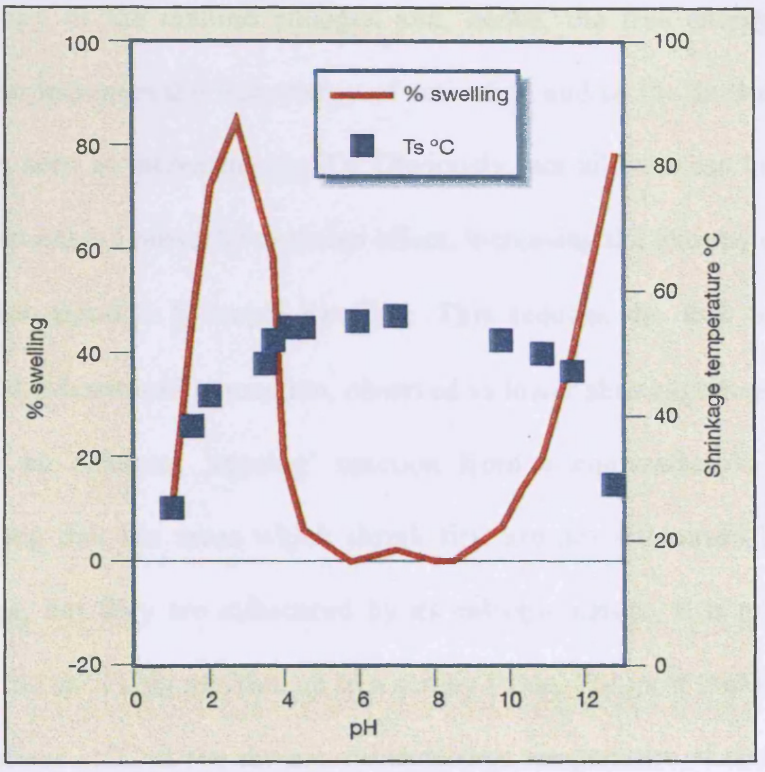

Figure 6.2: Change in swelling and shrinkage temperature as a function of pH

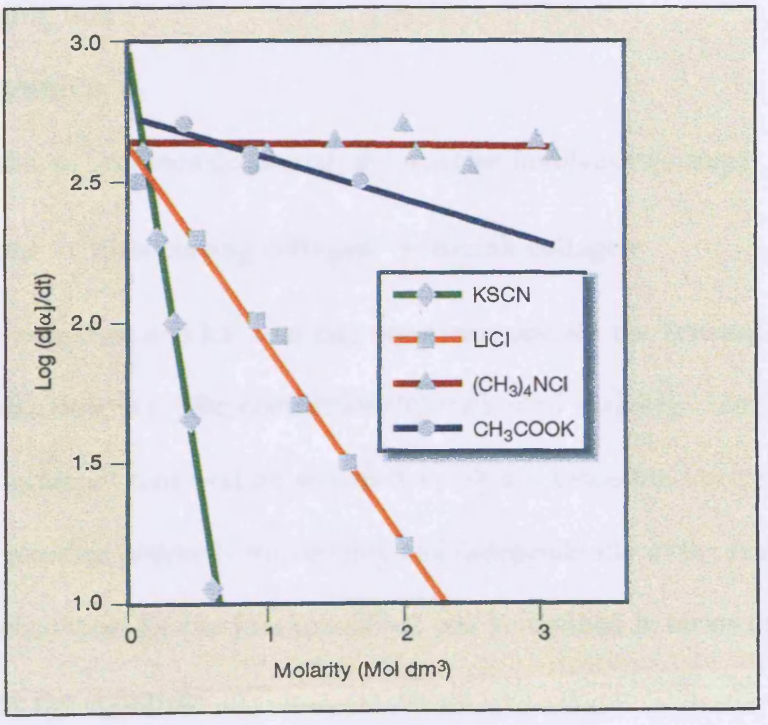

Figure 6.3: Log of initial rate of mutarotation of ichthyocol gelation at 3°C as a function of the molarity of salt added

respect to temperature. These additions reduce the rotational degrees of freedom and the conformational entropy of the random collagen and, hence, the free energy of the system increases. This in turn increases the free energy of activation and so the denaturation proceeds more slowly. This is seen as increasing the Ts. Obviously, not all salts can have this primary effect, since many can exert a powerful negative effect, increasing the entropy of the system by breaking the structure through lyotropic swelling. This reduces the free energy, $\Delta G^{\ddagger}$ and increases the rate of the denaturation reaction, observed as lower shrinkage temperature.

Since there can be an apparent 'tanning' reaction from a non enthalpic interaction, the inference can be made that the areas which shrink first are not influenced by the enthalpic nature of the tannage, but they are influenced by its entropic nature. It is proposed that this entropic term slows the shrinking reaction up to a certain value. For most tannages this is in the range 75- 80°C, ie about 15°C above the natural shrinkage temperature of raw skin. It will be recognised that many tannages stabilise collagen with respect to heat to about these temperatures. However, above about 80°C, the enthalpy begins to play the major role and this involves a 'co-operating unit'.

6.3.2 Thermodynamics

When collagen shrinks, ie becomes denatured, the reaction involves two steps:

Intact collagen ⇆ dissociating collagen → shrunk collagen

The first reaction is reversible and has two rate constants, one for the forward reaction, k_1 and one for the reverse reaction, k_{-1}. The conventionally measured shrinkage temperature, Ts, can be thought of as the notional temperature at which $k_1 >> k_{-1}$. Once the denatured collagen has begun to shrink, the reaction proceeds irreversibly and independently of the tannage.

And the equilibrium constant for the first transition, can be defined in terms of the free energy of the reaction, G°, by the equation:

$$\Delta G^{o} = -RT\ln K = -RT \ln k_1/k_{-1}$$

where: R = gas constant

T = absolute temperature of the reaction

K = equilibrium constant for the reaction

To relate this to the enthalpy and entropy of the system, the following derivation can be used. The free energy of activation, $\Delta G^{\ddagger}$, is defined as follows:

$$\Delta G^{\ddagger} = \Delta H^{\ddagger} - T\Delta S^{\ddagger}$$

where: $\Delta H^{\ddagger}$ = activation enthalpy of the reaction (kJ/mol)

$\Delta S^{\ddagger}$ = activation entropy of the reaction (J/K/mol)

For an endothermic reaction, the Hammond postulate says that the transition state is more like the products than the reactants[108], so the free energy of activation has a similar value to the free energy of reaction, illustrated in figure 6.4.

Therefore: $\Delta G^{\ddagger} = \Delta G^{o}$

And, thus,

$$\Delta H^{\ddagger} - T\Delta S^{\ddagger} = -RT\ln k_1 + RT\ln k_{-1}$$

So, when $k_1 >> k_{-1}$,

$$\ln k_1 = \frac{\Delta S^{*}}{R} - \frac{\Delta H^{*}}{RT}$$

Thus, the rate of the dissociation reaction depends on two factors: the entropy of activation, the degree of disorder in the formation of the transition state, and the enthalpy of activation, the bond energy change in the formation of the transition state.

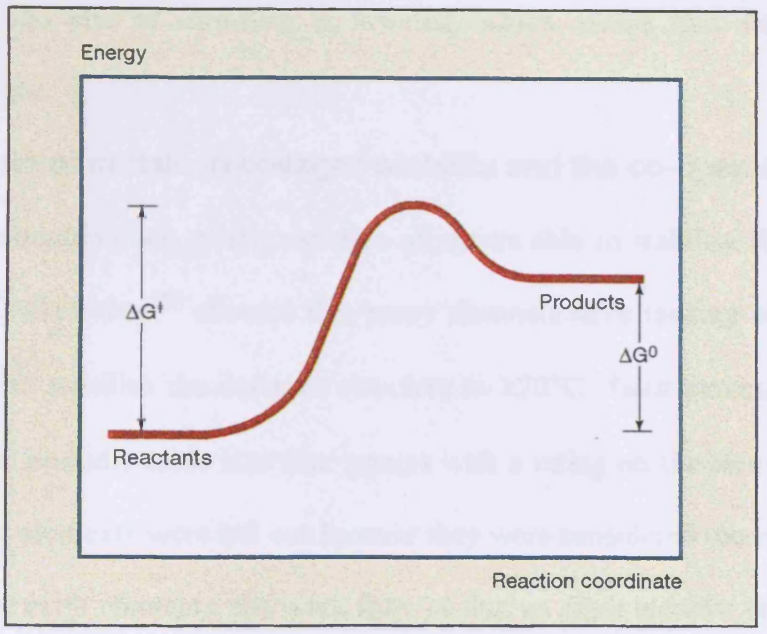

Figure 6.4: The energetics of an endothermic reaction

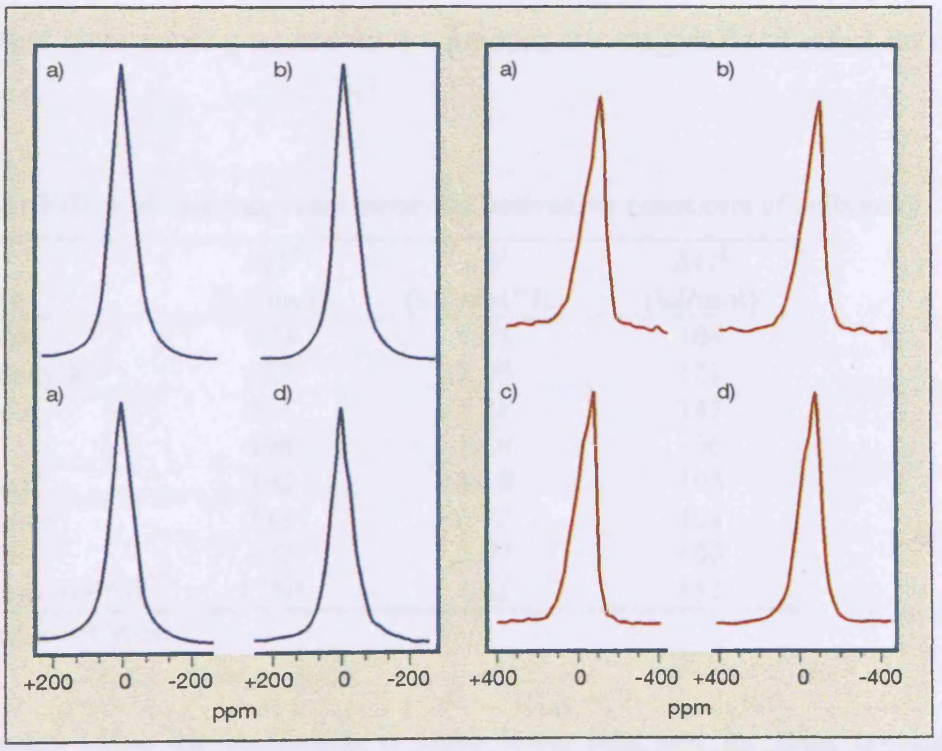

Left: Aluminium (III) sulfate tanned: Temperatures A=315K, B=325K, C=335K, D=345K

Right: Citrate masked aluminium (III) sulfate: Temperatures A=340K, B=350K, C=360K, D=370K,

Figure 6.5: Variable temperature ^{27}Al NMR spectra for aluminium (III) tanned hide powder

This means that, with a decrease in the entropy of activation and/or an increase in the enthalpy of activation, the rate of shrinking is lowered, which means that the apparent shrinkage temperature rises.

6.3.3 The role of metals in collagen stability and the co-operating unit

Mineral salts comprise one of the varieties of agents able to stabilise the collagen structure. Nursten and Chakravorty[109] showed that many elements have tanning ability, if the criterion for tannage is to stabilise the collagen structure to ≥70°C. Their extensive work divided the elements of the periodic table into four groups with a rating on the element's ability to 'tan'. Although some elements were left out because they were considered too expensive at that time, such as the rare earth elements, the work showed that no other element could match chromium (III).

Weir[110] showed that chromium (III) salts markedly increased the enthalpy of activation. This increases the $\Delta G^{\ddagger}$ value and so increases the value of the shrinkage temperature. He also showed that other tanning agents do not produce this magnitude of effect on the $\Delta H^{\ddagger}$ value, table 6.3.

Table 6.3: Effect of tanning treatments on activation constants of collagen‡

Tannage	$\Delta H^{\ddagger}$ (kJ/mol)	$\Delta S^{\ddagger}$ (kJ/mol/°K)	$\Delta G^{\ddagger}$ (kJ/mol)
Bated pelt	673	1.71	104
Formaldehyde	473	1.05	121
Zirconium	573	1.28	147
Iron	498	1.18	106
Vanadium	493	1.18	105
Aluminium	343	0.72	104
Uranium	427	0.97	106
Chromium (0.6%)†	1350	3.61	151

†modified from Weir

The enthalpy value for aluminium is much lower than that for other tanning agents. It is noteworthy that a small entropy of activation accompanies this. Covington *et al* [111], presented

an argument based on entropy considerations to explain the effect of aluminium (III) on accelerating the rate of chrome tanning. The argument centres on the role of Al(III) species orientating the carboxyl groups ready for reacting with chromium. There is an analogy with solvation, in which the interaction between the metal ion and solvating or coordinating solvent molecules is labile. That means the bond is easily made and broken. Therefore, the formation of the solvate results in little loss of disorder. So reaction between aluminium and collagen occurs with little entropy penalty. This has the effect of lowering the activation energy terms for any reaction with the sidechain carboxyls. Then incoming chromium (III) complexes find the sidechains already in conformations, which favour co-ordination, so the result is a more rapid fixation of chromium. From the data in Table 6.3, the free energy of activation for coordination of aluminium (III) is lower than that for chromium (III) due to the combined effects of the enthalpy and entropy terms, which operate in the same direction. This means that there is favourable energy for the formation of activated complexes between Al(III) and collagen, therefore reducing the energy penalty paid by chromium (III).

One of the reasons for chromium compounds producing high stability leathers seems to be due to the chromium complexes which, when attached to collagen, are kinetically stable.

Both Weir[112] and Covington[113] showed that chromium (III) salts exert their maximum influence when the chrome content of the leather is about 0.6 - 0.7% Cr_2O_3. This corresponds to a shrinkage temperature of about 77°C, which is within the range of hydrothermal stability that is controlled by entropy. At higher chrome contents, although the Ts increases, the chrome is less effective. This observation is consistent with the idea that more than one factor determines hydrothermal stability, with a transition point at moderate shrinkage temperature.

6.3.4 The shrinking reaction

Table 6.4[114] illustrates the relationship between the shrinkage temperature and the free energy of activation at 60°C for the shrinking transition and the enthalpy of the endothermic reaction.

The samples referred to in table 6.4 are raw collagen from kangaroo tail tendon or sheepskin flesh layer tanned with either formate masked aluminium (III) sulfate or basic chromium (III) sulfate.

Table 6.4: The kinetics and thermodynamics of collagen shrinking in wet heat at 60°C.

Tannage	Ts (°C)	$\Delta G^{\ddagger}$(kJ/mol)	ΔH_{endo}(kJ/mol)
Raw	60	103	104
Aluminium (III)	73	112	49
Chromium (III)	107	139	52

The relationship between Ts and ΔH_{endo} indicates that breakdown of the tanning interaction is not the cause of shrinkage. If the metal tanning bonds did break during shrinking, there would be a difference in the enthalpy of shrinking, with more energy being needed to break the more stable Cr (III)-collagen bonds. Ioannidis[115], using ^{27}Al nuclear magnetic resonance studies demonstrated the weak, hydrolysable aluminium tannage is not reversed during shrinkage. Figure 6.5 shows that at temperatures ranging from 67 to 97°C, ie below and above the shrinkage temperature of the samples, the ^{27}Al-nmr spectrum of aluminium (III) tanned hide powder is not altered by heat shrinkage.

This means that there is no change in the inner or outer co-ordination spheres of the bound aluminium (III) species. Also, the fact that the line intensity is not affected shows that the bound aluminium (III) species are not hydrolysed to $Al[H_2O]_6^{3+}$ species during shrinking.

Thus, the reaction of shrinking in wet heat is probably a breakdown of the hydrogen bonding in collagen or leather; that is, irrespective of the tanning process, the shrinking reaction is the same. The NMR data confirm the view postulated by Weir and Carter that hydrothermal shrinking is due to hydrogen bonds breaking.

6.3.5 Cooperating unit

As discussed above, the shrinking reaction can be treated like any other chemical reaction. Thus, it is assumed that there is a reactant, which must have a defined molecular mass. In this case, it is necessary to postulate the existence of collagen moieties, which serve this function. These moieties are portions of the macromolecule that cooperate as though they function as single molecular units. Such elements of collagen structure are defined as 'cooperating units'. The molecular weight of the cooperating unit, M_{eff}, corresponds to the size of the cooperatively interacting peptide units within the tertiary structure, which collapse during the denaturation of the specimen upon heating. These units of structure are involved in the initiation and propagation of the shrinking process along the collagen chain.

From the thermodynamic equations, the more positive $\Delta G^{\ddagger}$ is, resulting from either a more positive $\Delta H^{\ddagger}$ or by a more negative $\Delta S^{\ddagger}$, the smaller the rate constant k_1 becomes, so the forward reaction becomes slower. If the rate of shrinking is slow, then the temperature at which shrinking rate becomes appreciable, the shrinkage temperature, is higher.

For mineral tanning, $\Delta G^{\ddagger}$ values correlate well with the size of the cooperating unit when the cooperating unit is larger, k_1 is smaller and the shrinkage temperature is higher. This is illustrated in figure 6.6 and shown in table 6.5, which shows the size of cooperating units, based on the measured rate of shrinking and the calculated activation entropy.

Table 6.5: The effect of tannage on the size of the putative crosslink

Tannage	Shrinkage temperature (°C)	Number of amino acid residues in Cooperating unit
None	60	25
Aluminium (III)	73	71
Chromium (III)	107	206

The figure shows that the greater the influence of the cooperating unit the higher the shrinkage temperature. The extent of the cooperating unit seems to be a function of the tannage, and the

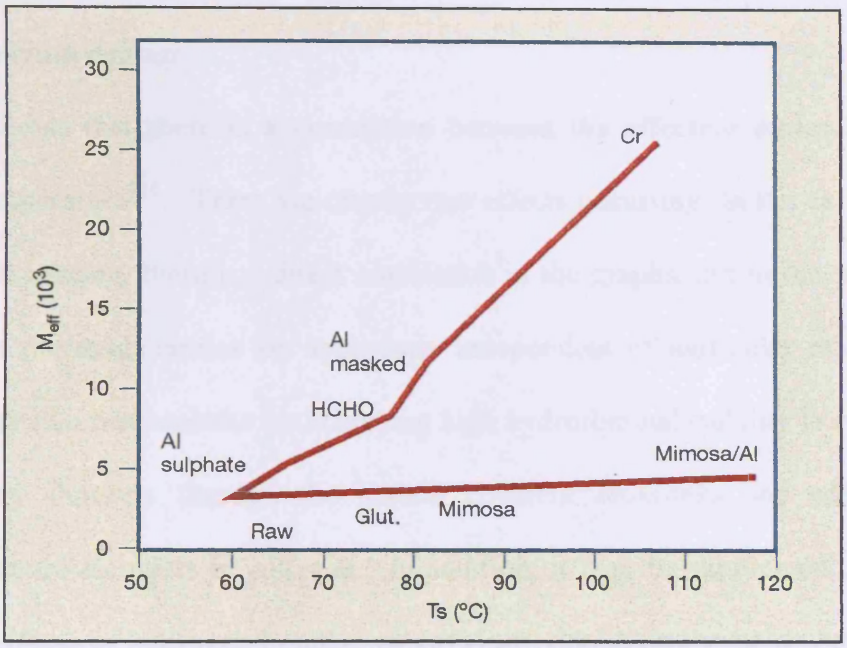

Figure 6.6: Relationship between the size of the cooperating unit and the shrinkage temperature for raw collagen, masked and unmasked aluminium (III), mimosa, formaldehyde, glutaraldehyde and chromium

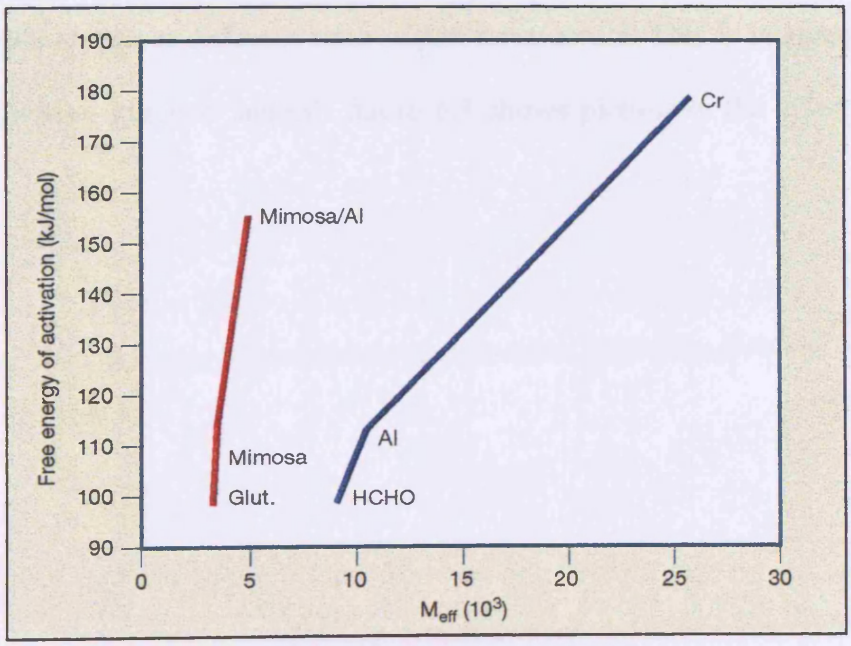

Figure 6.7: The relationship between the free energy of activation and the size of the co-operating unit. Tannages with masked aluminium (III), mimosa, formaldehyde, glutaraldehyde or chromium (III)

results fit with the observation that chromium tannage imparts hydrothermal stability better than an aluminium tannage.

Figure 6.7 shows that there is a correlation between the effective molecular mass and the shrinkage temperature[116]. There are clearly two effects occurring. In the cases of mineral and formaldehyde tanning, there is a direct correlation in the graphs, but in the cases of polymeric tannages, the thermodynamics are apparently independent of molecular mass. This indicates there might be two mechanisms for achieving high hydrothermal stability in tanned collagen. A crosslink may function through the natural covalent crosslinks and additional hydrogen bonding structure elements in collagen. In addition, it may be supplemented or modified by the tanning effects of hydrogen bonding or covalent crosslinking at polar groups on the amino acid side chains or through multiple interactions at the peptide link itself. With chromium (III) tannages the influence of the cooperating unit extends approximately 50 residues either side of the covalent linkage. It has been estimated that only 10% of the bound chrome is involved in crosslinking[117], and assuming chrome crosslinking is the sole source of hydrothermal stability[118] and that those crosslinks are evenly distributed over the triple helix length, the collagen should shrink at different rates within its structure. This is in agreement with Weir's idea of a shrinking nucleus. Indeed, figure 6.8 shows pictorially the effects that he saw [119].

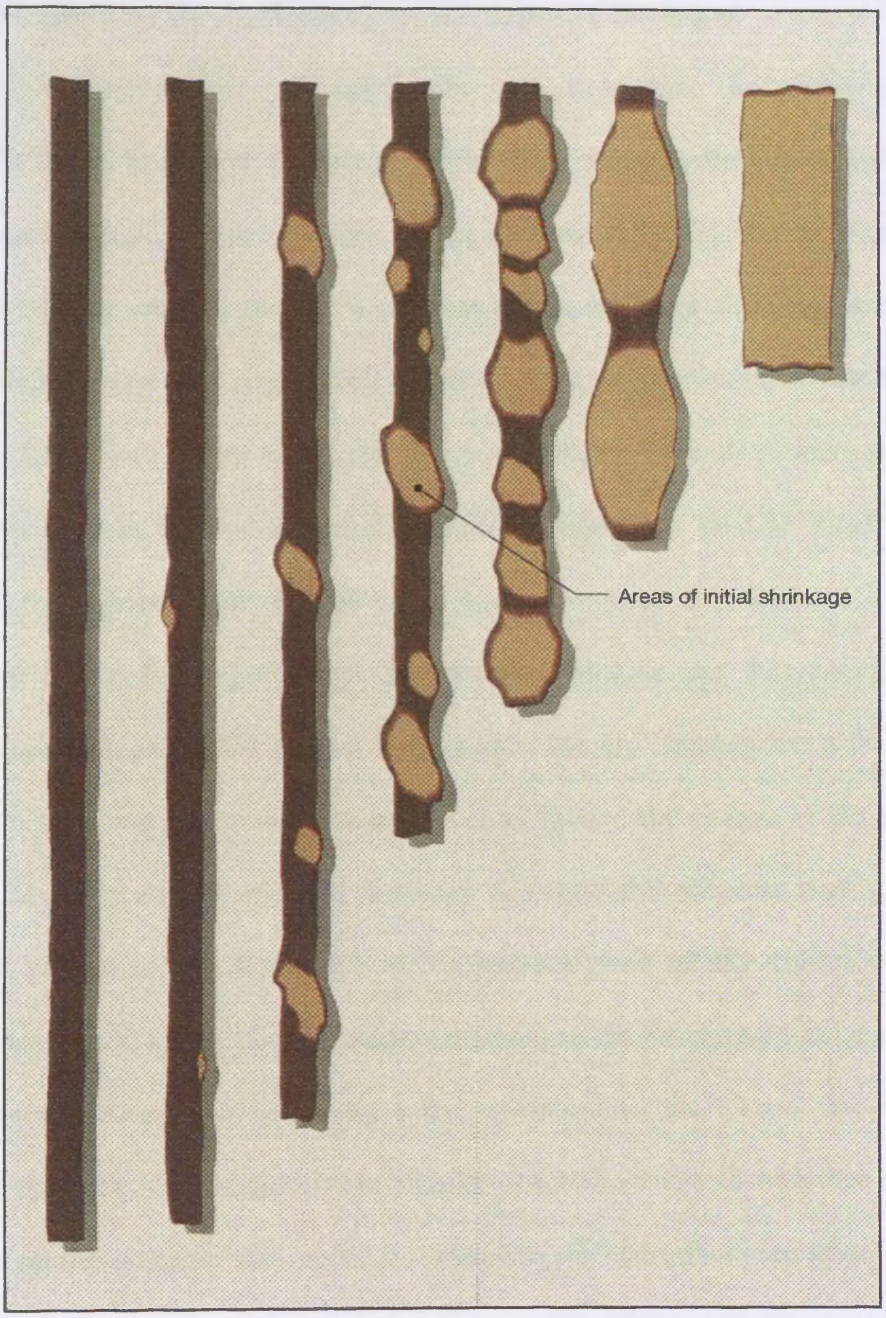

Figure 6.8: The non-uniform behaviour of collagen during thermal shrinkage

6.3.6 The effect of the hydrophilic/hydrophobic balance

Many chemical compounds will apparently 'tan' raw skin; the problem for the leather technologist lies in producing a tannage which will give the hydrothermal and other properties necessary to make the leather useable. As an extreme example, neutral salts such as sodium chloride or sulfate are said to give a salt tannage because the shrinkage temperature is over 70°C. While no one would suggest this is truly leather, the increase in hydrothermal stability is interesting. There can be no crosslinks in the conventional covalent, ion pairing or hydrogen bonding sense. Thus, the hydrothermal stability in these cases must be occurring through ionic bonding, steric effects or dehydration.

The use of the hydrophilic/hydrophobic balance, used in the determination of surfactant properties, may be an indicator here. It is known that dry collagen has a far higher shrinkage temperature than wet collagen. Witnauer[120] *et al* likened the change in the behaviour of hide substance in the presence of small amounts of compatible diluents such as water, ethylene glycol and phenol to the depression of the melting point of any crystalline substance by a diluent. They suggest that: 'the shrinkage temperature can be elevated quite simply by limiting the amount of diluent that can solvate the polypeptide coils.' Thus, the only difference in stabilising the collagen structure is the amount of water associated with that structure, which is dependent on the tannage. This could be related to the hydrophobicity of the system and, thus, it may then be possible to predict which type of tanning agents are best at stabilising the collagen.

To take a crude analogy, the hydrophilic vegetable tannages have a lower shrinkage temperature than the more hydrophobic metal tannages. Witnauer suggests the reason for this is that vegetable tannins act like a diluent themselves, through the loose associations of its polar groups with the polypeptide chains. Given that leather, which has been waterproofed

shows greater apparent stability to shrinking than one which has not, then it does seem likely that the hydrophilicity of the tannage is important in determining the stability of the leather.

Taking this idea further, it may be the interfacial tension effects that are important rather than the actual solvent. BLC[121] and Japanese workers have extended the use of HHB to dyes. It is possible to determine the properties of the dye by investigating the HHB values in different solvents. This gives the tanner an idea of how the dye will work in production. It should also be possible to use the system for fatliquors, as these are basically modified surfactants. So, it is not too difficult to see a way of extending the idea to include tanning agents; the variation in their tanning ability being partially due to their hydrophilicity.

The introduction of highly charged or polar molecules tends to decrease the stability of the folded structure, typically by lyotropic effects. It will also increase the hydrophilicity of the system and, hence, make the collagen more labile. This may be a contributory reason why aluminium (III) does not increase the enthalpy of activation as much as chromium (III). In the region surrounding the Al-collagen interaction, there is greater disruption in the crystallinity, that is higher entropy or greater lability in the interaction, and this offsets the stabilising effects of tanning. The argument applies to other mineral tanning agents, such as titanium (IV) and zirconium (IV), which fix to collagen principally by charge-charge or ion pair interactions.

6.3.7 Crystallinity

Crystallinity may also explain why other tanning agents do not have effects as big as chromium (III). In chrome tanning reactions, the number of chromium atoms complexed together is around three or four[122]. Thus, they are discrete moieties, small and precisely defined molecules, which interact specifically with the collagen molecule.

Most tanning agents, other than chromium (III), are polymeric to a greater or lesser extent and although they have a positive enthalpic effect, the longer crosslinks do not enhance crystallinity in the same way as chromium (III) complexes.

Montgomery *et al.*[123] employed a method of introducing short, non-labile crosslinks into the collagen, mimicing the action of chromium taning. They reacted collagen with pyromellitic dianhydride and retanned them with aluminium. The shrinkage temperature of the leather was in excess of 120°C. The large increase in hydrothermal stability is probably due to short crosslinks being formed between the metal, the organic compound and the rigid non-labile collagen-peptide link.

6.4 Conclusions

- Shrinkage temperature is related to the size of the cooperating unit involved in the shrinking reaction. This determines the kinetics of shrinking: the bigger the cooperating unit is, the slower the rate of shrinking is, which makes the conventionally measured shrinkage temperature higher.
- The size of the cooperating unit is determined by the nature of the crosslinking reaction, in particular the power of the crosslink to confer a localised higher degree of structure to collagen.
- The magnitude of the effect of a tannage is controlled by two factors: the interaction of the crosslinking species with collagen (the lability of the bonding) and the nature of the crosslinking moiety itself. If the crosslink is formed by a second interaction, linking species directly bound to collagen, there is a third factor, the lability of this bonding.
- High shrinkage temperature is achieved by the introduction of 'stiff' structure making crosslinks: this means they must necessarily be short.
- Structure-making crosslinks must be short and non labile; the former depends on crosslink stereochemistry and geometry, the latter is achieved either by covalent reactions or by multiple weaker bonding.

- When the lability is determined by weak bonding, structure-making or rigidity can be introduced by short, covalent (non labile) crosslinks between the weakly bonded species.
- For hydrogen bonding tanning species, there is a critical magnitude of reaction, at which the interaction with collagen constitutes low lability, but allows short crosslinks to be formed. In the absence of structure-making crosslinking, hydrogen bonded interactions at both ends of the crosslink in collagen constitute a labile crosslink.
- In the crosslinking of species bound to collagen, the crosslinks must be short; this means that the crosslinker must have greater affinity for the substrate than for itself, in order to avoid an extended, polymeric crosslink.

In this way, the differences between tannages can be explained. Tannages that conform to the rules of low lability and stiffness in the crosslinking will confer high hydrothermal stability to collagen.

6.5 Overview and future work

The research set out in this thesis has developed a number of new areas in leather science. These include:

- the first use of X-ray absorption techniques such as EXAFS and XANES to investigate the interaction of transition metals with collagen. There is still much work that needs to be done in these areas, such as varying the process conditions. Although, the data obtained with the XANES spectra proved difficult to analyse, this was more due to the inexperience of the operator than the information not being there. If a programme could be extended from the EXAFS, then XANES could prove very useful in determining the structure of the complexes involved in tanning
- the use of ENDOR AND ESR to investigate the effect of transition metals on the stability of leathers produced both as a solo tannage and via the semi-metal tannage route. It was gratifying that with the vanadium tannage we were able to determine where the complex bonded to the collagen. This would obviously be useful to repeat with chromium, where the interaction with collagen is already better understood.
- the role of the metal in the production of free radicals that may attack the polyphenolic moieties of the veg tan could be investigated using ESR or ENDOR. The addition of scavengers, such as those used in reducing the yellowing effects and fading of dyes, may reduce the effect of the free radical oxidation process on the degradation of the tannage, seen with vanadium tannages. Further investigation is needed and tests such as repeating the semi-vanad tannage and measuring how the shrinkage temperature changes with time or how the aqueous extract pH changes with time may help determine how the vanadium/collagen/veg complexes are changing with time. This work could be carried out with vanadium (IV) salts, since the salt is easily available, easy to use and stable in air.

- the first use of NMRD to investigate the interaction of transition metals and soluble collagen. Again, there is much that could be done, such as varying the process conditions and investigating the changes in chromium species during processes such as basifying.
- a new theory of hydrothermal stability was developed from this research into titanium (III), chromium (III) and semi-metal tannages, and by reinterpreting data from various papers already published. This work should help to develop bespoke tanning agents, which can be used for specific properties.

The research into titanium (III) as an alternative tanning agent highlighted the unique characteristics of chromium (III) as a tanning agent. It seems that no other mineral element's chemistry can satisfy the need for oligomeric rather than polymeric complexes, the right pH values that maximise both the size of the complexes without leading to precipitation and the interaction with collagen. Using titanium (III) highlighted the problems associated with using elements that polymerise at pH values where interaction with the collagen is a necessity. However, the research also showed that titanium (III) was useful as a retanning agent in semi-metal tannages and it would probably be beneficial to investigate this interaction, to determine whether the leather produced is suitable for bookbinding leathers.

An example of the future of tanning is illustrated in work discussed by Covington[124]. He showed that by pretanning with synthetic resins with the right molecular dimensions and then crosslinking them in situ, a high stability tannage could be obtained. The shrinkage temperature of leathers tanned with melamine-formaldehyde polymer, which is then crosslinked by tetrakis hydroxymethyl phosphonium sulfate, depends primarily on the size of the polymer particle. Smaller than optimum size species either provide too labile an interaction with collagen or do not crosslink. Bigger than optimum size species reduce the rigidity of the crosslink and either effect reduces the hydrothermal stability and the magnitude of the reduction depends on how far the particle size is from optimum. Another factor is the hydrophobic nature of the tannage, which is likely to have a positive effect on the shrinkage temperature. The future of tanning probably lies in this direction.

References

1. Covington AD and Ma S, UK patent 2 287 953, June 1996
2. Bailey AJ and Paul RG, Heidemann Symposium, proceedings of IULTCS Centenary Congress 1997, 17
3. Gustavson, KH, '*Chemistry and reactivity of collagen*', p225, Academic press Inc, New York
4. Privalov PL, *'Adv in Protein Chemistry'* 35 56
5. Covington AD, *J Soc Leather Technol Chem* 1986 70 **2** 33
6. Covington AD, *J American Leather Chem Assn* 1987 82 **11**
7. Thorstensen TC, *J American Leather Chem Assn* 1930 25 **116**
8. Heidemann E, Tonigold L and Hein A, S8, Proceedings of IULTCS XX, 1989, Philadelphia
9. Cotton FA & Wilkinson G, *'Advanced Inorganic Chemistry'* 5th Ed, 1988 pg 660
10. Pecsok RL and Fletcher AN, *Inorganic Chemistry* 1962 **1** 1 155-159
11. Baes CF, '*Hydrolysis of Cations*', pg 19, Plenum Press, New York, 1976
12. Brunschwig BS and Sutin N, *Inorganic Chemistry* 1979 **18** 7 1731-1736
13. Hugi AD, Helm L, Merbach AE, *Inorganic Chemistry* 1987 **26** 11 1763
14. Hugi AD, Helm L, Dellavia I, *Inorganic Chemistry* 1992 **31** 11 2230-2233
15. Chaudhuri P & Diebler H, *Z Fur Phys Chem* 1984 **139** 191-202
16. Chaudhuri P and Diebler H, *JCS Dalton* 1976 1693-1695
17. Chaudhuri P and Diebler H, *JCS Dalton* 1977 596-601
18. Hartmann H and Schläfer HL, *Z Physik Chem* 1951 **197** 116
19. Wessel K and Ijdo, F, *Acta Cryst* 1957 **10** 466 from '*The chemistry of titanium and vanadium – An introduction to the chemistry of the early transition metals*', RJ Clark, Elsevier, London 1968

20. Birk JP and Logan TP, *Inorganic Chemistry* 1973 **12** 3 580-584

21. Goroshchenko G and Godneva MM, *Russian Journal of Inorganic Chemistry* 1961 **6** 6 744-746

22. Cservenyak I, Kelsall GH and Wang W, *Electrochimica Acta* 1996 **41** 4 563-567

23. Whitney JE and Davidson NJ, *J Amer Chem Soc* 1947 **69** 2076-77

24. McConnell H and Davidson NJ, *J Amer Chem Soc* 1950 **72** 5557

25. See *reference 21*

26. McConnell H and Davidson NJ, *J Amer Chem Soc* 1950 **72** 3168

27. Browne CI, Craig N and Davidson NJ, *J Amer Chem Soc* 1951 **73** 1946

28. Whitney JE and Davidson NJ, *J Amer Chem Soc* 1949 **71** 3809

29. Swamy MP, Bangaruswamy S, Chatterjea JN and Rao JB, *Leather Science* 1983 **30** 10 291-306 and p325-342

30. Covington AD, Lampard GS and O'Brien P, Proceedings of the XXV IULTCS Congress 1999, SLO-6, 62

31. Petroselli R, *LEATHER* 1995 **197** 4638 31

32. Society of Leather Technologists and Chemists's Official Methods of Analysis, 1996, SLC 8

33. Vogel A, *'Quantitative Inorganic Analysis'*, Vol 4, 750 (XIII,28 – determination of titanium)

34. Covington AD, *J Amer Leather Chem Assn* 1991 **86** (11) 456

35. Rusakova Z, *Kozh Obuvn Prom* 1981 **23** 24

36. Heidemann E, '*Fundamentals of Leather Manufacturing*' Pg 338, Eduard Roether KG, Darmstadt, 1993

37. Celades R, Duque J and Palma JJ, S9, Proceedings of IULTCS Congress, Philadelphia 1989

38. Peng J, *Personal communication*, November 1999

39. Swamy MP, Bangaruswamy S, Chatterjea JN and Rao JB, *Leather Science* 1983 **30** 10 325-342

40. Francke H, T4 .9, pg 837, *Proceedings of the IULTCS Congress*, Barcelona 1991

41. Hernandez JH and Kallenberger WE, *J Amer Leather Chem Assoc* 1984 **79** (5) 182

42. Slabbert NP *J Amer Leather Chem Assn* 1981 76 231

43. Sykes RL, Hancock RA and Orszulik S T, *J Soc Leather Technol Chem* 1980 **64** 32

44. Kallenberger W and Hernandez JF *J Amer Leather Chem Assn* 1983 78 217

45. Kallenberger W, *Personal communication*

46. Covington AD, *Personal communication*

47. Covington AD, *Chem Soc Rev*, 1997 124

48. Theis ER and Blum WA, *J Amer Leather Chem Assn* 1942 **37** 553

49. Slabbert NP *J Amer Leather Chem Assn* 1981 **76** 231

50. Evans NA, Milligan B, Montgomery KC, *J Amer Leather Chem Assn* 1987 **82** 91

51. Van Benschoten JJ, Tasset DG, Eversole R and Kallenberger WE, *J Amer Leather Chem Assn* 1985 **80** 237

52. Covington AD and Shi B, *J Soc Leather Technol Chem* 1998 **82** (2) 64

53. Covington AD and Shi B, *J Soc Leather Technol Chem* 1999 **83** (1) 8

54. Covington AD, Lampard GS and Pennington M, *J Soc Leather Technol Chem* 1998 **82** (3) 78

55. Weir C, *J Res Natl Bur Std* 1949 **43** 17

56. Covington AD and Lampard GS, Second Freiberg Conference on Collagen, May 25-26,2000

57. Pierce W & Conabere GO, *J Soc Leather Trades Chem* 1942 **26** 99

58. Murphy DM, Lecture to Postgrad students at Cardiff University, Feb 1999

59. Banwell CN and McCash EM, *'Fundamentals of Molecular Spectroscopy'*, p251, 4th edition, McGraw Hill, London 1994

60. Wilson RC and Myers RJ, *J Chem Phys*, **1976** 64 2208

61. Premović PI and West PR, *Can J Chem* 1975 **53** 1630-1634

62. Tachikawa H, Ichikawa T and Yoshida H, *J Amer Chem Soc* 1990 112 977-982 and 982-987

63. Segal BG, Kaplan M, Fraenkel GK, *J Chem Phys* 1965 **43** 4191 and correction Allendoerfer RD, *J Phys Chem* 1971 **55** 3615

64. Li H, Biglino D, Erickson R, Lund A, *Chem Phys Lett* 1997 **266** 417

65. Hornak JP, '*The basics of Magnetic Resonance Imagery*' Rochester Institute of Technology', USA 1996

66. See reference 59, page 251

67. Clementi V and Luchinat C, *Acc Chem Res* 1998 **31** 351-361

68. Aime S, Botta M, Fasano M and Terreno E, *Chem Soc Rev*, 1998 **27** 19-29

69. Koenig SH, Brown RD, III, '*NMR spectroscopy of Cells and Organisms*' Gupta RK, Ed, CRC Press, Boca Raton, FL, 1987, Vol 2 .

70. Bertini I, Luchinat C and Xia Z, *Inorg Chemistry* 1992 **31** 3152-3154

71. Teo BK and Joy DC, *'EXAFS Spectroscopy –Techniques and applications'*, p13, 1980, Plenum Press

72. Bianconi A, *'XANES Spectroscopy'* Chapter 11, page 575 in 'X-Ray Absorption', Edited by Koningsberger DC and Prins R, 1980, Plenum Press

73. McCarthy PJ and Richardson MF, *Inorg Chem* 1983 **22** 2979-2983

74. Beattie JK and Best SP, *Coordination Chemistry Reviews* 1997 **166** 391-415

75. Irving HMNH, *J Soc Leather Technol Chem* 1974 **58** (3) 51

76. Stunzi H and Marty W, *Inorg Chem* 1983 **22** 2145

77. Gafford BG *et al, Inorg Chem* 1990 **29** 4652, Nakahanda M *et al, ibid* 1992 **31** 1315

78. Finholt JE et al, *Inorg Chem* 1965 4 43

79. Lytle F, *Personal communication*, 22 August, 1999

80. Schroeder S, *Personal communication*, 30 October, 1999

81. Covington AD, Hancock RA and Ioannidis IA, *J Soc Leather Technol Chem* 1989 **73** (1) 1

82. Brown EM, Dudley RL and Elsetinow AR, *J Amer Leather Chem Assn* 1997 **92** (9) 225

83. Apperley DC, *Personal communication*, 19 February, 1999

84. Apperley DC, *Personal communication*, 9 February, 1999

85. Jordan-Lloyd, DJ and Balfe MP, *'Progress in Leather Science'*, Chapter 23, III, 487, 1948, BLMRA

86. Gustavson KH, *'The chemistry of the tanning process'*, P3, Academic Press, New York, 1956

87. Pauling L, *J Amer Chem Soc* 1940 **62** 2643

88. Wilson JA, *J Amer Leather Chem Assn* 1941 **36** 584

89. Braybrooks I, et al *J Int Soc Leather Trades Chem* 1939 **23** 111, 135

90. Astbury WT, *J Int Soc Leather Trades Chem* 1940 **24** 69

91. Weir CE and Carter J, *J Res Natl Bur Std* 1950 **44** 599

92. Miles CA and Bailey AJ, '*Trends in Collagen*', Chemical Sciences, Feb 1999, **111**, (1),71 Indian Academy of Sciences, Bangalore .

93. Gustavson KH, *'The chemistry and reactivity of collagen'*, P 225, Academic Press, New York, 1956

94. Woodhead-Galloway J, '*Collagen – the anatomy of a protein*' P26, Edward Arnold, London, 1980

95. Berg RA and Prockop DJ, *Biochem and Biophys Res Comm* 1973 **52** 1 115-119

96. Privalov PL and Tiktopulo EI, *Biopolymers* 1970 9 127-139

97. Ramachandran GN & Ramakrishnan C, *Biochemistry of Collagen*, 1976, Plenum Press, Chapter 2

98. Privalov PL, *Advances in Protein Chemistry* 1982 **35** 1-104

99. Bella J, Brodsky B and Berman HM, *Structure* 1995 **3** (9) 893-906

100. Kramer RZ, Vitagliano L, Bella J, Berisio R, Mazzarella L, Brodsky B, Zagari A and Berman HM, *J Mol Biol* 1998 **280** 623-28

101. Cooper A, *J Mol Biol* 1971 **55** 123-127

102. Williams JMV, *'Shrinkage temperature and other studies'*, ALC, Leathersellers' College, Dec 1964

103. Engel J, Chen H-T and Prockop DJ, *Biopolymers* 1977 **16** 601-622

104. Raines RT, Holmgren SK, Taylor KM and Bretscher LE, *Nature* 1998 **392**, 666

105. Theis ER & Steinhardt RG, *J Amer Leather Chem Ass* 1942 **37** 433

106. Von Hippel PH and Wang KY, *Biochemistry* 1962 **1** 664-674

107. Hofmeister W, in Principles of Leather Manufacture, Ed: HR Procter, Spon, p 625, 1936

108. Hammond GS, *J Amer Chem Soc* 1955 **77** 334

109. Nursten HE and Chakravorty HP, *J Soc Leather Technol Chem* 1958 **42** (1) 2

110. Weir C, *J Res Natl Bur Std* 1949 **43** 17

111. Covington AD, *J Soc Leather Technol Chem* 1986 **70** (2) 33

112. Weir C, *J Res Natl Bur Std* 1949 **43** 17

113. Covington AD, *Chrome Management*, 1995, UNIDO workshop, Ljubljana, Slovenia

114. See reference 81

115. Ioannidis IA, Covington AD, and Hancock RA, IULTCS XXth Congress 1989, paper S2

116. Covington AD, *personal communication*

117. Gustavson KH, *'Chemistry of the Tanning Process'*, Academic Press, 1956

118. Sykes RL, *J Amer Leather Chem Assoc* 1956 **51** (5) 235

119. Weir C, *J Amer Leather Chem Assoc* 1949 **44** (3) 108

120. Witnauer LP and Fee JG, *J. Amer. Leather Chem. Assoc* 1959 **54** (7) 374

121. Dyson W, Knight M and Britten P, BLC Laboratory report 178 (Restricted Circulation)

122. Covington AD, *Chromium Review* 1985 **5**

123. Montgomery KC, *Proceedings of the IULTCS Congress,* Philadelphia 1989, *S1*

124. Covington AD and Ma S, Proceedings of the IULTCS Centenary Congress, London 1997

Appendix 1: Tanning processes

All percentages based on pickled weights, unless stated

Tannage used in section 3.3.1

X% Ti as titanium (III) sulfate

Run 4 hours at 25°C

Basify to pH 4 with sodium bicarbonate over 2 hours

Drain and rinse.

Tannage used in section 3.3.2

X% Ti as titanium (III) sulfate

Run 4 hours at 20°C or 30°C

Basify to pH 4 with sodium bicarbonate over 2 hours

Drain and rinse.

Tannage used in section 3.3.5

5% Ti as titanium (III) sulfate

2 moles sodium citrate to 1 mole of titanium

Run 4 hours, under nitrogen, at 35°C

Basify with HMT at 1,2,5 and 10% over 1 hour

Neutralise to pH 4 using sodium hydroxide

Sample not basified with HMT was basified with sodium hydroxide only

Shrinkage temperature was measured using SLP 18.

Tannage used in section 3.5.2.2

Depickle sheepskins to pH 4 with sodium acetate and sodium bicarbonate

5% Ti as titanium(III) sulfate or titanium(IV) potassium oxalate

Mask with 2 moles of masking salt to 1 mole of titanium

Basify to pH 3 with sodium hydroxide

Run overnight at 25°C

Basify to pH 4 with sodium bicarbonate

Drain and rinse

Tannage used in section 3.5.3

5% Ti as titanium (III) sulfate

Add 2 moles of masking agent per mole of titanium (III)

Run overnight at 20°C

Add 5% HMT

Basify to pH 4 using sodium hydroxide over 2 hours

Drain and rinse

Tannage used in section 3.7

Depickle: 150% buffer solution (60g/l sodium chloride, 40g/l sodium acetate trihydrate,

10g/l sodium bicarbonate

pH 4.5

Leave overnight, drain.

Cut blue to bromocresolgreen

100% cold water Run 30 minutes

Drain

Divide samples

100% water at 25°C

5% syntan (100% solids)

Run overnight. Take sample to measure shrinkage temperature.

Acidify with formic acid to pH 3.5

Retan: + 5% titanium oxide using either titanium (III) sulfate or potassium titanium oxalate

Run 4 hours

Basify with sodium bicarbonate aliquots to pH 4

Drain. Samm

Samples were recombined and fatliquored.

100% water at 40°C

2% sodium bicarbonate, pH 5.5

+5% highly sulfited cod oil

Run 60 minutes

Acidify with formic acid to pH 3.6

Drain

The samples were hang dried.

Tannages used for semi-metal leathers in section 3.92 and 4.5.1.4

Wash:	100% brine solution (10% w/v) at 20°C	
		Run 10 minutes
	Drain	
Pretan		
	100% brine solution (10% w/v) at 20°C	
	3% glutaraldehyde [as Relugan GT50 ex BASF]	
		Run 60 minutes
	+ 1% sodium formate	
	+ 0.75% sodium bicarbonate.	pH 4.6
	Drain	
	6% sodium sulfate	
	2% sulfated fatliquor [Remsynol ESA]	
	4% pretanning syntan [Neosyn N]	
		Run 30 minutes
	+ 0.2% sodium hydrogen sulfite	Run 20 minutes
Tannage	+ 5% vegetable tannin	Run 30 minutes
	+ 5% vegetable tannin	Run 30 minutes
	+ 50% water at 30°C	Run 1 hour
		penetration checked with $FeCl_3$
	Drain, wash off, samm and horse up.	

Toggle dry, stake and bag ready for the metal tannages

The leathers were redivided and half were tanned with 1% metal content of the following metals:

- aluminium (III) [as Neosyn 9P {10% Al_2O_3, ex Hodgson Chemicals}]
- chromium (III) [as 25/33 powder]
- titanium (III) [as freshly made titanium (III) sulfate]
- titanium (IV) [as potassium titanyl sulfate]

Vegetable leathers were wetted back in an excess of water and reweighed.

Wash	200% water at 40°C	Run 10 minutes
Drain		
Fatliquor	100% water at 40°C	
	5% highly sulfited fatliquor [Paradol MIR]	
		Run 40 minutes
Acidify	+ 2% formic acid [diluted 1:10 with water]	
	+ 0.5% oxalic acid [diluted in 10x water]	Add in 3 lots
		Run 3 x 10 minutes
		pH:3.7
Metal tannage	100% water at 35°C	
	+ 1% metal ion concentration on weight of leather	
	+ 1% sodium acetate	Run 1 hour
Basify	2% magnesium oxide [as Tanbase]	Run 4 hour
	+ x % sodium bicarbonate	to give pH 3.8-4.0

Drain		
Fixation	**150% water at 35°C**	
	1% neutral syntan [as Neosyn N]	
	+ 0.5% calcium formate	**Run 30 minutes**
	+ 1.5% sodium bicarbonate	**Run 30 minutes. PH 4.0**

The leathers were sammed, toggled dried and finished at CF Stead & Co Ltd, Leeds, England.

Tannages for use in X-ray absorption spectroscopy (section 5.65)

The titanium and chromium leathers for use in EXAFS and XANES analyses were produced using the following tannages.

1 Titanium

50% water at 20°C

10% salt Run 10 minutes

+4% sodium acetate

+1% sodium bicarbonate Run 20 minutes pH 4.2, cut blue to bromo-cresol green

Drain and store in plastic bag

5% titanium, as titanium (III) chloride or as potassium titanium (IV) oxalate, masked in a 1:1 mole ratio with sodium citrate, sodium tartrate or sodium gluconate.

Adjust to pH 4. Run overnight

Adjust to pH 4

+5% Neosyn N

+2% synthetic fatliquor. Run 45 minutes. Drain.

Chromium

Standard hide powder was treated as follows:

100% water at 25°C

2% chrome powder as either 33%, 42% or 50% basicity. All contained 25% Cr_2O_3

Run 4 hours at 25°C. Adjust to pH 4 and run overnight at 35°C in a shaking waterbath.

pH adjusted to 4 in the morning using sodium bicarbonate.

No masking agents were used. All samples were air dried, ground using a Wiley Mill and bagged

Appendix 2: Two-way analysis of variance of tannages set out in section 3.7

Analysis of Variance for shrinkage

Source	DF	SS	MS	F	P
Titanium	1	105.1	105.1	6.89	0.018
Pretan	7	652.0	93.1	6.11	0.001
Interaction	7	228.9	32.7	2.14	0.098
Error	16	244.0	15.2		
Total	31	1230.0			

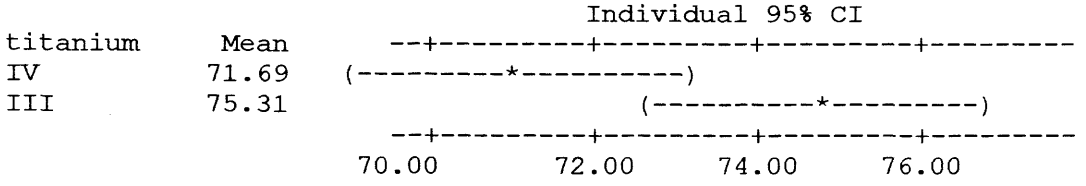

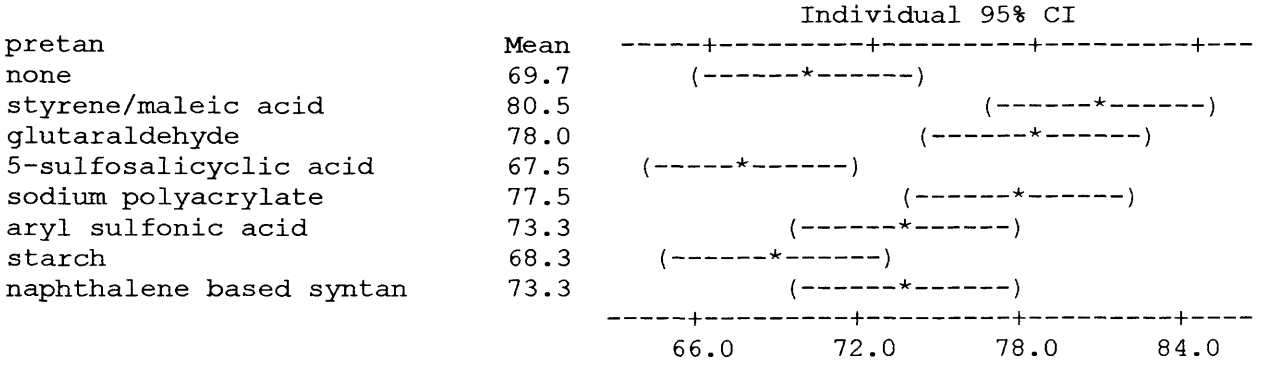

Analysis of Variance for shrinkage

Source	DF	SS	MS	F	P
titanium	1	105.1	105.1	5.11	0.034
pretan	7	652.0	93.1	4.53	0.003
Error	23	472.9	20.6		
Total	31	1230.0			

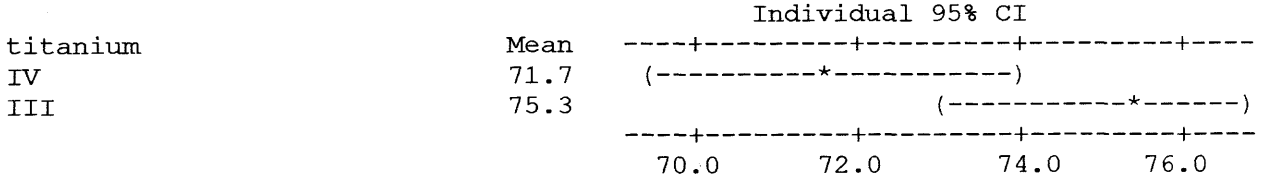

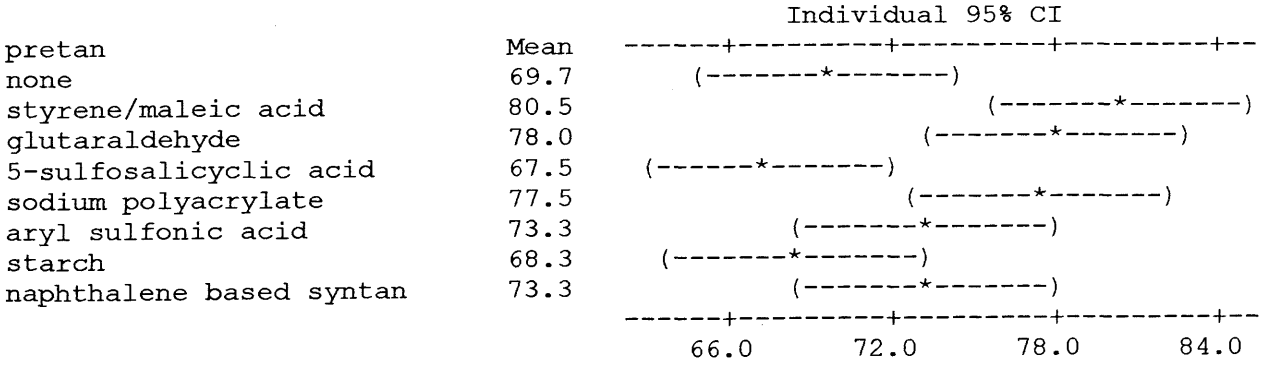

Analysis of Variance for energy of shrinkage

Source	DF	SS	MS	F	P
titanium	1	1.6	1.6	0.02	0.880
pretannage	7	718.8	102.7	1.58	0.280
Error	7	454.3	64.9		
Total	15	1174.7			

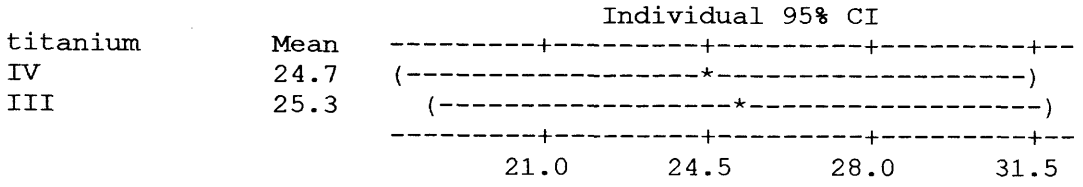

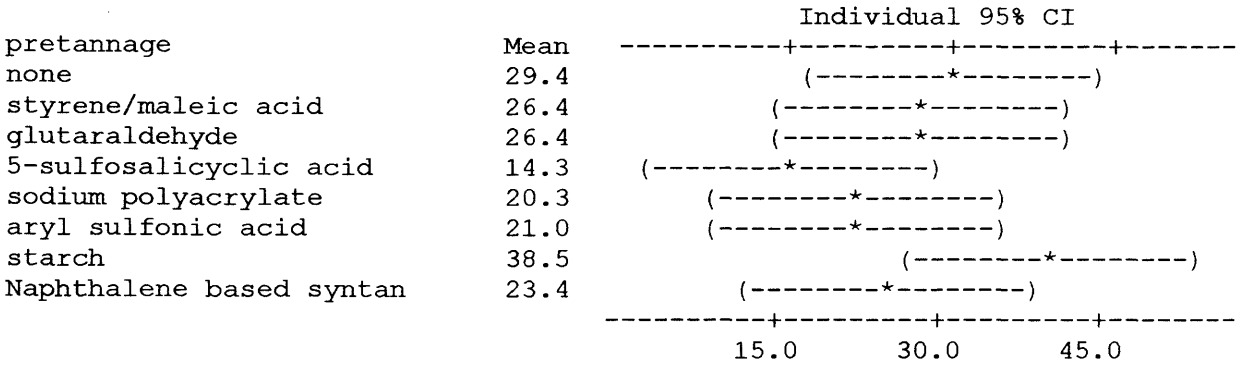

Analysis of Variance for tear strength

Source	DF	SS	MS	F	P
titanium	1	1733.9	1733.9	17.84	0.004
pretannage	7	1846.3	263.8	2.71	0.106
Error	7	680.2	97.2		
Total	15	4260.4			

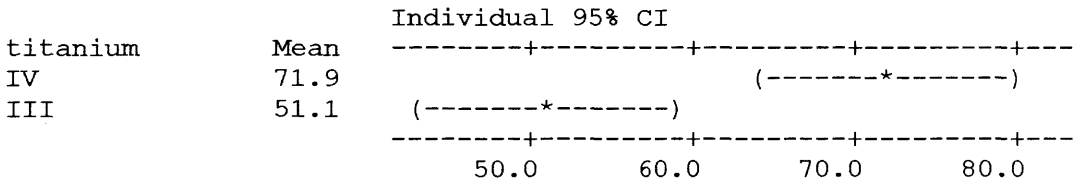

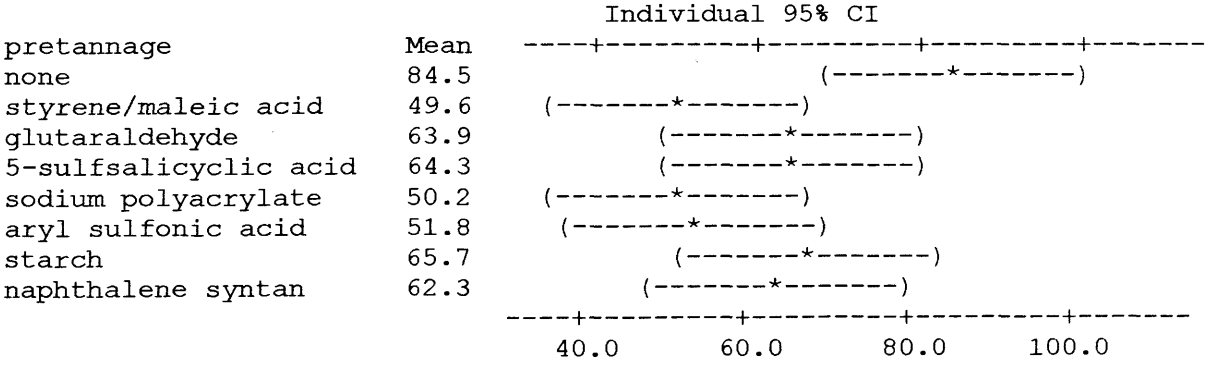

Analysis of Variance for thickness

Source	DF	SS	MS	F	P
titanium	1	1.0878	1.0878	15.48	0.001
pretan	7	0.8929	0.1276	1.82	0.153
Interaction	7	0.4415	0.0631	0.90	0.531
Error	16	1.1240	0.0703		
Total	31	3.5462			

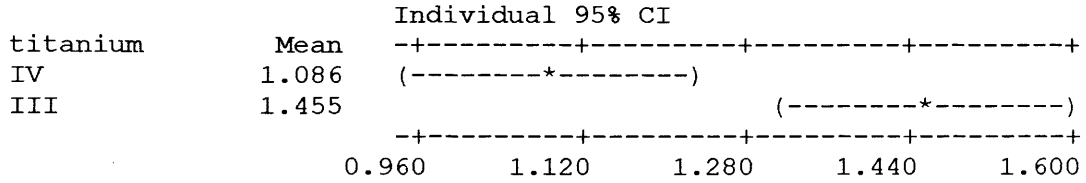

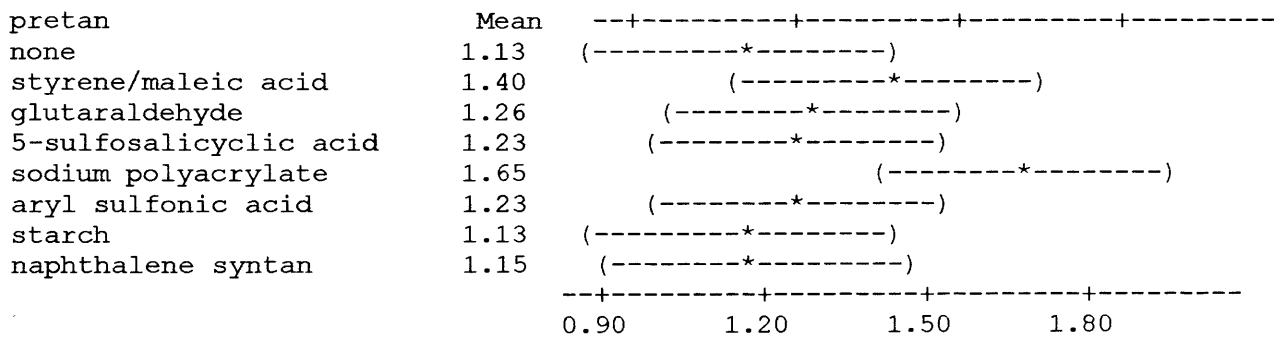

Appendix 3: Tannage for comparative trials in section 3.10

All products ex Hodgson Chemicals, Beverley, UK unless stated

Tannage	80% water at 20°C	
	6% salt	Run 10 minutes
	Add skins	Run 20 minutes
	+ 1% neutral syntan [Neosyn N]	
	+ 1% neutralising agent [Neutrol DP]	Run 30 minutes
	+ 0.25% acetic acid	pH 2.8
	+ 2% Synthetic/natural oil blend [Remsynol OCS]	Run 20 minutes
	+ 2.5% chromium oxide or titanium (III) oxide	Run 1 hour
	Basified to pH 3.9 for chromium and 4.3 for titanium	
Drain, samm, horse up overnight . Packs were added together		
	Skins were shaved to 1.0 mm	
Wash	300% water at 40°C	
	+ 0.25% anionic surfactant [Remcoil KTU]	
	+ 0.25% Acetic acid	Run 20 minutes,
Drain		
Retan	160% water at 40°C	
	2% synthetic/natural oil blend [Remsynol OCS]	
	6% chrome syntan [Neosyn HL]	pH 3.5
	+ 2% oxazolidine [Neosyn TX]	
	+ 0.3% formic acid	pH 4.3
Wash and Drain	300% water at 40°C	Run 10 minutes

Drain

Neutralise	150% water at 40°C	
	2% synthetic/natural oil blend [Remsynol OCS]	
	1% ammonium bicarbonate	
	1.5% neutral syntan [Neosyn BS3]	Run 45 minutes
		pH 5.5

Drain and wash

Dye & Retan	80% water at 60°C	
	4% Black dye	Run 30 minutes
	+10 % synthetic oil blend [Remsynol SOL] (dil x5)	Run 30 minutes
	+2% acrylic syntan [Neosyn ACN] (dil x 5)	Run 10 minutes
	+2% melamine formaldehyde syntan [Neosyn MFN]	Run 30 minutes
	+ 1.5% formic acid (dil x 10)	Run 20 minutes
	+ 1.0% formic acid (dil x 10)	Run 15 minutes
		pH 3.5

Drain and wash off at 60°C

Top fatliquor	100% water at 60°C	
	3% sulfated vegetable/synthetic oil [Remsynol AV2M]	Run 30 minutes

Drain

Rinse cold

Horse up

Toggle dry and finished at a H Goodman and Sons, Kettering, UK.

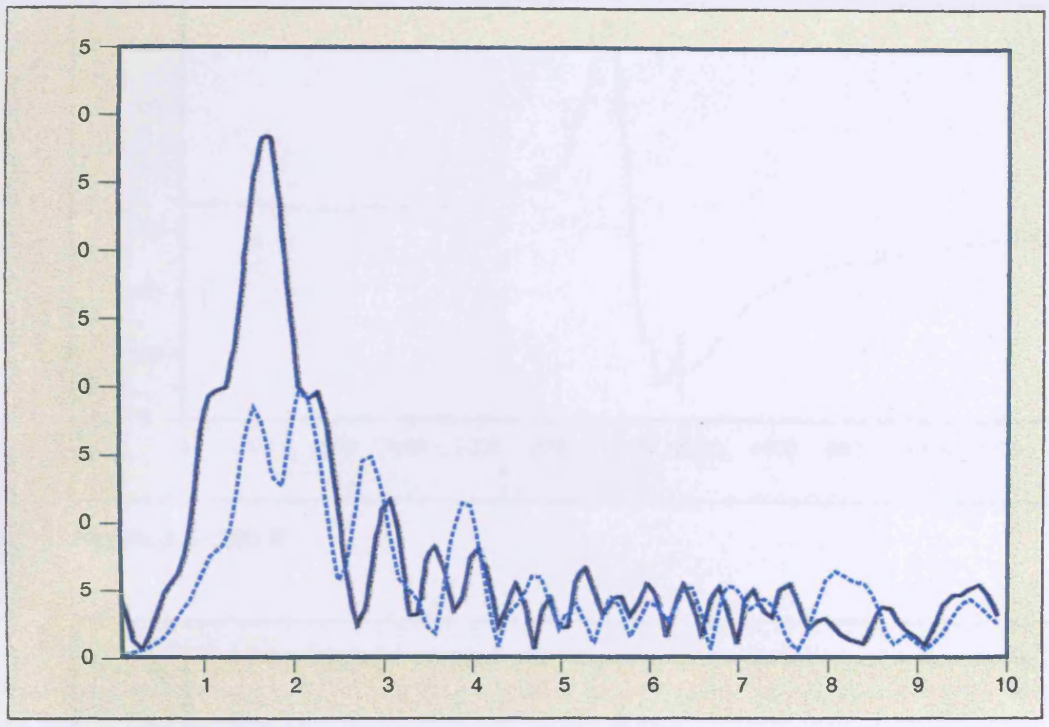

Appendix 4:
K edge spectra of titanium (III) leather (above) and titanium (IV) leather (below)

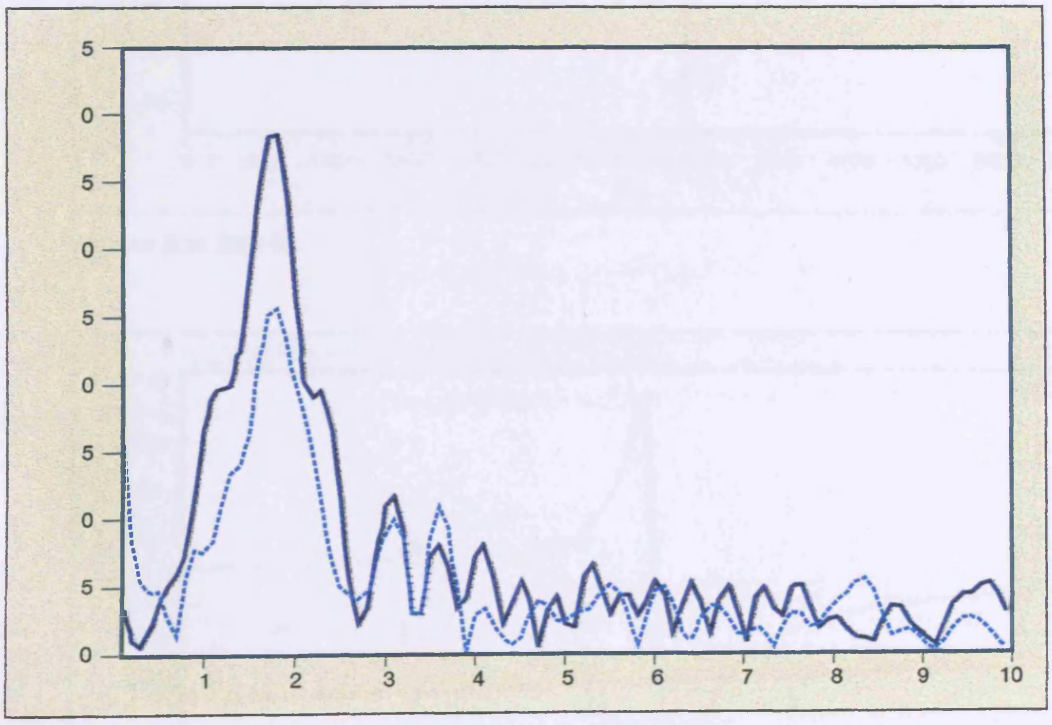

Appendix 5: Electron spin resonance spectra of semi-titanium leathers

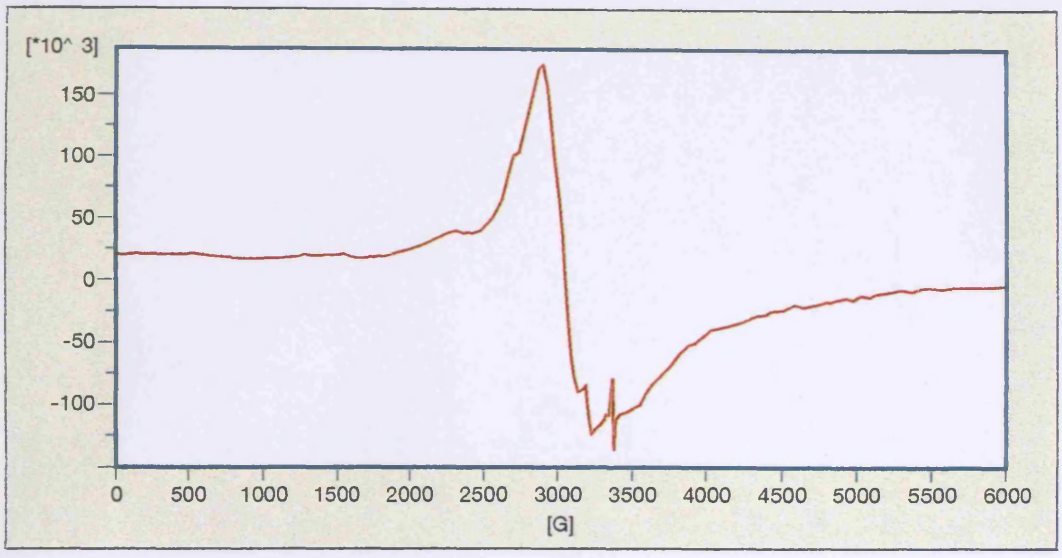

Figure 5.1: 295 K

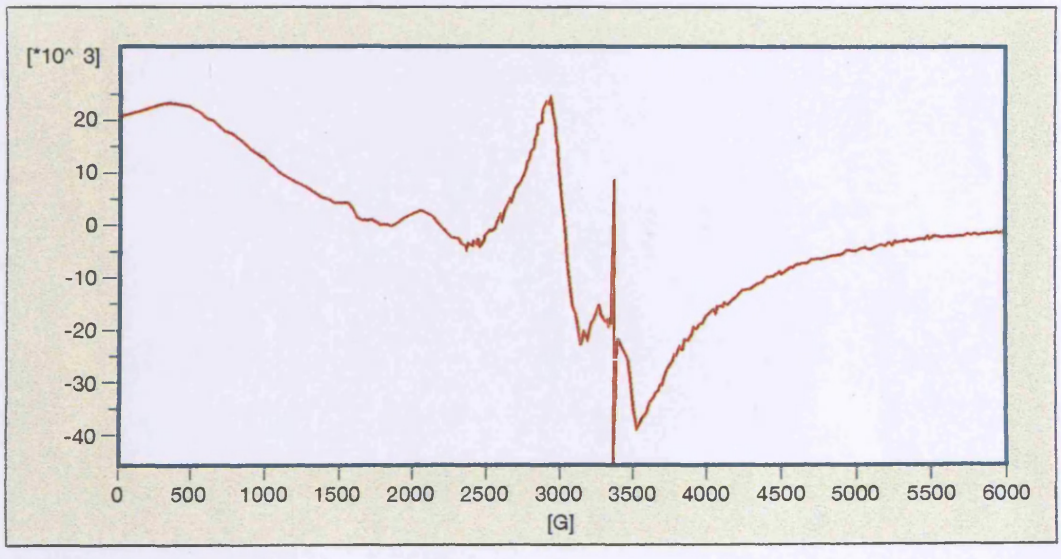

Figure 5.2: 290 K

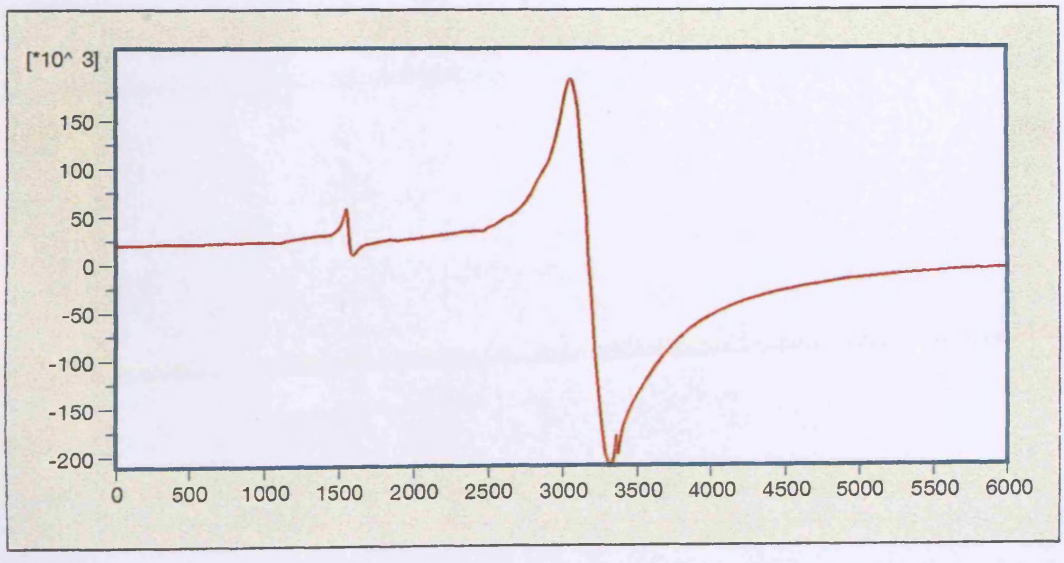

Figure 5.3: 100 K